M 2016

U.PORTO

FEUP FACULDADE DE ENGENHARIA
UNIVERSIDADE DO PORTO

DEVELOPMENT OF AN IN-HOUSE TOOL FOR LIQUEFACTION ASSESSMENT OF SOILS

BERNARDO JOSÉ ANDRADE PEREIRA CARVALHO

DISSERTAÇÃO DE MESTRADO APRESENTADA
À FACULDADE DE ENGENHARIA DA UNIVERSIDADE DO PORTO EM
ENGENHARIA CIVIL – ESPECIALIZAÇÃO EM GEOTECNIA

U.PORTO

FEUP FACULDADE DE ENGENHARIA UNIVERSIDADE DO PORTO

ch2m:SM

DEVELOPMENT OF AN IN-HOUSE TOOL FOR LIQUEFACTION ASSESSMENT OF SOILS

BERNARDO JOSÉ ANDRADE PEREIRA CARVALHO

Dissertação submetida para satisfação parcial dos requisitos do grau de

MESTRE EM ENGENHARIA CIVIL — ESPECIALIZAÇÃO EM GEOTECNIA

Orientador: Professor Doutor António Milton Topa Gomes

Coorientador: Doutor Iain John Tromans

Coorientador: Engenheira Manuela Daví

JULHO DE 2016

MESTRADO INTEGRADO EM ENGENHARIA CIVIL 2015/2016

DEPARTAMENTO DE ENGENHARIA CIVIL

Tel. +351-22-508 1901

Fax +351-22-508 1446

✉ miec@fe.up.pt

Editado por

FACULDADE DE ENGENHARIA DA UNIVERSIDADE DO PORTO

Rua Dr. Roberto Frias

4200-465 PORTO

Portugal

Tel. +351-22-508 1400

Fax +351-22-508 1440

✉ feup@fe.up.pt

http://www.fe.up.pt

Aos meus Pais,

"One's destination is never a place, but a new way of seeing things"

Henry Miller

ACKNOWLEDGMENTS

Firstly I would like to express my thanks for this opportunity at CH2M and to the persons who made it possible. It was an incredible experience and it represents a remarkable period of my life, contributing to the development of my capabilities, allowing me to expand my knowledge and to get a closer look at the work developed within the engineering practice. My special gratitude goes then to the mentor of this agreement between the company and FEUP, Eng. João Fonte, who integrated me and made sure I was adapting not only to the company, but also to my life in London.

I would also like to acknowledge my gratefulness to my supervisors at CH2M. Eng. Manuela Daví, who from my first day at the company provided me the best conditions to develop a solid work and steered me in the right direction. Once again, my special gratitude for her availability and supervision, without whom it would not have been possible to accomplish the objectives set. Also to Dr. Iain Tromans, whose advice was indispensable for the development of my work. It was undoubtedly a privilege to have the possibility to work with such a great professional and an incredible team leader.

I would also like to acknowledge my thesis advisor at FEUP, Professor António Topa Gomes, whose virtual office had the door always open to any questions. I also thank him for his guidance during my Masters in Geotechnical Engineering, proving to be extremely professional and always maintaining a close relationship with his students.

I also want to express my gratitude to my colleague and friend Ana Rita, with whom I shared this experience abroad and whose support was vital during this period. My fingers are crossed for her and I am totally sure she will succeed in this new thrilling stage in her life.

I want to express my gratefulness to my friend Filipa, who even far away showed an incredible and indispensable support. I hope her to have a bright future as she deserves it and to be there to celebrate it with her.

To Diogo and Tiago, whose friendship was indeed one of the greatest gifts I had. I know for sure that we will keep improving it through great dinners and vacations.

To all my colleagues and friends at FEUP that accompanied me through the last five years, of which I underline Pinto, Zé, Francisca and Lili. It was a pleasure to share this ride with them and I wish them the best of lucks in their futures.

Last but not least, a very special thank you to my family, especially to my parents who provided me a great education but more importantly, values that I honour. Without their accompaniment, it would not have been possible to live this experience or to graduate.

ABSTRACT

An in-house soil liquefaction assessment tool based on CPT procedures is developed using Mathcad as platform. Three software packages are assessed by mutual comparison, namely CLiq (Geologismiki), LiquefyPro (CivilTech) and Settle^{3D} (Rocscience). The aim of the developed in-house tool is to validate the software CLiq, as it is the only that embodies the same CPT-based liquefaction assessment procedure implemented on the tool. The validation is based on case histories selected from the New Zealand Geotechnical Database (NZGD), which provides an extensive archive of CPT data and post-earthquake information from the 2010-2011 Canterbury earthquake sequence. The seismic parameters as well as the post-earthquake information extracted are related to the M_W 6.2, 2011 Christchurch earthquake, the most damaging event in terms of liquefaction occurrence within the 2010-2011 Canterbury sequence.

The three software packages are validated by comparing their calculated parameters against each other, using the Robertson and Wride (1998) liquefaction evaluation procedure, as it is one of the most established methods in earthquake engineering practice. The predicted liquefaction-induced settlements are also compared using the methods incorporated within LiquefyPro and CLiq, since Settle^{3D} does not allow settlement estimation for CPT-based procedures (Tokimatsu and Seed, 1987; Ishihara and Yoshimine, 1992; Zhang et al., 2002 and Robertson and Shao, 2010).

Within the aim of this thesis, the tool has been developed to implement the latest and widely used method for liquefaction assessment in the engineering practice, i.e. Robertson (2009), an update of the Robertson and Wride (1998) procedure, as it was concluded through the literature review presented in chapter 2 and engineering practice in actual project in CH2M. A second part of the validation consists in plotting the parameters estimated by the tool and the software CLiq against each other using Robertson (2009).

This study helps in identifying capabilities and limitations of the three commercially available software packages and highlights the benefits of having a custom-made in-house tool to assess soil liquefaction, flexible to adaptation and updates as new techniques become available.

KEYWORDS: Liquefaction, Mathcad, LiquefyPro, Settle^{3D}, CLiq.

RESUMO

No âmbito desta tese é desenvolvida uma ferramenta baseada em métodos CPT para avaliar o solo à liquefação. Três programas são avaliados através da comparação dos seus resultados, nomeadamente CLiq (Geologismiki), LiquefyPro (CivilTech) e Settle^{3D} (Rocscience). O objetivo da ferramenta desenvolvida é o de validar o programa CLiq, uma vez que é o único dos três que incorpora o mesmo método CPT para avaliação do solo à liquefação que foi introduzido na ferramenta. A validação é baseada em casos históricos selecionados a partir da New Zealand Geotechnical Database (NZGD), que providencia um extenso arquivo de dados CPT e informação pós-sismo da sequência sísmica de Canterbury, 2010-2011. Os parâmetros sísmicos, assim como a informação pós-sismo são retirados do abalo sísmico de 2011 em Christchurch de magnitude 6.2, o evento que causou mais danos relacionados com a ocorrência de liquefação da sequência sísmica de Canterbury, 2010-2011.

A validação dos três programas consiste em comparar os parâmetros calculados entre eles, com recurso ao método de Robertson and Wride (1998) de avaliação em relação à liquefação, por ser um dos métodos mais utilizados pela comunidade de engenharia sísmica. Os assentamentos induzidos por liquefação estimados pelos programas são também comparados, usando os métodos incorporados no LiquefyPro e no CLiq, uma vez que o Settle^{3D} não permite estimar assentamentos para análises baseadas em ensaios CPT (Tokimatsu and Seed, 1987; Ishihara and Yoshimine, 1992; Zhang et al., 2002 e Robertson and Shao, 2010).

No âmbito do objetivo da tese, a ferramenta é desenvolvida para incorporar o método mais recente e currentemente utilizado pela comunidade de engenharia sísimica em avaliações à liquefação, i.e. Robertson (2009), uma atualização do método de Robertson and Wride (1998), como foi concluido após a pesquisa bibliográfica apresentada no capítulo 2 e pela prática em projeto na CH2M. A segunda parte da validação consiste em representar gráficamente os parâmetros estimados pela ferramenta desenvolvida e pelo CLiq através do método de Robertson (2009).

Este estudo ajuda a identificar as capacidades e limitações dos três programas comerciais e realça os beneficios de possuir uma ferramenta interna para avaliar o solo em relação à liquefação, flexível para adaptações e atualizações que possam surgir com novas técnicas desenvolvidas.

PALAVRAS-CHAVE: Liquefação, Mathcad, LiquefyPro, Settle^{3D}, Cliq.

GENERAL INDEX

FIGURES INDEX

TABLES INDEX

SYMBOLS, ACRONYMS AND ABBREVIATIONS

Latin Alphabet:

AASHTO- American Association of State Highway and Transportation Officials

a_{max}- maxi mum acceleration at ground surface

BPT- Becker Penetration Test

c- Normalization exponent

C_0 – Fitting parameter for $CRR_{7.5}$

C_{FC} – Fitting parameter for FC

C_N- Correction factor for overburden stress

C_Q- Correction factor for overburden stress

CPT- Cone Penetration Test

CPTu- Piezocone Penetration Test

CRR- Cyclic Resistance Ratio

$CRR_{7.5}$- Cyclic Resistance Ratio for magnitude of 7.5

CSR- Cyclic Stress Ratio

CSR^*- Equivalent uniform CSR for a magnitude of 7.5

D_r – Relative density

d- depth

DMT- Flat Dilatometer Test

DWF_M- Duration Weighting Factor

e_0- initial void ratio

e_c- critical void ratio

e_{ss}- void ratio for the steady state line

F- Normalized friction ratio from CPT

F_r - Normalized friction ratio from CPT

FC- Fines Content

FS- Factor of Safety

f_s- sleeve friction from CPT

g- gravitational acceleration

G_0- Small strain shear modulus

GWT- Ground Water Table

I_C- Soil Behaviour Type Index

IND- Indicator of liquefaction occurrence

K_0 – In-Situ earth pressure coefficient

K_α- Static shear stress reduction factor

K_σ – Overburden stress correction factor

K_C- Fines correction factor

LFRD – Load and Resistance Factor Design

LiDAR- Light Detection And Ranging

LL- Liquid Limit

LPI- Liquefaction Potential Index

M- Moment magnitude scale

M_W- Moment magnitude scale

MSF- Magnitude Scaling Factor

m- Stress exponent

N_C - Equivalent number of cycles

$(N_1)_{60,cs}$ – Normalized penetration resistance in clean sands for SPT

n- Stress exponent

NZGD- New Zealand Geotechnical Database

NCEER- National Center for Earthquake Engineering Research

p_a- Reference pressure

PGA- Peak Ground Acceleration

PI- Plasticity Index

P_L – Probability of liquefaction

P_S – Probability of exceeding a specific settlement

Q- Normalized cone penetration resistance

Q_{tn}- Normalized tip resistance correct for overburden stress from CPT

$Q_{tn,cs}$- Normalized clean sand tip resistance from CPT

q_c- tip resistance from CPT

$q_{c,1}$- Normalized tip resistance from CPT

$q_{c,1,mod}$ – Modified normalized tip resistance from CPT

q_{c1N}- Normalized tip resistance corrected for overburden stress from CPT

$q_{c1N,cs}$- Normalized clean sand tip resistance from CPT

R_f - Friction ratio

r_d- stress reduction factor

S- Settlement

S_{D1} – Spectral acceleration coefficient at 1.0-sec. period

S_d – Dry soil settlement

S_s – Saturated soils settlement

S_t – Total settlement

SCPT- Seismic Cone Penetration Test

SPT- Standard Penetration Test

SSL- Steady State Line

USGS- United States Geological Survey

V_s- Shear wave velocity

WT_e – Earthquake water table

WT_i – In-situ water table

w_c- water content

z- depth

Greek Alphabet:

Δ_{qc} – Fines adjustment factor

Δ_z - Thickness of the soil layer

ε_v- Vertical strain

ε_{vol} - Volumetric strain

$\varepsilon_{vol\ (15)}$ - Volumetric strain equivalent to 15 cycles

γ- shear stress

γ_{cyc}- cyclic shear stress

γ_s- soil unit weight

γ_w- water unit weight

μ- Mean

σ- Standard deviation

$\sigma_{ln(R)}$ – Fitting parameter for $CRR_{7.5}$

σ_v- Total vertical stress

σ_{v0}- Total vertical in-situ stress

σ'_v- Effective vertical stress

σ'_{v0}- Effective vertical in-situ stress

τ_{av} – Average cyclic shear stress

τ_{max}- Maximum shear stress

Φ – Standard normal cumulative distribution function

Φ^{-1} – Inverse normal cumulative distribution function

1
INTRODUCTION

1.1. MOTIVATION AND GOALS

Soil liquefaction is one of the great issues affecting foundations in sandy soils. The propensity of cohesionless soils to densify when submitted to ground shaking is well known, however when the water table is near the surface the hazard increases. When the soil is saturated, cyclic loading occurs rapidly and under undrained conditions, causing an increase in pore water pressure with the tendency of the soil to densify. If the magnitude of the cyclic loading reaches high values, the pore water pressure may even the soil's total stress, causing the effective stress to reach a value of zero which decreases the soil stiffness and strength, and produces large deformations. After the earthquake, the pore water pressure excess tends to dissipate, causing a rearrangement of the soil's particles and consequently producing settlement of the ground surface. Obviously, this phenomenon has catastrophic effects in structures founded upon soils that experience it, causing severe structural damage as it can be observed in Figure 1. Liquefaction may be also evidenced by the ejection of liquefied soil through cracks on the ground caused during the earthquake, defined as sand boils and noticed in Figure 2.

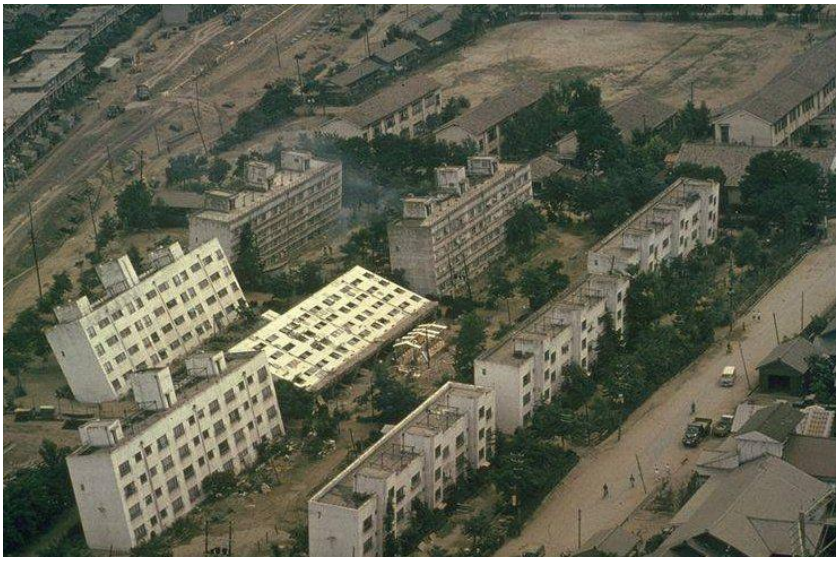

Figure 1- Damage caused by liquefaction on buildings after the 1964 Niigata earthquake (Japan National Committee on Earthquake Engineering, 1968)

Once it became an important topic of study, several methods to assess and analyse it were developed over time, based on laboratory or field testing. In chapter two of the current thesis, some of the proposed

methods based on field testing (CPT) are presented, from liquefaction evaluation to liquefaction-induced settlement estimation methods.

There is then a requirement for liquefaction assessment of soils within seismic design for structures by implementing these methods. However, it was found important by the engineering practice to develop an automated liquefaction assessment calculation based on some of the methods in the literature, which led to the formulation of several commercial software products.

Figure 2- Sand boils evidencing liquefaction in the 2011 Christchurch earthquake at the Queen Elizabeth II Park (New Zealand Defence Force, 2011)

Nonetheless, some of the software products used in engineering practice offer little transparency to the user, providing only the calculation results as output, which does not convey confidence and may not be acceptable in the scope of some projects. Emerged then the necessity of validating the commercial software products employed in seismic design, in order to better understand their procedures and the legitimacy of the calculations performed.

In the scope of this thesis is developed a tool, running on Mathcad and implementing some of the methods available in literature. Its aim is to validate some commercial software products, by comparing the results of a liquefaction analysis developed in both. The operation of the developed tool is presented in chapter three. The analyses performed are grounded in case histories selected from the New Zealand Geotechnical database (NZGD), since it provides quality information from the 2010-2011 Canterbury earthquake sequence.

It should be noted the importance of having an in-house tool that strictly follows the literature methods, flexible to adaptation and updates as new techniques become available, and capable of identifying the capabilities of the commercial software products.

This thesis was developed in business environment within CH2M in its London office.

1.2. THESIS ORGANIZATION

This dissertation can be divided into five main sections and one appendix.

Chapter two presents the state-of-the-art in which this thesis is grounded. A brief introduction to the liquefaction phenomenon is presented along with the methods available in the literature to evaluate it and to estimate associated settlements. It is discussed the types of liquefaction, the methods available to evaluate it and the effects of this phenomenon on the ground. CPT-based methods are emphasized, having been selected as the field testing technique of most interest for the curent research project. Liquefaction evaluation methods are divided in deterministic and probabilistic, while settlement estimations methods are separated into those for saturated soils and those for dry soils.

Chapter three presents the CPT-based in-house tool developed in Mathcad. A brief discussion of this software is made, by presenting its capabilities and functionalities that support the selection of Mathcad to be the platform in which the tool runs. The calculation sequence is also presented by describing, for each step, the methods implemented and discussed in chapter two, as well as the data required by the tool to run the analysis and the parameters provided after the calculation. Snapshots of the calculation spreadsheet are provided, including the input area and graphical output of calculated parameters, in order to better understand the tool's operation. The full worksheet developed for the tool is presented in appendix.

In chapter four, the case histories selected to perform the assessment of three software products and the validation of the developed tool against one of them are presented, as well as the criteria implemented in their selection. Three case histories are selected from the New Zealand Geotechnical Database, created after the 2010-2011 Canterbury earthquake sequence in New Zealand. A geological characterization of the Canterbury region is provided, emphasizing the Christchurch area, since the case histories selected are within it. The data available in the NZGD is presented, as well as the methods adopted to obtain it. After the selection of the case histories, it is provided the stratification of each location based on boreholes nearby.

In chapter five is carried out a validation of three commercial software products: LiquefyPro, Settle^{3D} and CLiq. The three software products are assessed and characterized by describing their functionality and methods available to perform a liquefaction evaluation or a liquefaction-induced settlement estimation. The validation is based on the methods of the software products and it is achieved by evaluating each of the three case histories selected in chapter four and plotting the calculated parameters from each software against the others. The results of the liquefaction assessments are also compared with the post-earthquake information available in NZGD. A final discussion gathers the findings of the validation process and summarizes the characteristics and limitations observed for each software.

Chapter six presents the validation of the developed tool against one of the three commercial software products, CLiq. The validation process is similar to the one implemented in chapter five with a liquefaction evaluation made of one of the case histories, plotting the results computed from the tool against the same parameters obtained by CLiq. A sensitivity analysis is also developed herein, in order to check the influence on the results of some modifications made to the literature procedures implemented in the tool and in CLiq. To conclude, the results of the validation and the sensitivity analysis are discussed, presenting an overview of the developed tool.

Chapter seven summarizes the work developed and the conclusions obtained after each validation. A proposal for further developments of the work realized is also presented in this chapter, considering the opportunities for enhancement of the tool and the process of validation, from the point of view of the author.

The appendix provides the worksheet developed for the Mathcad tool, presented in chapter three.

2
LITERATURE REVIEW

2.1. SOIL LIQUEFACTION

2.1.1. DEFINITION

Liquefaction is an important topic to study and to consider in the design of structures constructed upon saturated sandy soils, due to its devastating effects. Although Duton had already noticed liquefaction evidence in the 1886 Charleston earthquake, and Mogami and Kubo (1953) conceived the term liquefaction as the total loss of strength of vibrated sands, according to Scawthorn (2006), the process of studying the liquefaction phenomenon had only intensified after the Niigata and the Alaska earthquakes in 1964, where both earthquakes produced examples of liquefaction-induced damage, such as slope failures, bridge and building foundation failures and flotation of buried structures – Kramer (1996).

Terzaghi and Peck (1963) defined liquefaction as the sudden drop of shear strength under undrained conditions from the yield strength to the substantially smaller critical state strength. This loss of strength induces a behaviour in the soil similar to a liquid. When a saturated cohesionless soil is submitted to a rapid loading under undrained conditions, its tendency to densify will produce an increase in the excess pore water pressure, causing a decreasing of the effective stresses – Kramer (1996). Ishihara developed a scheme to better explain what happens in terms of stresses during the occurrence of liquefaction, presented in Figure 3.

As there is not an established and prevailing approach to assess the triggering of liquefaction phenomena in a soil, due to the several procedures and methods of analysis, it is still a controversial topic, the understanding of which has been improved after major earthquake events such as the Loma Prieta (1989), Kobe (1995), Kocaeli (1999) and more recently the Canterbury earthquake sequence (2010-2011) in New Zealand.

Liquefaction phenomena can be divided in two major groups: flow liquefaction and cyclic softening. Although this dissertation will only focus on liquefaction cases of cyclic softening, it will be made a brief distinction between both so it is clearer to understand what the soil is experiencing in each situation.

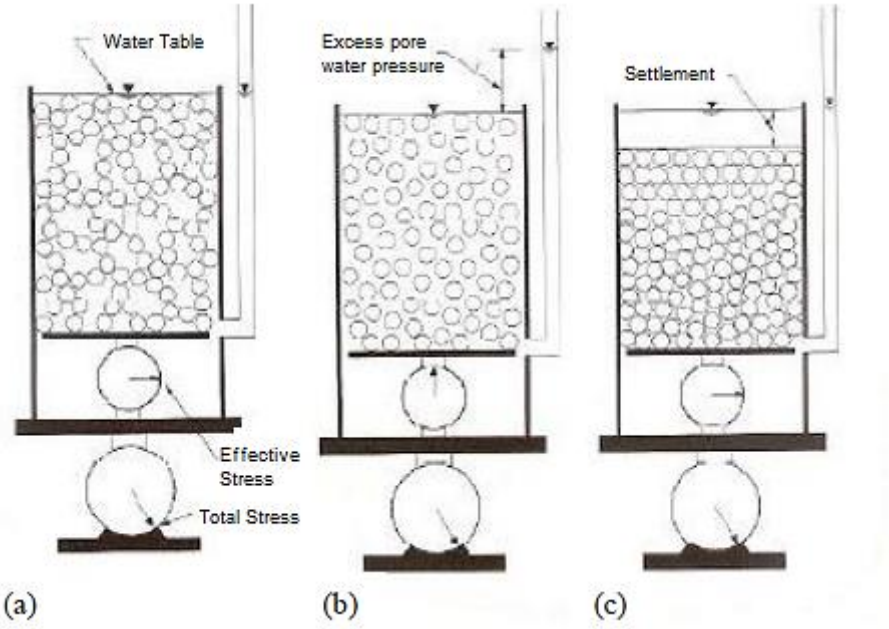

Figure 3- Scheme presented by Ishihara (1985) to explain liquefaction phenomena (modified after Matos Fernandes, 2006): a) before liquefaction occurred b) during liquefaction c) after liquefaction

2.1.2. Evaluation of Soil Liquefaction

2.1.2.1. Flow Liquefaction

Flow liquefaction applies to strain softening soils and it occurs when the static shear stress is greater than the shear stress of the soil in its liquefied state – Kramer (1996). It can be triggered by a loading either monotonic or cyclic in loose and cohesionless deposits, very sensitive clays and silt deposits. For soil failure to occur, a sufficient volume of material should strain soften, and the resulting failure can be a slide or a flow depending on the material characteristics and the ground geometry – Robertson (2004). Although it is not very frequent to perceive an example of a failure due to flow liquefaction, when it happens the results are catastrophic as it was exemplified in the Aberfan flow slide – (Bishop, 1973), Zeeland sub-marine flow slides – (Koppejan et al., 1948) and the Sheffield and the Lower San Fernando dams.

2.1.2.1. Cyclic Softening

Cyclic softening can occur in saturated cohesionless soils with a strain hardening behaviour and it is characterized by a decreasing of the effective stresses in the soil due to an undrained cyclic loading. Cyclic softening may also be divided into two groups depending on the reversal of the shear stress. If it occurs, the soil experiences cyclic liquefaction, otherwise the phenomenon is called cyclic mobility. For shear reversal to occur, ground conditions must be level or gently sloping – Robertson and Wride (1998). If it occurs, the effective stress can reach a value of zero, causing a decrease in the soil stiffness and producing large deformations. The magnitude of the deformations depends on the density of the soil, the magnitude and duration of the cyclic loading and the extent to which shear stress reversal occurs (Robertson and Wride, 1998).

If there is no shear stress reversal and the cyclic loading is moderate, the effective stress barely drops to a value of zero, causing smaller deformations than cyclic liquefaction.

Robertson (1994) produced a flowchart evaluating liquefaction and characterizing its different types, as shown by Figure 4.

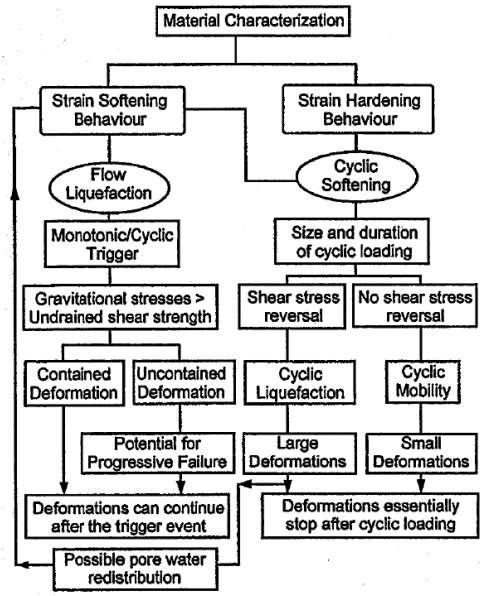

Figure 4- Flowchart for evaluation of soil liquefaction (Robertson 1994)

2.1.3. LIQUEFACTION SUSCEPTIBILITY

The first step in a liquefaction evaluation is the assessment of the susceptibility of a soil to liquefaction, since not all soils are potentially liquefiable. Liquefaction susceptibility can be evaluated through several criteria, presented below.

2.1.3.1. Compositional Criteria

As the aim of this project is to develop a tool to assess liquefaction linked to earthquake events, only cyclic liquefaction will be evaluated. The first step to evaluate cyclic liquefaction in level ground sites is to evaluate the soil susceptibility to this phenomenon. The Guide to Cone Penetration Testing for Geotechnical Engineering – Robertson and Cabal (2015), suggests that the susceptibility to cyclic liquefaction should be evaluated based on the plasticity index (PI), the liquid limit (LL) and the natural water content (w_c) of a soil. The criteria followed by this guide was proposed by Bray and Sancio (2006), and is presented in

Figure 5.

It also should be considered the level of risk of each project before deciding whether a soil is susceptible or not. If a project has low risk, it should be assumed that a soil is susceptible to cyclic liquefaction based on the Bray and Sancio (2006) criteria, unless previous local experience shows otherwise – Robertson and Cabal (2015). If the risk of the project is high, it should be assumed that the soil is susceptible to liquefaction or high quality samples should be obtained and properly tested on laboratory.

If a soil is considered susceptible to cyclic liquefaction, the next step in liquefaction evaluation should be taken. In other words, it should be evaluated the triggering of cyclic liquefaction, presented hereafter.

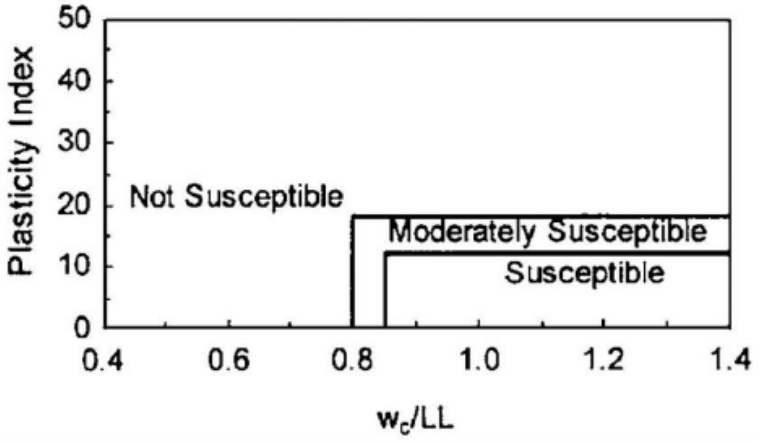

Figure 5- Liquefaction susceptibility criteria (Bray and Sancio, 2006)

2.1.3.2. Historical and Geological Criteria

An important source of information in the evaluation of the susceptibility of a soil to liquefaction comes from historical data on previous earthquakes that caused liquefaction. Post-earthquake field investigations have shown that liquefaction often occurs at the same location if soil and groundwater conditions have remained unchanged – Youd (1984). Based on these investigations, Ambraseys (1988) compiled data from case histories to propose a relationship between the epicentral distance of sites at which liquefaction was observed and the magnitude of the earthquakes that produced liquefaction. This relationship is presented in Figure 6.

The geological criteria to assess the susceptibility of a soil to liquefaction is based on the depositional and hydrological environment, as well as the age of the deposit – Kramer (1996). Soils that are sorted into uniform grain size distributions and deposited in loose states have a high liquefaction potential. The water level has also great influence in liquefaction susceptibility, since liquefaction only occurs in saturated soils, causing fluvial and estuarine deposits to have high liquefaction potential. The susceptibility of older soils to liquefaction is lower than newer deposits – Kramer (1996).

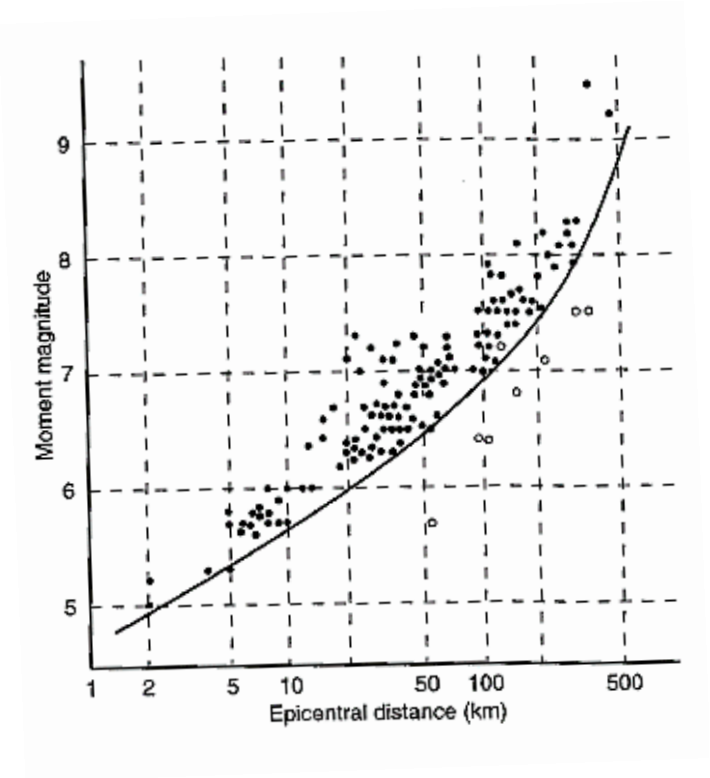

Figure 6-Relationship between epicentral distances of sites at which liquefaction was observed and the magnitude of the earthquake (Kamer, 1996 after Ambraseys, 1988)

2.1.3.3. State Parameter Criteria

As mentioned previously, the base of liquefaction triggering is the generation of excess pore pressures when the soil is submitted to a cyclic loading. Since the tendency to generate pore pressure of a soil is influenced by its initial state, defined by density and initial stress conditions – Kramer (1996), liquefaction susceptibility can be evaluated through state criteria, as the state parameter.

To understand the concept of state parameter, it is necessary to discuss the concept of steady state of deformation, defined by Castro and Poulos (1977). Based in several stress-controlled undrained triaxial tests, the steady state of deformation was defined as the state in which the soil flowed continuously under constant shear stress and constant effective confining pressure at constant volume and velocity – Kramer (1996). The spatial distribution of the points that correlate the void ratio with the effective confining pressure of the soil in the steady state of deformation is defined as the steady-state line (SSL). The correlation between the state parameter and the steady state line is presented on Figure 7.

The state parameter represents the proximity of the soil's initial state to the steady state line, and was defined by Been and Jeffries (1985) as:

$$\psi = e_0 - e_c \tag{1}$$

Where e_0 is the initial void ratio and e_c, also represented as e_{ss}, is the void ratio of the steady-state line (SSL) for the same effective confining pressure, defined as critical void ratio.

The SSL has been proved to be useful identifying the susceptibility of a soil to flow liquefaction, since it can only occur in soils with positive values of the state parameter, in other words, soils with an initial void ratio higher than the critical, defined as soils with contractive behaviour. On the other hand, cyclic softening can occur in soils with contractive or dilative behaviour, with the initial void ratio lower than the critical. Given that, the state criteria does not represent a useful criteria in cyclic liquefaction evaluation.

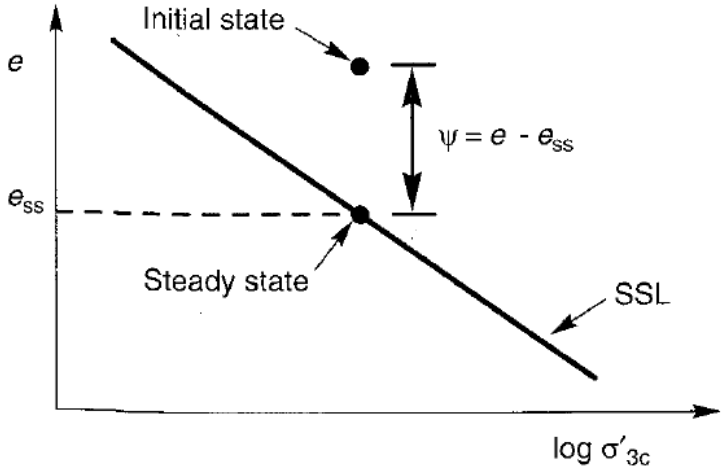

Figure 7 - Definition of state parameter (Kramer, 1996)

2.1.4. INITIATION OF LIQUEFACTION

There are several approaches to evaluate the potential for initiation of liquefaction, the most common to use in geotechnical engineering practice are the cyclic stress and the cyclic strain approaches. The work reported on this thesis will be only based on the cyclic stress approach, once it may only require in-situ tests for the characterization of the liquefaction resistance.

To evaluate the initiation of liquefaction, this approach expresses the earthquake-induced loading in terms of cyclic shear stresses, and compares it with the liquefaction resistance of the soil, also expressed in terms of cyclic shear stress. At locations where the loading exceeds the resistance, liquefaction is expected to occur – Kramer (1996).

Seed and Idriss (1971) proposed a simplified procedure to evaluate the susceptibility of a soil to liquefaction, consisting on comparing the soil resistance with the cyclic loading by the means of a factor of safety against liquefaction. This parameter is defined by equation (2) and is estimated for each depth where soil resistance and earthquake loading are characterized.

$$FS = \frac{CRR}{CSR} \tag{2}$$

Where CRR is the cyclic resistance ratio and CSR the cyclic stress ratio. Both parameters will be presented further ahead. For depths where CSR is greater than CRR (FS < 1), it is considered the soil layer to be liquefiable, otherwise it is assumed that liquefaction will not occur.

2.1.4.1. Characterization of Earthquake Loading

To express the seismic loading in terms of cyclic shear stress, it can be made a ground response analysis or use a simplified approach – Kramer (1996). In this thesis it will be used the simplified approach developed by Seed and Idriss (1971) and presented in Figure 8. The following procedure for the estimation of the cyclic shear stress was extracted from Matos Fernandes (2011):

Consider a soil column with level ground conditions and height equal to z, submitted to horizontal accelerations. When they reach their maximum value at the surface, the peak ground acceleration (PGA), is installed in the bottom of the considered soil column a shear stress defined by:

$$(\tau_{\max})_r = \frac{a_{\max}}{g} \times \sigma_{v0} \tag{3}$$

As the soil column is not stiff, the shear stress installed is smaller than the defined by the equation (3), and it can be obtained by introducing a stress reduction factor r_d:

$$(\tau_{\max})_d = \frac{a_{\max}}{g} \times \sigma_{v0} \times r_d \tag{4}$$

There are several approaches to define the stress reduction factor, in this thesis it will be assumed a set of expressions proposed by Liao and Whitman (1986), equations (5) and (6), Robertson and Wride (1997), equation (7), and William F. Marcuson in an oral communication, equation (8) – Youd and Idriss (1997). The expressions proposed by Liao and Whitman (1986) were recommended in the 1997 National Centre for Earthquake Engineering Research (NCEER) workshop and Youd et al. (2001):

$$r_d = 1 - 0.00765 \times z \qquad \text{if } z < 9.15\text{m} \tag{5}$$

$$r_d = 1.174 - 0.0267 \times z \qquad \text{if } 23\text{m} < z \leq 9.15\text{m} \tag{6}$$

$$r_d = 0.744 - 0.008 \times z \qquad \text{if } 30\text{m} < z \leq 23\text{m} \tag{7}$$

$$r_d = 0.5 \qquad \text{if } z \geq 30\text{m} \tag{8}$$

These expressions provide a mean of a wide range of possible r_d, and the range increases with depth – Golesorkhi (1989), once there is a considerable variability in the soil's flexibility at field sites. However, the participants of the workshop agreed that these expressions are suitable for use in engineering practice – Youd et al. (2001).

As the amplitude of an earthquake cyclic loading is quite odd, the shear stress will vary, so the assumption of a peak ground acceleration to characterize the seismic loading is not the more accurate. Seed and Idriss (1971) defined a uniform and equivalent cyclic loading with constant frequency and amplitude, with an amplitude equal to 65% of the maximum earthquake amplitude. The uniform cyclic shear stress is defined by:

$$\tau_{cyc} = 0.65 \times \frac{a_{\max}}{g} \times \sigma_{v0} \times r_d \tag{9}$$

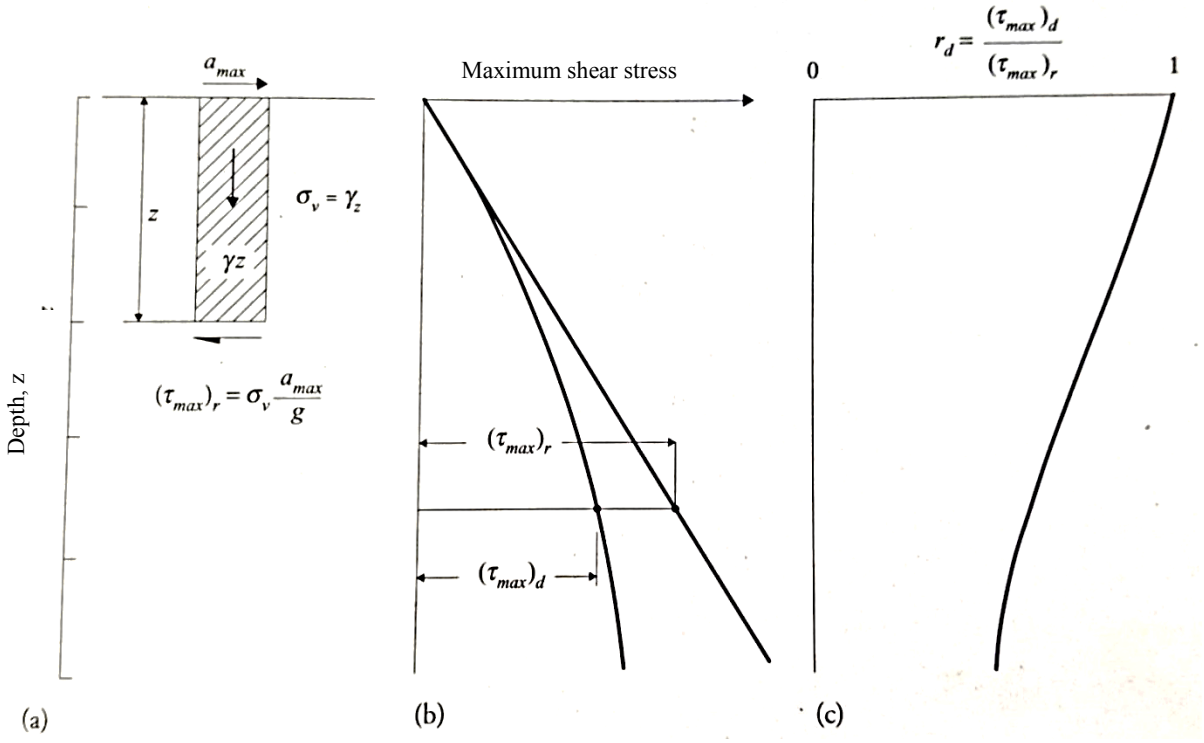

Figure 8- Simplified method to estimate shear stresses induced by earthquake (adapted from Seed and Idriss, 1971 after Matos Fernandes, 2011) : a) soil column considered; b) propagation in depth of shear stresses considering a stiff or flexible soil mass; c) evolution in depth of the stress reduction factor, r_d.

Regardless of whether a detailed ground response analysis or the simplified procedure is used, the earthquake-induced loading is characterized by a level of uniform cyclic shear stress applied for an equivalent number of cycles – Kramer (1996). The equivalent number of cycles depends on the earthquake magnitude, and the correlation between them was proposed by Seed et al. (1975) and presented on Figure 9

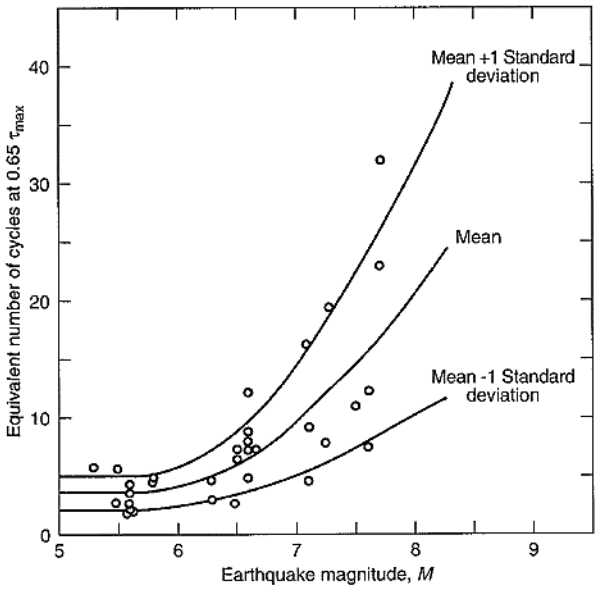

Figure 9- Correlation between the number of equivalent uniform stress cycles with the earthquake magnitude (Seed and Idriss 1975)

Dividing both members of the equation (9) by the initial effective overburden pressure to normalize the cyclic stress, it is obtained the cyclic stress ratio, CSR:

$$CSR = \frac{\tau_{cyc}}{\sigma'_{v0}} = 0.65 \times \frac{a_{\max}}{g} \times \frac{\sigma_{v0}}{\sigma'_{v0}} \times r_d \tag{10}$$

2.1.4.2. Characterization of Liquefaction Resistance

Resistance to cyclic loading is usually represented in terms of a cyclic stress ratio that causes cyclic liquefaction – Robertson and Wride (1998). To denote this ratio, different authors gave it different symbols but, as they used the symbol CSR with or without a subscript to signify liquefaction resistance, it generated some sort of confusion. So, in the workshop of the NCEER, Robertson and Wride proposed the term cyclic resistance ratio (CRR) to denote the liquefaction resistance – Youd and Idriss (1997).

Cyclic resistance can be obtained both by laboratory testing and by field testing. Laboratory test consist in submitting soil samples to cyclic loading by means of cyclic triaxial, cyclic simple shear or cyclic torsional tests – Robertson and Wride (1998). For cyclic simple shear test, the CRR is taken as the ratio of the cyclic shear stress to cause liquefaction to the initial vertical effective stress. In the cyclic triaxial test, CRR is taken as the ratio of the maximum cyclic shear stress to the initial effective confining pressure – Kramer (1996). Liquefaction failure in a laboratory test is defined as the point at which the soil sample achieves a strain level of 5% for axial strain amplitude in a cyclic triaxial test – Robertson and Wride (1998). Although laboratory testing was the basis of the early works related with cyclic resistance, there are several issues that hamper its broader use in evaluating the CRR. The in-situ stress state is very difficult to reply on laboratory and the samples are easily disturbed during the sampling, which destroy the effects of the depositional and historical environment of a soil deposit that influence liquefaction resistance – Kramer (1996). A solution to surpass these limitations is ground freezing, used

to obtain undisturbed samples of cohesionless soil, but the implementation of this procedure is usually costly, so it is only adopted in high-risk projects, where laboratory tests are necessary.

An alternative to estimate the liquefaction resistance of a soil is through liquefaction case histories and soil parameters measured by field tests, and due to the costs and the difficulties associated with recovering good quality and undisturbed samples to use in laboratory tests, field tests are the dominant approach in engineering practice for evaluating liquefaction potential. – Juang et al. (2013)

The first approaches were based on measured standard penetration test (SPT) parameters, plotted with the cyclic stress ratio that characterized the earthquake loading. The plotted points were distinguished whether liquefaction was observed or not, and a conservative boundary was drawn dividing the combinations that have or have not produced liquefaction in the past earthquakes – Kramer (1996). The observance of liquefaction cases is proven by the appearance of sand ejected through cracks and forming sand boils at ground surface. One of the first studies based on SPT was developed by Seed et al. (1975) plotting the cyclic stress ratio for an earthquake magnitude of 7.5 versus the blow count, presented in Figure 10.

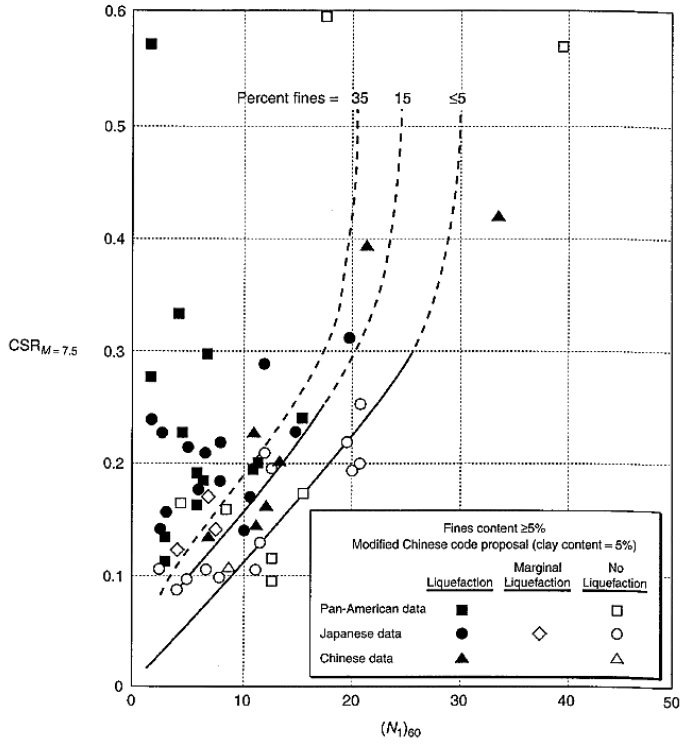

Figure 10- Relationship between CSR and N160 values for silty sands in M=7.5 earthquakes (Kramer, 1996 after Seed et al. 1975)

The development of studies following this procedure and the introduction of new case histories, allowed the development of methodologies considering the fine content (Seed et al. 1985) and new approaches based on cone penetration test (CPT) results – Matos Fernandes (2011). Among the in-situ tests, CPT is the preferred tool for liquefaction evaluation, due to its repeatability, accuracy and the capacity of providing continuous profiling of the soil throughout the measured parameters, cone tip resistance (q_c) and sleeve friction (f_s) – Juang et al. (2013).

There are several more examples of field tests that can be used on the liquefaction assessment and that were object of research through the years, such as the Becker penetration test (BPT), the shear wave velocity measurement (V_S) and the flat dilatometer test (DMT). The advantages and disadvantages of some methods available for liquefaction assessment based on field tests were gathered by Youd and Idriss (2001) and presented on Table 1.

Table 1- Comparison of Advantages and Disadvantages of Various Field Tests for Assessment of Liquefaction Resistance, Youd et al. (2001)

Feature (1)	Test Type			
	SPT (2)	CPT (3)	V_s (4)	BPT (5)
Past measurements at liquefaction sites	Abundant	Abundant	Limited	Sparse
Type of stress-strain behavior influencing test	Partially drained, large strain	Drained, large strain	Small strain	Partially drained, large strain
Quality control and repeatability	Poor to good	Very good	Good	Poor
Detection of variability of soil deposits	Good for closely spaced tests	Very good	Fair	Fair
Soil types in which test is recommended	Nongravel	Nongravel	All	Primarily gravel
Soil sample retrieved	Yes	No	No	No
Test measures index or engineering property	Index	Index	Engineering	Index

In this thesis, the procedure to be followed on liquefaction assessment is the use of field tests to characterize liquefaction resistance of a soil, more specifically the CPT, since it provides good outcome and it is widely implemented. Within the CPT based procedures, there are several methods to assess liquefaction triggering, from deterministic approaches that express liquefaction potential in terms of a factor of safety, to probabilistic approaches that consider the uncertainties inherent to the parameters and express the liquefaction potential in terms of the probability of liquefaction – Juang et al. (2013). Those different methods will be presented and detailed hereafter along with their approaches to characterize the cyclic resistance of the soil.

The CRR is typically taken at about 15 cycles of uniform loading to represent an equivalent earthquake loading of magnitude, M, equal to 7.5, i.e., $CRR_{7.5}$ – Robertson and Wride (1998). To obtain the cyclic resistance for the design earthquake loading, the $CRR_{7.5}$ provided from the CPT procedures should be affected by a factor that accounts for the duration effects. The magnitude scaling factor, MSF, account for how the characteristics of the irregular cyclic loading produced by different magnitude earthquakes affect the potential for triggering of liquefaction – Boulanger and Idriss (2014). Each procedure to evaluate liquefaction triggering has a specific recommendation for MSF and they will be presented herein this thesis, in section 2.2.

The CRR for the design earthquake magnitude comes as:

$$CRR_M = CRR_{7.5} \times MSF \tag{11}$$

2.1.5. Liquefaction Effects

As it was mentioned previously, liquefaction causes devastating damages on structures, sometimes more severe than the earthquake motion. These damages are due to the effects that a liquefied soil layer has on building foundations, on the surface, or even on the ground motion.

The effects of liquefaction provide evidence that a soil layer beneath the surface has liquefied, and are the base of case histories used by geotechnical earthquake engineering for progressing on this area.

2.1.5.1. Alteration of Ground Motion

The alteration of the ground motion is one effect of cyclic liquefaction that may cause damages on pile foundations and on the ground oscillation. The development of excess pore pressures during an earthquake will decrease the soil stiffness to values that can affect the transmission of the bedrock motion to the ground surface. Also, the occurrence of liquefaction beneath a level ground surface can decouple the liquefied soils from the surficial soils and produce transient ground oscillations – Kramer (1996). The soils at the surface may crack, causing liquefied soils to emerge and developing sand boils. Ground oscillation was the cause of the ground movements that fractured the pavements of the Marina District of San Francisco during the Loma Prieta earthquake in 1989. – Youd (1993). Figure 11 and Figure 12 represent the damage that the alteration of ground surface can induce.

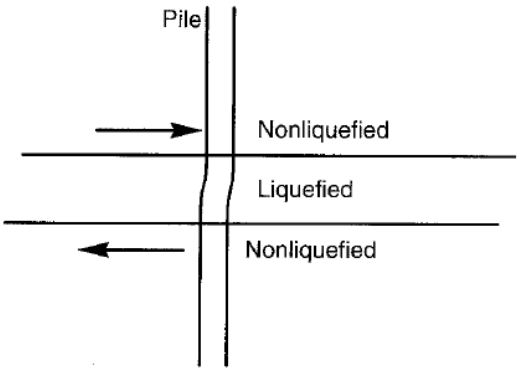

Figure 11- Potential effects of liquefaction on pile foundations. The strains that may develop in a liquefied layer can induce high bending moments in piles. (Kramer, 1996)

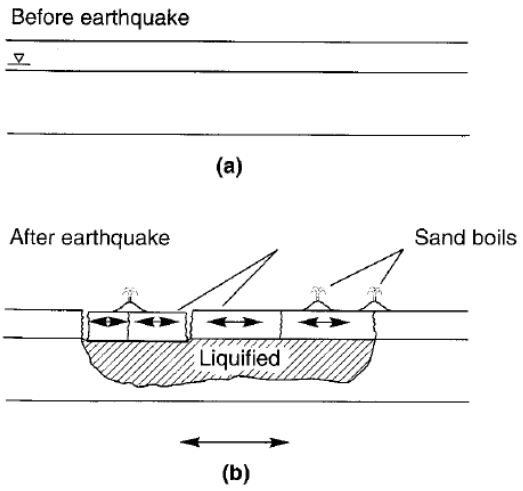

Figure 12- Ground oscillation (a) before and (b) after earthquake (Kramer, 1996)

2.1.5.2. Sand Boils

The excess pore pressures developed during the earthquake motion tend to dissipate by an upward flow of pore water, producing forces on soil particles in the same direction. These forces can loosen the upper portion of the deposit and leave it in a state susceptible to liquefaction in a future earthquake event – Youd (1984). If the hydraulic gradient driving the flow reaches a critical value, the vertical effective stress will drop to zero and the soil will be in quick condition – Kramer (1996). The soil particles may be carried upwards by the water movement and be ejected at the surface through localized cracks, forming sand boils. The development of sand boils depends on the characteristics of the liquefied soil layer and the soil layer above, and on the magnitude of the excess pore pressure – Kramer (1996).

Sand boils do not produce any damage but are a proper evidence of liquefaction, as it can be noticed in Figure 13

Figure 13- Photo of sand boils formed after the 1989 Loma Prieta earthquake (J.C. Tinsley, 1989)

2.1.5.1. Settlement

Cohesionless soils tend to densify when submitted to an earthquake loading, causing settlements on the ground surface. It can be divided in dry soils settlements, that are usually fast, and in saturated soils settlements, that take longer to occur depending on the time that excess pore pressures take to dissipate. As settlement causes more damage on structures and lifelines than other liquefaction effects, it will be object of further studies on subsequent chapters.

2.2. CPT BASED LIQUEFACTION TRIGGERING PROCEDURES

Due to its repeatability, accuracy and the capacity of providing continuous profiling of the soil throughout the measured parameters, cone tip resistance (q_c) and sleeve friction (f_s) – Juang et al. (2013), the CPT is the preferred in-situ test to be the basis of a liquefaction assessment. The CPT-based procedures present their recommendations to estimate $CRR_{7.5}$ and MSF. Seed and Idriss (1971)

recommendation to estimate CSR is considered accurate, so it is recommended by all presented methods. However, some may introduce new procedures to estimate r_d, rather than the suggested by NCEER. From the several CPT based procedures in the literature, only five will be presented in this chapter, divided into deterministic and probabilistic approaches.

2.2.1. DETERMINISTIC APPROACH

The deterministic approaches to determine the liquefaction potential of a soil give as an output, the factor of safety (FS) against liquefaction triggering. The FS correlates the seismic loading with the soils resistance to cyclic loading through a ratio between the CRR_M and the CSR. For the depths in which the FS is lower than 1 cyclic loading exceeds cyclic resistance, so liquefaction is expected.

The deterministic approaches to be followed in this report are the Robertson and Wride (1998) and the Robertson (2009). The latter can be considered as an update of Robertson and Wride (1998), but this will be analysed in more detail further ahead.

2.2.1.1. Robertson and Wride (1998)

This method suggests the Seed and Idriss (1971) approach, detailed in the subchapter 2.1.4.1. and defined by the equation (10) to estimate the CSR.

The authors suggest the use of CPT to estimate the CRR, since it provides great repeatability and a more continuous profile than the SPT – Robertson and Wride (1998). The output of a CPT test is the cone tip resistance (q_c) and the sleeve friction (f_s), and these values alongside with the total vertical in-situ stress (σ_{v0}) and the effective vertical in-situ stress (σ'_{v0}) are the basis for the CRR calculation.

The $CRR_{7.5}$ expressions proposed by Robertson and Wride (1998) are based on the equivalent clean sand normalized CPT penetration resistance ($q_{c1N,cs}$), and they are defined by:

$$CRR_{7.5} = 93 \times \left(\frac{q_{c1N,cs}}{1000} \right)^3 + 0.08 \qquad \text{if } 50 \le q_{c1N,cs} < 160 \tag{12}$$

$$CRR_{7.5} = 0.833 \times \left(\frac{q_{c1N,cs}}{1000} \right)^3 + 0.05 \qquad \text{if } q_{c1N,cs} < 50 \tag{13}$$

To obtain the $q_{c1n,cs}$ it must be made a normalization and a correction for overburden stress, and also it must be implemented a correction factor that accounts for the grain characteristics of the soil:

$$q_{c1N,cs} = K_C \times q_{c1N} \tag{14}$$

Where K_C is the grain characteristics correction factor, which will be presented further ahead, and q_{c1N} is the normalized cone penetration resistance corrected for overburden stress:

$$q_{c1N} = \left(\frac{q_c}{P_{a2}} \right) \times C_Q = \frac{q_{c1}}{P_{a2}} \tag{15}$$

Where C_Q, defined in equation (16), is the correction for overburden stress and P_{a2} is the reference pressure that must be in the same unit as q_c – Robertson and Wride (1998).

$$C_Q = \left(\frac{P_a}{\sigma'_{v0}} \right)^n \tag{16}$$

To establish a correction factor for the grain characteristics of the soil, it is necessary to estimate grain characteristics such as apparent fines content of the soil, once the correlations proposed for the CRR are very sensitive to the plasticity of the fines within the sand – Robertson and Wride (1998). The grain characteristics can be estimated from CPT results, by using soil behaviour charts. This method uses the normalized CPT soil behaviour type chart, proposed by Robertson (1990) and presented here in Figure 14, to obtain the soil behaviour type index (I_C):

$$I_C = \sqrt{(3.47 - Q)^2 + (\log F + 1.22)^2} \tag{17}$$

Where Q is the normalized CPT penetration resistance and F is the normalized friction ratio:

$$Q = \left(\frac{q_c - \sigma_{v0}}{P_{a2}} \right) \times \left(\frac{P_a}{\sigma'_{v0}} \right)^n \tag{18}$$

$$F = \left(\frac{f_s}{q_c - \sigma_{v0}} \right) \times 100\% \tag{19}$$

The soil behaviour type chart proposed by Robertson (1990) uses a normalized cone penetration resistance (*Q*) based on a stress exponent of n = 1.0, whereas the expressions proposed by Robertson and Wride (1998) to estimate CRR (equations (12) and (13)) are based on a normalized cone penetration resistance, q_{c1N}, that uses a stress exponent n = 0.5 (equations (15) and (16)).

The stress exponent is complex to obtain, and Olsen and Malone (1988) suggested that it varies from 0.5 in sands to 1.0 in clays. The approach followed by Robertson and Wride (1998) begins by assigning a stress exponent equals to 1.0 to calculate Q and, therefore, an initial value of I_C. If $I_C > 2.6$, it should be assumed that $q_{c1N} = Q$. However, if $I_C \leq 2.6$, the exponent to calculate Q should be assumed as 0.5 and I_C should be recalculated based on q_{c1N} and F. If the recalculated I_C remains less than 2.6, it should be used the q_{c1N} based on the stress exponent of 0.5 to estimate CRR, otherwise, a stress exponent of 0.75 should be used to calculate q_{c1N} and then, estimate CRR – Robertson and Wride (1998). This

complex process of normalization can be better understood by consulting the flowchart that illustrates the method of evaluating CRR proposed by this approach. The flowchart is represented on Figure 16.

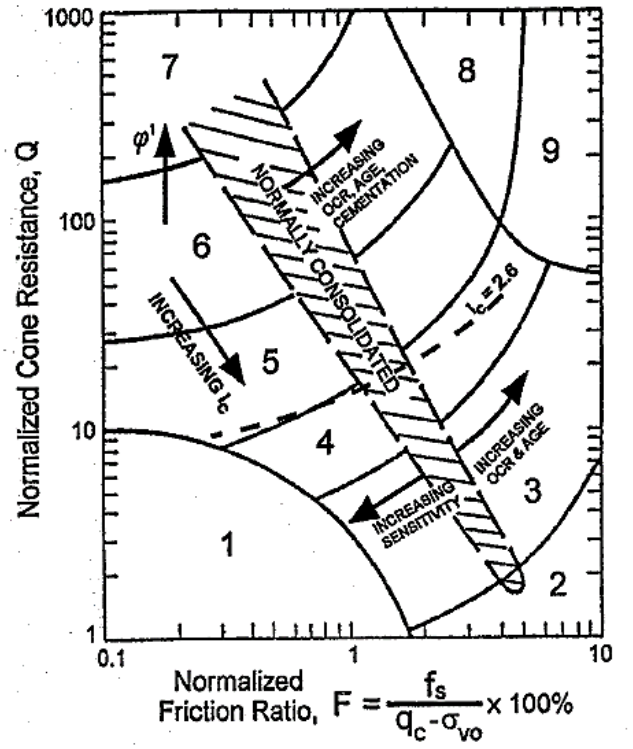

Figure 14- Normalized CPT soil behaviour chart type (Robertson, 1990)

It is now possible to estimate the K_C from the latter I_C values resultant from the process of normalization of the tip resistance. K_C can be estimated from the following expressions:

$$K_C = -0.403 \times I_C{}^4 + 5.581 \times I_C{}^3 - 21.63 \times I_C{}^2 + 33.75 \times I_C - 17.88 \quad \text{if } 2.6 > I_C > 1.64 \tag{20}$$

$$K_C = 1.0 \quad \text{if } I_C < 1.64 \tag{21}$$

$$K_C = 1.0 \quad \text{if } 1.64 < I_C < 2.36 \text{ and } F < 0.5\% \tag{22}$$

In depths where the I_C is greater than 2.6, the soil must be considered as non-liquefiable. However, if at the same time F is lower than 1%, the soil can be very sensitive and possibly susceptible to cyclic liquefaction. Hence, it should be used other criteria to assess liquefaction triggering. If the soil has an I_C value between 1.64 and 2.36 and F lower than 0.5%, it must be assumed that it is a clean sand and set K_C to a value of 1. This assumption is made to avoid the confusion between very loose clean sands and denser sands containing fines – Robertson and Wride (1998). The grain characteristic correction to obtain clean sand equivalent penetration resistance is obtained by the curve presented on Figure 15.

To assess the liquefaction potential of a soil is required the CRR for the design earthquake magnitude. Once this method provides a CRR for an equivalent magnitude of 7.5 it is needed to perform a correction

through the MSF. There are several approaches for an MSF expression, this method suggests the implementation of an MSF expression presented in the NCEER workshop of 1997 and in Youd et al. (2001), defined as:

$$MSF = \frac{10^{2.24}}{M^{2.56}} \tag{23}$$

With the MSF and the $CRR_{7.5}$ calculated, applying equation (11) it is possible to obtain the CRR values for each depth. The next step of this assessment is to compare the CRR with the CSR to obtain the factor of safety. The equation (2) provides the FS.

After the liquefaction potential of the soil is calculated it should be carried out a settlement assessment. Some of the methods available in the literature to estimate settlements are presented in chapter 2.4.

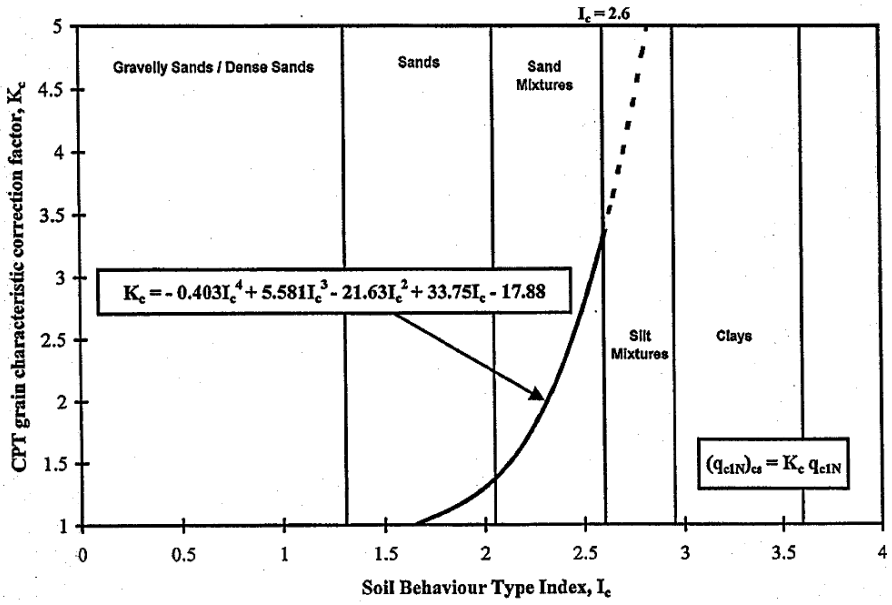

Figure 15- Recommended grain characteristic correction to obtain clean sand equivalent CPT penetration resistance in sandy soils (Robertson and Wride, 1998)

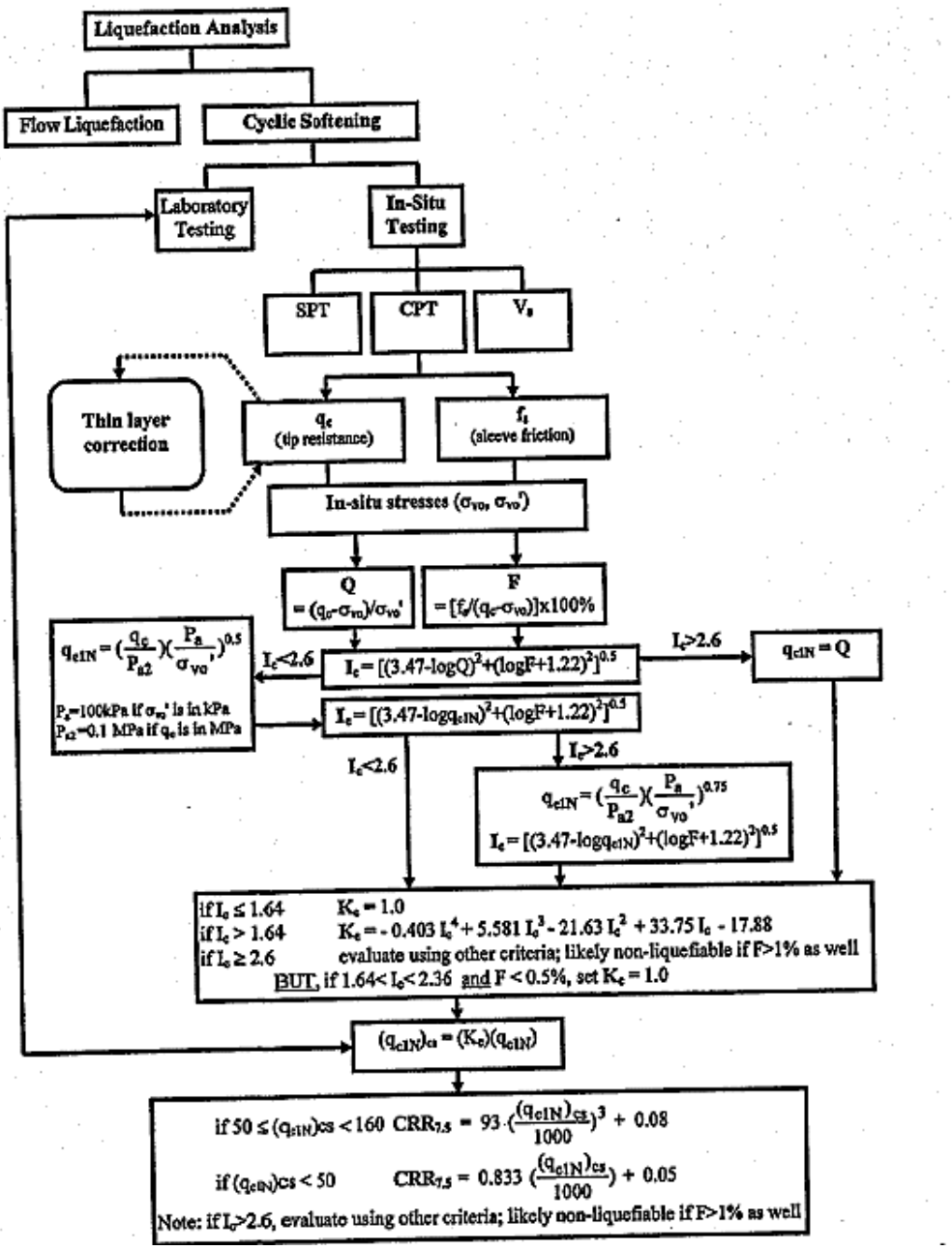

Figure 16- Flowchart illustrating the calculation of the cyclic resistance ratio (Robertson and Wride, 1998)

2.2.1.2. Robertson (2009)

This method developed by Robertson arrives as an update of the previous CPT based procedure proposed by Robertson and Wride (1998). One of the differences between them is related with a new stress normalization, where this latter method adopts a stress exponent that captures the change in soil response with increasing overburden stress – Robertson (2009). The inclusion of a transition region related with the I_C values to embody a smoother shift between cohesionless and cohesive soils, and a more appropriate interpretation of the soil type is also implemented within this method, with a new recommendation to K_C when I_C values fall between 2.5 and 2.7. But the most important update presented in this method is the cyclic softening estimation for clay-like soils, combining the Robertson and Wride

(1998) approach for cohesionless sand-like soils with the Boulanger and Idriss (2007) recommendations for cohesive clay-like soils – Robertson (2009).

The new stress exponent proposed by Robertson (2008) and implemented herein intents to capture the correct state response for soils at high stress level and to avoid further stress level correction in liquefaction analysis – Robertson (2009). It is defined by:

$$n = 0.381 \times I_C + 0.05 \times \frac{\sigma'_{v0}}{P_a} - 0.15 \tag{24}$$

This expression has a threshold value of 1.0, and its implementation requires an iterative process, starting with an initial stress exponent of 1.0. The iterative process comes as a result of both n and I_C being dependent on each other. The stopping criteria is defined by a difference between successive stress exponent values below 0.01.

The K_C expressions proposed by Robertson and Wride (1998), presented on equations (20) to (22) are complemented by a new proposal for the transition region ($2.5 < I_C < 2.7$). The introduced K_C expression to be added to the previous K_C recommendations from Robertson and Wride (1998) is defined by:

$$K_C = 6 \times 10^{-7} \times I_C^{16.76} \qquad \text{if } 2.5 < I_C < 2.7 \tag{25}$$

As well as cohesionless soils, clay-like soils can also develop excess pore pressures during undrained cyclic loading, but generally they never reach zero effective stress, causing them to retain some stiffness and hence deform less than sand-like soils. The criteria used to define the CRR in clay-like soils is deformation, assuming a shear strain $\gamma = 3\%$ - Robertson (2009). The $CRR_{7.5}$ recommendation for clay-like soils ($I_C > 2.7$) presented on equation (26) is additional to $CRR_{7.5}$ recommendations of Robertson and Wride (1998) given by equations (12) and (13).

$$CRR_{7.5} = 0.053 \times Q_{tn} \times K_\alpha \qquad \text{if } I_C > 2.7 \tag{26}$$

Where Q_{tn} represents the normalized cone resistance corrected by a variable stress exponent, which represents the same as the term q_{c1N} used in Robertson and Wride (1998). K_α is a reduction factor based on the static shear stresses at the time of the earthquake, suggested by Boulanger and Idriss (2004). For level ground conditions, $K_\alpha = 1.0$.

A chart based on the soil behaviour type was developed to be used as a guide for choice of engineering procedures to help identifying zones of potential cyclic softening – Robertson (2009). The soils in regions A_1 and A_2 are both cohesionless and to evaluate their liquefaction potential, CPT based correlations can be used. Soils within this zones are susceptible to cyclic liquefaction, and the soils in region A_2 are also susceptible to strength loss, once they are looser. Zones B and C are characterized by representing cohesive clay-like soils. They are both susceptible to cyclic softening and soils in zone C may suffer strength loss once they are more sensitive. The chart proposed is presented in Figure 17.

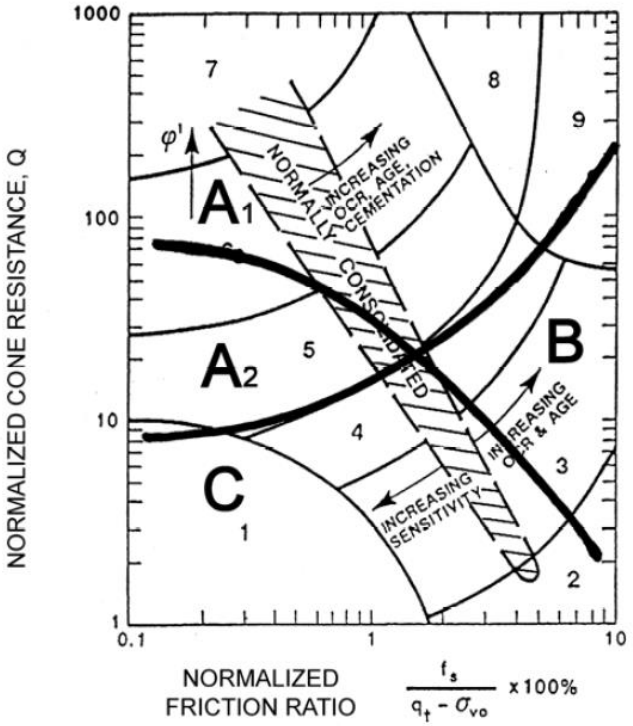

Figure 17- CPT Soil Behaviour Type chart for liquefaction and cyclic softening (Robertson, 2009)

The parameters presented within this section will be added or replace the proposed by Robertson and Wride (1998), once the proposal of Robertson (2009) represents an update of the former procedure. The remaining parameters will be estimated by following Robertson and Wride (1998) recommendations. Some modifications were implemented on the symbols convention, with the normalized tip resistance, normalized friction ratio, correction factor for overburden stress and the equivalent clean sand normalized tip resistance being now defined as Q_{tn}, F_r, C_N and $Q_{tn,cs}$, respectively.

A flowchart presenting the calculation sequence proposed by Robertson (2009) and detailed above is presented in Figure 18:

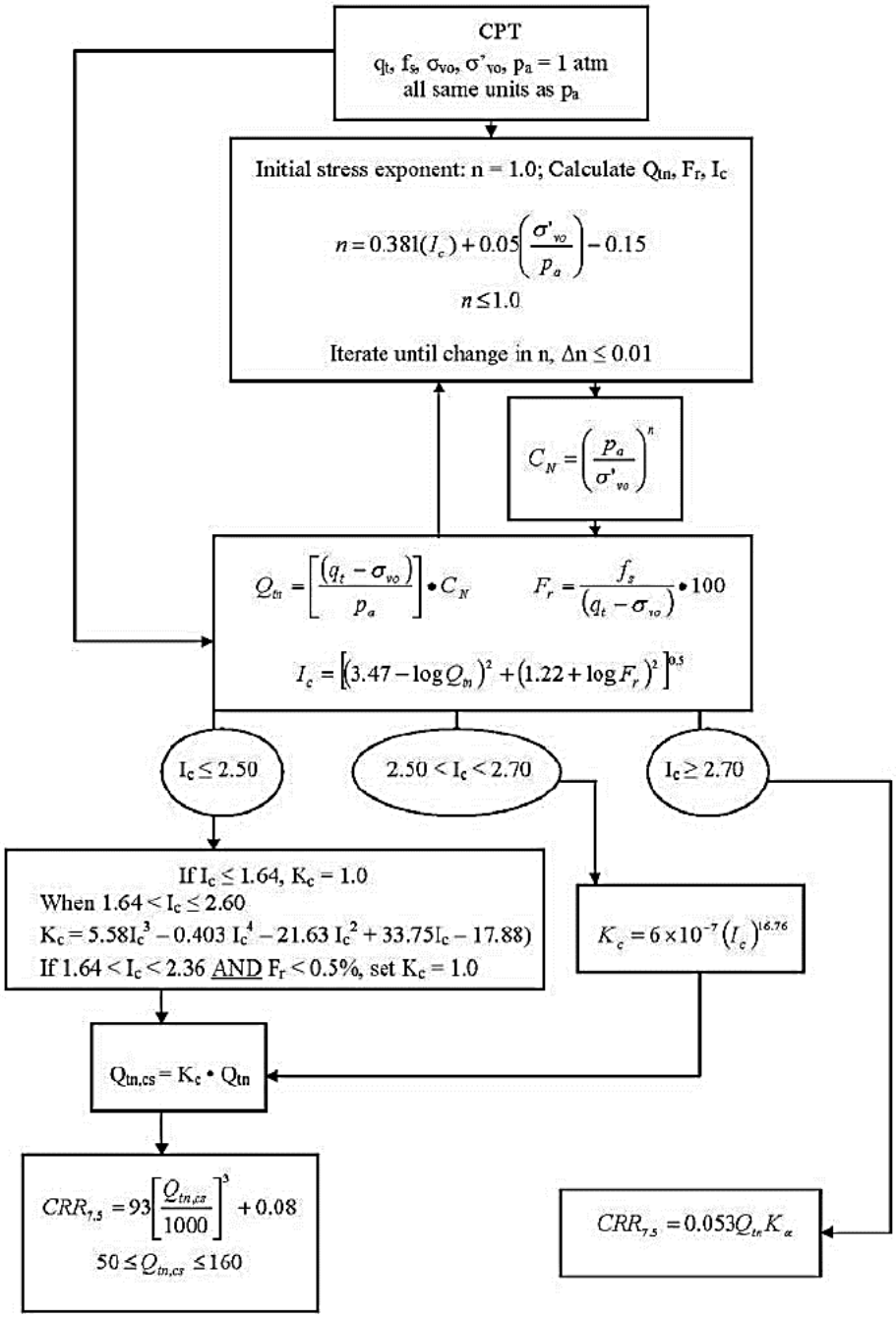

Figure 18- Flowchart illustrating the calculation of CRR (after Robertson, 2009)

2.2.2. PROBABILISTIC APPROACH

The probabilistic approaches to calculate the cyclic resistance of a soil, based on CPT test results, consider the uncertainties inherent to the parameters and express the liquefaction potential in terms of the probability of liquefaction – Juang et al. (2013). Two of the most implemented methods are the Moss et al. (2006) and the Boulanger and Idriss (2014) and they will be object of a further analysis.

2.2.2.1. Moss et al. (2006)

In this study, the threshold of liquefaction triggering usually located deterministically by engineering judgment, is implemented using engineering statistics, Bayesian updating and reliability methods – Moss et al. (2006). The seismic loading is characterized by the cyclic stress ratio proposed by Seed and Idriss (1971) and presented in this thesis in equation (10). The factor that accounts for nonlinear ground response of the soil, r_d, follows the Cetin (2000) approach and it is defined by:

$$r_d = \frac{1+\frac{-9.147-4.173\times a_{\max}+0.652\times M_W}{10.567+0.089\times e^{0.089\times(-d\times 3.28-7.76\times a_{\max}+78.576)}}}{1+\frac{-9.147-4.173\times a_{\max}+0.652\times M_W}{10.567+0.089\times e^{0.089\times(-7.76\times a_{\max}+78.576)}}} \qquad \text{if } d < 20\,\text{m} \tag{27}$$

$$r_d = \frac{1+\frac{-9.147-4.173\times a_{\max}+0.652\times M_W}{10.567+0.089\times e^{0.089\times(-d\times 3.28-7.76\times a_{\max}+78.576)}}}{1+\frac{-9.147-4.173\times a_{\max}+0.652\times M_W}{10.567+0.089\times e^{0.089\times(-7.76\times a_{\max}+78.576)}}} - 0.0014\times(d\times 3.28-65) \qquad \text{if } d \geq 20\,\text{m} \tag{28}$$

Where d is the depth in meters, M_W the magnitude and a_{max} the peak ground acceleration, PGA, in units of gravity.

This approach for r_d was specifically implemented for this CPT correlation, since previous r_d recommendations were not compatible with the one proposed by this paper.

This study proposes the correction of the equivalent uniform CSR to represent this ratio for a typical duration of an earthquake with a magnitude of 7.5, CSR*. The factor of correction is represented as a duration weighting factor, DWF_M and it depends on the specific M_W. The approach for DWF_M used in this study is the proposed by Cetin et al. (2004) and defined by:

$$DWF_M = 17.84\times M_W^{-1.43} \tag{29}$$

This approach is only valid for magnitudes between 5.5 and 8.5.

The CRR calculation stands, as in other methods, in the parameters obtained from the CPT test, the tip resistance, q_c and the sleeve friction, f_s. As the effective overburden stress can influence these measurements – Olsen and Mitchell (1995), it is required to perform a normalization of the tip resistance and the vertical effective stress to a reference pressure of 1 atm. The normalized tip resistance, $q_{c,1}$ is defined as:

$$q_{c,1} = C_q \times q_c \tag{30}$$

The tip normalization factor, C_q, is defined by:

$$C_q = \left(\frac{P_a}{\sigma'_v} \right)^c \tag{31}$$

Where P_a is the reference pressure, 1 atm, σ'_v is the effective stress and c is the normalization exponent, defined by:

$$c = f_1 \times \left(\frac{R_f}{f_3} \right)^{f_2} \tag{32}$$

Where:

$$\begin{aligned} f_1 &= 0.78 \times q_c{}^{-0.33} \\ f_2 &= -\left(-0.32 \times q_c{}^{-0.35} + 0.49 \right) \\ f_3 &= abs\left[\log\left(10 + q_c\right) \right]^{1.21} \\ R_f &= \frac{f_s}{q_c} \end{aligned} \tag{33}$$

As in other CPT based approaches, the process of deriving the normalization exponent is iterative. The recommended procedure in this study is to start the iterative process by calculating the normalization exponent based on the raw measurements from the CPT, then following the entire process and repeating it until an acceptable convergence tolerance is obtained. The tip normalization factor, C_q, should not exceed a value of 1.7.

A modification in the normalized tip resistance accounting for the effect of the fine content is also presented, and is defined by:

$$q_{c,1,\mathrm{mod}} = q_{c,1} + \Delta q_c \tag{34}$$

Where the fines adjustment factor, Δq_c, can be defined by:

$$\Delta q_c = 0.38 \times R_f - 0.19 \times \ln\left(CSR\right) + 1.46 \times R_f - 0.73 \tag{35}$$

This expression is valid for R_f values between 0.5 and 5.0. For values of R_f below 0.5, Δq_c is equal to 0.

The last step is then to estimate the probability of liquefaction based on the parameters calculated previously, and the CRR. In this approach, the CRR is calculated for a given probability of liquefaction and it is relative to the specific earthquake magnitude.

$$P_L = \Phi\left\{-\frac{\left[q_{c,1}{}^{1.045} + q_{c,1}\times(0.110\times R_f)+(0.001\times R_f)+c\times(1+0.850\times R_f)-7.177\times\ln(CSR)-0.848\times\ln(MW)-0.002\times\ln(\sigma'_v)-20.923\right]}{1.632}\right\} \quad (36)$$

Where ϕ (P_L) is the cumulative normal distribution. CRR is defined by:

$$CRR = \exp\left\{\frac{\left[q_{c,1}{}^{1.045} + q_{c,1}\times(0.110\times R_f)+(0.001\times R_f)+c\times(1+0.850\times R_f)-0.848\times\ln(M_W)-0.002\times\ln(\sigma'_v)-20.923+1.632\times\Phi^{-1}(P_L)\right]}{7.177}\right\} \quad (37)$$

Where ϕ^{-1} (P_L) is the inverse cumulative normal distribution.

It was developed a plot, presented in Figure 19 with different thresholds of liquefaction for different probabilities of liquefaction and it correlates the CSR for a magnitude of 7.5 with the fines normalized CPT tip resistance, $q_{c,\,1,\,mod}$.

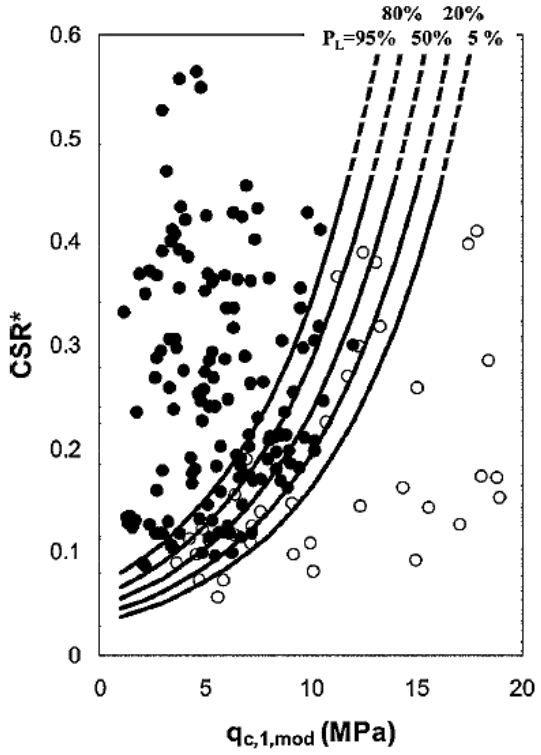

Figure 19 - Contours of 5, 20, 50, 80 and 95% probability of liquefaction triggering as function of CSR* and qc,1,mod. Close circles are liquefied case histories and open circles are non-liquefied case histories (Moss et al., 2006)

The major differences in the outcome of this approach when compared to previous CPT based procedures is related with the evaluation of liquefaction for silts and sands with fine content. This study proposes a much smaller modification in the CPT tip resistance with an increase in the fine content than

the earlier relationships – Moss et al. (2006), as it can be seen in Figure 20. The comparison is made for a probability of liquefaction of 15%, once the curve proposed by Robertson and Wride (1998) is compatible with the PL=15% curve – Moss et al. (2006).

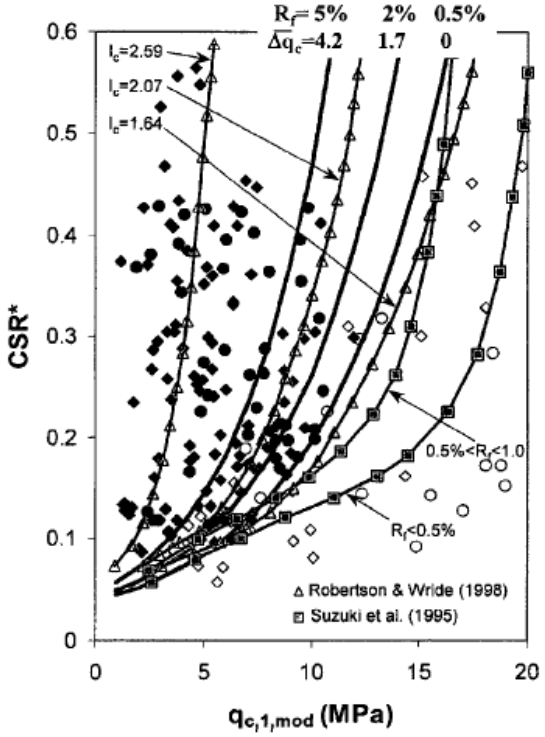

Figure 20- Comparison of fines adjusted curves for PL=15% with previous curves (Moss et al., 2006)

2.2.2.2. Boulanger and Idriss (2014)

Boulanger and Idriss (2014) proposed a CPT and a SPT based procedure for liquefaction triggering based on the previous work developed by Idriss and Boulanger (2008), although herein it will only be discussed the CPT-based procedure. This update presents a new approach for MSF and a procedure to estimate fines content (FC), as well as an updated database of CPT case histories, improved with the 2010-2011 Canterbury earthquake sequence in New Zealand and the 2011 Tohoku earthquake in Japan. The major update within this procedure is the development of a probabilistic version of the CPT-based liquefaction triggering procedure based on the updated database.

The cyclic loading is represented in terms of stress by the CSR. The approach for CSR used in this procedure is the same as the implemented in previous studies presented here, proposed by Seed and Idriss (1971) and presented in equation (10). The expression implemented herein to represent the shear stress reduction factor, r_d is proposed by Idriss (1999) and defined by:

$$r_d = \exp\left[\left(-1.012-1.126\times\sin\left(\frac{z}{11.73}+5.133\right)\right)+\left(0.106+0.118\times\sin\left(\frac{z}{11.28}+5.142\right)\times M\right)\right] \quad (38)$$

The cyclic resistance is also represented in terms of stress by the CRR, correlated with CPT resistances. As in other procedures, the raw tip resistance from the CPT must be normalized and corrected to account for overburden stresses and the proposed correction is defined by:

$$q_{c1N} = C_N \frac{q_c}{p_a} \tag{39}$$

Where q_c is the raw tip resistance from the CPT, P_a is the atmospheric pressure and C_N the overburden correction factor defined by:

$$C_N = \left(\frac{p_a}{\sigma'_v} \right)^m \leq 1.7 \tag{40}$$

Where m is the stress exponent, function of the normalized clean sand tip resistance, q_{c1Ncs}:

$$m = 1.338 - 0.249 \times (q_{c1Ncs})^{0.264} \tag{41}$$

As in others procedures, Boulanger and Idriss (2014) also impose a limitation of C_N to a maximum value of 1.7, once the expression was not validated for low effective stresses, and its implementation would produce large values of C_N within this range. The plot of C_N against the vertical effective stress normalized by the atmospheric pressure can be seen in Figure 21.

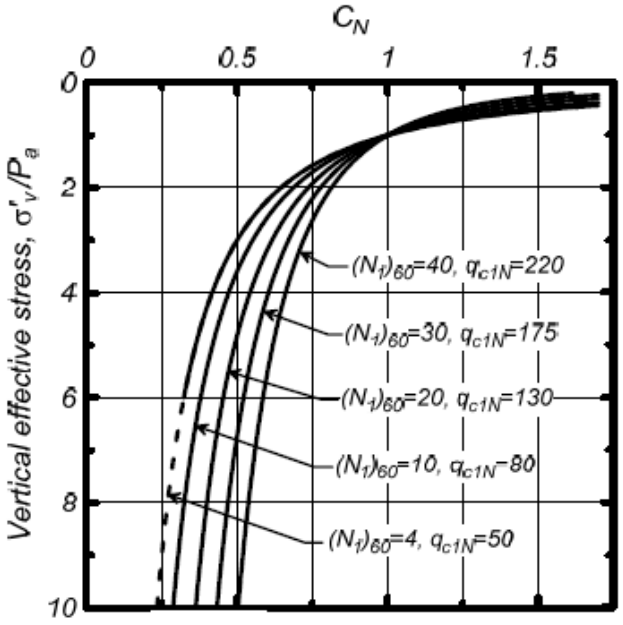

Figure 21- Correlation between the overburden correction factor (C_N) and the normalized vertical effective stress for different q_{c1Ncs} values (Boulanger and Idriss, 2014)

As the stress exponent, m, is function of q_{c1Ncs}, which in turn depends on q_{c1N}, this is an iterative process that should stop when an acceptable convergence is achieved. The relationship between q_{c1Ncs} and q_{c1N} is defined by:

$$q_{c1Ncs} = q_{c1N} + \Delta q_{c1N} \tag{42}$$

Where Δq_{c1N} is an equivalent clean sand adjustment, expressed as:

$$\Delta q_{c1N} = \left(11.9 + \frac{q_{c1N}}{14.6}\right) \times \exp\left(1.63 - \frac{9.7}{FC+2} - \left(\frac{15.7}{FC+2}\right)^2\right) \tag{43}$$

This expression was derived from liquefaction case history data, and accounts for the effects that fines content have on CRR and on CPT penetration resistance – Boulanger and Idriss (2014). The fines content is estimated based on the I_C, which is function of the data collected from the CPT test, and the proposed approach to estimate it, is the same recommended by Robertson and Wride (1998) and presented in equation (17). The developed relationship to estimate FC is defined by:

$$FC = 80 \times \left(I_C + C_{FC}\right) - 137 \tag{44}$$

Where C_{FC} is a fitting parameter that can be adjusted based the specific data available and accounts for the uncertainties in the relationship between FC and I_C and it varies from -0.29 to 0.29. According to Boulanger and Idriss (2014), when there is no soil sampling and lab testing data, and therefore the FC calculation is not reliable, a liquefaction assessment should be performed for C_{FC} values of -0.29, 0 and 0.29, to evaluate the sensitivity of CRR to FC.

With q_{c1Ncs} defined, $CRR_{7.5}$ can be estimated by:

$$CRR_{7.5} = \exp\left(\frac{q_{c1Ncs}}{113} + \left(\frac{q_{c1Ncs}}{1000}\right)^2 - \left(\frac{q_{c1Ncs}}{140}\right)^3 + \left(\frac{q_{c1Ncs}}{137}\right)^4 - 180\right) \quad (45)$$

As CRR is being estimated for a magnitude of 7.5, it must be applied an MSF to account for duration effects and to enable the correlation between cyclic resistance and cyclic loading. The proposed MSF is based on MSF and q_{c1Ncs} values, as it can be seen in Figure 22, and its expression, developed by Boulanger and Idriss (2014), is:

$$MSF = 1 + (MSF_{\max} - 1) \times \left(8.64 \times \exp\left(-\frac{M_W}{4}\right) - 1.325\right) \quad (46)$$

With MSF_{max} defined in function of q_{c1Ncs} as:

$$MSF_{\max} = 1.09 + \left(\frac{q_{c1Ncs}}{180}\right)^3 \leq 2.2 \quad (47)$$

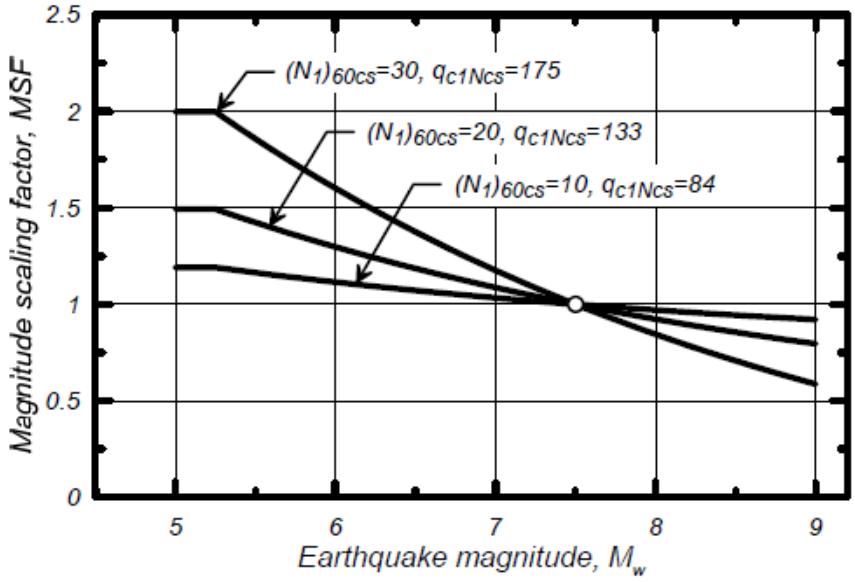

Figure 22- MSF estimation based on q_{c1Ncs} and earthquake magnitude values (Boulanger and Idriss, 2014)

The $CRR_{7.5}$ must be also affected by an overburden correction factor, K_σ, function of the relative density of the soil and its initial stress state. The relationship used in this study was developed by Boulanger (2003) and it is based on laboratory estimations of the relative state parameter index. Idriss and Boulanger (2008) recommended the calculation of K_σ based on the values of q_{c1Ncs} as:

$$K_\sigma = 1 - C_\sigma \times \ln\left(\frac{\sigma'_v}{P_a}\right) \leq 1.1 \tag{48}$$

The limit of 1.1 imposed to K_σ mitigates the uncertainties in the applicability of the expression above for low effective stresses. C_σ can be defined as:

$$C_\sigma = \frac{1}{37.3 - 8.27 \times q_{c1Ncs}^{0.264}} \leq 0.3 \tag{49}$$

The CRR for the design earthquake magnitude, can then be defined as:

$$CRR = CRR_{7.5} \times MSF \times K_\sigma \tag{50}$$

As in other procedures the factor of safety against liquefaction is obtained by estimating the ratio of CRR to CSR.

A probabilistic version of this procedure was also developed to consider the model uncertainties and it is based on sensitivity studies and likelihood analysis. The proposed $CRR_{7.5}$ expression can be defined as:

$$CRR_{7.5} = \exp\left(\frac{q_{c1Ncs}}{113} + \left(\frac{q_{c1Ncs}}{1000}\right)^2 - \left(\frac{q_{c1Ncs}}{140}\right)^3 + \left(\frac{q_{c1Ncs}}{137}\right)^4 - C_0 + \sigma_{\ln(R)} \times \Phi^{-1}(P_L)\right) \quad (51)$$

Where C_0 and $\sigma_{\ln(R)}$ represent respectively a fitting parameter that serves to scale the relationship while maintaining its shape – Boulanger and Idriss (2014), and the standard deviation of the total error associated to CRR calculation. Values of $C_0 = 2.60$ and $\sigma_{\ln(R)} = 0.20$ are recommended to implement in practice as they are considered reasonable. Φ^{-1} is the inverse of the standard cumulative normal distribution and P_L the probability of liquefaction, which can be defined as:

$$P_L = \Phi\left[-\frac{\exp\left(\frac{q_{c1Ncs}}{113} + \left(\frac{q_{c1Ncs}}{1000}\right)^2 - \left(\frac{q_{c1Ncs}}{140}\right)^3 + \left(\frac{q_{c1Ncs}}{137}\right)^4 - C_0 - \ln(CSR_{7.5})\right)}{\sigma_{\ln(R)}}\right] \quad (52)$$

Where ϕ is the standard cumulative normal distribution and $CSR_{7.5}$ is the CSR calculated for 15 cycles and an equivalent magnitude of 7.5, and it is estimated by affecting the CSR by the inverse of the MSF.

This probabilistic relationship only considers the model uncertainties and a liquefaction analysis must include parameters uncertainties related to the cyclic loading characterization and the q_{c1Ncs} values, that must be accounted for in previous stages of the liquefaction assessment. The recommended triggering curves for different probabilities of liquefaction values are presented in Figure 23. The deterministic liquefaction triggering correlation presented in equation (45) represents a probability of liquefaction of 16% - Boulanger and Idriss (2014).

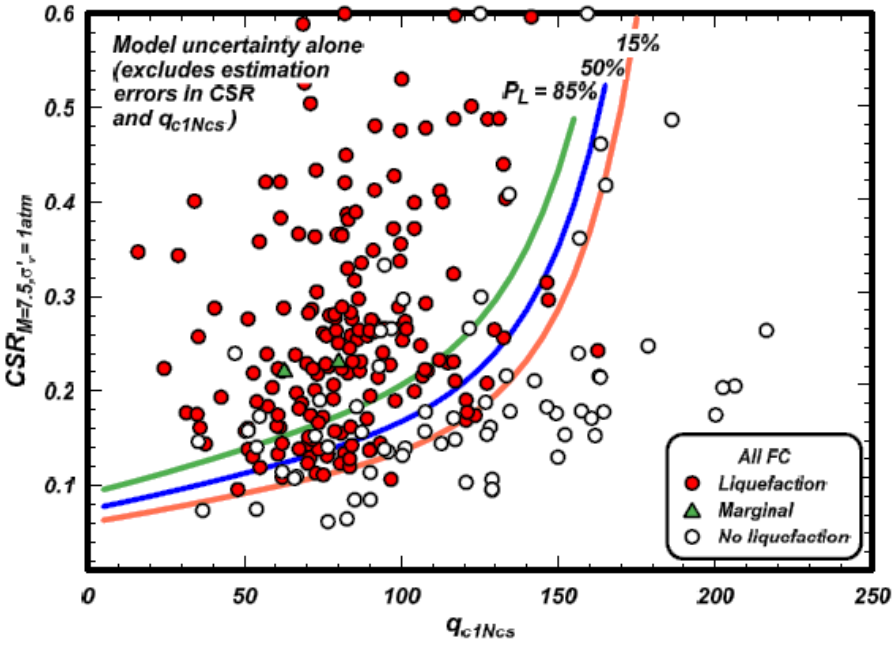

Figure 23- Liquefaction triggering curves for probabilities of liquefaction of 15%, 50% and 85% for all sands (Boulanger and Idriss, 2014)

2.2.2.3. Ku et al. (2011) – Probabilistic version of Robertson and Wride (1998)

The probabilistic model proposed by Ku et al. is considered an extension of Robertson and Wride (1998) and its recent Robertson (2009) update, since it is based on the factor of safety values provided by these two methods. Although there are several probabilistic models for evaluating the liquefaction probability as the presented above, since the Robertson and Wride (1998) is the most widely used CPT-based method, it was considered valuable to develop a probabilistic method based on it, that estimates the probability of liquefaction based on the factor of safety provided by Robertson and Wride (1998) with little extra effort – Ku et al. (2011).

This model somehow completes the deterministic Robertson and Wride (1998) and Robertson (2009), since in some situations it might be desirable to express the liquefaction potential in terms of a probability, rather than just the factor of safety – Ku et al. (2011).

The purpose of this method is then to develop a correlation between P_L and FS, based on a database with case histories taken from Robertson (2009), Moss et al. (2009) and Moss et al. (2011), and using the principle of maximum likelihood and the modelling error of the factor of safety. The probabilistic function comes as:

$$P_L = 1 - \Phi\left(\frac{0.102 + \ln(FS)}{0.276}\right) \tag{53}$$

Where Φ is the standard normal cumulative distribution function, with a mean of 0 and a standard deviation of 1, and FS is the factor of safety computed by Robertson and Wride (1998) or Robertson (2009).

It is noticed that FS=1.0 produces P_L=0.356, meaning that the deterministic Robertson and Wride (1998) can be considered as a conservative method. If it is implemented the minimum factor of safety against liquefaction of 1.2 recommended by the Building Seismic Safety Council (1997), the probability of liquefaction will be less than 15%, which is the same probability adopted by Moss et al. (2006) as a basis for deriving its deterministic curve, so it can be considered that this probabilistic version provides accurate results and consistent with the state of practice – Ku et al. (2011).

The plot of equation (53) is presented on Figure 24:

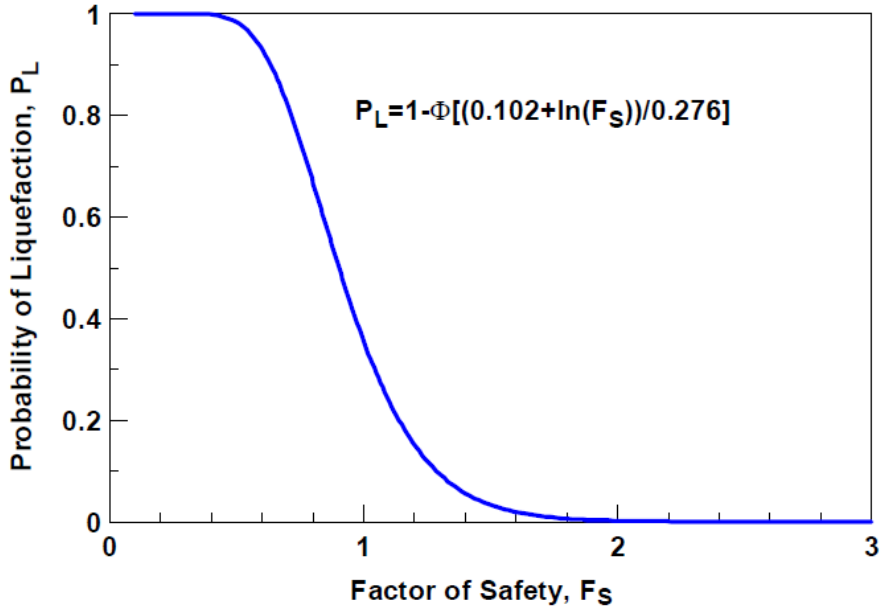

Figure 24- Correlation between Probability of Liquefaction and the Factor of Safety provided by Robertson and Wride (1998) (Ku et al., 2011)

2.3. LIQUEFACTION POTENTIAL INDEX

Proposed by Iwasaki et al. (1978), Liquefaction Potential Index, LPI, was developed to estimate the liquefaction potential capable to cause damage on foundations – Rodrigues et al. (2014). In the development of this parameter, it was considered that liquefaction susceptibility of a specific soil column is proportional to the thickness of the liquefiable layer, to the distance between ground surface and the liquefiable layer, and to the factor of safety against liquefaction. Only liquefiable soils (FS < 1) have contribution for this parameter, and an analysis at depths greater than 20 m is considered irrelevant.

Unlikely the simplified procedure proposed by Seed and Idriss (1971) that performs a liquefaction evaluation for each depth independently, LPI allows to execute an evaluation for the whole soil column and assess the consequences that a possible liquefaction triggering may produce at the ground surface – Rodrigues et al. (2014). LPI is defined by:

$$LPI = \int_0^{20} F \times w(z).dz \tag{54}$$

Where:

$$\begin{aligned} F &= 1 - FS && \text{if } FS \le 1 \\ F &= 0 && \text{if } FS > 1 \\ w(z) &= 10 - 0.5 \times z \end{aligned} \tag{55}$$

According to the estimated LPI values, Iwasaki et al. (1982) produced a table that related LPI with the risk of liquefaction triggering, updated by Luna and Frost (1998). Both approaches are presented in the table below.

Table 2-Characterization of liquefaction severity based on LPI values (after Iwasaki et al., 1982, and Luna and Frost, 1998)

LPI	Iwasaki et al. (1982)	Luna and Frost (1998)
LPI = 0	Very Low	Little or None
0 < LPI ≤ 5	Low	Minor
5 < LPI ≤ 15	High	Moderate
LPI > 15	Very High	Major

2.4. CPT BASED LIQUEFACTION INDUCED GROUND SETTLEMENTS ESTIMATION

Soils with sand-like behaviours have tendency to densify when submitted to a cyclic load, inducing settlements at the ground surface. There are differences in the estimation of dry sand and saturated sand settlements, once the former occur very quickly and the latter require the dissipation of the pore pressures generated with the cyclic loading to take place. The methods presented herein are based on the calculation of volumetric strains, what in the framework of this thesis correspond to vertical strains, once liquefaction assessment is made on sites with level ground conditions. Experience has shown that there is a reasonable agreement between the procedures results and the values obtained on field.

2.4.1. SATURATED SOILS SETTLEMENTS

The magnitude of the densification of saturated sands is influenced by the density of the soil, the maximum shear strain induced and the amount of excess pore pressure generated with the cyclic loading – Kramer (1996). The first approaches for the estimation of vertical strains were SPT based, such as Tokimatsu and Seed (1987) and Ishihara and Yoshimine (1992), although the latter also allows a correlation between vertical strains and CPT tip resistance. In the scope of this thesis, the procedures that will be discussed and later implemented in the Mathcad tool are the Zhang et al. (2002) and the Juang et al. (2013).

2.4.1.1. Zhang et al. (2002)

This CPT based approach estimates liquefaction induced ground settlements for level ground conditions, which makes reasonable the assumption that no lateral displacement occurs due to earthquake loading

and by that, the volumetric strain will be equal or close to the vertical strain – Zhang et al. (2002). By integrating the vertical strain in each soil layer in depth, it is obtained the ground settlement at the CPT location induced by liquefaction occurrence. The expression that allows the settlement calculation is defined by:

$$S = \sum_{i=1}^{j} \varepsilon_{vi} \times \Delta z_i \tag{56}$$

Where ε_{vi} and Δz_i are respectively the vertical strain and the thickness of the soil layer i, and j is the number of soil layers. The proposed method to estimate the vertical strain is based on Ishihara and Yoshimine (1992), which presented a set of curves based on laboratory test results on clean sand that correlated the factor of safety against liquefaction FS and the relative density D_r with the postliquefaction volumetric strain ε_v. These curves are presented in Figure 25. To estimate vertical strain based on CPT, this method proposes the use of an equivalent clean sand tip resistance $(q_{c1N})_{cs}$ first defined by Robertson and Wride (1998) to account for the effect of grain characteristics or fine content on CPT soundings – Zhang et al. (2002). The correlations between $(q_{c1N})_{cs}$ and ε_v for different values of FS that were developed based on Ishiara and Yoshimine (1992) are presented in Figure 26.

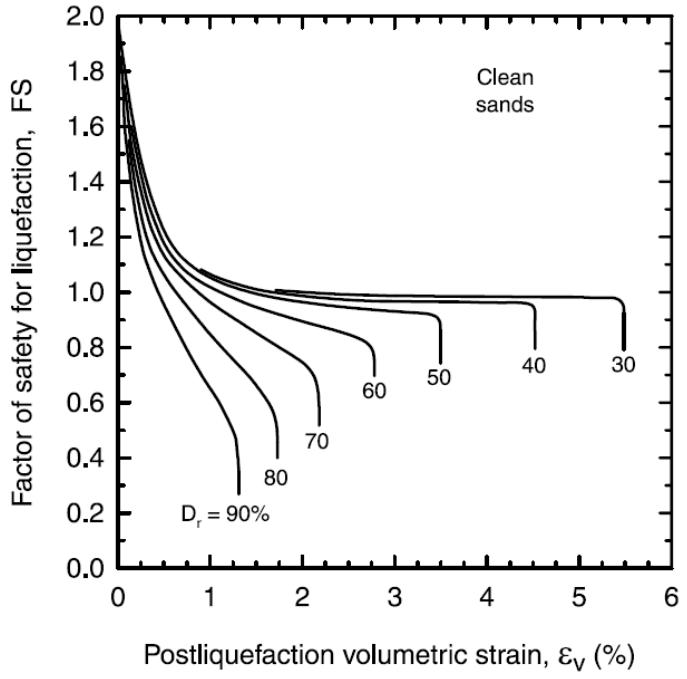

Figure 25- Estimation of postliquefaction volumetric strain of clean sands (modified from Ishihara and Yoshimine, 1992)

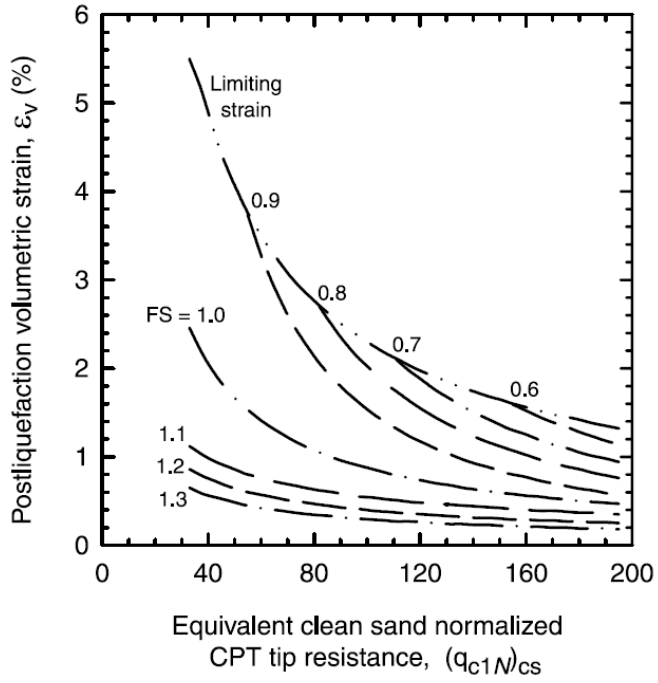

Figure 26- Correlation between postliquefaction volumetric strain and equivalent clean sand tip resistance for different factors of safety (Zhang et al., 2002)

The expressions that define the set of curves presented on Figure 26 are:

$$
\begin{aligned}
&\text{if } FS \le 0.5, && \varepsilon_v = 102 \times (q_{c1N})_{cs}^{-0.82} && \text{for } 33 \le (q_{c1N})_{cs} \le 200 \\
&\text{if } FS = 0.6, && \varepsilon_v = 102 \times (q_{c1N})_{cs}^{-0.82} && \text{for } 33 \le (q_{c1N})_{cs} \le 147 \\
&\text{if } FS = 0.6, && \varepsilon_v = 2411 \times (q_{c1N})_{cs}^{-1.45} && \text{for } 147 \le (q_{c1N})_{cs} \le 200 \\
&\text{if } FS = 0.7, && \varepsilon_v = 102 \times (q_{c1N})_{cs}^{-0.82} && \text{for } 33 \le (q_{c1N})_{cs} \le 110 \\
&\text{if } FS = 0.7, && \varepsilon_v = 1701 \times (q_{c1N})_{cs}^{-1.42} && \text{for } 110 \le (q_{c1N})_{cs} \le 200 \\
&\text{if } FS = 0.8, && \varepsilon_v = 102 \times (q_{c1N})_{cs}^{-0.82} && \text{for } 33 \le (q_{c1N})_{cs} \le 80 \\
&\text{if } FS = 0.8, && \varepsilon_v = 1690 \times (q_{c1N})_{cs}^{-1.46} && \text{for } 80 \le (q_{c1N})_{cs} \le 200 \\
&\text{if } FS = 0.9, && \varepsilon_v = 102 \times (q_{c1N})_{cs}^{-0.82} && \text{for } 33 \le (q_{c1N})_{cs} \le 60 \\
&\text{if } FS = 0.9, && \varepsilon_v = 1430 \times (q_{c1N})_{cs}^{-1.48} && \text{for } 60 \le (q_{c1N})_{cs} \le 200 \\
&\text{if } FS = 1.0, && \varepsilon_v = 64 \times (q_{c1N})_{cs}^{-0.82} && \text{for } 33 \le (q_{c1N})_{cs} \le 200 \\
&\text{if } FS = 1.1, && \varepsilon_v = 11 \times (q_{c1N})_{cs}^{-0.65} && \text{for } 33 \le (q_{c1N})_{cs} \le 200 \\
&\text{if } FS = 1.2, && \varepsilon_v = 9.7 \times (q_{c1N})_{cs}^{-0.69} && \text{for } 33 \le (q_{c1N})_{cs} \le 200 \\
&\text{if } FS = 1.3, && \varepsilon_v = 7.6 \times (q_{c1N})_{cs}^{-0.71} && \text{for } 33 \le (q_{c1N})_{cs} \le 200 \\
&\text{if } FS = 2.0, && \varepsilon_v = 0 && \text{for } 33 \le (q_{c1N})_{cs} \le 200
\end{aligned}
\qquad (57)
$$

This proposed methodology for the estimation of liquefaction induced ground settlements was validated with the Marina District and Treasure Island case histories from the 1989 Loma Prieta earthquake and it demonstrated good agreement between calculated and measured settlements.

2.4.1.2. Juang et al. (2013)

This procedure presents an evaluation of liquefaction-induced settlement using the CPT, and allows the estimation of the probability of exceeding a specified settlement at a given site. The estimation of liquefaction-induced settlements represents an important parameter in a liquefaction assessment, since it is of greater concern than the likelihood of liquefaction occurrence – Juang et al. (2013).

This procedure is based on the Zhang et al. (2002) deterministic model, presented in the previous subchapter, and it adopts a probabilistic approach using the concept of liquefaction probability and the maximum likelihood principles to develop a model based on a database of case studies – Juang et al. (2013). It should be noted that the deterministic procedures for estimate liquefaction-induced settlements are more suitable for assessments on free-field sites. To estimate the settlements at a site with high building loading, it should be performed a soil-structure analysis. Dashti et al. (2010) states that liquefaction-induced building settlement is dependent on the soil-structure interaction and on the ground motion. Based on centrifuge tests, it was concluded that liquefaction-induced building settlements were greater than free-field settlements.

The expression to estimate settlements is based on Zhang et al. (2002), presented in equation (56), with a modification based on the studies of Ueng et al. (2010) that stated that earthquake-induced settlement was mainly caused by liquefied soil, whereas the soil layer that did not liquefy had a small contribution in the settlement. The modified expression is then defined as:

$$S_p = \sum_{i=1}^{N} \varepsilon_{vi} \times \Delta_{zi} \times IND_i \tag{58}$$

Where the added parameter IND represents an indicator of liquefaction occurrence, equal to 0 if the i^{th} layer does not liquefy and equal to one otherwise. This parameter is related with the probability of liquefaction of the considered layer. Thus, the mean of the predicted settlement, S_p, can be defined as:

$$\mu_p = \sum_{i=1}^{N} \varepsilon_{vi} \times \Delta_{zi} \times P_{Li} \tag{59}$$

And the variance of S_p:

$$\sigma_p^2 = \sum_{i=1}^{N} \varepsilon_{vi}^2 \times \Delta_{zi}^2 \times P_{Li} \times \left(1 - P_{Li}\right) \tag{60}$$

Where the probability of liquefaction, P_L, can be given by the Ku et al. (2011) procedure presented in chapter 2.2.2.3. and equation (53).

Assuming that the model presented for S_p, equation (58), has limitations, it is required to obtain its error, characterized by a multiplicative model bias factor, M. Thus it can be obtained the actual settlement, S_a, based on M and S_p, by implementing:

$$S_a = M \times S_p \tag{61}$$

The model M was calibrated in this study using a database of case histories.

The mean and variance of S_a can be obtained based on the mean and variance of the parameters on that it depends:

$$\mu_a = \mu_M \times \mu_p \tag{62}$$

$$\sigma_a^2 = \mu_M^2 \times \sigma_p^2 + \mu_p^2 \times \sigma_M^2 + \sigma_M^2 \times \sigma_p^2 \tag{63}$$

Where μ_M and σ_M are respectively the mean and standard deviation of M and derived from a database of case histories. These parameters were optimized by using the principle of maximum likelihood and from 64 cases obtained from the 1989 Loma Prieta, the 1999 Kocaeli and the 1999 Chi-Chi earthquakes, divided in two types, according to the type of settlements. Type A for liquefaction-induced free field settlement and type B for liquefaction-induced building settlement. The parameters are presented inTable 3:

Table 3- Statistical parameters obtained to characterize the model bias M (after Juang et al., 2013)

	Type A (free-field settlement)	Type B (building settlement)
μ_M	1.2488	1.6583
δ_M	0.5331	0.7839

Where $\delta_M = \sigma_M / \mu_M$. An analysis to the values obtained reveals that the uncertainties associated with the estimation of liquefaction-induced building settlements are expressed in the type B, with greater values of mean and variation than type A.

With these parameters obtained, the probability of exceeding a specified settlement, s, can be expressed as:

$$P(S_a > s) = 1 - \Phi\left(\frac{\ln(s) - \ln\left(\frac{\mu_a}{\sqrt{1+\delta_a^2}}\right)}{\sqrt{\ln\left(1+\delta_a^2\right)}}\right) \quad (64)$$

Where ϕ is the standard normal cumulative distribution function, and $\delta_a = \sigma_a / \mu_a$. By repeating the calculation of the probabilities of exceedance for a number of settlement values, a plot of probability, $P(S_a > s)$ versus settlement, s, can be made, presenting a probabilistic liquefaction-induced settlement hazard curve – Juang et al. (2013). A curve based on a case history from the 1989 Loma Prieta earthquake was made in the scope of the Juang et al. procedure and it is presented on the figure below:

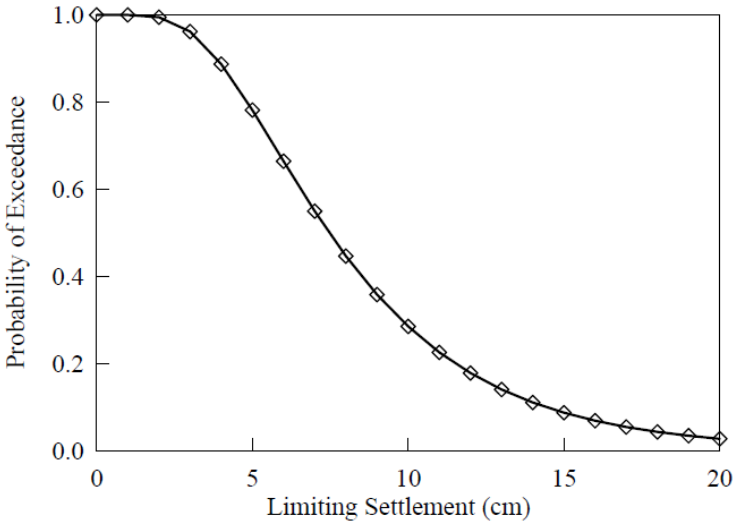

Figure 27- Probabilistic liquefaction-induced settlement hazard curve for a case history at the Marina District after the 1989 Loma Prieta earthquake (Juang et al., 2013)

2.4.2. Dry Soils Settlements

Based on Silver and Seed (1971) which suggested that the settlement of dry sands is function of its relative density, the amplitude and the number of cycles of the cyclic shear strain, Seed and Silver (1972) presented a procedure to evaluate settlements in dry sands, induced by earthquake events. Pradel (1998) proposed a simplified approach of Seed and Silver (1972), based on SPT results and only applicable to clean sands. In the scope of this thesis, the method discussed and implemented to estimate the settlements of dry soils is the Robertson and Shao (2010) which presents a modification of Pradel (1998), in order to base the settlements estimation on CPT and to extend its applicability to a wide range of unsaturated soils.

As mentioned above, this procedure presents a modification of the Pradel (1998) approach, by basing its methodology on the CPT and extending the settlement estimation to a wider range of dry soils. The procedure of this method starts by obtaining the cyclic shear stress τ_{av}, based on Seed and Idriss (1971)

method, and presented in equation (10). The following step is to determine the small strain shear modulus, estimated from the CPT, by implementing:

$$G_0 = 0.0188 \times 10^{0.55 \times I_C + 1.68} \times (q_t - \sigma_{v0}) \tag{65}$$

Where q_t is the tip resistance measured from the CPT, I_C is the soil behaviour type index and σ_{v0} is the total in-situ stress. After obtaining the small strain shear modulus, it calculates the cyclic shear strain, based on the ratio between the average shear stress and the small strain shear modulus. This relationship was proposed by Pradel (1998):

$$\gamma = \left(\frac{1 + a \times e^{b \times R}}{1 + a} \right) \times R \times 100 \tag{66}$$

Where R is the ratio between τ_{av} and G_0, and *a* and *b* are soil-type dependant parameters defined by:

$$\begin{aligned} a &= 0.0389 \times \left(\frac{p}{p_a} \right) + 0.124 \\ b &= 6400 \times \left(\frac{p}{p_a} \right)^{-0.6} \\ p &= \frac{1}{3}(1 + 2 \times K_0) \times \sigma_{v0} \end{aligned} \tag{67}$$

Where p is dependent of the total initial vertical stress and K_0, the ratio between the vertical and horizontal initial effective stresses.

Having the cyclic shear strain, it can be obtained the volumetric strain after 15 cycles, $\varepsilon_{vol(15)}$. The expression was proposed by Pradel (1998) after Silver and Seed (1971) and Tokimatsu and Seed (1987), it is based on normalized SPT penetration resistance in clean sands, $(N_1)_{60,cs}$, and it is defined by:

$$\varepsilon_{vol(15)} = \gamma \times \left[\frac{(N_1)_{60,cs}}{20} \right]^{-1.20} \tag{68}$$

As this method is based on CPT penetration resistance, it uses a modified correlation between SPT and CPT penetration resistance proposed by Lunne et al. (1997):

$$(N_1)_{60,cs} = \frac{Q_{tn,cs}}{8.5 \times \left(1 - \frac{I_C}{4.6}\right)} \tag{69}$$

Where $Q_{tn,cs}$ is the normalized tip resistance for clean sand, determined by Robertson and Wride (1998) and presented here in equation (14).

Proposed by Pradel (1998), the volumetric strain, ε_{vol}, is given by:

$$\varepsilon_{vol} = \varepsilon_{vol(15)} \times \left(\frac{N_C}{15}\right)^{0.45} \tag{70}$$

Where N_C is the equivalent number of cycles for a dynamic loading with a specific magnitude M, and it is defined by:

$$N_C = (M - 4)^{2.17} \tag{71}$$

By integrating the volumetric strain in depth, the vertical settlement due to the seismic event can be obtained as it is seen in equation (72). The settlement is obtained after the modified Pradel (1998) and the volumetric strain is doubled to consider the multidirectional nature of earthquake shaking – Pyke et al. (1975).

$$S = 2 \times \int_0^{GWT} \varepsilon_{vol}.dz \tag{72}$$

This method was evaluated at a site where were adopted vibro-compacted stone columns and compaction grouting to mitigate seismic settlements and presented great effectiveness.

2.5. Design Codes Approach for Liquefaction Assessment

Design codes require liquefaction assessment as an element in the project of some structures for earthquake resistance. They specify the cases in which liquefaction assessment is required and the procedures to assess it. In this thesis the design codes discussed are the Part 5 of the Eurocode 8: Design of structures for earthquake resistance, and the AASHTO Guide for LRFD Seismic Bridge Design.

2.5.1. AASHTO Guide for LRFD Seismic Bridge Design

This guide of specifications was published in 2009 to cover seismic design for bridges in the United States of America. It establishes four seismic design categories, based on the design earthquake response

spectral acceleration coefficient at 1.0-sec period, S_{D1}. This value shall be obtained from the national ground motion maps, provided by the U.S. Geological Survey, and the categories are presented on Table 4.

Table 4- Partitions for Seismic Design Categories (AASHTO Guide Specifications for LRFD Seismic Bridge Design, 2009)

S_{D1}	Seismic Design Category
$S_{D1} < 0.15$	A
$0.15 \leq S_{D1} < 0.30$	B
$0.30 \leq S_{D1} < 0.50$	C
$0.50 \leq S_{D1}$	D

According to this guide, liquefaction assessment is required for categories C and D if both of the following conditions are presented:

- The groundwater level is less than 50 ft. (about 15 m) deep;
- Soils less than 75 ft. (about 23 m) deep are characterized by one of the following conditions:
  - $(N_1)_{60} \leq 25$ blows/ft. in sand and nonplastic silt layers;
  - $q_{c1N} \leq 150$ in sand and nonplastic silt layers;
  - Normalized shear wave velocity, $V_{S1} < 660$ fps (about 200 m/s);
  - It was observed liquefaction at the site in past earthquakes.

When liquefaction of loose to very loose saturated sands can impact the stability of a structure at a site within category B, a liquefaction assessment shall also be performed.

According to the guide, there is not a prevailing or a required method to assess liquefaction. It predicts the use of empirically-based to complex numerical methods and even cyclic simple shear or cyclic triaxial tests can be performed to assess liquefaction susceptibility of soils.

The determination of the magnitude for the design earthquake parameters shall be made based on the earthquake data for the site, available at the USGS national seismic hazard website.

The guide proposes the implementation of Boulanger and Idriss (2006) and Bray and Sancio (2006) to assess the susceptibility of soils to liquefaction, since there is no consensus on the preferred criteria, and either method can be used based on the designer's preferences. The first method considers a soil non susceptible to liquefaction if PI $\geq$7, and the latter method states that a soil is susceptible to liquefaction if PI <12 and the ratio between the water content and the liquid limit is greater than 0.85 (w_c/LL > 0.85). This method is discussed with further detail on section 2.1.3.

As a guide for seismic bridge design, it also accounts for the effects of liquefaction on bridge response as well as the differences on the designing whether liquefaction occurs or not, but as it is out of the scope of this thesis, it will not be discussed in here.

2.5.2. EUROCODE 8: DESIGN OF STRUCTURES FOR EARTHQUAKE RESISTANCE – PART 5: FOUNDATIONS, RETAINING STRUCTURES AND GEOTECHNICAL ASPECTS. BRITISH STANDARD

Eurocode 8 is a European standard for the design of structures for earthquake resistance, and in its part 5 are presented the technical specifications required in liquefaction assessment. A set of conditions for which liquefaction assessment should be performed are presented in this standard, as well as the procedures required to implement it.

Following the Eurocode specifications, a liquefaction susceptibility evaluation shall be made if the foundation soils include extended layers or thick lenses of loose sand beneath the water table, and if the water table is close to the ground surface. This evaluation shall be performed for free-field site conditions prevailing during the lifetime of the structure. To perform liquefaction evaluation, the standard requires the execution of either SPTs or CPTs, as well as a laboratory determination of grain size distribution curves.

The standard also specifies the cases in which liquefaction evaluation may not be required:

- When saturated sandy soils are found at depths greater than 15 m from the surface;
- When PGA $\leq$ 0.15g and at least one of the following conditions is fulfilled:
  - The soils have a clay content greater than 20% with PI >10;
  - The soils have a silt content greater than 35% and $(N_1)_{60}$ >20;
  - The soils are clean sands with $(N_1)_{60}$ >20.

If liquefaction evaluation is required, it should be performed by correlating in situ measurements and a critical shear stress, here referred as CRR. A soil is considered to be susceptible to liquefaction whenever the earthquake-induced shear stress, CSR, exceeds a certain fraction λ of the CRR. The recommended value for λ is 0.8 which implies a factor of safety FS=1.25.

To obtain CRR, the standard proposes the implementation of empirical charts presented in Annex B of Eurocode 8 – Part 5, which correlate in situ measurements with CRR. Following the specification, charts can be based on SPT blowcount or on CPT resistance, although the Eurocode only presents a chart based on SPT resistance for different fine content and for an earthquake magnitude of 7.5. The proposed chart is presented in Figure 28.

CSR is obtained by implementing Seed and Idriss (1971) approach, presented in equation (10).

To obtain a CRR for different earthquake magnitudes rather than 7.5, a magnitude scaling factor, MSF should be applied. The proposed MSF values for different magnitudes are presented in Table 5.

Table 5- Magnitude scaling factors proposed by Eurocode 8 - Part 5

Magnitude, M	MSF EC8-Part 5
5.5	2.86
6.0	2.20
6.5	1.69
7.0	1.30

7.5	1.00
8.0	0.67

The standard also states that this assessment can only be performed for level ground conditions. To other ground conditions, more complex procedures should be implemented.

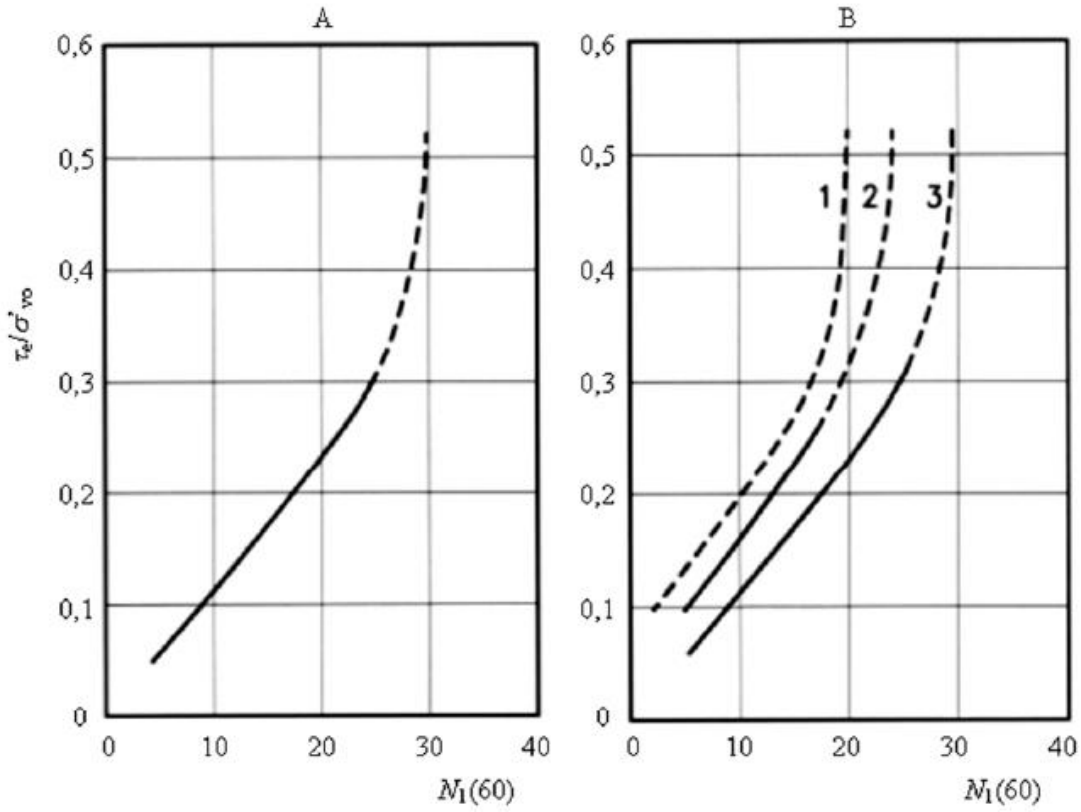

Figure 28 - Relationship between the stress ratio for M=7.5 earthquakes and $N_{1(60)}$ values for (A) - clean sands and (B) - silty sands with 1. 35% fines; 2. 15% fines; 3. <5% fines

3

IMPLEMENTATION OF A CPT BASED MATHCAD TOOL TO ASSESS LIQUEFACTION TRIGGERING

3.1. CAPABILITIES OF MATHCAD

Mathcad is an engineering calculation software owned by PTC and developed by Allen Razdow from the MIT and co-founder of MathSoft. It is mainly used to verify, validate and properly present engineering calculations in a friendly and ease-of-use worksheet, providing capability of manipulating the input values, which allows an easily recalculation of the worksheet. Mathcad allows the combination of mathematical expressions, text, graphs and images in a readable worksheet which makes this software product a valuable platform in the communication between clients and companies. The ability of applying and checking engineering units of the variables is indeed one of its greatest capabilities, once it prevents improper operations that could induce an error in the output. In the scope of this thesis the tool created to assess liquefaction triggering was developed on Mathcad 15.0, due to the capabilities presented above and the company procedures.

3.2. DEVELOPMENT OF THE TOOL

As CH2M is responsible for the design of several projects that require a liquefaction assessment of soils, there was a need to validate the commercial software products used to this purpose, as they operate with little transparency and flexibility, and use some superseded techniques. Therefore, the aim of this in-house tool is to validate them by understanding their capabilities and limitations, allowing user control over the calculation parameters and offering the transparency required in project designing.

After performing the literature review presented on chapter 2, it was concluded that due to its continuity and accuracy alongside with the great results performed and the strong implementation in soil testing, the liquefaction assessment and consequently the estimation of settlements performed by the tool should be based on CPT test results.

3.2.1. CALCULATION SEQUENCE OF THE DEVELOPED TOOL

Liquefaction assessment is based on the calculation and study of some defined indicators, in this case, the selected indicators are:

- Factor of Safety, FS;
- Probability of Liquefaction, P_L;
- Liquefaction Potential Index, LPI;
- Saturated Soil Settlement, S_s;
- Dry Soil Settlement, S_d.

Once selected the parameters in which the liquefaction assessment will be grounded, the objective of the tool is to attain them, based on the input data required for their calculation that can be divided in three categories:

- CPT Profile and Soil Parameters;
- Groundwater Depths;
- Seismic Parameters.

The implemented procedure to obtain the selected liquefaction indicators is represented in the Figure 29 flowchart and each step of the calculation sequence presented on the flowchart is exposed below, as well as the implemented methods to obtain them.

The developed Mathcad spreadsheet that performs the calculations and presents the outputs is presented on Appendix.

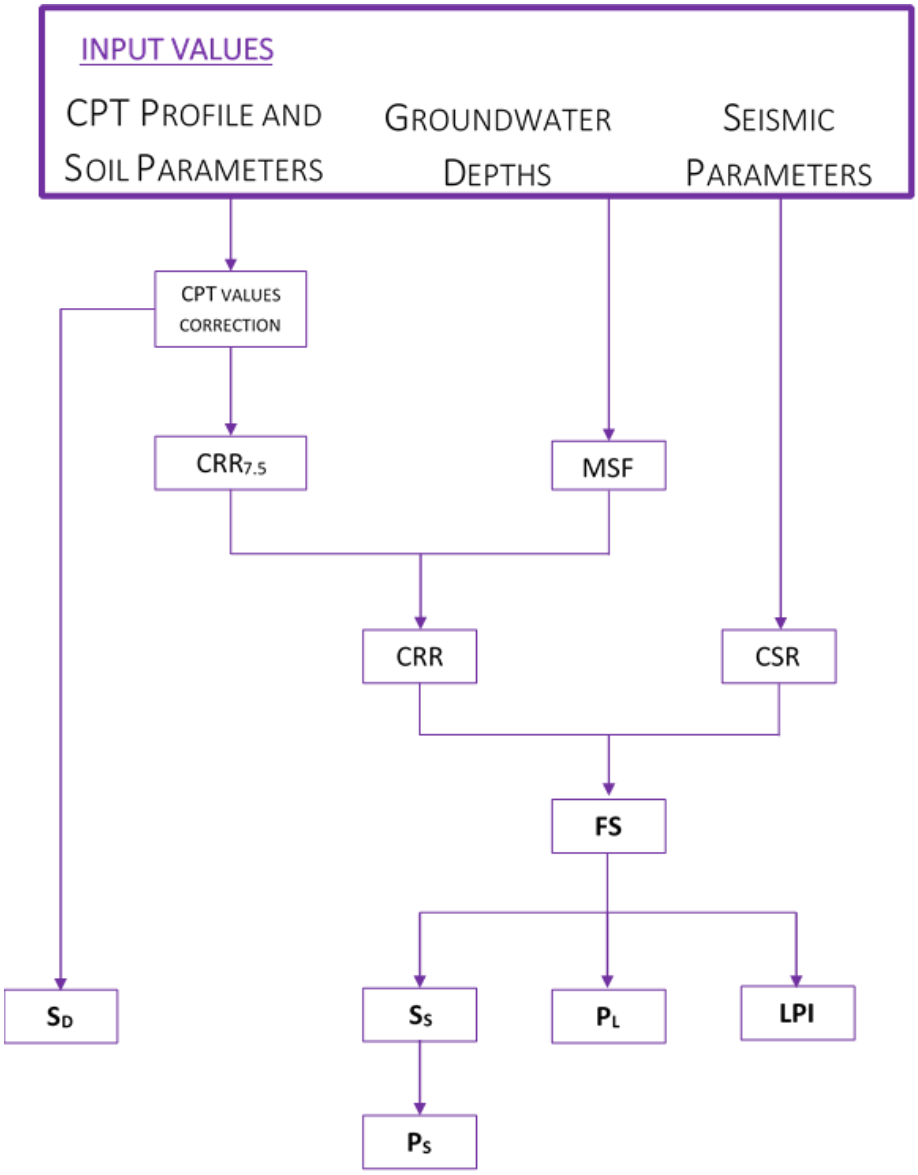

Figure 29- Calculation sequence performed by the developed tool

3.2.1.1. CPT Profile and Soil Parameters

The data input from the selected CPT is imported directly in Mathcad from an Excel file, with the attention of the user to define the range of data to be read by the tool. The correspondence between the parameters and the data columns from the Excel file is already defined, as well as the units, although both items can be easily changed. The default unit for both CPT measurements is MPa and the first three columns correspond to depth, tip resistance and sleeve friction, respectively. Other input parameters are introduced by the user directly in the tool, within the input area.

The data provided by the CPT tests and the soil unit weight, γ_s, are the basis of any liquefaction assessment, as the procedures available on the literature are grounded on these parameters. The parameters measured by the CPT are the tip resistance, q_c, the sleeve resistance, f_s and it is also possible

to measure the pore pressure, u, if it is used a piezocone, CPTU, and seismic wave velocities, V_S, if it is used a seismic CPT with geophones and accelerometers incorporated, SCPT. In the framework of this thesis, the liquefaction assessment will be only based on q_c and f_s values. The pore pressures measured will not be considered herein, thus the influence of the excess pore pressure generated with the CPT test is neglected. Since a liquefaction assessment is mainly performed for sandy soils, where the dissipation of pore pressures occurs in an easier way, this assumption is made in order to simplify the procedure and it does not bring inaccurate results. Summarily, the parameters considered from the CPT log are:

- Tip resistance, q_c;
- Sleeve resistance, f_s.

The soil unit weight can be estimated from laboratory testing or it can be assumed a value for the whole profile, although the latter approach provides less accuracy on the results. Also, it is possible to estimate the soil unit weight from the CPT data by implementing the following relationship proposed by Robertson and Cabal (2010):

$$\frac{\gamma}{\gamma_w} = 0.27 \times \log\left(R_f\right) + 0.36 \times \log\left(\frac{q_t}{p_a}\right) + 1.236 \tag{73}$$

Where γ_w is the water unit weight; q_t can be assumed as the raw tip resistance from the CPT, q_c, since this assumption is valid for sandy soils; p_a the atmospheric pressure and R_f is the friction ratio of f_s to q_c in percentage.

As this tool is based in CPT test results, it is assumed that the estimation of the soil unit weight by laboratory tests is not feasible, so to obtain the soil unit weight the adopted procedures were:

- Assumption of a single soil unit weight value for the whole profile;
- Estimation of the soil unit weight by implementing Robertson and Cabal (2010) approach presented above.

The input parameters to consider within this category are:

- CPT data: q_c and f_s;
- Unit Weight, γ_s: (may be estimated from CPT data if required).

In Figure 30 it is possible to see part of the input section of the tool.

3.2.1.2. Groundwater Depths

In the developed tool, as well as in some other software products, the calculation of CRR and CSR is based on different water levels. For the CRR calculation it is assumed the same water level value measured during the in-situ test, whereas the CSR calculation is grounded on the water level during the earthquake. The latter water level parameter can be obtained by event specific groundwater elevation measurements if the liquefaction assessment is performed as a back analysis, or by consulting monitoring based maps of the median water table if a forward analysis is performed. In short, the groundwater levels to consider and required for the procedure are:

- CRR calculation: Water level measured during the CPT test;
- CSR calculation: Water level during the earthquake event.

These two water levels that are required for the calculation need to be inserted by the user within the input field, thus the input parameters to consider in this category are:

- Water level measured during the CPT test (referred in the tool as WTi);
- Water level during the earthquake event (referred in the tool as WTe).

Part of the input area of the tool is represented in Figure 30.

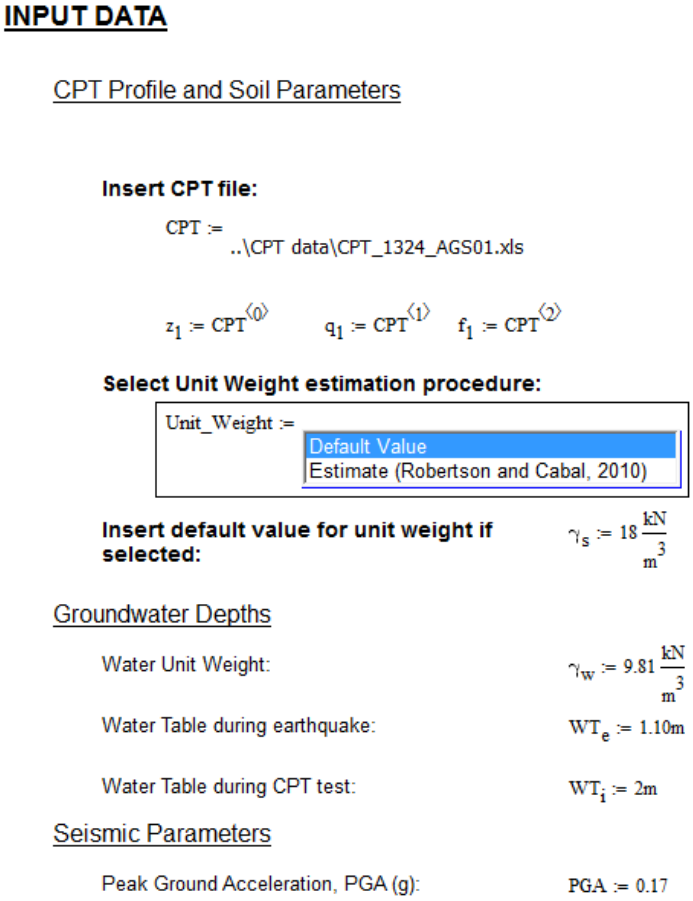

Figure 30- Part of the input area within the Mathcad tool

3.2.1.3. Seismic Parameters

The characterization of the cyclic loading and the consideration of the duration effects of the earthquake, require parameters from the seismic event, such as the peak ground acceleration, PGA, and the magnitude, M. The procedure to estimate these values is similar to the adopted in the groundwater depths estimation, if the assessment represents a back analysis, both parameters are estimated from the recordings of the strong motion stations near the site. In short, the values required to input in the tool are:

- Peak Ground Acceleration, PGA;
- Magnitude, M.

Figure 30 presents part of the seismic parameters input within the Mathcad tool.

3.2.1.4. CPT Values Correction

CPT log provides in some cases negative or null values of q_c and f_s. There are several conditions that can cause this issue, from measurements that can record negative values due to a zero drift of the cone in very soft soils or an insufficient sensor resolution – Ramsey (2010), but also due to temperature differences between the cone and the soil, in soft soils, once that temperature may have some effect on CPT readings, mainly on tip resistance – Kim et al. (2010). If that is noticed, it is required a correction of those values due to mathematical issues in following steps of the calculation procedure that include logarithmic functions. The solution adopted to outcome this issue, was the replacement of the negative values for a very low value, in this case the value implemented was 0.01 kPa to f_s and 0.01 MPa to q_c, to allow performing the mathematical operations without decreasing the accuracy of the results. This assumption was based on the CLiq (liquefaction analysis software presented and discussed in chapter 5) feature that allows to correct negative or null values.

3.2.1.5. $CRR_{7.5}$

The following step on the procedure is the characterization of the cyclic resistance of the soil through the CRR. The procedures presented and discussed in chapter 2.2. propose a CRR calculation for an equivalent earthquake loading magnitude of 7.5, $CRR_{7.5}$, with a posterior correlation with the design earthquake loading magnitude through a magnitude scaling factor, MSF.

The literature review carried out in the first stage of this thesis and presented in chapter 2 aimed at identifying the best method to implement in the developed tool. As one of the most widely used CPT-based liquefaction assessment procedures in the engineering practice is the Robertson and Wride (1998) and its updated Robertson (2009) version – Ku et al. (2011); as it is the recommended procedure on the Guide to Cone Penetration Testing for Geotechnical Engineering (Robertson and Cabal - 2015) to evaluate the triggering of cyclic liquefaction; the procedure implemented in the tool was the Robertson (2009), presented in section 2.2.1.2.

The calculation sequence implemented is presented on 2.2.1.2. and on the flowchart in Figure 29 with the following modifications to the original method:

- $CRR_{7.5}$ - $Q_{tn,cs}$ relationship is extended to $Q_{tn,cs}$ values of 200, slightly beyond the original limit of 160, to capture denser soils and larger earthquake loading;
- Adoption of a $CRR_{7.5}$ value of 4 for depths above the water table during the earthquake, WT_e, since the soil in that range is unsaturated, and therefore it will not liquefy;
- Implementation of a limit of 1.7 for the correction factor for overburden stress, C_N, referred in Robertson and Wride (1998) in chapter 2.2.1.1. as C_Q, presented on equation (16). This implementation is suggested by Youd et al. (2001) to outcome large values of this parameter at shallow depths, due to low overburden pressures.

The influence of the adjustment made in the $CRR_{7.5} - Q_{tn,cs}$ relationship, presented above, in the calculation is assessed on chapter 6 in a sensitivity analysis of the tool.

The modifications implemented in the tool are proposed by the commercial software product, CLiq, developed by Geologismiki in collaboration with Gregg Drilling Inc. and Professor Peter Robertson. The validation of this software product is presented and discussed on chapter 6.

One of the aims of the tool was to offer more transparency than the available software products and to allow user control over the methodology and the outputs, so, along the $CRR_{7.5}$ calculation procedure,

the plots of Q_{tn}, F_r, I_C and $Q_{tn,cs}$ in depth are provided, as well as the final $CRR_{7.5}$ result presented in Figure 31.

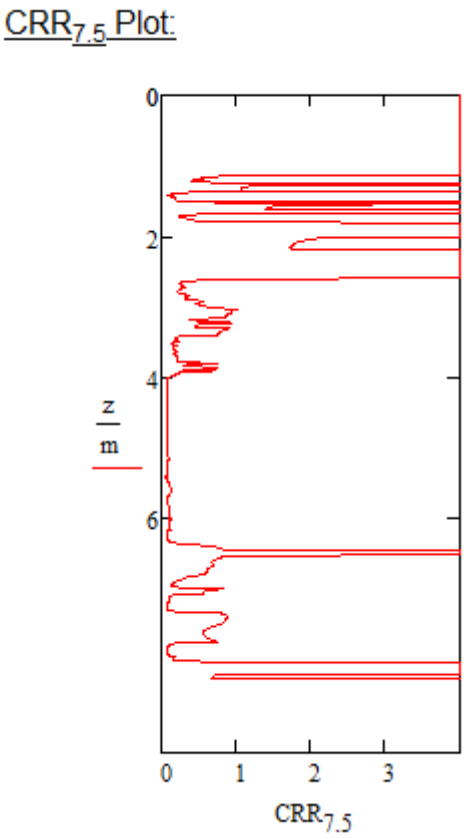

Figure 31- Example of a $CRR_{7.5}$ plot provided by the Mathcad tool.

3.2.1.6. Magnitude Scaling Factor, MSF

Once calculated the $CRR_{7.5}$, the following step is to account for the duration effects by implementing MSF. It is suggested that the MSF expression to implement be based on the selected method adopted for the estimation of the $CRR_{7.5}$. In this case, Robertson (2009) recommends the implementation of the MSF proposed by the NCEER and Youd et al. (2001) and presented here on equation (23).

The user is also allowed to select a different MSF expression, proposed by Idriss and Boulanger (2008) and presented in equation (46). The option for a different approach was implemented because this expression is considered to be more accurate, since it provides values based on the normalized clean sand tip resistance, although its implementation is more efficient if combined with the Boulanger and Idriss (2014) procedure.

3.2.1.7. CRR

The last step in the characterization of the cyclic resistance of the soil is the calculation of the CRR by combining the $CRR_{7.5}$ with the MSF, by implementing the equation (11). CRR plot is also provided alongside CSR plot as it shows Figure 32.

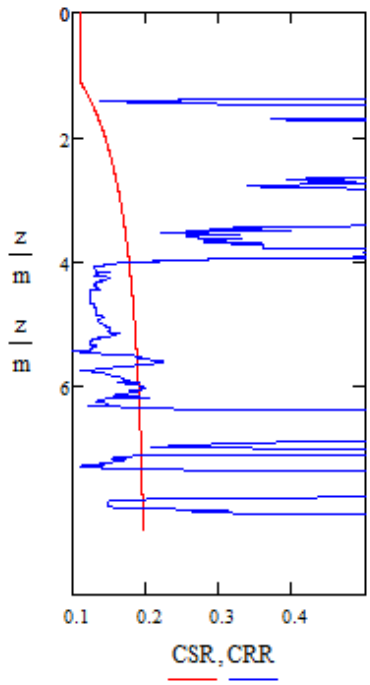

Figure 32- Example of a plot of CRR alongside with CSR provided by the tool.

3.2.1.8. CSR

The characterization of the cyclic loading in terms of stress is performed by implementing the procedure presented in chapter 2.1.4.1. developed by Seed and Idriss (1971) and recognized as an accurate method to define the seismic action. The implemented shear stress reduction factor, r_d, that accounts for the dynamic response of the soil in depth was proposed by Liao and Whitman (1986) and it is the approach recommended by the NCEER and Youd et al. (2001) and presented in equations (5) and (6). The expressions for r_d are suitable for use in engineering practice and, in the 1997 NCEER workshop, participants agreed that they are convenient for use in programming spreadsheets – Youd et al. (2001). Idriss and Boulanger (2008) also suggested a different approach for r_d, but it is associated with alternate values of CRR – Robertson and Cabal (2015), and hence it was not implemented. The plot of CSR is presented alongside with CRR in Figure 32.

3.2.1.9. Factor of Safety, FS

The selected method to evaluate liquefaction was the simplified procedure of Seed and Idriss (1971), that provides the factor of safety as a result of the ratio between CRR and CSR. The factor of safety against liquefaction is one indicator of liquefaction and a deterministic method to verify if liquefaction is triggered or not for each specific level of soil. In the depths where this parameter provides a value lower than 1, it is considered that liquefaction occurred or may occur, whereas if the value is greater than 1, the soil is non-liquefiable.

This parameter is estimated by comparing CRR with CSR through the expression defined in equation (2). The plot of FS is presented as it shows Figure 33.

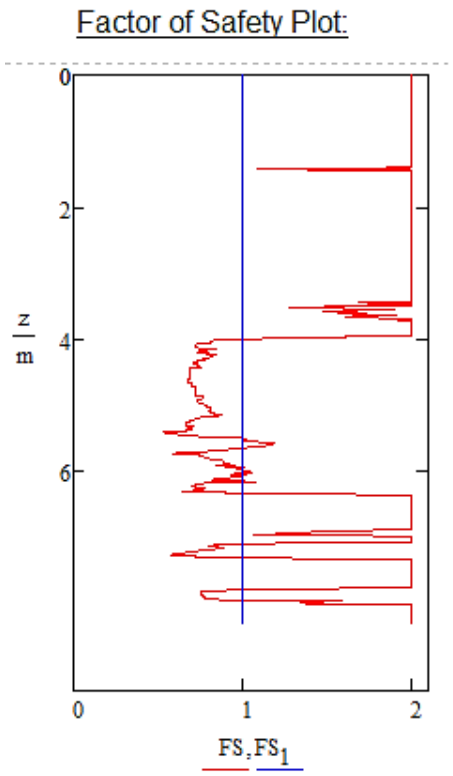

Figure 33- Example of a Factor of Safety plot provided by the tool.

3.2.1.10. Probability of Liquefaction, P_L

This parameter is obtained by implementing the Ku et al. (2011) approach presented in section 2.2.2.3. Although there are some other methods to estimate the probability of liquefaction that present accurate results, such as Boulanger and Idriss (2014) or Moss et al. (2006), they must be based on the deterministic expressions presented by these same methods, which were not implemented in the tool. Ku et al. (2011) present a simplified method to estimate P_L based on the Robertson and Wride (1998) and its Robertson (2009) update liquefaction triggering procedures, what makes it a valuable method to implement on the tool.

As the probability of liquefaction is one of the selected indicators of liquefaction and it represents a valuable method to assess this phenomenon, the tool provides this parameter in a plot, as presented in Figure 34, and its variation in depth.

PROBABILITY OF LIQUEFACTION *Ku et al. (2011)*

$$P_{L_j} := 1 - pnorm\left[\frac{\left(0.102 + \ln\left(FS_j\right)\right)}{0.276}, 0, 1\right]$$

Probability of Liquefaction Plot:

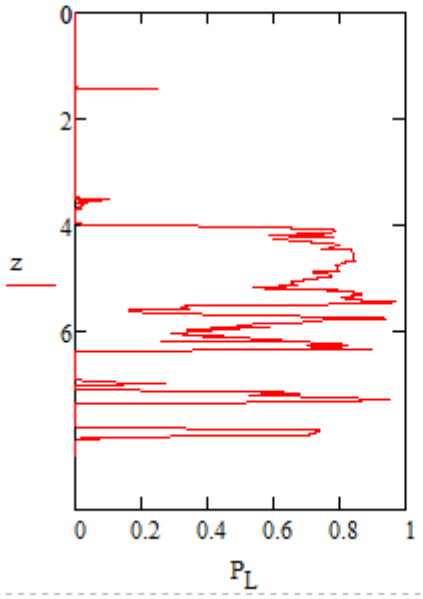

Figure 34- Example of the P_L expression and plot as presented in the Mathcad tool.

3.2.1.11. Liquefaction Potential Index, LPI

To estimate LPI, it was performed the analysis presented on chapter 2.3, proposed by Iwasaki et al. (1978, 1982) by implementing equation (54). The plot of the evolution of LPI along depth is presented in the tool as it can be seen in Figure 35, as well as the liquefaction severity parameters proposed by Luna and Frost (1998) and presented in Table 2 in section 2.3. The tool correlates the estimated LPI values with liquefaction severity parameters and present the final result, evaluating the soil column.

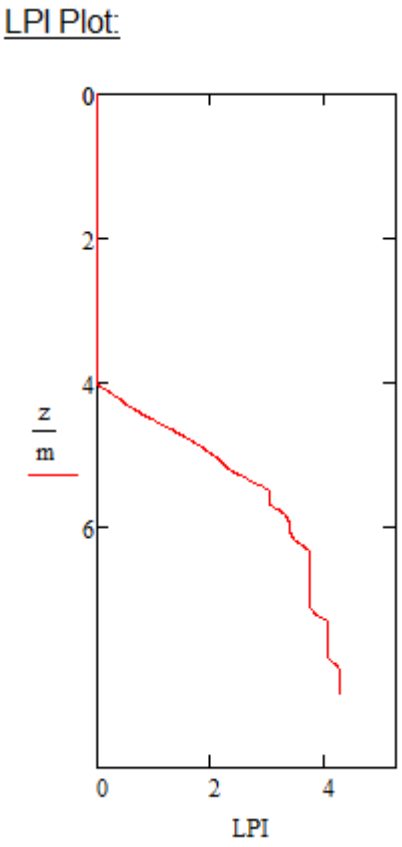

Figure 35- Example of the provided LPI plot within the tool.

3.2.1.12. Saturated Soil Settlements, S_s

The calculation of settlements due to the seismic event is divided into settlements in saturated soils, induced by liquefaction, and settlements in dry soils, caused by seismic compression. The method implemented to estimate settlements in saturated soils is the one developed by Zhang et al. (2002), presented on section 2.4.1.1. This method, based on Ishihara and Yoshimine (1992) approach to estimate the volumetric strain, provides a detailed vertical profile and represents a conservative approach, since it is applied for the whole CPT log – Robertson and Cabal (2015). It is also implemented in some commercial software products, as CLiq.

This procedure presents a couple of limitations in the estimation of the volumetric strains, since it only provides expressions for specific values of the factor of safety, and for $q_{c1N,cs}$ values greater than 33. To surpass this, a set of instructions provided in the Technical Specification for Liquefaction Evaluation of CPT Investigations by the New Zealand Geotechnical Database were followed as detailed below. The purpose and the scope of this database will be presented in chapter 4, as the tool's validation is performed based on its data.

The recommendations presented in the specification to outpace the issues presented in Zhang et al. (2002) are:

- Perform linear interpolation for the values between the published expressions;
- When $q_{c1N,cs} < 33$, adopt the strain values from the boundary, $q_{c1N,cs} = 33$.

Another modification of the procedure was implemented in order to properly reply the soil behaviour. Robertson and Cabal (2015) report that in clay-like soils the post-earthquake volumetric strains due to cyclic softening will be less than those experienced by sand-like soils due to cyclic liquefaction. Concerning this, it is suggested and implemented in this tool a maximum value for the volumetric strain of 0.5% to clay-like soils, $I_C > 2.7$. The plot of S_s as provided in the tool is presented in Figure 36.

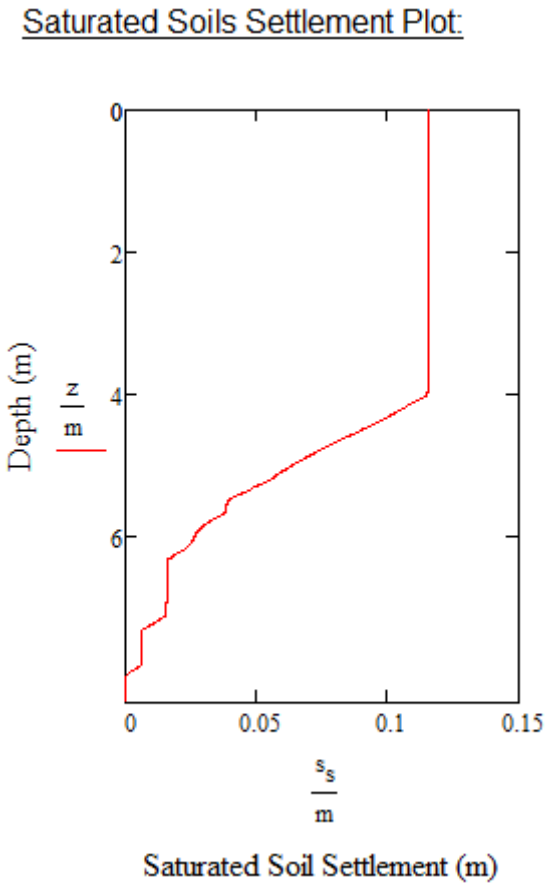

Figure 36- Example of the provided plot of S_s for a specific case.

3.2.1.13. Dry Soil Settlements, S_d

To estimate the settlements in unsaturated soils it was implemented the Robertson and Shao (2010) approach presented in chapter 2.4.2. It presents a reliable and widely implemented method, since it is based on CPT data and it was extended to a wider range of unsaturated soils, whereas the previous approach from Pradel (1998) was restricted to sandy soils. This method is also implemented in CLiq and it is the method suggested by the CPT Guide from Robertson and Cabal (2015) to perform the evaluation of seismic compression in dry soils.

The calculation of the cyclic shear strain, γ_{cyc}, presented on equation (66), depends on the in-situ earth pressure coefficient, K_0. To simplify and avoid the calculation of this parameter, it was considered a value of 1, as it was the same procedure implemented in CLiq and it can be considered a conservative approach. The influence of this assumption in the final results should be evaluated in future developments. The plot of S_d provided by the tool is presented in Figure 37.

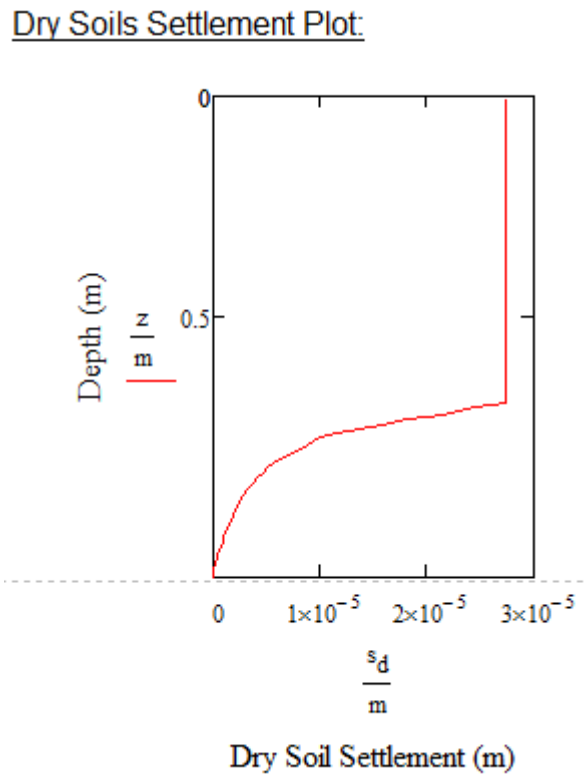

Figure 37- Example of the settlement of dry soils as provided by the Mathcad tool.

3.2.1.14. Probabilistic Settlements, P_S

This feature comes as an improvement in the settlement calculation, once it provides the probability of exceeding a specified settlement for the specific site. The calculation method is based on the Juang et al. (2013) approach presented on section 2.4.1.2. and it provides a plot of the probability of exceeding a settlement, s, shown in Figure 38.

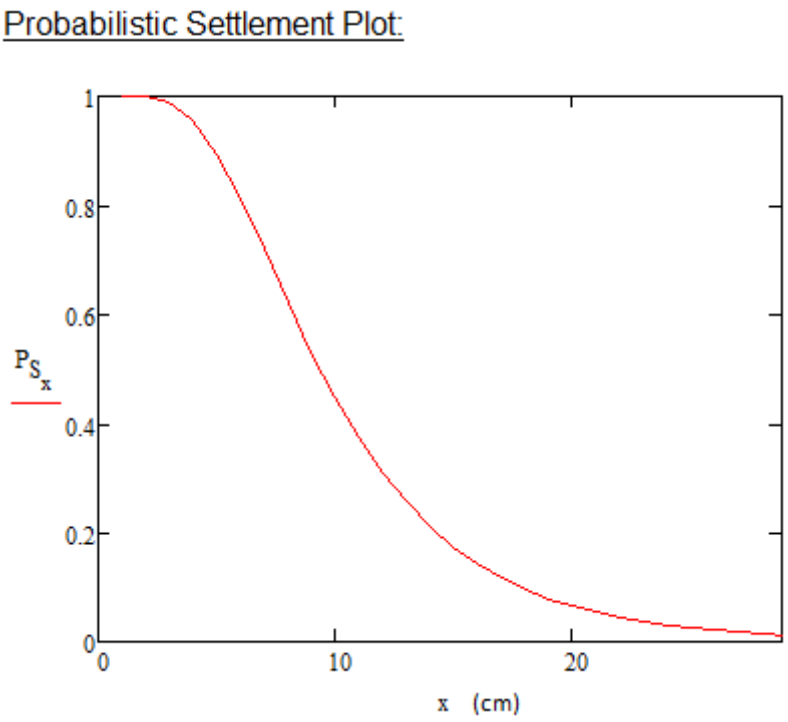

Figure 38- Example of the plot presenting P_S within the tool.

3.2.2. PROVIDED OUTPUTS

As a tool developed to overcome the limitations of the available software related with little transparency on the implementation of the methods, all the parameters calculated within the procedure can be easily accessed and presented in plots. The parameters provided as plots are:

- Normalized friction ratio, F_r;
- Normalized tip resistance, Q_{tn};
- Soil behaviour type index, I_C;
- Normalized clean sand tip resistancd, Q_{tn_cs};
- Cyclic resistance ratio equivalent for a magnitude of 7.5, $CRR_{7.5}$;
- Cyclic resistance ratio, CRR;
- Cyclic stress ratio, CSR;
- Factor of safety against liquefaction, FS;
- Probability of liquefaction, P_L;
- Liquefaction potential index, LPI;
- Saturated soils volumetric strain, ε_v;
- Saturated soils settlement, S_s;
- Dry soils volumetric strain, ε_{vol};
- Dry soils settlement, S_d;
- Total vertical settlement, S_t;
- Probability of exceeding a specified settlement, P_S.

Note that he symbols presented above are the same used in the tool.

The table below gathers the characteristics of the developed tool:

Table 6- Characteristics of the developed tool

Parameters	
Input	CPT data; γ_s; γ_w; Water Table during earthquake (WT_e); Water Table during CPT (WT_i); M; PGA
CRR	Robertson (2009)
MSF	NCEER; Idriss and Boulanger (2008)
CSR / r_d	Seed and Idriss (1971) / NCEER
P_L	Ku et al. (2011)
LPI	Iwasaki et al. (1978) / Luna and Frost (1998)
Saturated Soils Settlement	Zhang et al. (2002)
Dry Soils Settlement	Robertson and Shao (2010)
Probabilistic Settlement	Juang et al. (2013)
Output	F_r; Q_{tn}; I_C; Q_{tn_cs}; $CRR_{7.5}$; CRR; CSR; FS; P_L; LPI; ε_v; S_s; ε_{vol}; S_d; S_t; P_S

3.3. TOOL USER'S MANUAL

In this section, it is explained in further detail the calculation process of the tool, starting with the definition, by the user, of the parameters required. With this stage completed, the tool automatically performs the liquefaction assessment and presents, in plots, the parameters estimated along the process.

3.3.1. STARTING A NEW PROJECT AND DEFINING CALCULATION PARAMETERS AND PROCEDURES

The developed in-house tool uses Mathcad as platform, so it is required a license of this software in order the tool to run. When it starts, the whole spreadsheet is presented, having the user to define the parameters.

The input data can be divided in three categories: CPT profile and soil parameters; Groundwater depths; and Seismic Parameters.

Figure 39 presents the procedure that the user must follow to insert in the tool the data required to perform a liquefaction analysis.

Note that in Mathcad, the vector and matrix elements by default are numbered starting with row zero and column zero, which explains the reason why the tool assigns the depth to the column zero of the imported excel file with the CPT data, as noticed in Figure 39.

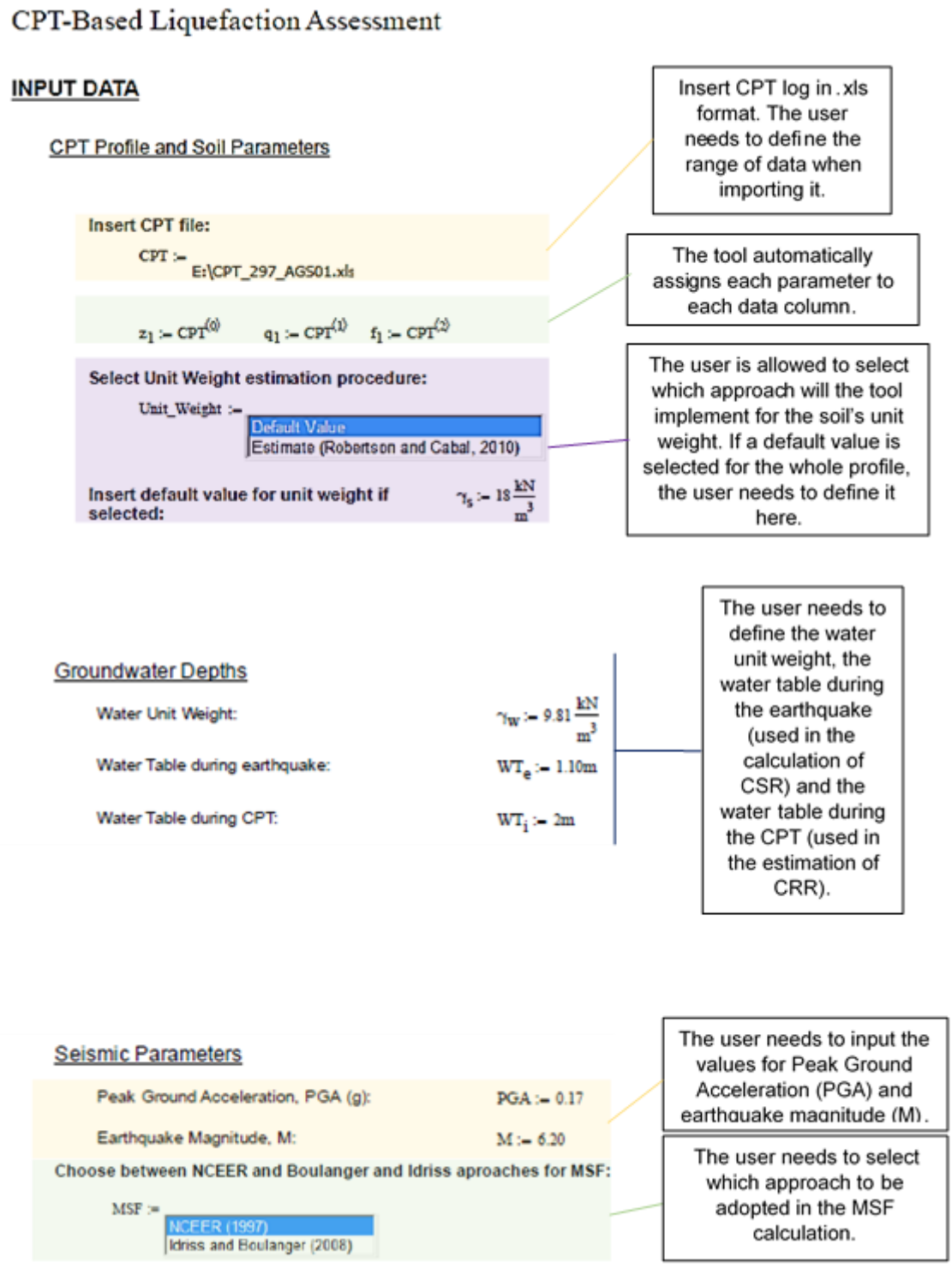

Figure 39- Procedure to input the data and define the parameters required by the tool for a liquefaction assessment.

3.3.2. Performing the Calculation

After the user defines all the information required by the tool, it automatically performs a liquefaction assessment based on the methods presented previously, and presents the calculated parameters, defined in section 3.2.2., in plots. The parameters estimated in a liquefaction evaluation are presented in Figure 40.

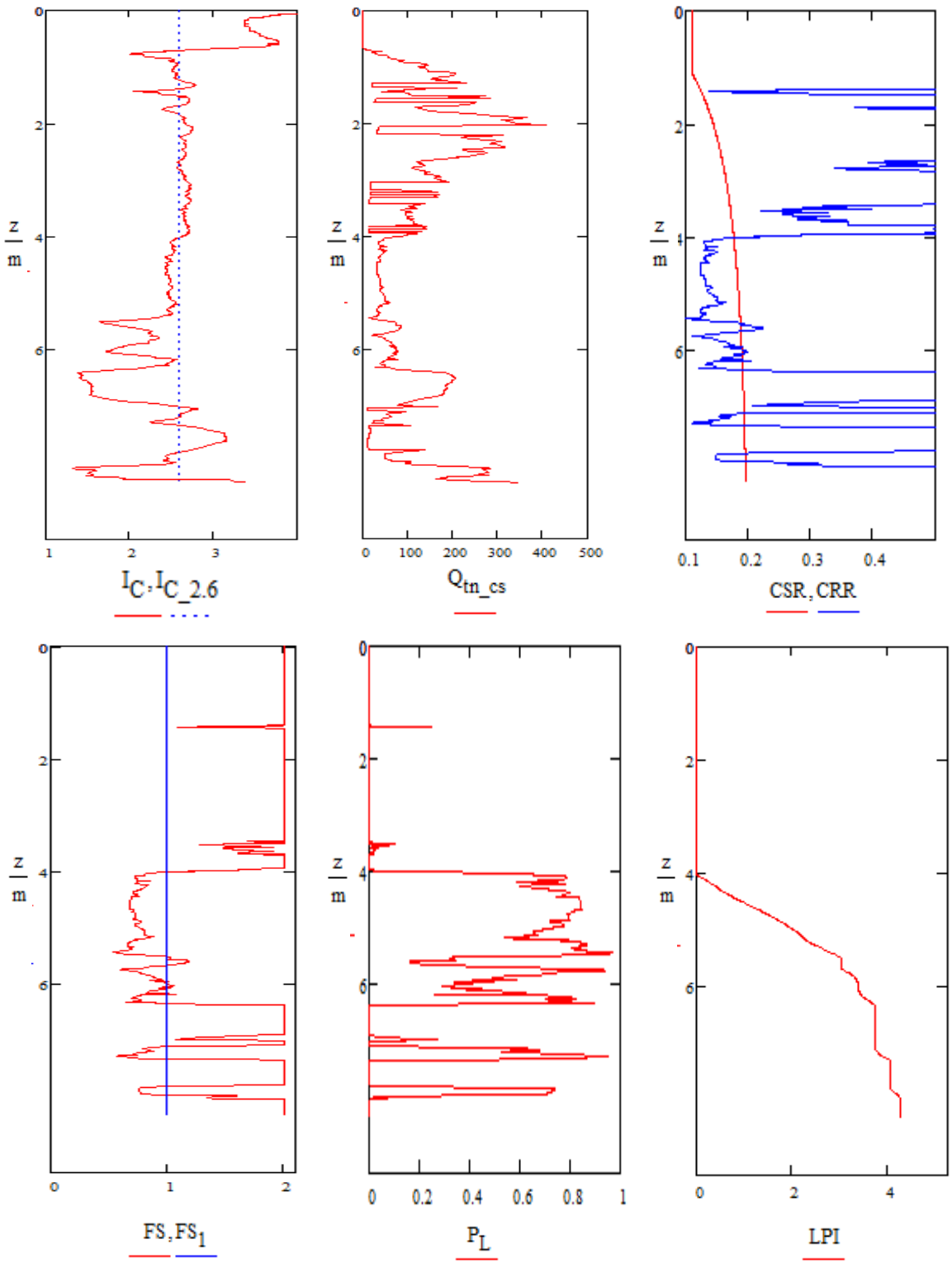

Figure 40- Parameters estimated by the tool in the course of a liquefaction evaluation.

The parameters estimated in the course of a settlement estimation are presented in Figure 41.

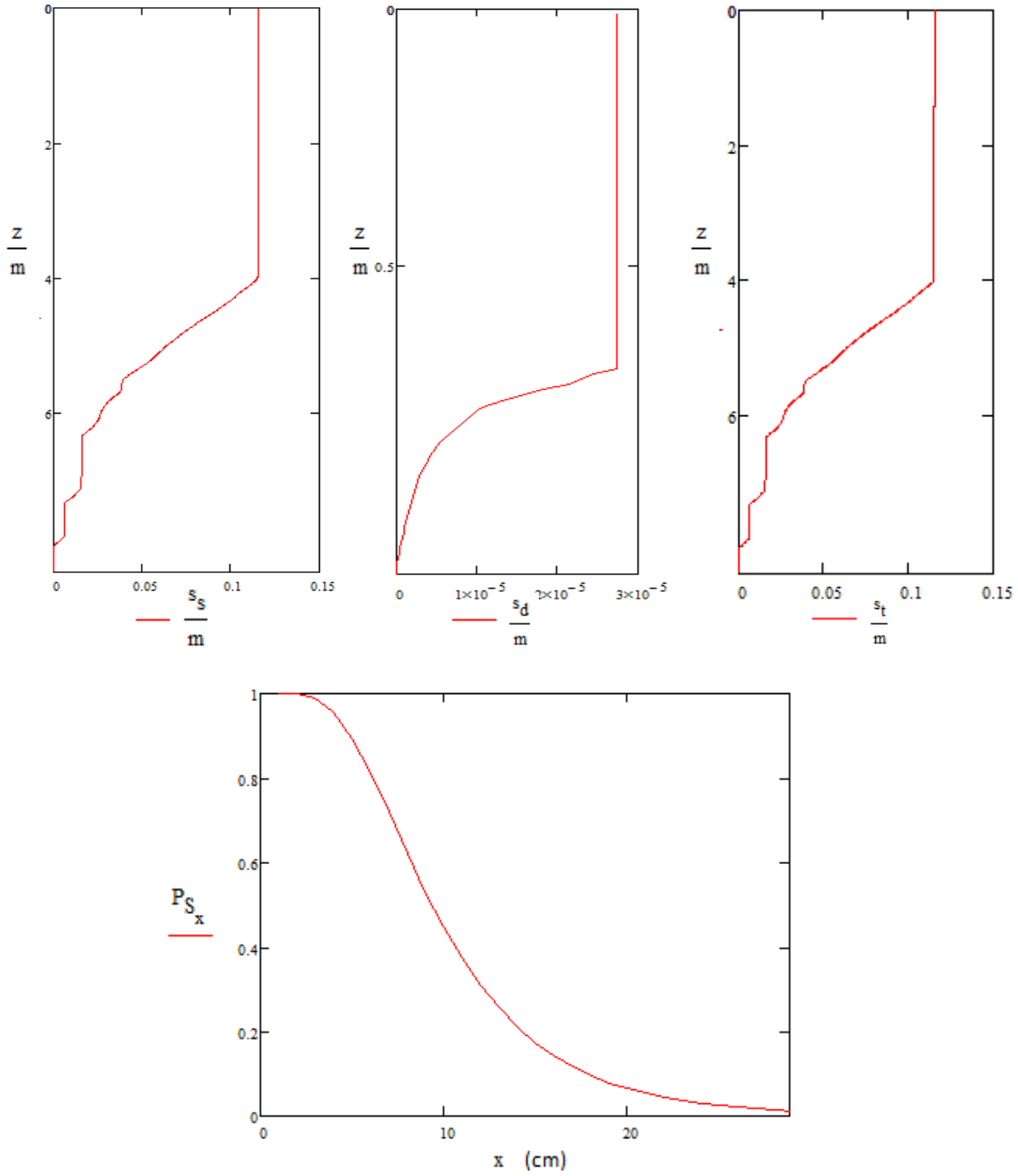

Figure 41- Parameters estimated by the tool in the course of a settlement estimation.

All the parameters calculated during an assessment are easily obtained in the worksheet, which allows the user to have control over the process and to extract the parameters to an Excel spreadsheet. The expressions introduced in the tool can also be easily modified in order to study the influence of some assumptions made.

4
SELECTION OF CASE HISTORIES

4.1. INTRODUCTION

In order to assess the different commercial software available, as well as the developed tool, it was proposed to perform a validation using some case histories collected from a database.

The case histories were selected from a wide range of data presented in the New Zealand Geotechnical Database (NZGD), created after the 2010-2011 Canterbury earthquake sequence, in New Zealand. The selection of the case histories, as well as the criteria used, will be focus of a detailed discussion in this chapter. Note that the New Zealand Geotechnical Database was designated as Canterbury Geotechnical Database until the 2nd of June of 2016.

4.2. CANTERBURY GEOLOGICAL CHARACTERIZATION

Christchurch is located on the east coast of the South Island of New Zealand, more precisely on the Canterbury plains, a large area formed from the deposition of eroded material from the Southern Alps, that represent the convergent boundary between the Australian and the Pacific tectonic plates. The material was deposited during the Quaternary, transported by the Waimakiriri River that flows about 25 km north from the city, and it is constituted of alternating layers of eroded gravel and fine grained marine sediments – Taylor et al. (2012).

Consulting Figure 42 it is possible to notice that the city of Christchurch is grounded on Quaternary deposits, defined as thick and poorly consolidated, mainly constituted by fluvial gravels and sands – Browne et al. (2012) after Bal (1996), that interfinger eastward with estuarine and shallow marine sediments – Browne et al. (2012) after Browne and Naish (2003). Figure 43 presents a cross section of the mentioned Quaternary deposits, where it is possible to observe that the shallow depths of Christchurch's sub soil are characterized by the Christchurch Formation, which is constituted by beach, estuarine, lagoonal dune and coastal swamp deposits of gravel, sand, silt, clay, shell and peat – Brown et al. (1988).

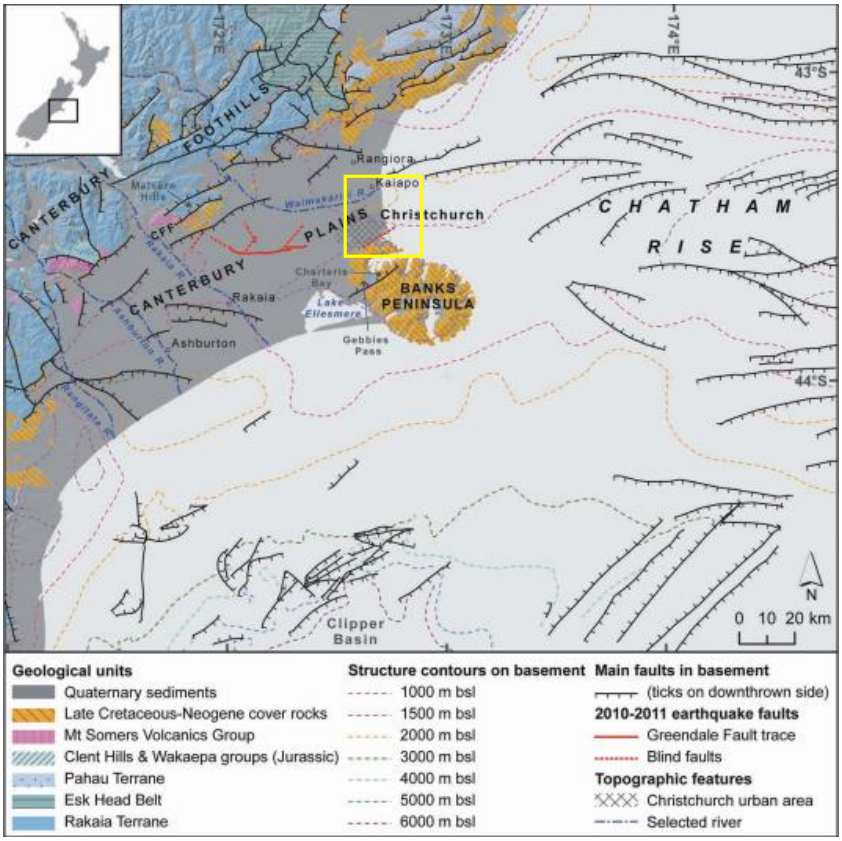

Figure 42- Geological features of Canterbury area. Christchurch location is highlighted by a yellow square. (Modified after Browne et al., 2012. Modified after Field & Browne, 1989 Wood et al., 1989, Cox & Barrell, 2007 and Forsyth et al., 2008)

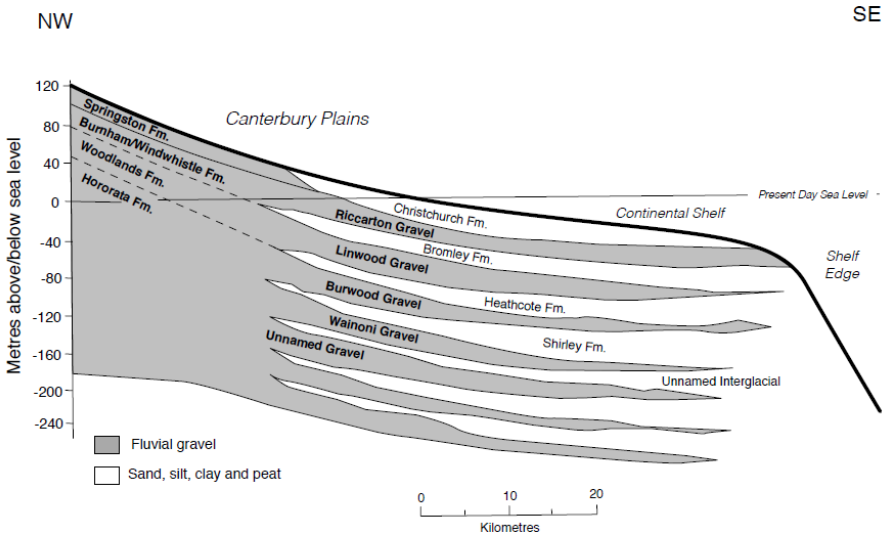

Figure 43- Cross section of the Quaternary deposits underlying Christchurch (Taylor et al., 2012 after Brown and Weeber, 1992)

Figure 44 presents a soil texture map developed by Environmental Canterbury, characterizing the soil in the Christchurch area, highlighted in Figure 42. These soils integrate the Christchurch Formation

described before and coincide with the set of soils that characterize it. Christchurch city area is characterized by silt loam, peaty loam and fine sandy loam and is represented in the figure below by a black star. Further ahead, after the case histories being selected, soil profiling of their locations will be presented, based on log reports of boreholes extracted from the NZGD. The knowledge of the stratification of the soil improves the assessments developed based on ground parameters and presents a great source of information to better understand soil's behaviour.

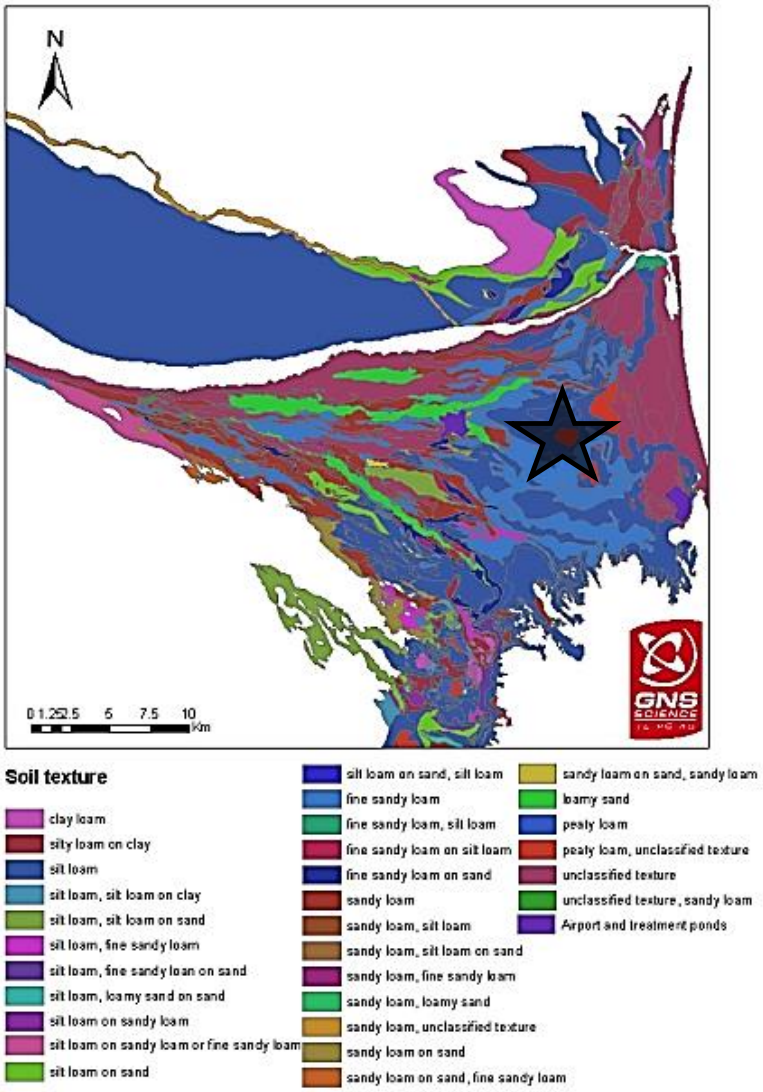

Figure 44- Soil texture of Christchurch city area. Christchurch city area is highlighted by a black star. (GNS Science report after Environment Canterbury pers. comm.)

4.3. SELECTION OF CASE HISTORIES

The New Zealand Geotechnical Database, NZGD, is an on-line database created to provide and promote the exchange of geotechnical data after the 2010-2011 Canterbury earthquake sequence in New Zealand. This sequence began with the 4th of September 2010, M_W 7.1 Darfield earthquake and includes up to ten events that induced liquefaction, with the most notable case being the 22nd February 2011, M_W 6.2 Christchurch earthquake – Green et al. (2014). The seismic parameters used on the validation are based on the latter earthquake event.

The NZGD is free of access for all the academic and scientific community, only requiring a registration on their website (https://www.nzgd.org.nz/). The geotechnical data available in the database is easily accessed by a map viewer, where it is possible to combine different layers of data and observe the location of the in-situ tests. The type of data available and the methods that were used to obtain it, will be presented hereafter.

4.3.1. NZGD- Methodology Used to Obtain Data Values

NZGD provides geotechnical investigations, aerial photograph, field observations, LiDAR data and some data analysis. From the information available in the database, not all was considered relevant to the scope of the validation, thus, the selected data is:

- Geotechnical Investigation Data;
- Liquefaction Interpreted from Aerial Photography;
- Vertical Ground Movements;
- Event Specific Groundwater Surface Elevations;
- Conditional PGA for Liquefaction Assessment.

From the data selected above, some will be the basis of the assessments to be performed by the developed tool and the software products, and other will be used to be compared with the assessments results, in order to validate the methodology implemented. The relationship between the data obtained from the database and the parameters provided or introduced in the software products/tool will be presented further ahead. According to NZGD, the soil's stress state can be reasonably well approximated using an average soil unit weight of 18 kN/m^3. This assumption was implemented in the validations performed.

4.3.1.1. Geotechnical Investigation Data

The geotechnical investigation data available in the database is composed by more than 22000 CPT, 4300 DCP tests, 10000 Boreholes and some other field tests performed in several locations throughout the Canterbury region affected by the earthquakes of 2010-2011. Due to the scope of this thesis, only the CPT's were selected to be the basis of the liquefaction assessments performed, by providing not only the soil's penetration resistance and sleeve friction but also the value of the water level, measured during the execution of the CPT. Figure 45 presents the field tests available in the NZGD, although the map file only allows to display a small amount of data at the same time and it is necessary to zoom in the required location in order to have access to the information available for that specific site.

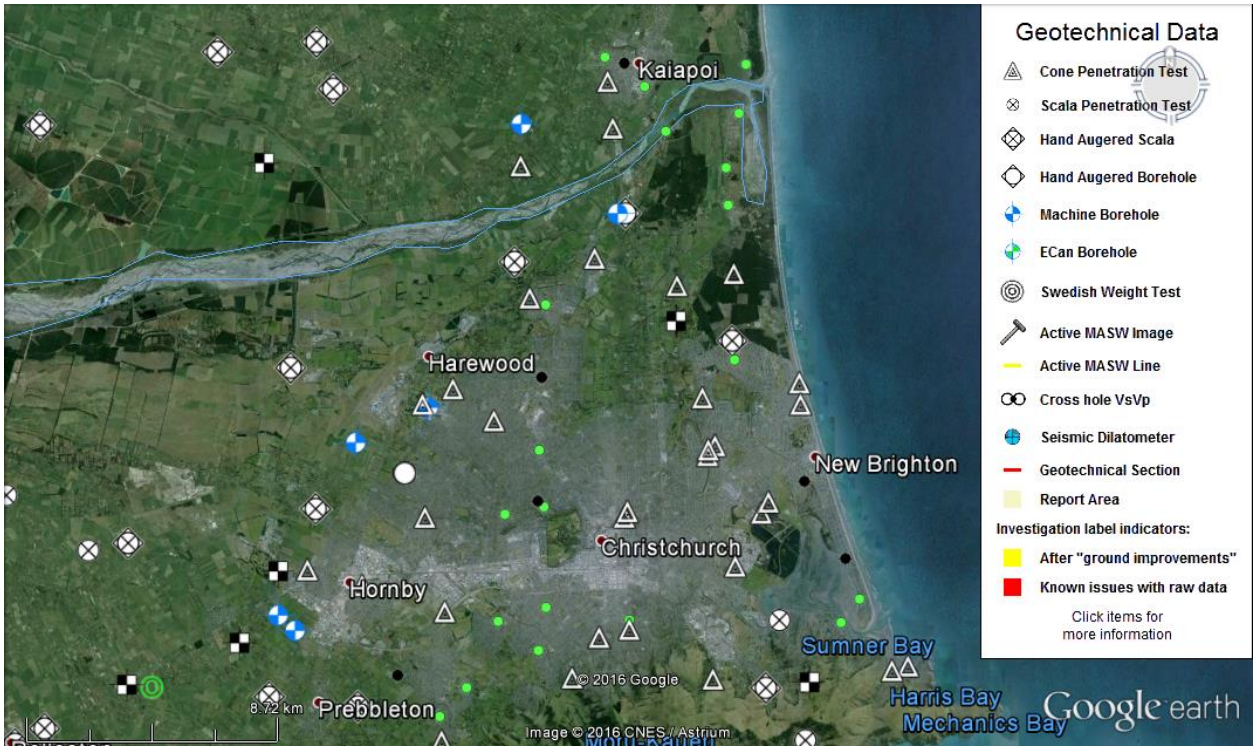

Figure 45- Types of field tests available in Christchurch area. (New Zealand Geotechnical Database (2016) "Geotechnical Investigation Data", Map Layer CGD0010, retrieved 15/06/2016 from https://canterburygeotechnicaldatabase.projectorbit.com/)

4.3.1.2. Liquefaction Interpreted from Aerial Photography

Based on the quantity of liquefaction material ejected, observed from aerial photographs taken after the significant earthquakes, it was performed a regional map divided in three scales according to the apparent liquefaction severity. The criteria used in the definition of the severity is presented in Table 7.

However, there is not great accuracy in the classification made, once the photographs that were used did not have the same quality or light conditions, and shadows due to low sun angles might have caused some misclassifications. Also, there is the possibility of the ejected material had been removed before the photographs were taken.

Table 7- Criteria implemented to define liquefaction severity (after New Zealand Geotechnical Database)

Classification	Apparent Features
Moderate to Severe	Roads had either ejected material or wet patches wider than a typical vehicle width; Ejected material in grass or roads; Groups of 2-3 ejected material boils within properties or parks.
Minor	Roads had either ejected material or wet patches narrower than a typical vehicle; Only one or two ejected material boils within a property or a park.

None	None of the above features were observed.

4.3.1.3. Vertical Ground Movements

Vertical elevation changes estimated between pairs of Digital Elevation Models (DEM) created from airborne Light Detection and Ranging (LiDAR), approximate the vertical ground movements during significant earthquakes. These elevation differences were colour banded in maps presented in the NZGD, are associated with an accuracy of ± 0.15 m, and were calibrated against land-based survey provided by the Christchurch City Council.

4.3.1.4. Event Specific Groundwater Surface Elevations

Based on water level dip measurements from wells installed since the beginning of the earthquake sequence (September 2010), surface models were produced with the water levels prior to the significant earthquakes. These groundwater depths are suitable for back analysis, since they approximate in a good way the water level at the time of each earthquake. The accuracy of the estimated groundwater elevations grows with the proximity to the measurement location. Figure 46 presents an example of a map layer with the derived groundwater depths and the well locations, in the NZGD.

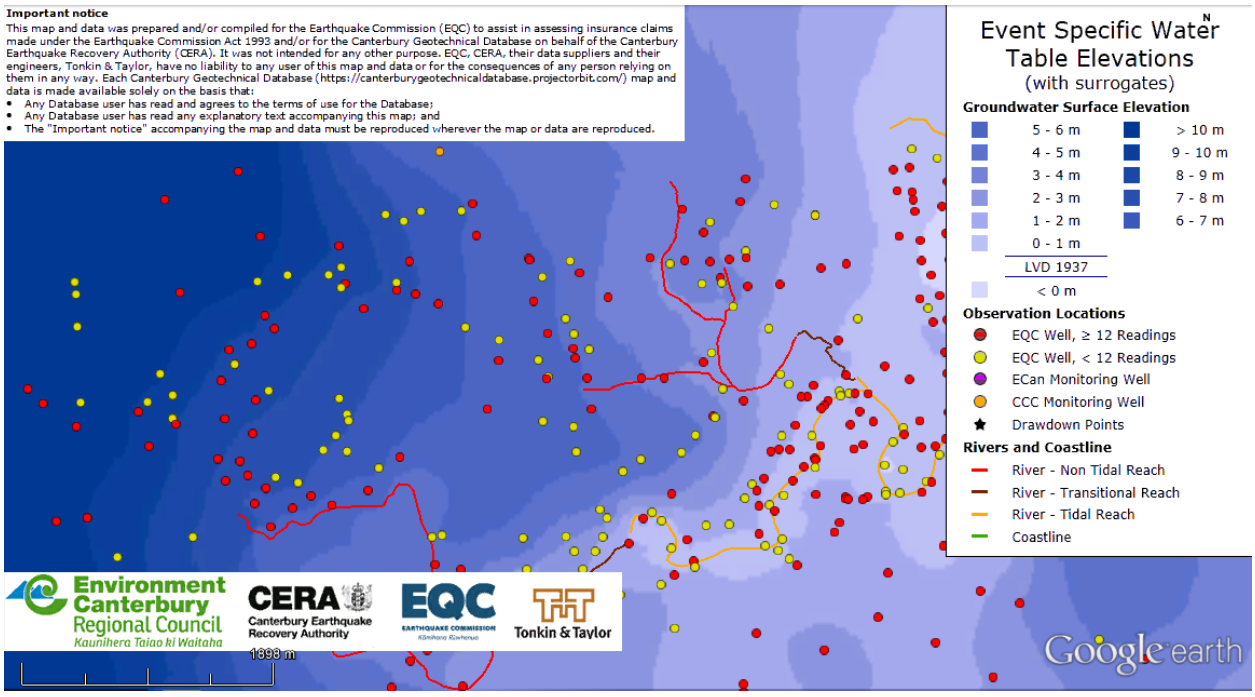

Figure 46- Water table elevations based on dip measurements. (Canterbury Geotechnical Database (2014) "Event Specific Groundwater Surface Elevations", Map Layer CGD0800 – 12 June 2014, retrieved 15/06/2016 from https://canterburygeotechnicaldatabase.projectorbit.com/)

4.3.1.5. Conditional PGA for Liquefaction Assessment

The PGA for each location in the region was estimated by combining empirical ground motion models of the fault rupture with the recorded PGA values at strong motion stations. Locations near to the strong motion stations present greater accuracy than farther locations, since in the latter case, the values are

more influenced by the PGA predicted from the empirical model. Figure 47 presents the map layer in the NZGD that provides the median and standard deviation of the conditional PGA for the Christchurch event, as well as the strong motion stations location.

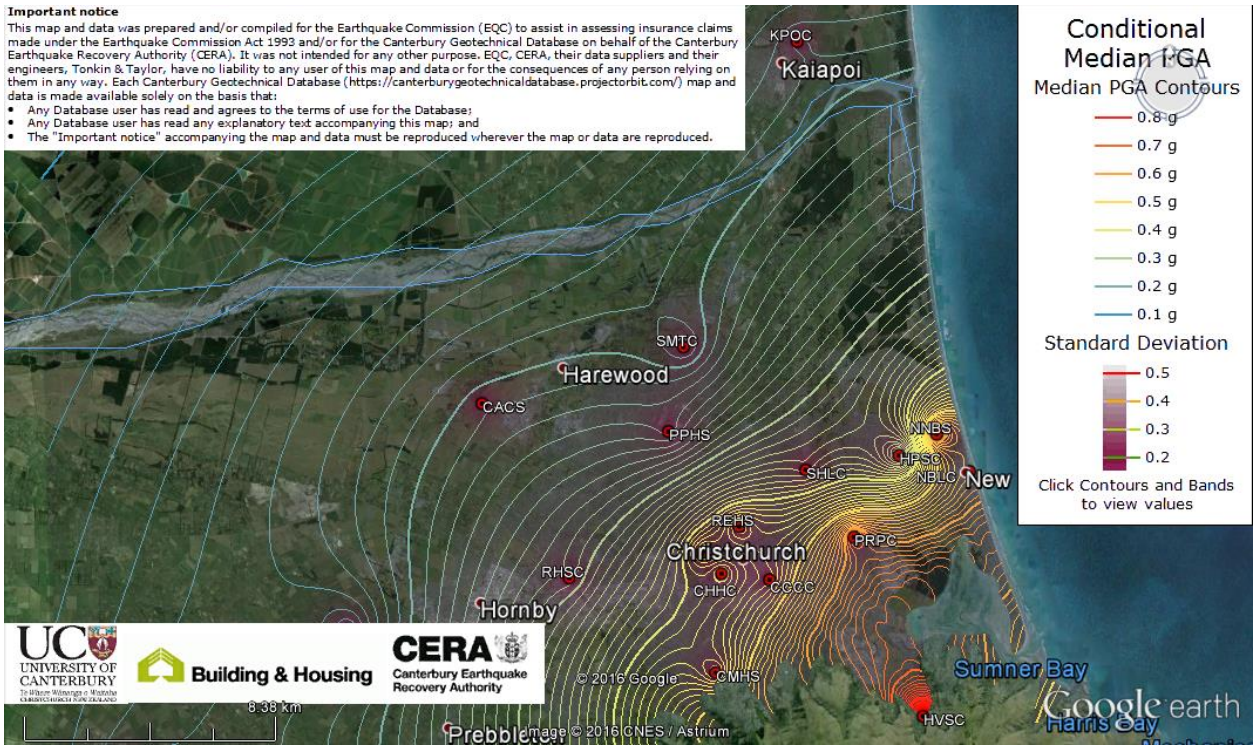

Figure 47- Map layer with the strong motion station network available in the Christchurch area (Canterbury Geotechnical Database (2015) "Conditional PGA for Liquefaction Assessment", Map Layer CGD5110 – 30 June 2015, retrieved 15/06/2016 from https://canterburygeotechnicaldatabase.projectorbit.com/)

4.3.2. Selected Case Histories

After understanding the approaches implemented to estimate the data available in the NZGD, it is possible to reduce the cases available to the ones with greater accuracy, in order to perform a rigorous validation. As mentioned, the case histories correspond to the CPT tests available in the database, thus the basis of the selection is the location of the CPT data available. The database presents data for the different earthquakes of the Canterbury sequence, so it was necessary to select a single earthquake event in which the data is based. Since the earthquake that produced more evidence of liquefaction was the 22nd February 2011, M_W 6.2 Christchurch, it was the selected.

4.3.2.1. Criteria Implemented

At first, it was decided to select three case histories, representing the three different classifications for liquefaction severity, in order to check for the sensibility of the software products/tool, as well as the accuracy of the evaluation performed. As it was stated before, the data values would be more accurate when nearer to the measurement locations, which is valid for both PGA and groundwater data, so it was decided to select case histories as close as possible to the measurement locations. Figure 49 presents the conditional PGA estimated for the Christchurch event, along with the selected case histories for the

validation. The ground motion stations that measured the specific PGA for this event are the basis of the developed map and are represented as well in red dots.

In order to refine even more the remaining data available, it was decided to consult a case study developed by Green et al. (2014), based on high quality CPT data from the NZGD. The purpose of this study was to evaluate three deterministic CPT liquefaction evaluation procedures by using 50 high quality CPT case histories. From the 50 cases selected, 5 are presented within the paper, and 2 match the criteria above.

The criteria implemented in the selection of the case histories is grouped in Table 8:

Table 8- Criteria adopted in the selection of case histories

Parameters	Criteria
Liquefaction Interpreted from Aerial Photograph	Select one case history for each of the three liquefaction severity levels.
Event Specific Groundwater Surface Elevations	Select case histories coinciding with the water level measurement locations.
Conditional PGA for Liquefaction Assessment	Select case histories as close as possible to strong motion stations.
High Quality of CPT data	Select case histories from Green et al. (2014)

The case histories that matched these criteria are CPT-NBT-03 and CPT-KAN-26. As no case where no liquefaction was observed is presented on Green et al. (2014), it was selected CPT-KAS-19, based only on the first three criteria of Table 8. The description of each one of these case histories is presented on Table 9.

Table 9- Description of the selected case histories

CPT Code	CPT-KAS-19	CPT-KAN-26	CPT-NBT-03
Test date	11/11/2010	15/11/2010	28/01/2011
Earthquake Event	Christchurch 22/02/2011	Christchurch 22/02/2011	Christchurch 22/02/2011
Magnitude	6.2	6.2	6.2
Liquefaction Severity	None	Minor	Moderate-Severe
WT during CPT test (m)	2.0	1.5	2.4
WT during earthquake (m)	0.94	0.5	1.18
PGA (g)	0.21	0.18	0.34
Distance to strong motion station (m)	1350	720	360
Vertical ground movement (m)	0 - 0.1	0 - 0.1	0.1 - 0.2

Some of the map layers used to obtain the parameters described in the Table 9 are presented below. Figure 48 presents the map developed after the observations of aerial photographs, dividing the region according to the liquefaction severity observed. Figure 49 presents the contour map that provided the PGA for each case history, while the vertical displacements were obtained by consulting the map in Figure 50.

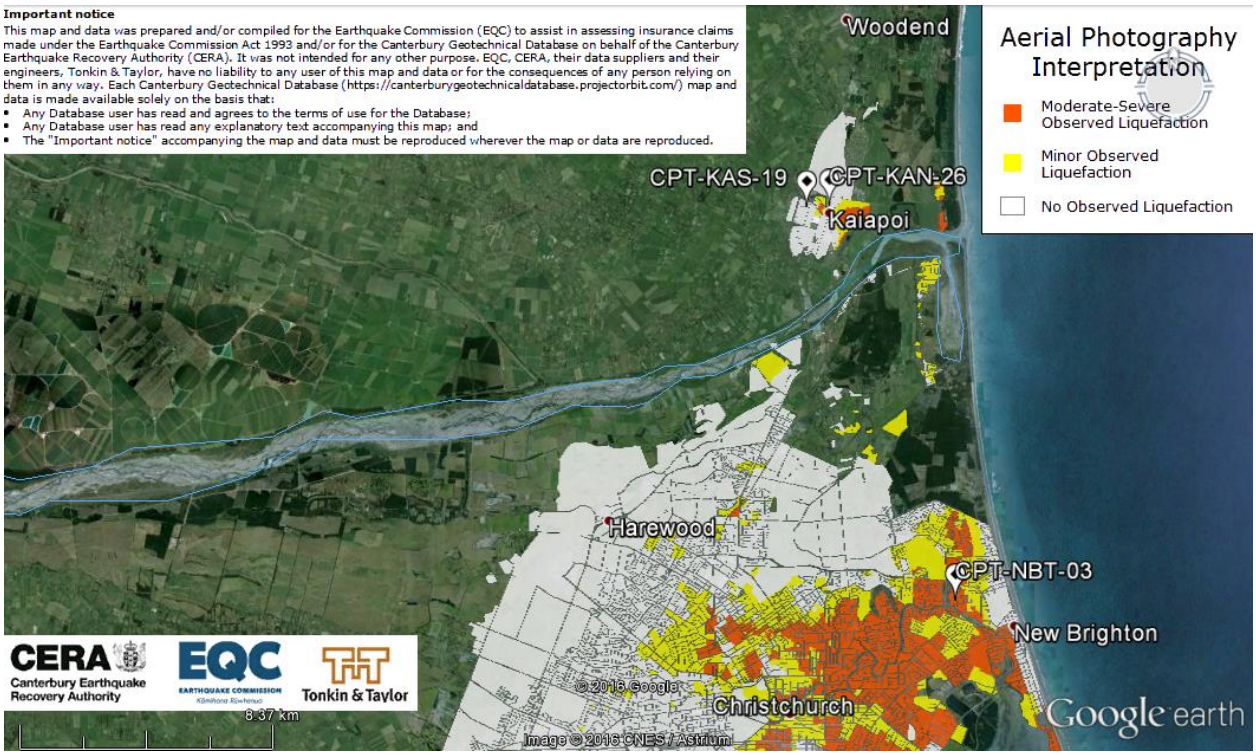

Figure 48- Map layer of liquefaction interpreted from aerial photographs, with each CPT selected represented (Canterbury Geotechnical Database (2013) "Liquefaction Interpreted from Aerial Photography", Map Layer CGD0200 - 11 Feb 2013, retrieved 15/06/2016 from https://canterburygeotechnicaldatabase.projectorbit.com/)

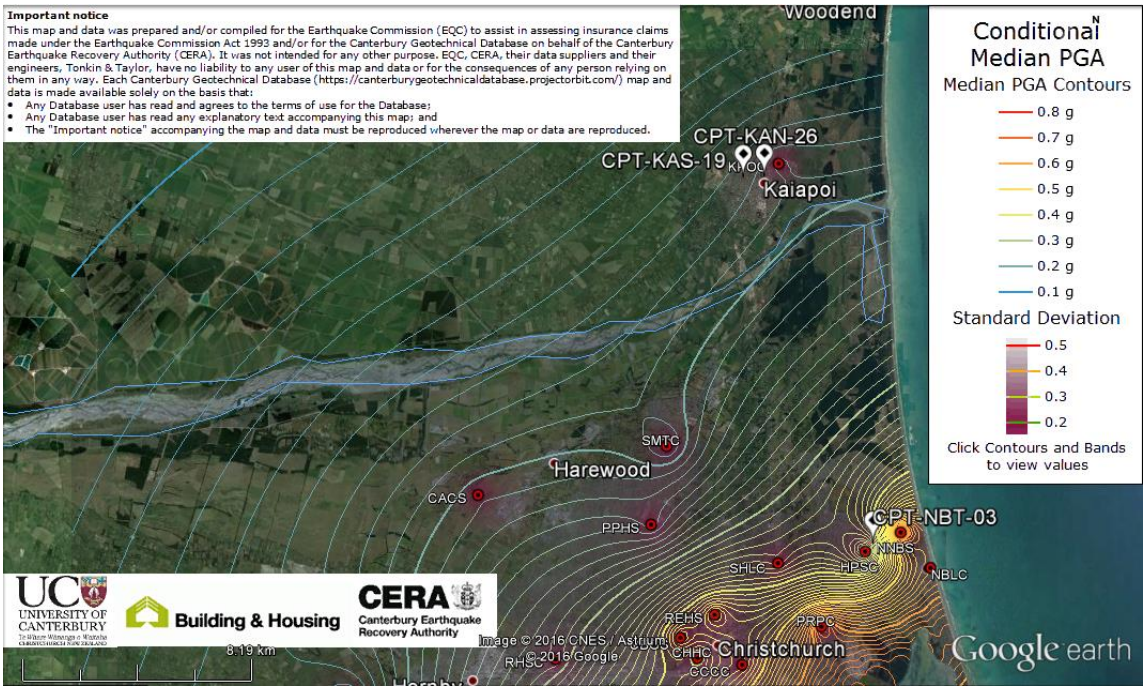

Figure 49- Map layer available in NZGD with the median PGA contours for the Christchurch earthquake event. The red dots represent the ground motion stations and the selected CPT's are presented as well. (Canterbury Geotechnical Database (2015) "Conditional PGA for Liquefaction Assessment", Map Layer CGD5110 – 30 June 2015, retrieved 15/06/2016 from https://canterburygeotechnicaldatabase.projectorbit.com/)

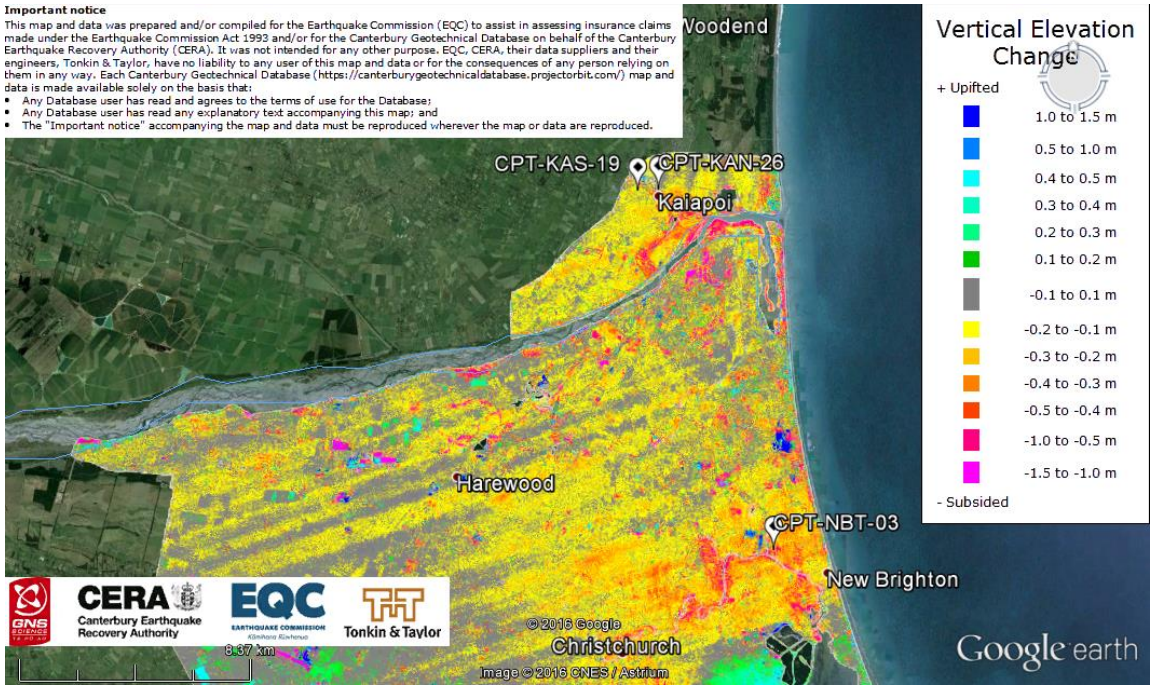

Figure 50- Vertical ground movements for each CPT location provided by NZGD (Canterbury Geotechnical Database (2012) "Vertical Ground Surface Movements", Map Layer CGD0600 - 23 July 2012, retrieved 15/06/2016 from https://canterburygeotechnicaldatabase.projectorbit.com/)

With the case histories selected, it was possible to extract the CPT log for each one of them, and thus perform a liquefaction assessment for each location. However, it would be valuable to have a more detailed characterization of the subsoil for each case, than the provided previously on the general geologic characterization of Christchurch.

Firstly it was consulted a geological map of Christchurch that concluded that the locations of CPT-KAS-19 and CPT-NBT-03 are characterized by river alluvium, comprising gravel, sand and silt, while CPT-KAN-26 is located at an area characterized by river sand dunes. Still, it is required more detailed information on the subsoil of the three selected cases, so by accessing borehole logs performed near the CPT locations and available on NZGD, it was performed a soil profile for each site that was compared with the CPT log.

4.3.2.2. CPT-NBT-03

Figure 51 presents the distance between the CPT-NBT-03 location and the borehole used to perform the soil profile. Figure 52 presents the normalized data provided from the CPT and its comparison with the soil profile. The soil profile is only presented up to 12 m deep once it was the maximum depth of the performed borehole. When comparing the CPT log with the strata, it can be noticed some similarity, although the stratification presents only an approximation of the soil profile for the exact location of the CPT.

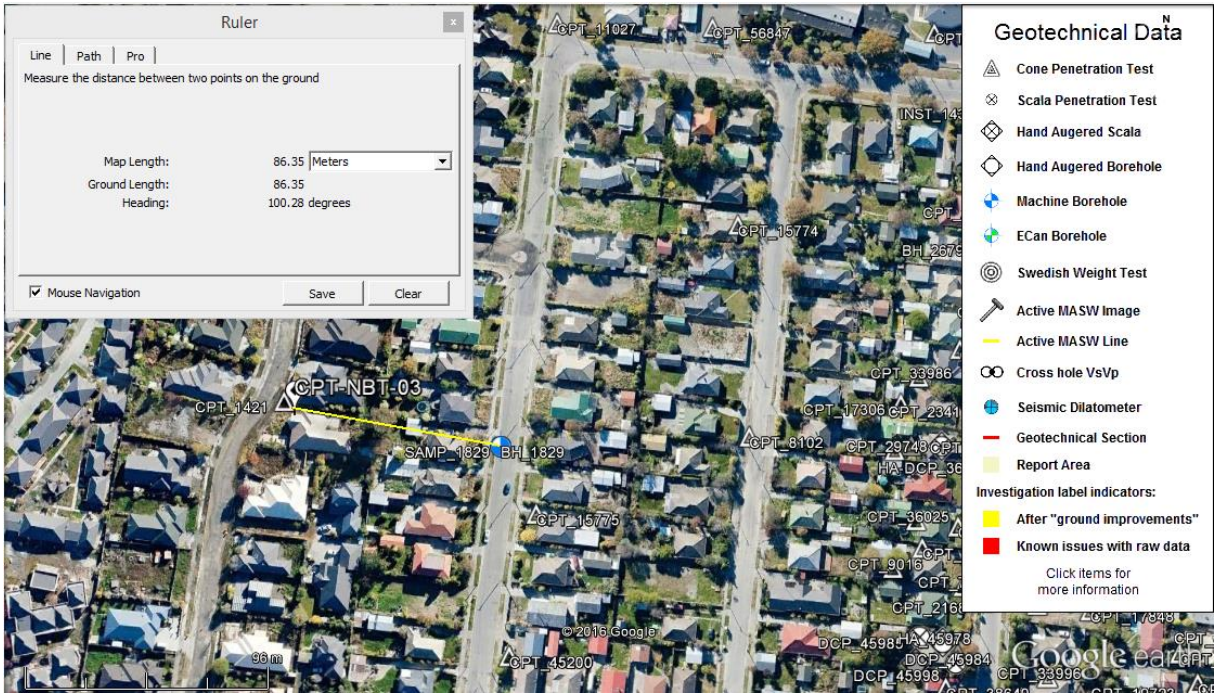

Figure 51- Distance between CPT-NBT-03 location and the borehole used to perform the soil profile, represented by the line in yellow. (New Zealand Geotechnical Database (2016) "Geotechnical Investigation Data", Map Layer CGD0010, retrieved 15/06/2016 from https://canterburygeotechnicaldatabase.projectorbit.com/)

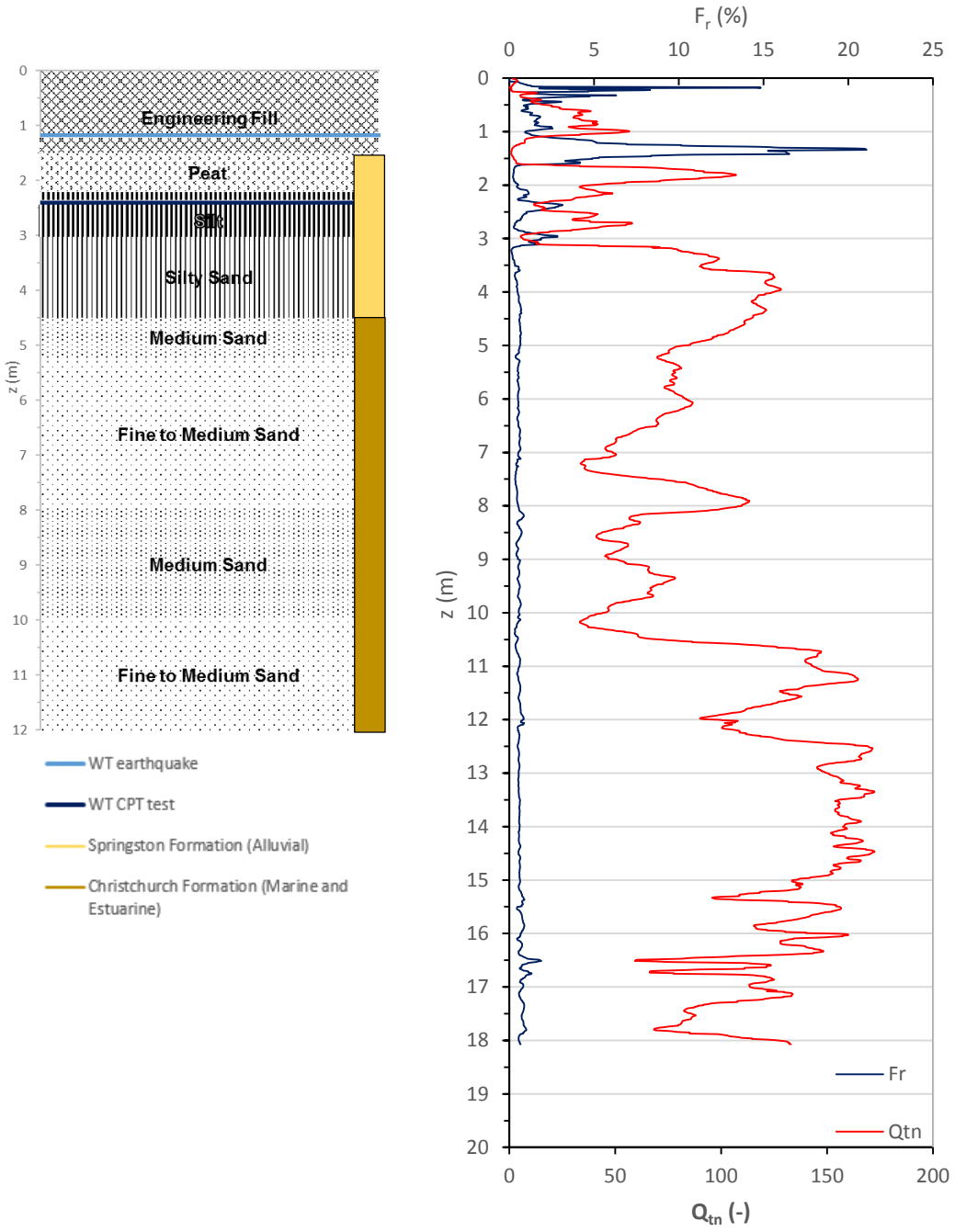

Figure 52- Plot of F_r and Q_{tn} compared with soil profile of CPT-NBT-03

The peat stratum is clearly identified in the plot, once it has low tip resistance and a considerable sleeve friction, producing high values of friction ratio, as noticed. The friction ratio has his maximum value in the peat layer, but it is also noticed that the layers with some fines content (Silt and Silty Sand) have friction ratio values higher than the average. This parameter has a low and approximately constant value (less than 1%) for the remaining strata. The normalized tip resistance in turn, has higher values at the

depths of 4 m and from 10 m, but between these two depths, Q_{tn} is low, apart from a local peak noticed at 8 m. There is not a completely accurate resemblance between the normalized CPT data and the strata.

4.3.2.3. CPT-KAN-26

Figure 53 presents the distance between CPT-KAN-26 location and the borehole used to perform the soil profile. By analysing the plot with the normalized CPT data and its comparison with the soil's stratification (Figure 54), it is noticed that the tip resistance along the thick sand stratum is almost constant and around 100, apart from a layer with less than 1 m thick and starting at 1 m deep that presents a local nadir and can be potentially liquefiable and two local peaks at the depths of 2.5 and 4 m. At lower depths it is possible to observe the influence of the thin sand layer in-between the two gravel strata with a sudden decrease of the normalized tip resistance at 7.5 m. Although the sand layer may be represented at 7 m deep in the soil profile, this was performed based on a borehole made at around 150 m of the CPT location, which cause that this thin sand layer may be deeper in this area.

The plot of the friction ratio does not present large peaks as in CPT-NBT-03, with the maximum value being lower than 2%. F_r values are confined in almost the entire column to values lower than 1%, what is plausible for sands.

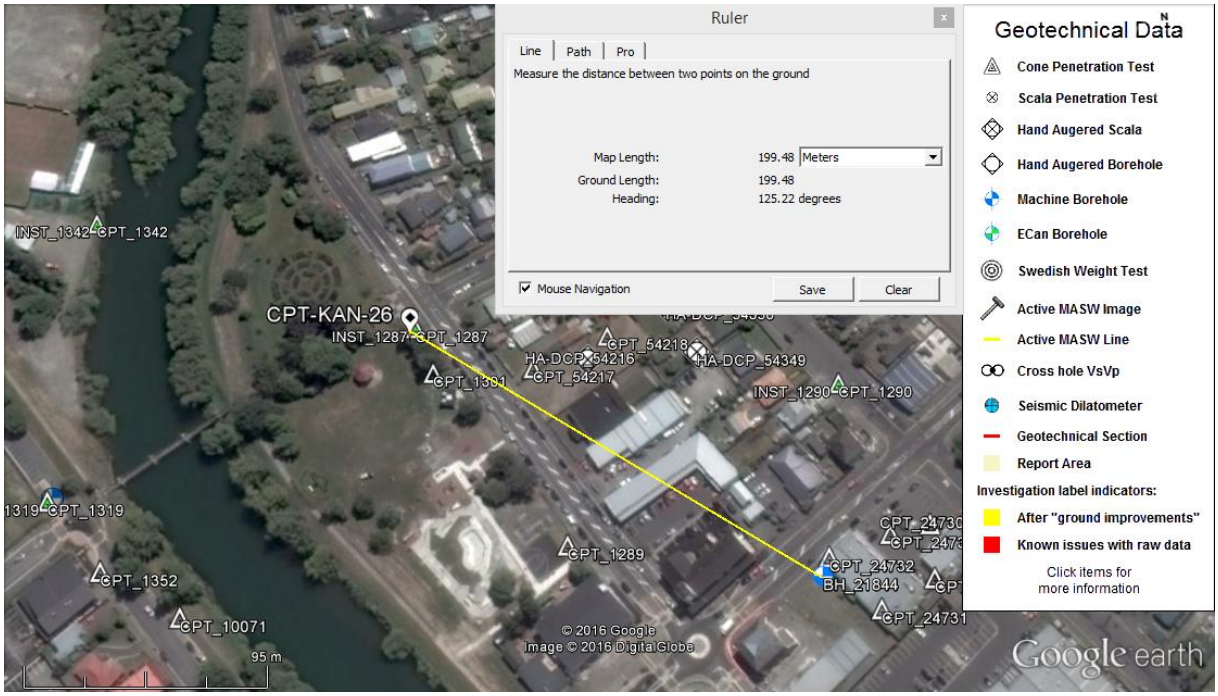

Figure 53- Distance between CPT-KAN-26 location and the borehole used in the performance of the soil profile, represented by the line in yellow. (New Zealand Geotechnical Database (2016) "Geotechnical Investigation Data", Map Layer CGD0010, retrieved 15/06/2016 from https://canterburygeotechnicaldatabase.projectorbit.com/)

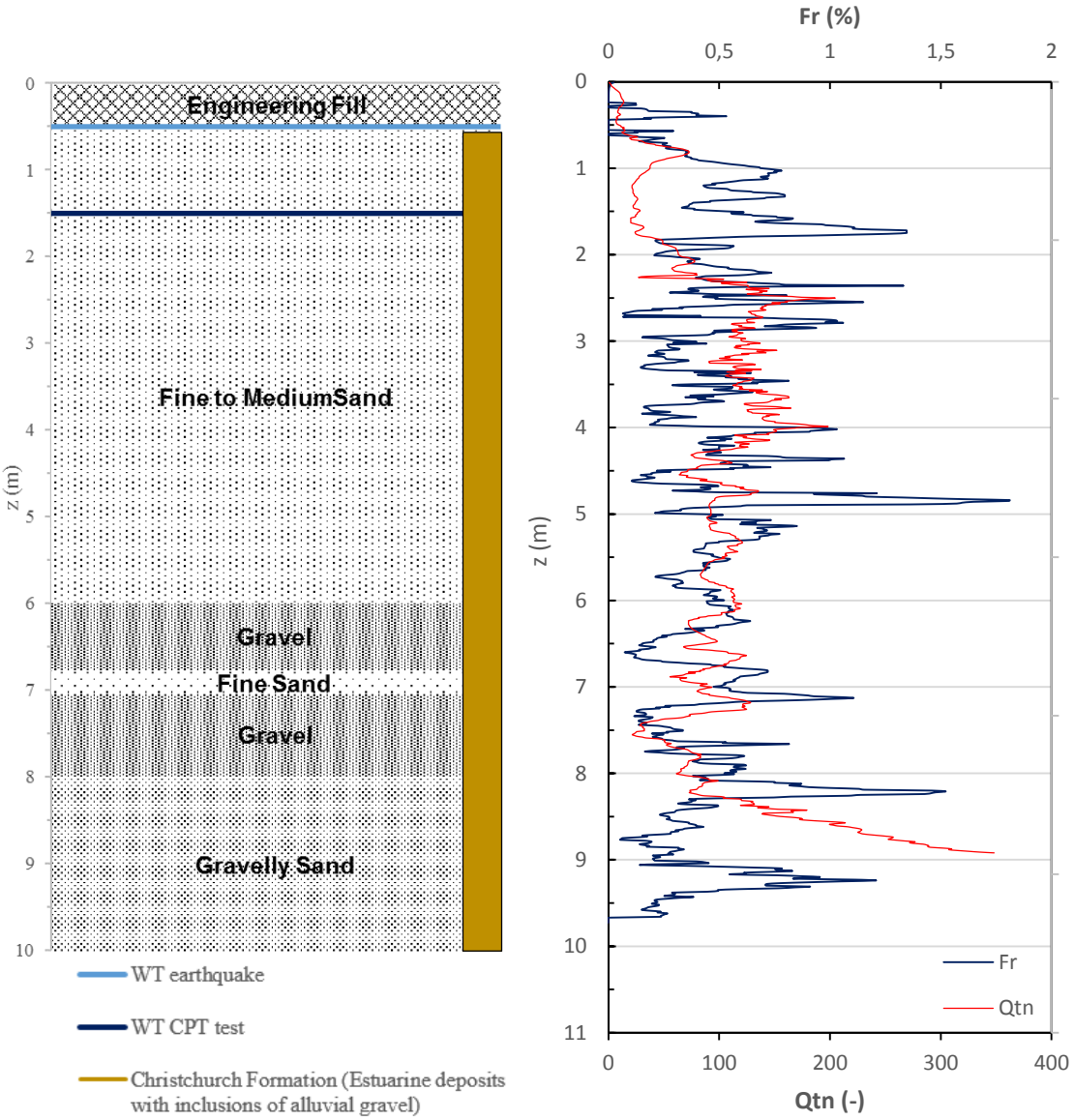

Figure 54- Plot of F_r and Q_{tn} compared with the soil stratification

4.3.2.4. CPT-KAS-19

Figure 55 presents the distance between CPT-KAS-19 location and the borehole selected to perform the soil profile. By observing the plot that gathers the normalized resistances from the CPT and the soil's stratification in Figure 56, it can be noticed some resemblance between the strata and the values of the tip resistance and sleeve friction ratio. The top silt stratum is clearly identified in the plot, with high values of the friction ratio from 1 m up to 3.5 m deep, reaching a value of 6%, and a relatively small normalized tip resistance in that range. The gravel stratum that lays around 7 m deep is also identified in the normalized tip resistance graph, once from 6 m to 8 m the values of this parameter are greater than the average, reaching 250. The values of both F_r and Q_{tn} are generally low for the entire profile, with the friction ratio under 1%, apart from the case mentioned above, and the normalized tip resistance with values lower than 50, apart from the mentioned gravel layer. It was also noticed at the depth of 9

m a huge and sudden increase in both parameters, but it is not clear that it is caused by the fine sand stratum presented in the soil profile.

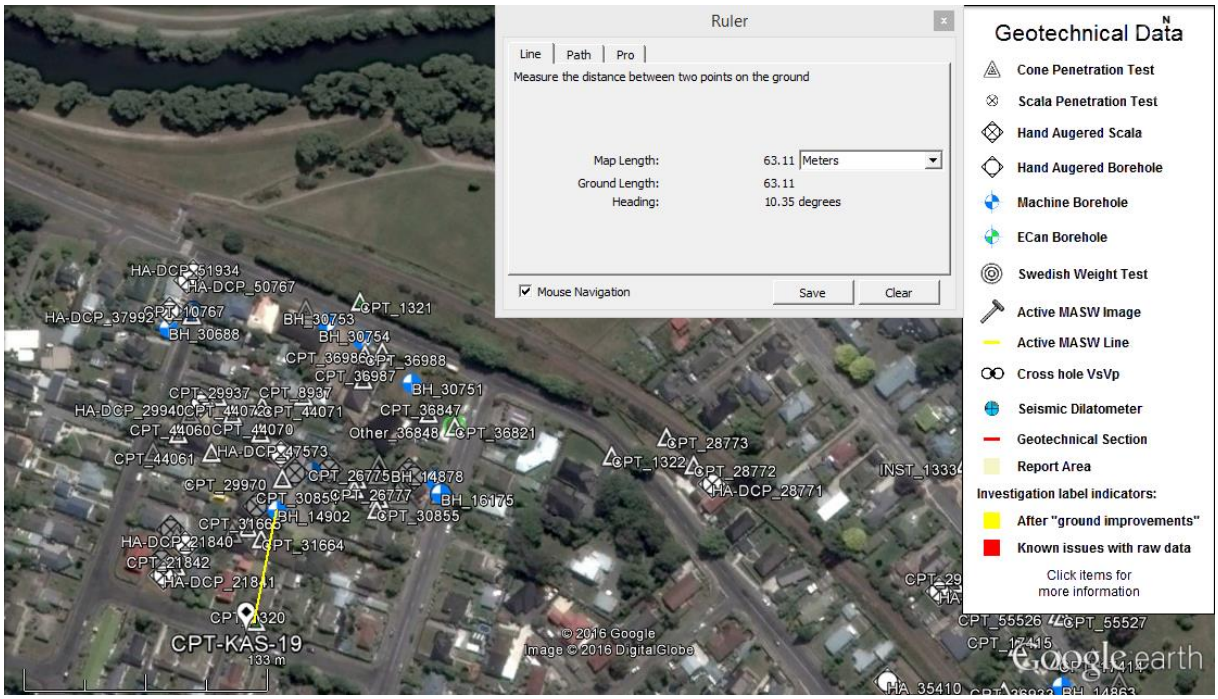

Figure 55- Distance between CPT-KAS-19 and the borehole selected to perform the soil profile, represented by the line in yellow. (New Zealand Geotechnical Database (2016) "Geotechnical Investigation Data", Map Layer CGD0010, retrieved 15/06/2016 from https://canterburygeotechnicaldatabase.projectorbit.com/)

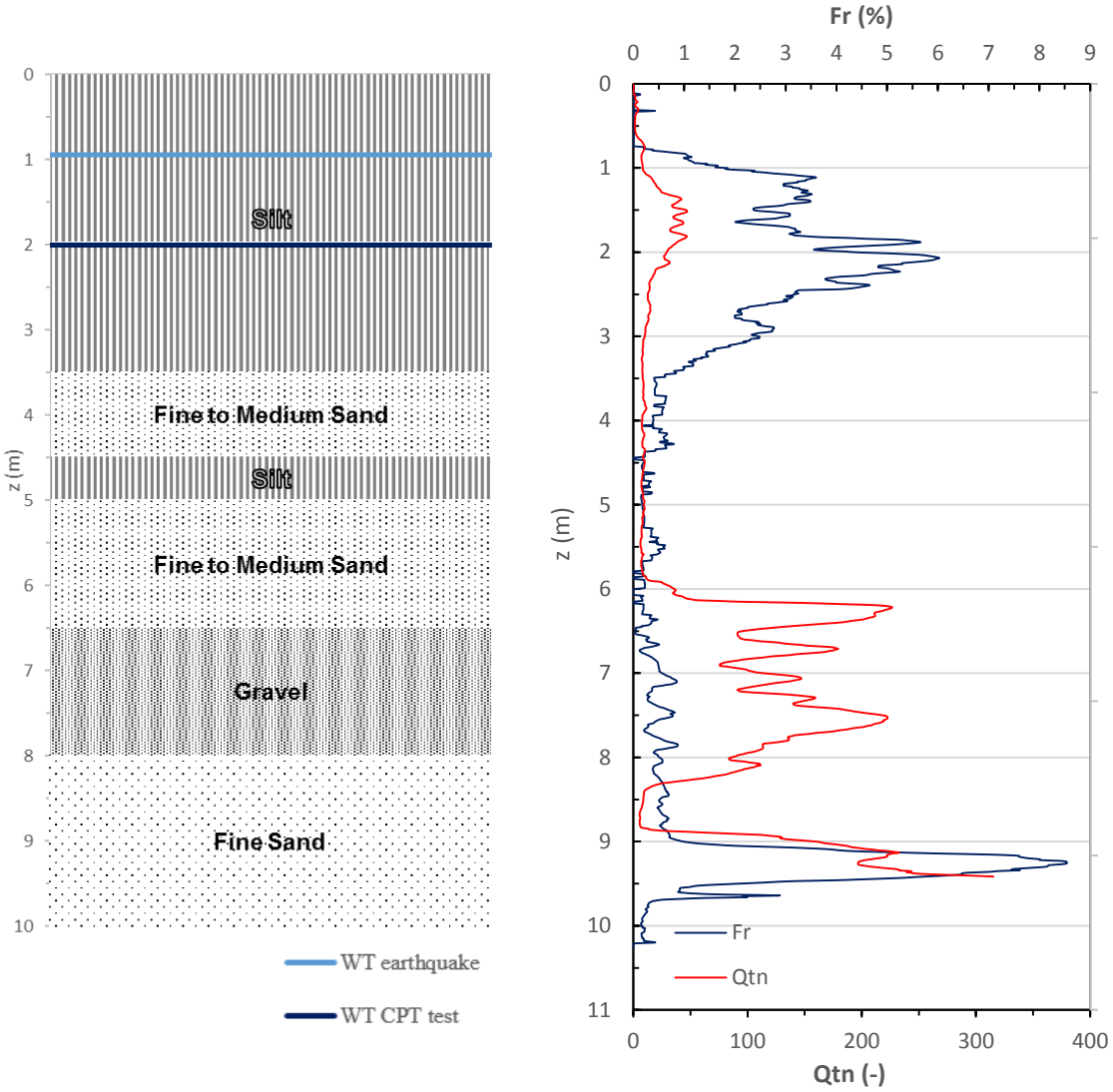

Figure 56-Plot of F_r and Q_{tn} compared with the soil profile of CPT-KAS-19

5

VALIDATION OF SOFTWARE PRODUCTS

5.1. INTRODUCTION

The validation performed in the scope of this thesis is divided in three parts. The first one has the purpose of comparing three software products that perform liquefaction analysis, and to study their limitations and the impact caused by these limitations in a liquefaction assessment. In the second part of the validation is made a comparison of the developed tool with one of the three software products. The selected software for this part of the validation was the one that presented greater accuracy as well as transparency during its assessment. Finally, the last part of the validation consists in submitting the tool to a sensitivity analysis, in order to study the effect of some modifications that were made to the original methods in the final outcome of the assessment. In this chapter only the first part of the validation will be discussed, letting the other two parts for chapter 6.

The commercial software products selected to perform the validation were CLiq v.1.7, developed by GeoLogismiki; LiquefyPro v.5.9a, from CivilTech Software; and Settle^{3D} v.3.17 from Rocscience Inc. These products were provided by the company (CH2M) and they can be used for design purposes.

The aim of performing a comparison of different software available is to understand their capabilities, as well as their limitations. The comparison between them is made by plotting the main output of the liquefaction assessment and intermediate parameters, using the same procedures against each software.

In this chapter, it is carried out at first, a brief introduction to each software, describing their capabilities and the procedures available to develop a liquefaction evaluation. Then, based on the case histories selected and their capabilities, it is performed a validation by comparing their results, followed by a discussion of the results and the limitations noticed for each one.

5.2. LIQUEFYPRO

Developed by CivilTech Software, a company specialized in structural and geotechnical software, LiquefyPro evaluates liquefaction potential and estimates settlement of soils due to seismic loads. It performs liquefaction assessments based on SPT, BPT or CPT data, implementing some of the procedures available in the literature. As the scope of this thesis is CPT-based liquefaction triggering procedures, it will only be assessed the capabilities offered by this software when an assessment is performed based on CPT data.

5.2.1. INPUT

The CPT data can be introduced in the software by importing it from a text file or by introducing it into a spreadsheet provided. Geotechnical, groundwater and seismic parameters can also be defined in the page presented for the input, with special attention for the soil unit weight and the grain size that must be defined by the user. The fine content can whether be defined, or estimated from CPT data if the Modified Robertson method is selected. Figure 57 and Figure 58 present the input pages of LiquefyPro.

LiquefyPro performs the liquefaction assessment based on two different water table values, defined by the user. One related with the earthquake, used in the calculation of CSR, and the other referent to the CPT-test, adopted in CRR calculation.

One of the limitations detected in the input was the restriction on the number of data rows handled by the software. It only allows to input data up to 1200 rows, which means that if it is required a liquefaction evaluation based on a CPT log with more data rows than the limit, the user has to manipulate the input data in order to overcome this limitation.

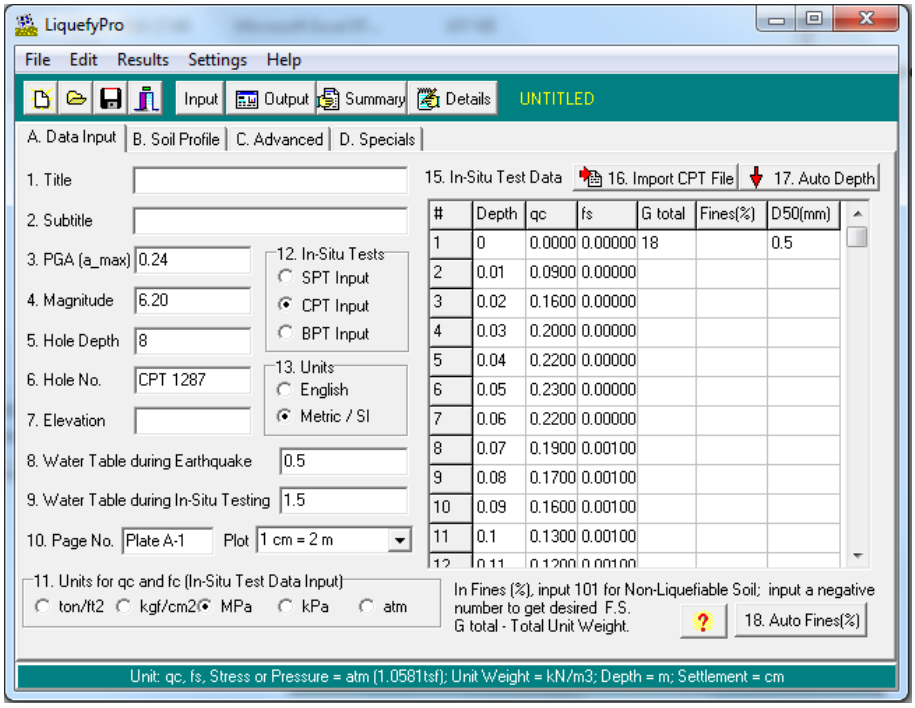

Figure 57- Example of CPT data input in LiquefyPro

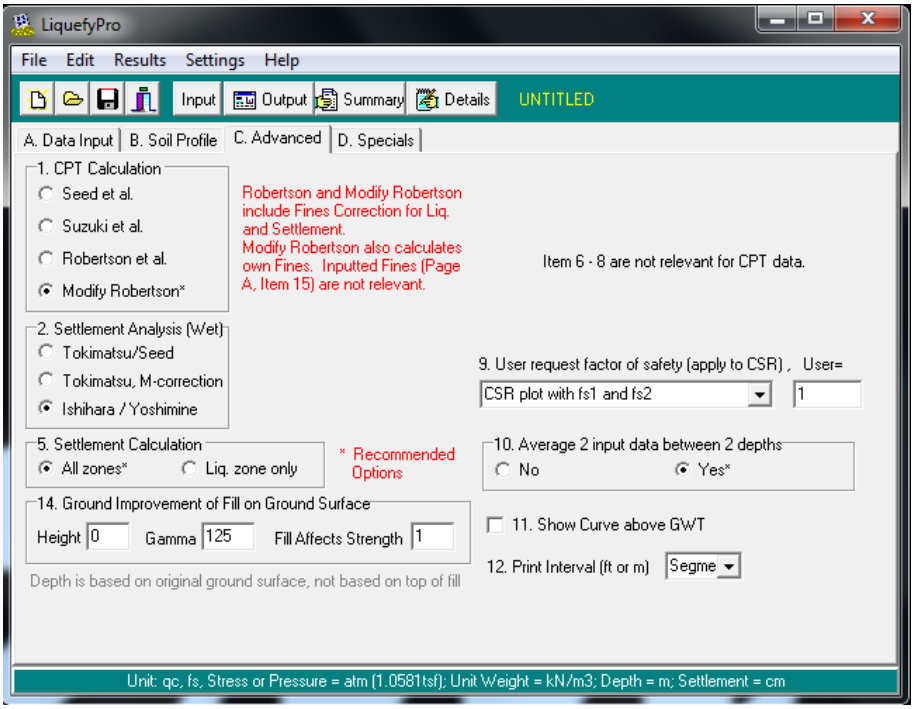

Figure 58- Selection of calculation methods in LiquefyPro

5.2.2. Capabilities and Implemented Methods

LiquefyPro performs a liquefaction evaluation by calculating the factor of safety against liquefaction, FS, and divides its estimation of settlements into dry soil and saturated soils settlements. It does not implement any probabilistic method either on the liquefaction evaluation or in the estimation of settlements.

To obtain FS, it performs the ratio of CRR by CSR, as the simplified procedure of Seed and Idriss (1971), presented in chapter 2 and equation (2). The method implemented to obtain CSR is the presented by Seed and Idriss (1971) and discussed previously on chapter 2.1.4.1.

The calculation of CRR can follow four different methods:

- Seed and de Alba (1986)
- Suzuki et al. (1997)
- Robertson and Wride (1997)
- Modified Robertson and Wride (1998)

The MSF implemented by the software is the proposed by the NCEER workshop (1997) and in Youd et al. (2001), presented in equation (23).

As discussed previously, the software divides the estimation of settlements in dry soils settlements and saturated soils settlements and for both, it converts the CPT data into SPT through relationships between $(N_1)_{60}$ and D_r. In the estimation of dry soils settlements, it implements Tokimatsu and Seed (1987), and for saturated soils the procedures available are Tokimatsu and Seed (1987) and Ishihara and Yoshimine (1992).

LiquefyPro has also the capability of assessing the influence of ground improving, by placing a fill on surface, on a liquefaction analysis.

5.2.3. OUTPUT

LiquefyPro presents the results of liquefaction analysis in the form of graphics, as the presented on Figure 59, that correlate CRR with CSR and show the Factor of Safety and the settlements along the depth. It also provides a calculation summary, in the form of a text file, presenting the input data, the calculation details and the output data.

The relevant parameters provided by the calculation report are:

- I_C;
- CRR;
- CSR;
- FS;
- Volumetric Strain for Unsaturated Sands;
- Unsaturated Sands Settlement;
- Voulmetric Strain for Saturated Sands;
- Saturated Sands Settlement;
- Total Settlement.

Though these results already present the information needed to properly perform a liquefaction evaluation, the estimation of other parameters like LPI or P_L could complement the assessment made and provide more reliability. Also, the calculation summary provided by LiquefyPro presents the output values in a form not as continuous as the CPT data introduced, providing values with 2 or 3 cm of interval and with few decimal places (only two), what may mislead to rounding errors.

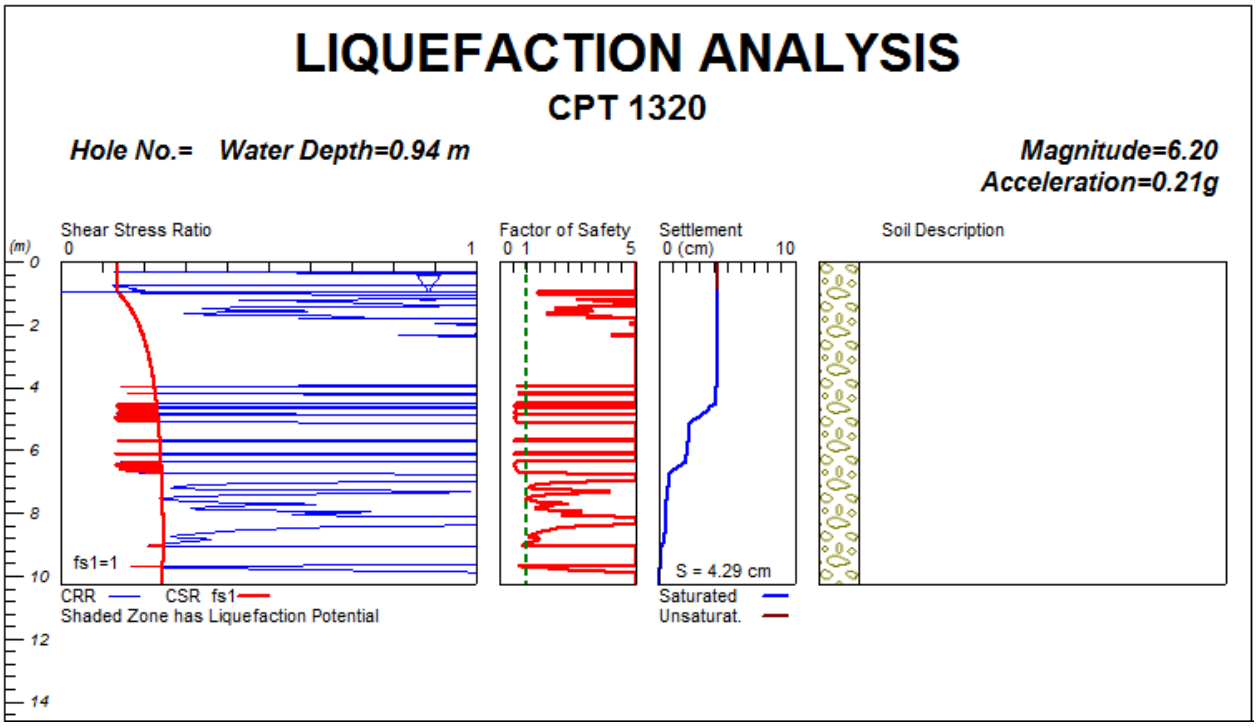

Figure 59- Example of an output graph report in LiquefyPro

5.3. SETTLE^{3D}

Settle^{3D} is a 3-dimensional geotechnical software developed by Rocscience to perform analysis of vertical consolidation and settlements, with a functionality that allows the realization of a liquefaction analysis. Only the latter feature will be discussed in the scope of this thesis, by presenting the capabilities and the procedures available to perform a liquefaction assessment.

5.3.1. INPUT

The input of CPT data on Settle^{3D} is performed by inserting the values relative to depth, cone tip resistance and sleeve friction into a spreadsheet provided, and presented here in Figure 60. The seismic parameters are also defined in this phase, as well as the geotechnical parameters, such as the unit weight and the fines content.

Some limitations were found during the input of the geotechnical parameters, since the unit weight cannot be defined alongside the CPT data. Instead, the user has to assign a value of the unit weight for a specific and defined soil layer, and in order to adopt different values in depth, it is necessary to define different soil layers along the profile.

Also, the software requires the implementation of a fines content for the soil profile. In this case, even if during the calculation is selected a method that implements a fines correction based on CPT data, the software assumes the same fines content provided by the user, instead of following the method's procedure. The input of the fines content may be done by inserting it alongside with the CPT data, or by assigning it for each defined soil layer, as in the input of the unit weight.

Other limitation was found related with the CPT values. Settle^{3D} does not correct automatically null values of the CPT data, having the user to manually correct them, or an input error is shown and the calculation is not performed.

At defining the water table, it was noticed that Settle^{3D} uses the same value whether for calculate CSR or CRR and it is up to the user to define which one to implement.

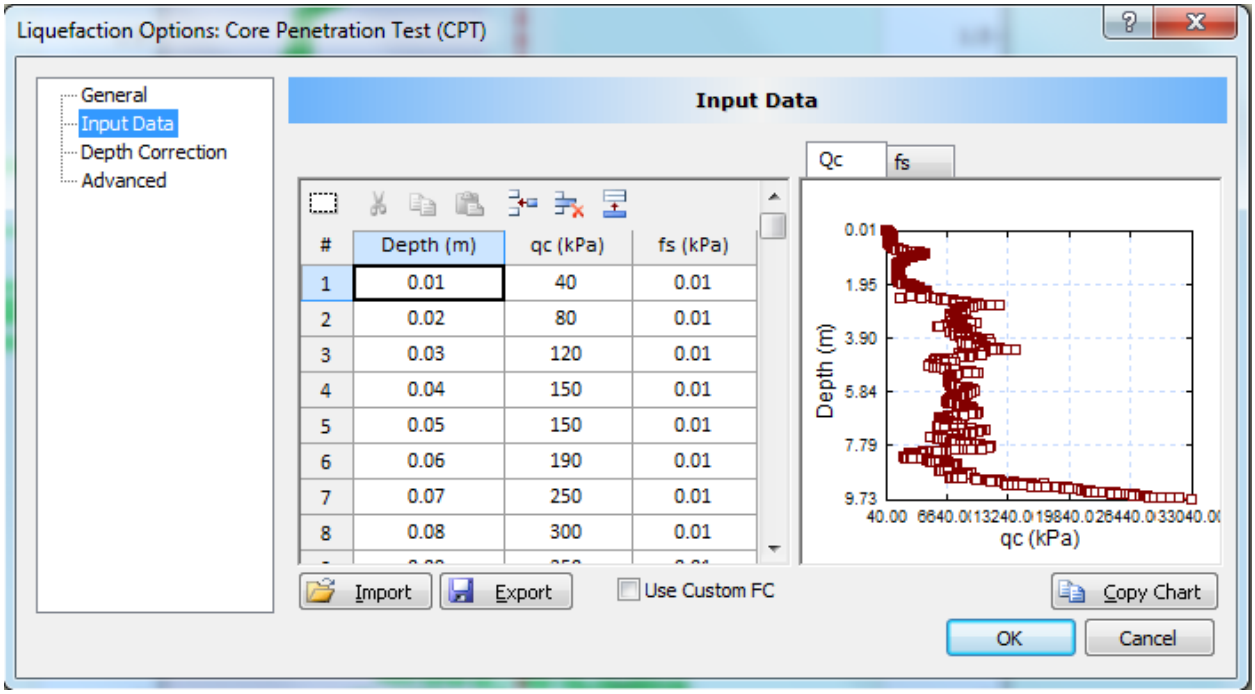

Figure 60- Spreadsheet provided by Settle^{3D} to insert the CPT data

5.3.2. Capabilities and Implemented Methods

The software presents an analysis based on CPT, SPT or VST by obtaining values for the factor of safety and probability of liquefaction along depth. The CPT procedures available to estimate CRR are:

- Robertson and Wride (1997)
- Modified Robertson and Wride (1998)
- Boulanger and Idriss (2004)
- Moss et al. (2006) – deterministic
- Moss et al. (2006) – probabilistic

The probability of liquefaction is only estimated if the Moss et al. (2006) probabilistic method is selected, so it does not estimate a probability of liquefaction based on the Modified Robertson and Wride (1998).

The calculation of CSR is performed according to Seed and Idriss (1971) procedure, while the stress reduction factor, r_d, can be estimated based on 5 different methods:

- NCEER (1997)
- Idriss (1999)
- Kayen (1992)
- Cetin et al. (2004)
- Liao and Whitman (1986)

The formulation referred as NCEER (1997), proposed in this workshop, was first defined by Liao and Whitman (1986) and it is here presented in equation (5) and (6).

As the CRR values computed from the procedures presented above are relative to a magnitude of 7.5, it is required to correct them for the earthquake magnitude by implementing an MSF. The methods available to estimate MSF are:

- Tokimatsu and Seed (1987)
- Idriss (1999)
- Andrus and Stokoe (1997)
- Idriss and Boulanger (2008)
- Youd and Noble (1997)
- Cetin et al. (2012)

It was noticed that the MSF recommended by the NCEER in the 1997 workshop, presented in Youd et al. (2001) and implemented by the other software products, is not implemented by Settle^{3D}, however, by assessing each MSF expression available on Settle^{3D}, it was noticed that the expression referred as Andrus and Stokoe (1997) presents values similar to the estimated from the proposed NCEER expression revised by Idriss after Seed and Idriss (1982), thus it will be the MSF estimation procedure implemented in Settle^{3D}.

Despite being a software in which the main functionality is the analysis of settlements, if in a liquefaction assessment is selected a CPT-based method, it does not estimate liquefaction-induced settlements.

5.3.3. OUTPUT

Settle^{3D} does not provide any intermediate calculated parameter, offering little transparency in the implementation of the methods. The parameters that can be obtained after a liquefaction analysis on Settle^{3D} are:

- R_d
- CSR
- CRR
- FS
- P_L – if a probabilistic method is selected

They are provided in the form of graphs, as presented in Figure 61, and it is possible to extract the values of these parameters along depth, into an Excel spreadsheet.

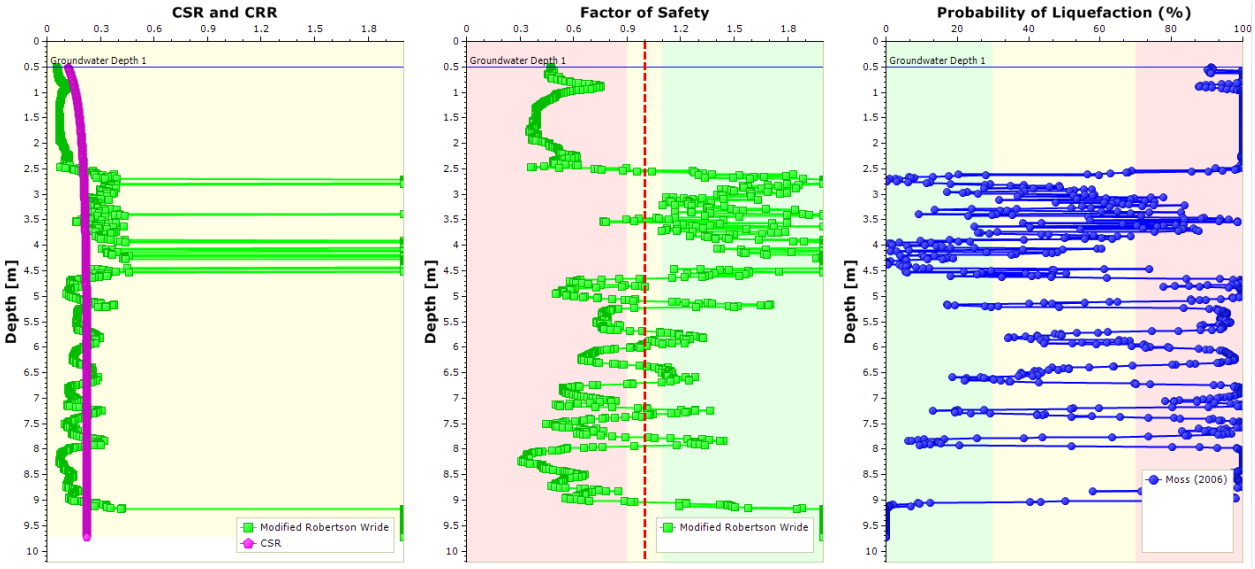

Figure 61- Example of an output provided by Settle3D

5.4. CLIQ

CLiq is a CPT-based soil liquefaction software, developed by GeoLogismiki in collaboration with Gregg Drilling Inc. and Professor Peter Robertson. The software is mainly focused on a CPT or CPTu-based assessment, once it allows to input pore pressure values, however, it also presents a functionality to perform liquefaction analysis based on SPT or V_S data. Once again, the software assessment will be made only to the methodology implemented on a CPT-based analysis.

5.4.1. INPUT

CLiq can import CPT data directly from text files or from an Excel spreadsheet, having an option that allows the user to convert the data units in the required by the software. The following step is to define the calculation parameters by introducing the seismic, geotechnical and groundwater specifications. The software allows the user to define a single value of the unit weight for the whole CPT profile; to assign different unit weight values to different defined soil layers; and also to perform a unit weight calculation based on the input CPT data, although it does not declare what method is being applied in this calculation.

CLiq uses two different water tables, defined by the user, in the calculation of CRR and CSR. The first is based on the water table at the moment of the earthquake, while the latter uses the water table measured during the CPT test.

It was noticed while using this software, that it allows great user control over the inputs and the methodology, once it is possible to change some parameters in order to adapt the calculation to the project's specifications. CLiq allows to modify the I_C threshold, with a default value of 2.6 suggested by Robertson and Wride (1998); or the limit of the correction for overburden stress, C_Q, mentioned as C_N on Robertson (2009) and on CLiq, where it is implemented the default value of 1.7 suggested by Youd et al. (2001). Figure 62 presents a part of the input where it is possible to notice the flexibility inherent to the implemented methodology.

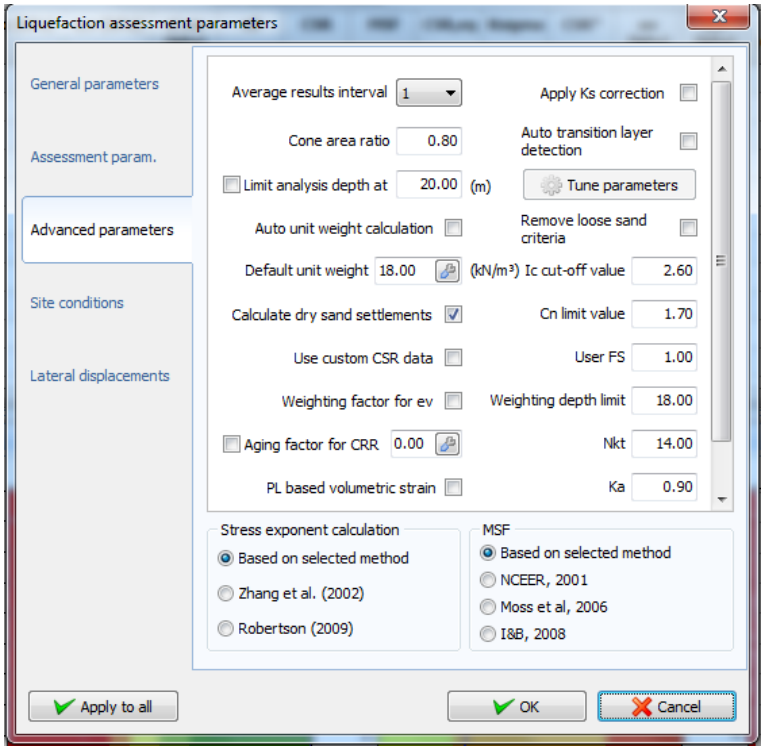

Figure 62- Example of the parameters definition in CLiq

5.4.2. Capabilities and Implemented Methods

The liquefaction assessment performed by CLiq consists on calculating the values of the factor of safety against liquefaction, probability of liquefaction, dry soils settlement and saturated soils settlement. It has also the capability to obtain lateral displacements and to check for strength loss, however these parameters will not be discussed herein.

The factor of safety is based on CRR and CSR values, as the simplified procedure of Seed and Idriss (1971). To obtain CSR, CLiq implements the Seed and Idriss (1971) procedure, presented in section 2.1.4.1., and to estimate CRR the available methods are the following:

- Robertson and Wride (1998)
- Robertson (2009)
- Moss et al. (2006)
- Idriss and Boulanger (2008)
- Boulanger and Idriss (2014)

To estimate r_d, CLiq does not implement the set of expressions recommended by the NCEER and in Youd et al. (2001), developed by Liao and Whitman (1986). Instead, it applies an alternative approach to these expressions, proposed by Blake (1996):

$$r_d = \frac{1 - 0.4113 \times z^{0.5} + 0.04052 \times z + 0.001753 \times z^{1.5}}{1 - 0.4177 \times z^{0.5} + 0.05729 \times z - 0.006205 \times z^{1.5} + 0.00121 \times z^{2}} \quad (74)$$

Where z is the depth in meters.

Opposite to Settle^{3D}, this software can also estimate the probability of liquefaction based on the deterministic Robertson and Wride (1998) and its update by Robertson (2009), by implementing the Ku et al. (2011) procedure, presented in section 2.2.2.3.

Although it suggests to implement the stress exponent based on the selected method, it also allows to choose from two different approaches for this parameter:

- Zhang et al. (2002)
- Robertson (2009)

The same procedure is implemented in the selection of the MSF expression, where it suggests to implement the one that is based on the selected method, but at the same time allows to select from the following:

- NCEER (1997)
- Moss et al. (2006)
- Idriss and Boulanger (2008)

As mentioned previously, the estimation of settlements is divided in saturated and dry soils. It is also available a feature that allows to estimate the probabilistic settlements based on the Juang et al. (2013) procedure, presented in chapter 2.4.1.2. CLiq allows the user to define and implement a threshold on the estimation of volumetric strains for clays, having 0.5% as default value, recommended by Robertson and Cabal (2015). The methods available to estimate settlements are:

- Saturated Soils Settlement:
  - Zhang et al. (2002);
  - Idriss and Boulanger (2008).
- Dry Soils Settlement:
  - Robertson and Shao (2010).

The Idriss and Boulanger (2008) settlement method is integrated in the CRR calculation procedure proposed by Idriss and Boulanger (2008) and Boulanger and Idriss (2014), thus it can only be selected if the liquefaction evaluation is based on these two methods. However, if one of these two methods is implemented, the software allows the user to estimate the settlements based on Zhang et al. (2002). Both Zhang et al. (2002) and Robertson and Shao (2010) were presented and discussed on section 2.4.

CLiq calculation report presents a modification to Robertson and Shao (2010) in the estimation of dry sand settlements. The calculation of the cyclic shear strain, γ_{cyc}, presented on equation (66), depends on the in-situ earth pressure coefficient, K_0. To simplify and avoid the calculation of this parameter, it was considered a value of 1, which may be considered as conservative for current geotechnical scenarios.

5.4.3. OUTPUT

CLiq provides a tabular and graphical presentation of all steps of the procedure, what is considered as a great advantage when compared to the other software products. The transparency noticed along the calculation allows the user to validate the methodology implemented and to assess the influence that each parameter may have in the final result. The graphical output provided by CLiq is presented in Figure 63. The output parameters provided by CLiq are:

- $CRR_{7.5}$;
- MSF;

- CSR;
- FS;
- P_L;
- LPI;
- Liquefaction Volumetric Strain;
- Saturated Soil Settlement;
- Dry Volumetric Strain;
- Dry Soil Settlement;
- Total Settlement;
- Probabilistic Settlement.

CLiq also presents the intermediate steps of the calculation that can easily be exported to an Excel spreadsheet. Assessing Robertson (2009) the parameters provided are:

- Normalized penetration resistance, Q_{tn}
- Normalized Friction Ratio, F_r
- Soil Behaviour Type Index, I_C
- Fines Correction Factor, K_C
- Clean Sand Resistance, $Q_{tn,cs}$

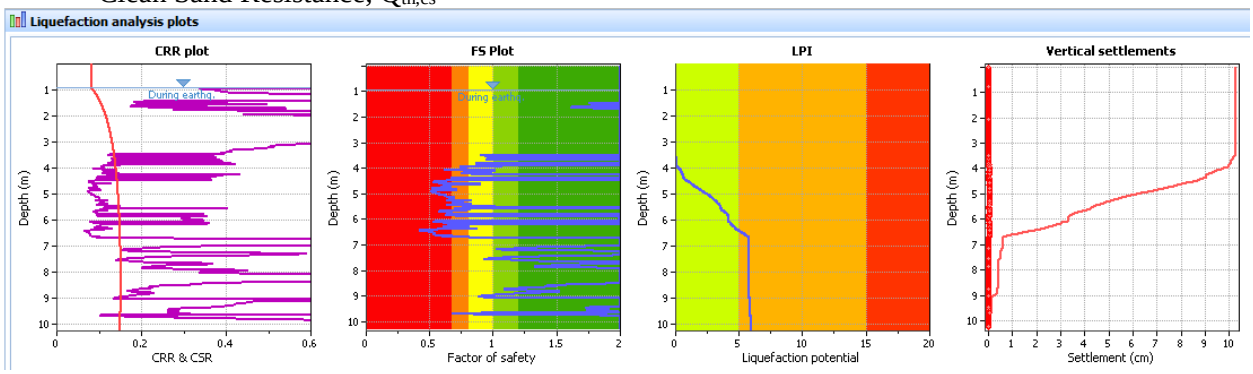

Figure 63- Example of the graphical output provided by CLiq

5.5. Comparison of Software Products

To validate the three software products, it was decided to perform a liquefaction assessment of the three selected case histories and compare the final results of the calculation and some intermediate parameters. The parameters were selected based on their relevance and whether the software products provide them or not. The comparison is then based on:

- I_C - only in LiquefyPro and CLiq;
- CRR;
- CSR;
- FS;
- Saturated Soils Settlement – only in LiquefyPro and CLiq;
- Dry Soils Settlement - only in LiquefyPro and CLiq.

For some specific cases other parameters may be presented in order to help and improve the discussion.

Since Settle^{3D} does not provide a settlement estimation if implemented a CPT-based procedure, it was only possible to compare settlements calculated by LiquefyPro and CLiq. Although it is not possible to implement the same procedure in both for this calculation, it was decided to select for saturated soils

settlement, Tokimatsu and Seed (1987) and Ishihara and Yoshimine (1992) in LiquefyPro, and Zhang et al. (2002) in CLiq. For the calculation of dry soils settlement, it was implemented Tokimatsu and Seed (1971) in LiquefyPro and Robertson and Shao (2010) in CLiq. These options allow to check for the differences between the methods by comparing the results.

I_C values are also compared, although only LiquefyPro and CLiq provide them.

The only method to estimate $CRR_{7.5}$ shared between the three software products was Robertson and Wride (1998), referred as Modified Robertson and Wride on LiquefyPro and Settle^{3D}, thus it was selected to perform the validation. To estimate MSF, it was selected the NCEER recommendation for LiquefyPro and CLiq and the Andrus and Stokoe (1997) expression for Settle^{3D}, since it provided similar results. CSR calculation was based on Seed and Idriss (1971). The stress reduction factor, r_d, was estimated by implementing the expressions proposed by Liao and Whitman (1986) and recommended by NCEER in LiquefyPro and Settle^{3D}, and the equation presented by Blake (1996) in CLiq. Since the latter method to estimate r_d provides similar results to the former, the assumption of different alternatives should not make the further comparison inaccurate.

The limitation presented by LiquefyPro on the maximum number of rows allowed to input CPT data, makes impossible to introduce CPT-NBT-03 in the software, since this test was performed up to 18.07 m deep with 1 cm of interval between successive measurements (about 1800 data rows). In order to surpass this limitation, the CPT data was manipulated by introducing it with 2 cm interval between rows, which may produce an error on the final result of the assessment, since a significant part of the information collected from the CPT was not introduced.

Due to the limitations presented on Settle^{3D} regarding the fines content input and the definition of a single water table, it was required to manipulate the calculation in order to allow a comparison with the other software products. The implemented procedure was:

- Perform a fines content calculation outside the software based on Modified Robertson and Wride (1998) and introduce the calculated values on Settle^{3D} as an input. As the FC depends on I_C, this latter parameter was extracted from CLiq;
- Perform liquefaction analysis based only on the water table during earthquake. Ideally it should be made two liquefaction analysis for each case history, one with the water table during the CPT, from which would be extracted CRR, and another with the water table during the earthquake, providing CSR. However, Settle^{3D} only estimates CSR and CRR for depths below the water table, what makes unreasonable to compare both values.

Considering all this, the methodology implemented to perform the validation is gathered on Table 10:

Table 10- Methodology implemented on the validation of the three software products

	LiquefyPro	Settle^{3D}	CLiq
CRR	Robertson and Wride (1998)	Robertson and Wride (1998)	Robertson and Wride (1998)
MSF	NCEER	Andrus and Stokoe (1997)	NCEER
CSR	Seed and Idriss (1971)	Seed and Idriss (1971)	Seed and Idriss (1971)
R_d	Liao and Whitman (1986)	Liao and Whitman (1986)	Blake (1996)

Dry Soils Settlement	Tokimatsu and Seed (1987)	-	Robertson and Shao (2010)
Saturated Soils Settlement	Tokimatsu and Seed (1987); Ishihara and Yoshimine (1992)	-	Zhang et al. (2002)
Considerations	Manipulation of CPT-NBT-03 to comply the limitation on the input.	Analysis made for water table at the earthquake; Input previously estimated fines content.	-

Note that in the plots legend some assumptions were made regarding the naming of software products or methods in order to simplify the presentation, thus hereafter:

- LiquefyPro is referred as LP;
- Settle^{3D} is referred as S3D;
- CLiq is referred as CL;
- Water Table at the earthquake is referred as WTe;
- Tokimatsu and Seed (1987) is referred as TS87;
- Ishihara and Yoshimine (1992) is referred as IY92;
- Zhang et al. (2002) is referred as Z02;
- Robertson and Shao (2010) is referred as RS10.

5.5.1. CPT-NBT-03

As presented on chapter 4.3.2., at the site location where this CPT was performed, it was noticed, from aerial photographs, moderate to severe liquefaction after the earthquake event of Christchurch, producing a settlement in the range of 10 to 20 cm. The results of the liquefaction assessment performed in the three software products will be compared with this information presented in the database. The soil characterization for this location is presented in Figure 52 alongside with the CPT data.

5.5.1.1. Liquefaction Evaluation

An analysis of the I_C plot presented in Figure 64 reveals great similarity between the values calculated from the two different software products, apart from the upper zone. In this area the values are more distinct, once it was noticed that LiquefyPro does not implement the threshold of 1.7 for the overburden stress correction factor, C_Q, proposed by Youd et al. (2001) to avoid large C_Q values at shallow depths due to low overburden pressure. It is also noticed that apart from the peat and silt strata that lay at shallow depths (as noticed in Figure 52), the soil column is entirely constituted by soil with sand-like behaviour.

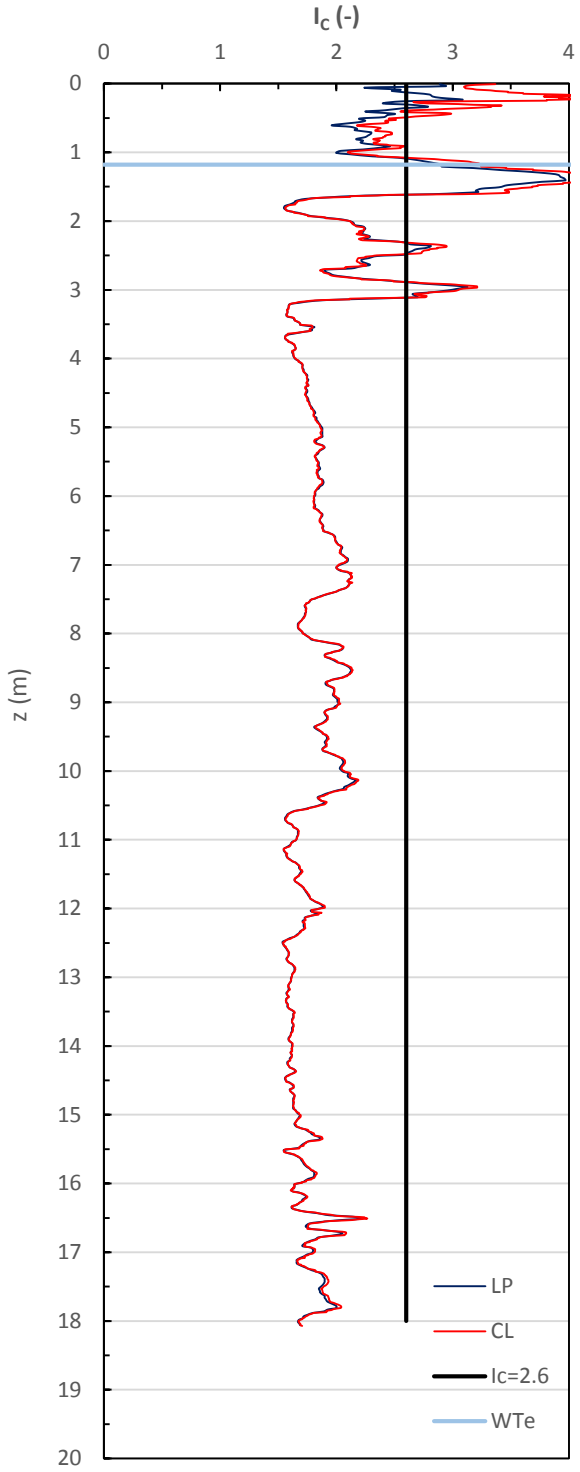

Figure 64- Comparison of I_C values estimated in CLiq and LiquefyPro

It is noticed in Figure 65a) a great resemblance between the CRR values estimated from CLiq and LiquefyPro apart from the first meters, where CLiq applies a value for CRR of 4 above the water table,

since the soil within this region will not liquefy. Herein, the threshold for CRR of CLiq was modified to 2, in order to agree with the value implemented by LiquefyPro and Settle^{3D}.

Although the shape of the CRR curve from Settle^{3D} is similar to the estimated by CLiq and LiquefyPro, it is much less conservative, providing higher CRR values than the other two products for the entire profile. The reason for this overestimation of the resistance is not very clear, once this software does not provide any intermediate calculation that could help understanding if an improper implementation of the method is performed. One of the reasons could be the MSF implemented by Settle^{3D}, different from the recommended by NCEER that is used by the other two software products. However, since for the earthquake magnitude of 6.2, the MSF implemented in Settle^{3D} has a value of 1.628 and the MSF proposed by the NCEER is 1.62, that might not be the reason of the gap noticed. It could also be related with the fines content correction, since it was noticed that the software has some limitations in this field. The implemented Robertson and Wride (1998) method is capable of performing a fines correction based only on the CPT data, however, Settle^{3D} requires the input of the fines content by the user when implementing this method. Following the same logic, the software may also be performing a fines content correction different than the proposed by the method, but as it was already mentioned, without any intermediate calculation results, it is not possible to completely understand what is being performed in the software and hence the reason behind the overestimation of the resistance.

The method to estimate CSR and r_d is the same for the three software products, apart from CLiq that implements for the stress reduction factor the expression proposed by Blake (1996). However, by analysing the CSR plot in Figure 65a), it is noticed great similarity between the three estimations, thus the implementation of these different approaches for r_d does not have any considerable impact on the final results. The major differences are noticed at greater depths, where r_d values obtained from CLiq start to differ from the estimations of the other two software products. Also, the fact that LiquefyPro provides its output with less precision (only presents two decimal places maximum) and with higher spacing between depths (values are presented with 2 or 3 cm interval), causes in parameters with little variation in depth, as CSR, little continuity, as it can be noticed.

The plot of the factor safety in Figure 65b) reflects what was noticed in the CRR, there is great resemblance between the estimations of LiquefyPro and CLiq, apart from higher depths, where CSR starts to have some differences. However, this noticed gap between the two estimations does not have a major effect on the final evaluation, since the layers evaluated as liquefiable are the same for both of them, only with CLiq being slightly more conservative. The overestimation of the resistance by Settle^{3D} is also reflected in the FS plot, with this software providing higher factor of safety values and less and thinner liquefiable layers. It can be concluded from analysing the plots that the CPT data manipulation performed in LiquefyPro to allow its input, did not produce a significant error in the evaluation results.

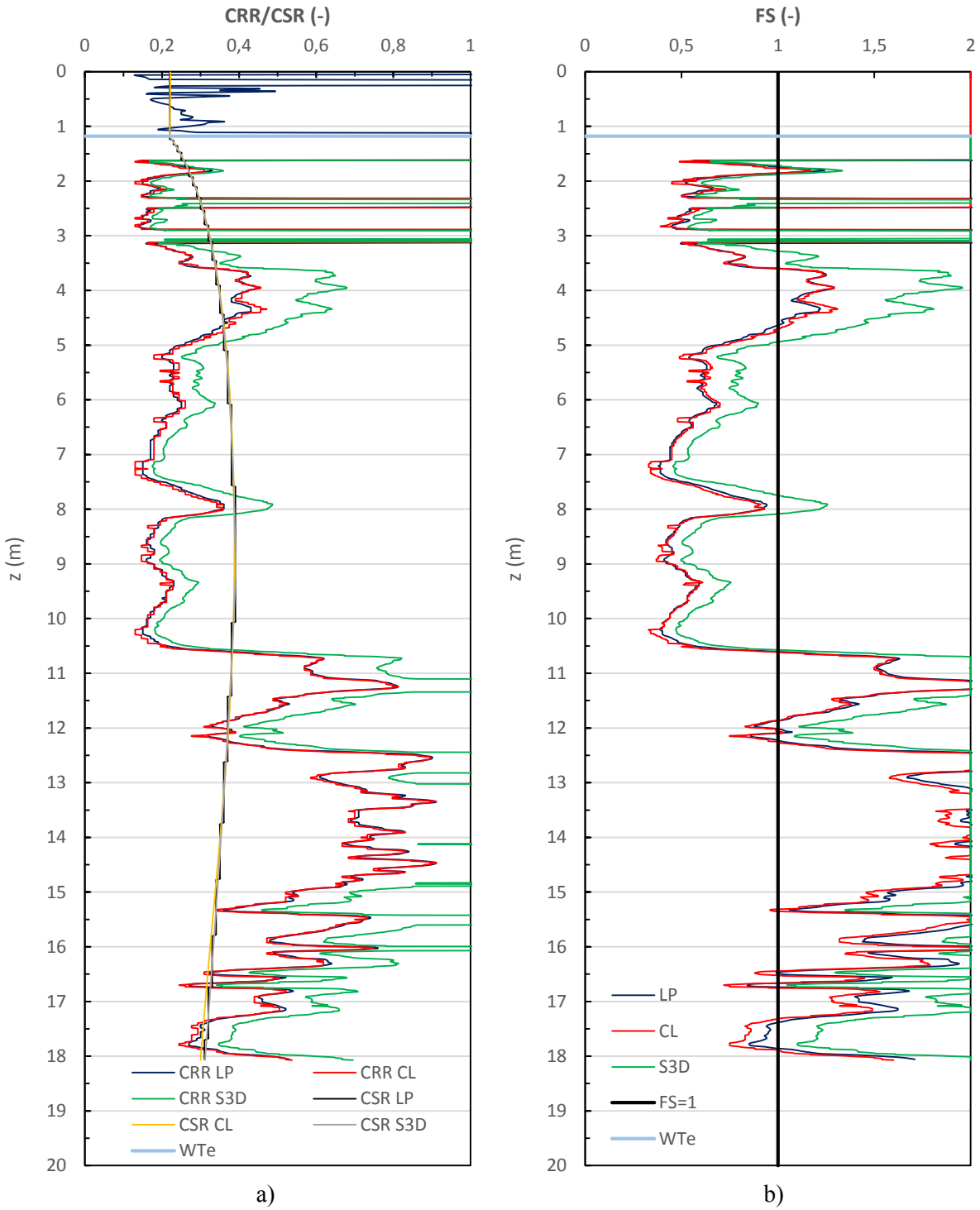

Figure 65- Comparison of values estimated by the three software products for CPT-NBT-03: a) CSR/CRR; b) FS

It is noticed in Figure 65b), a major liquefiable layer within the Christchurch formation, with a thickness of 6 m starting at the depth of 4.5 m, and other three less thick layers between 1.5 m and 3.5 m. The noticed liquefiable layer is almost in agreement with the critical layer proposed for this case history in

Green et al. (2014), since this study, based on geotechnical properties of the soil and liquefaction surface manifestations, presents a critical layer about 3 m thick, starting at the depth of 7 m. It is also possible to observe the effect of the fines of the silty sand layer in the value of the factor of safety, once that this layer that lays around 4 m deep it is considered as non-liquefiable.

The information available in the database and already presented in this thesis, points to a moderate to severe liquefaction occurrence in this location, which is in total agreement with the result of the liquefaction evaluation performed of several liquefiable layers at shallow depths.

5.5.1.2. Liquefaction-Induced Settlements

The comparison of the settlements estimated by LiquefyPro and CLiq is presented on Figure 66. It were implemented three different methods in the calculation of saturated soil settlements to better understand their differences.

Starting by saturated soils, in Figure 66a), the methods implemented by LiquefyPro produced the same final settlement at surface of approximately 22 cm, although the evolution of the settlement in depth is completely different. In Tokimatsu and Seed (1971) it was estimated an almost uniform settlement of the entire soil column, from the water table and until the final soil layer, while in Ishihara and Yoshimine (1992), despite the settlements are also being estimated until the final of the soil column, they are more influenced by the liquefiable layers, being noticed a greater slope in this depths.

The method implemented by CLiq, Zhang et al. (2002), was based on Ishihara and Yoshimine (1992), so it is noticed some resemblance between their plots, more specifically in the shape of their curves. It is possible to observe that CLiq only predicts a contribution to the settlement, in this case, of layers up to 12 m deep, unlike the methods implemented in LiquefyPro. However, it is more conservative, estimating higher settlements for the same liquefiable layers, resulting in a ground settlement about 1 cm higher. All of the methods predict settlements not only for liquefiable layers, although, apart from Tokimatsu and Seed (1987), these layers have a greater impact, being responsible for most of the ground settlement predicted.

Analysing the unsaturated soils settlement predicted in Figure 66b), it is noticed that there is no correspondence between both estimations, either in the ground settlement or in its evolution in depth. In this case, the method implemented by LiquefyPro (Tokimatsu and Seed, 1987) is much more conservative, predicting a ground settlement about four times higher than the predicted in CLiq (Robertson and Shao, 2010). Regarding the evolution of the settlement in depth, it is noticed that the estimation made by LiquefyPro predicts the contribution of only two thin layers (less than 5 cm thick) at the depths of 0.1 m and 0.85 m for the ground settlement, while CLiq forecasts a thicker layer (a little more than 50 cm thick) settling at 0.5 m deep. Nevertheless, the dry soils settlement has little expression in the total settlement of the soil column, with the more conservative estimation predicting a value of 0.02 cm for this parameter. Note that the plot only presents values in depth up to the water table, in order to have a clearer perception.

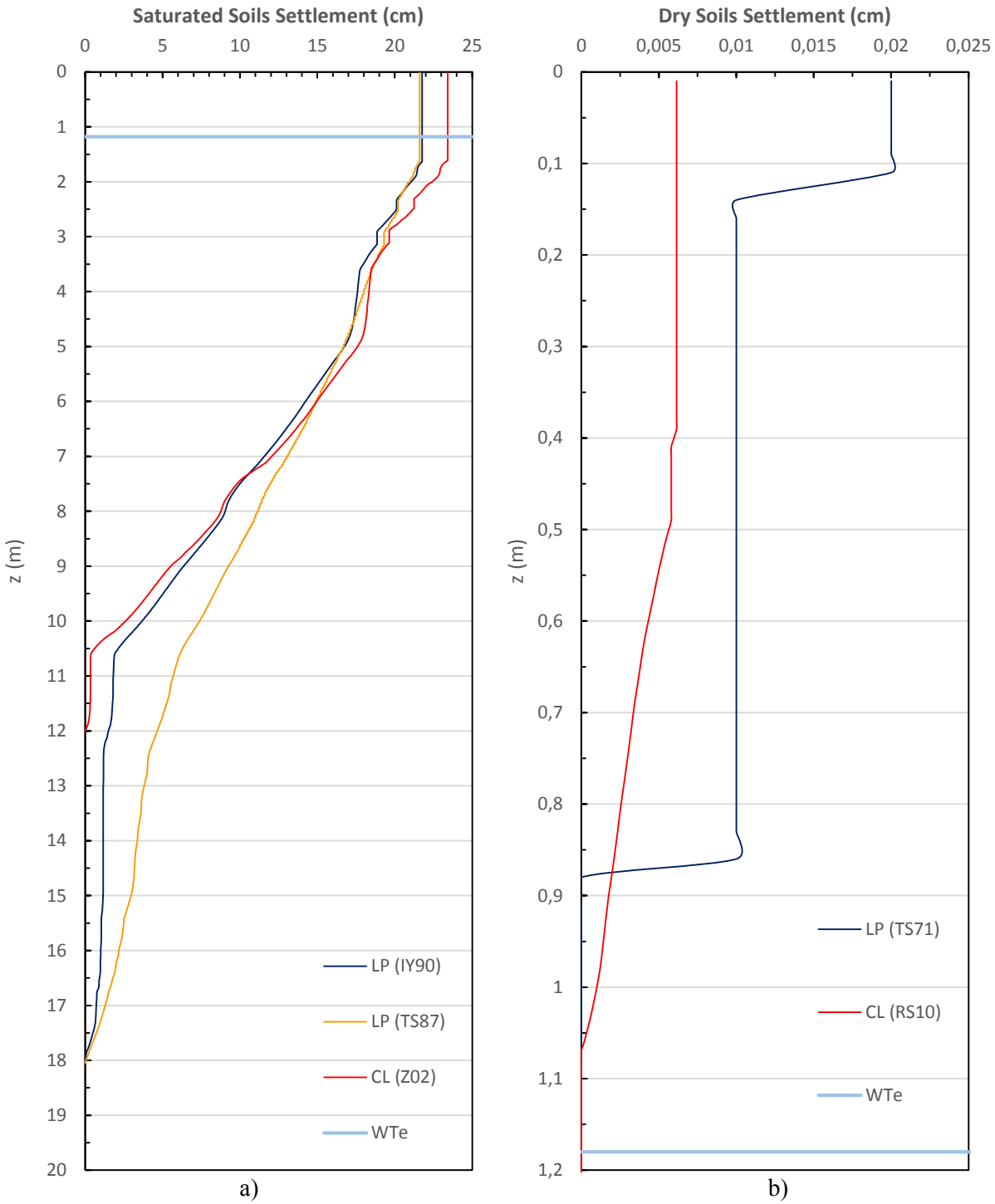

Figure 66- Comparison of settlements estimated by LiquefyPro and CLiq for CPT-NBT-03: a) saturated soils; b) dry soils.

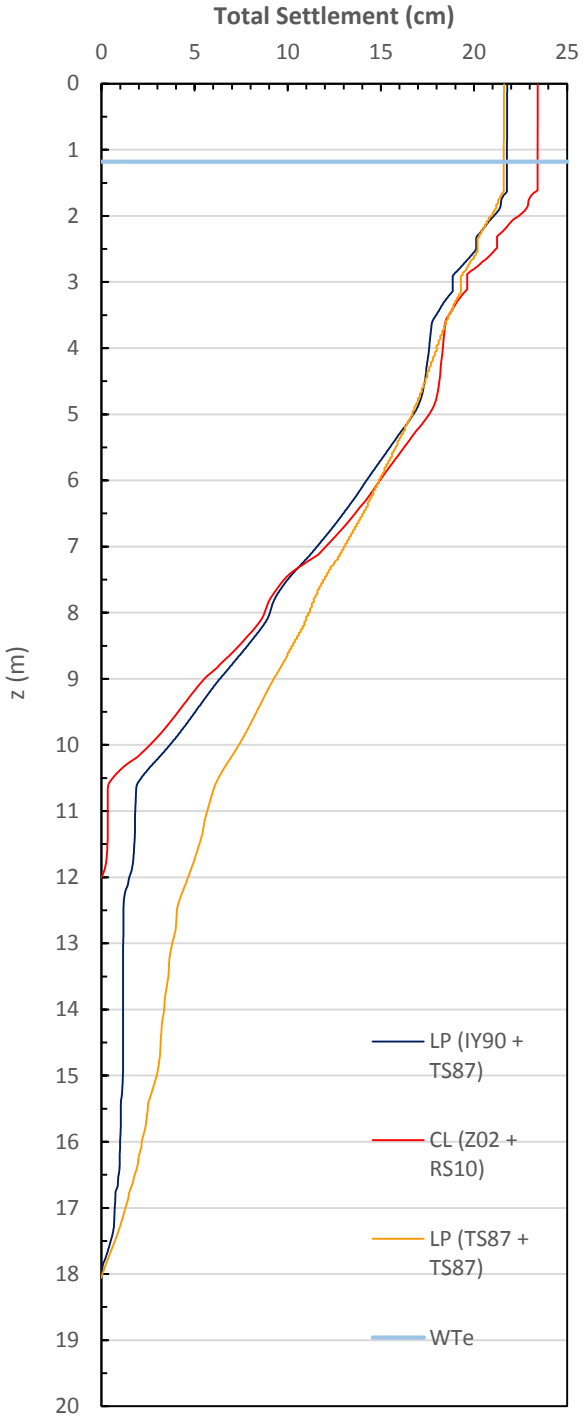

Figure 67-Total Settlement estimated by LiquefyPro and CLiq for CPT-NBT-03

The total settlement predicted by the software products, and presented on Figure 67, is between 20 and 25 cm, which is slightly higher than the values presented in the database for this location and estimated based on Digital Elevation Models, of 10 to 20 cm. The error associated to the vertical elevation changes

estimation in the database, along with the conservatism inherent to the implemented methods, lead to the difference noticed between the settlement estimations.

5.5.2. CPT-KAN-26

At this CPT location it was observed and registered minor liquefaction, based on aerial photographs, resulting in a settlement in the range of 0 to 10 cm. This values will be compared with the results from the assessment after the calculation is done. The characterization of the soil for this location is presented in Figure 54.

5.5.2.1. Liquefaction Evaluation

Figure 68 provides the comparison between the I_C values estimated from LiquefyPro and CLiq. According to what was noticed in the analysis to the I_C plot of CPT-NBT-03, in this case there is also a great resemblance between the two different estimations apart from the upper area, where LiquefyPro does not implement the limit value for C_Q, recommended in Youd et al. (2001), what produces high and unreasonable values of this parameter. The entire soil profile, apart from the first 0.5 m, has I_C values that fall under the threshold of 2.6, what corroborates the presented stratification composed by sand strata in Figure 54.

It was noticed during the assessment of LiquefyPro, that this software was performing a implementation of the fines content correction different than the proposed by Robertson and Wride (1998). This method assigns a value of 1.0 to K_C if the soil has an I_C between the values of 1.64 and 2.36 and F is lower than 0.5%, as presented in equation (22). However, for the depths in which the soil respects these conditions, LiquefyPro does not follow the method and implements equation (20). This issue can be noticed in Figure 69, where it is presented side by side, the plots I_C, F and K_C estimated by LiquefyPro. It is possible to observe that in the depths where the soil respects the I_C and F conditions presented above, K_C has a different value than 1.0, therefore the method is not being followed. This issue is noticed at several depths along the soil column and it may cause a less accurate liquefaction evaluation.

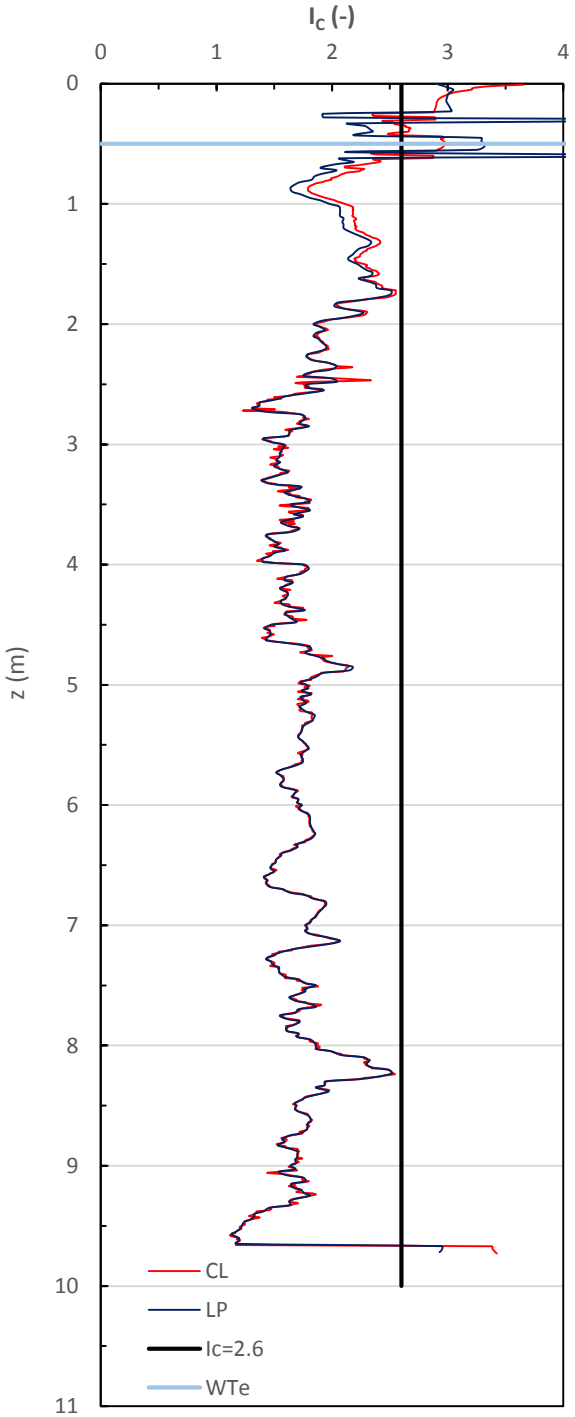

Figure 68- Plot comparing I_C values estimated by LiquefyPro and CLiq

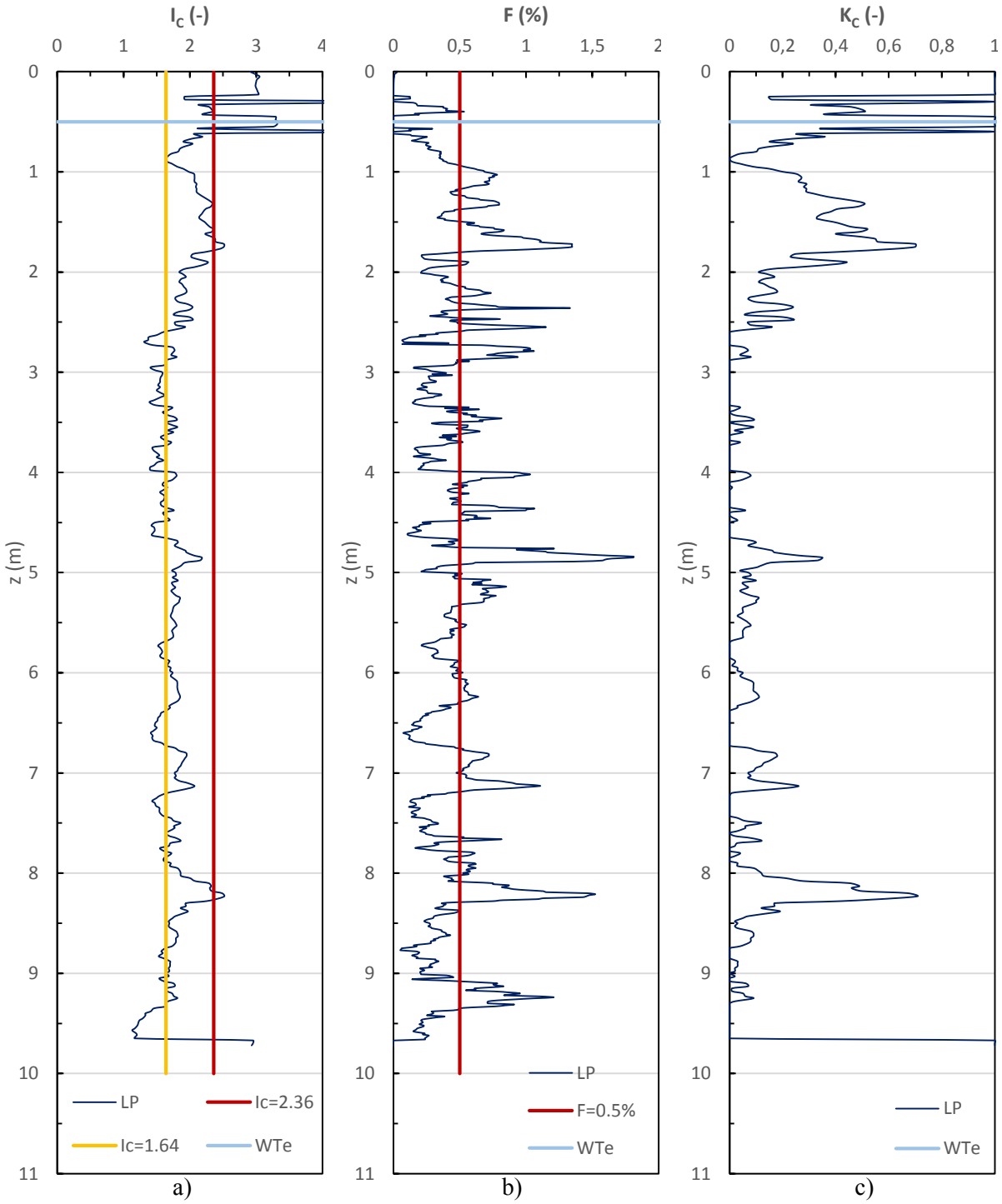

Figure 69- Comparison of values estimated by LiquefyPro: a) I_C; b) F and c) K_C

By analysing the CRR plot in Figure 70a), it is noticed the effect of the different implementation of the fines content correction in LiquefyPro on the estimation of this parameter, especially at the depth of around 1 m where it can be observed a huge discrepancy between the estimations of LiquefyPro and

CLiq. At other depths where LiquefyPro is also estimating the fines content correction different than the approach proposed by the method, as it is noticed in Figure 69, this issue has little expression on CRR values, with the estimations from both software products producing less distinct values. The fact that LiquefyPro is presenting a less conservative value of CRR at the depth around 1 m, due to the fines content correction estimation implemented, has a considerable impact in the values of FS (Figure 70b)). As it can be noticed, at this same depth there is a disagreement between the liquefaction evaluation of LiquefyPro and CLiq, with the first software defining the soil layer as non-liquefiable, whereas the latter computes a FS value lower than 1.0 for the same soil. There is then a disagreement between the layers defined as liquefiable by both software products, and considering that the soil in question lays at a considerable shallow depth (0.5 m) and it has a thickness of about 25 cm, it can be concluded that the improper implementation of the fines content correction in LiquefyPro has some impact on the results of the liquefaction evaluation.

Settle^{3D} reveals once again overestimation on the calculation of CRR and consequently FS, which causes an estimation of less and thinner liquefiable layers. This issue has greater expression in depths between 2.5 and 7 m, where it is noticed a considerable gap between the curve estimated by this software and the others. The cause of this difference is once again unclear and difficult to assess without knowing the intermediate calculations made within Settle^{3D}, although it is reasonable to consider that it may have to do with a fines content correction different than the proposed by the method.

The CSR estimation provides once again similar results between the three software products, even with a different method being implemented for r_d in CLiq (Blake, 1996).

By analysing the plot of FS, it is noticed an agreement between the values computed from both LiquefyPro and CLiq, apart from the upper area already discussed above. Nevertheless, CLiq is clearly more conservative, providing for the entire depth, values of FS lower than the predicted from LiquefyPro and consequently Settle^{3D}. This does not have great impact in the final result in this case, once that the only problem noticed where both software products define differently the same layer, according to its liquefiability, is related to a different implementation of the method, rather than a lack of conservatism.

The assessment carried out, provides two different liquefiable layers to consider. One more critical, due to its closeness to the surface (about 1 m deep and 1 m thick) and other at the depth of 8 m and about 1 m thick. Thus, it can be claimed that the assessment results are in agreement to the interpretation of liquefaction available in the database and presented herein, considering that minor liquefaction occurred in this location. Also, the case study developed by Green et al (2014), presents for this case history and based on CPT data, I_C, D_r and the liquefaction manifestations observed, a critical layer that matches this one. Green et al. (2014) also states: “For example, the relatively loose and thin upper critical layer has a depth-thickness-density combination that could result in minor surface manifestations if it liquefied.”

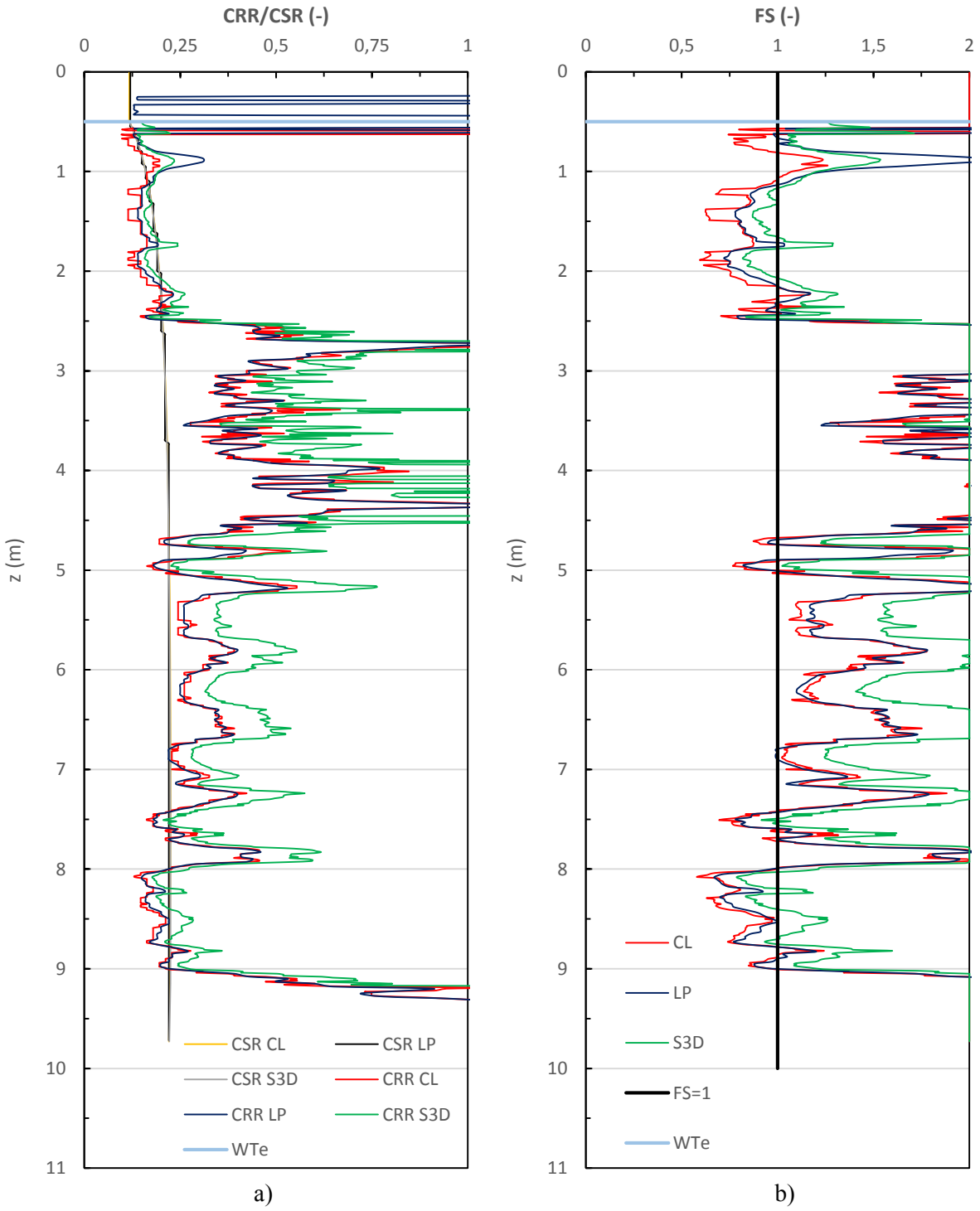

Figure 70- Comparison of parameters estimated from three software products for CPT-KAN-26: a) CRR/CSR; b) FS.

5.5.2.2. Liquefaction-Induced Settlements

Figure 71 presents the estimation of settlements in LiquefyPro and Settle^{3D}, implementing the methods already mentioned. As it was noticed in CPT-NBT-03, for saturated soils Tokimatsu and Seed (1987) presents an evolution of settlements in depth smoother than the other two methods, estimating a settlement almost uniform for the entire soil column, while in Ishihara and Yoshimine (1992) and in Zhang et al. (2002) it is more influenced by the layers defined as liquefiable, noticed by the slope of the curve at the depths of 1 m and 8 m. An analysis to the ground settlement shows, once again, more conservatism in the values estimated by CLiq than the two methods implemented in LiquefyPro. Zhang et al. (2002) predicts a settlement of about 11 cm, while Tokimatsu and Seed (1987) estimates a value slightly lower than 9 cm and Ishihara and Yoshimine (1992) has the less conservative forecast of the three, with a value around 8 cm. The differences between the estimation made by CLiq and LiquefyPro, using the Ishihara and Yoshimine (1992), are greater in the upper liquefiable layer, around 1 m deep, with CLiq predicting higher values of settlements for this area, proven by the greater slope noticed in its curve, and resulting in a ground settlement almost 1.5 times higher.

The method implemented in LiquefyPro for the estimation of dry soils settlement (Tokimatsu and Seed, 1987), predicted no settlement in the location of CPT-KAN-26, as it is noticed in Figure 71b), whereas CLiq (Robertson and Shao, 2010) estimated a ground settlement due to dry soils of about 0.0222 cm, an extremely low value that barely affects the total ground settlement. The reason for LiquefyPro not predict a settlement of these soils is not very clear, since it may be related with the lack of precision of the output values provided by LiquefyPro or with a lack of precision of the method.

Figure 72 presents the total settlement estimated, obtained by combining the approaches of LiquefyPro and CLiq for both dry and saturated soils settlement. The information available in the database points to the occurrence of a settlement in the range of 0 to 10 cm in the CPT-KAN-26 location, caused by the 2011 Christchurch event. Comparing this value with the predicted from both products, it is concluded that it is in agreement with LiquefyPro estimations, and that CLiq predicted a higher value. However, it is not reasonable to consider the CLiq estimation less accurate based only on this, once the estimation of the settlement range available in the database is not very accurate, as discussed previously.

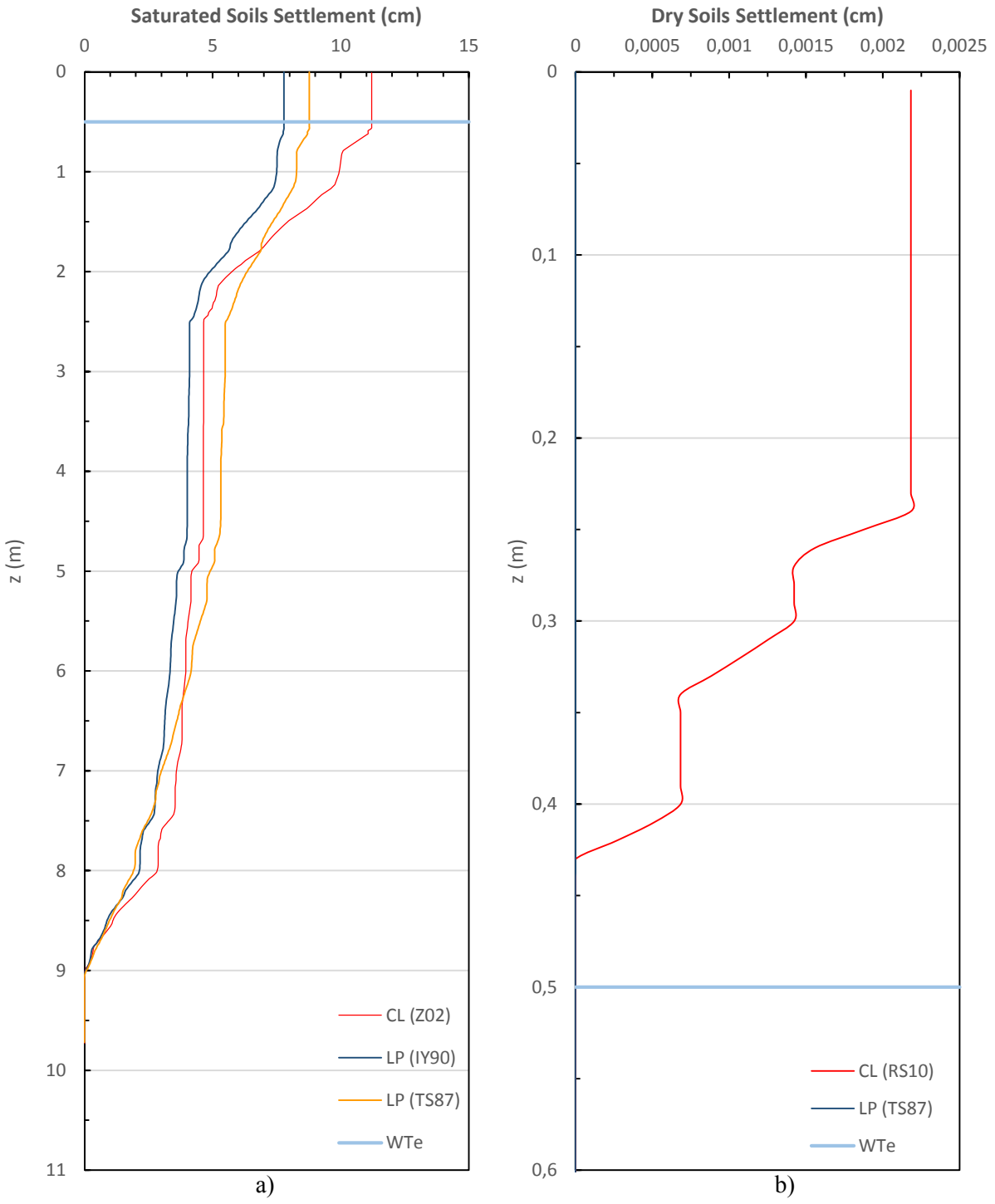

Figure 71- Settlement estimated by LiquefyPro and CLiq for CPT-KAN-26: a) Saturated Soils; b) Dry Soils

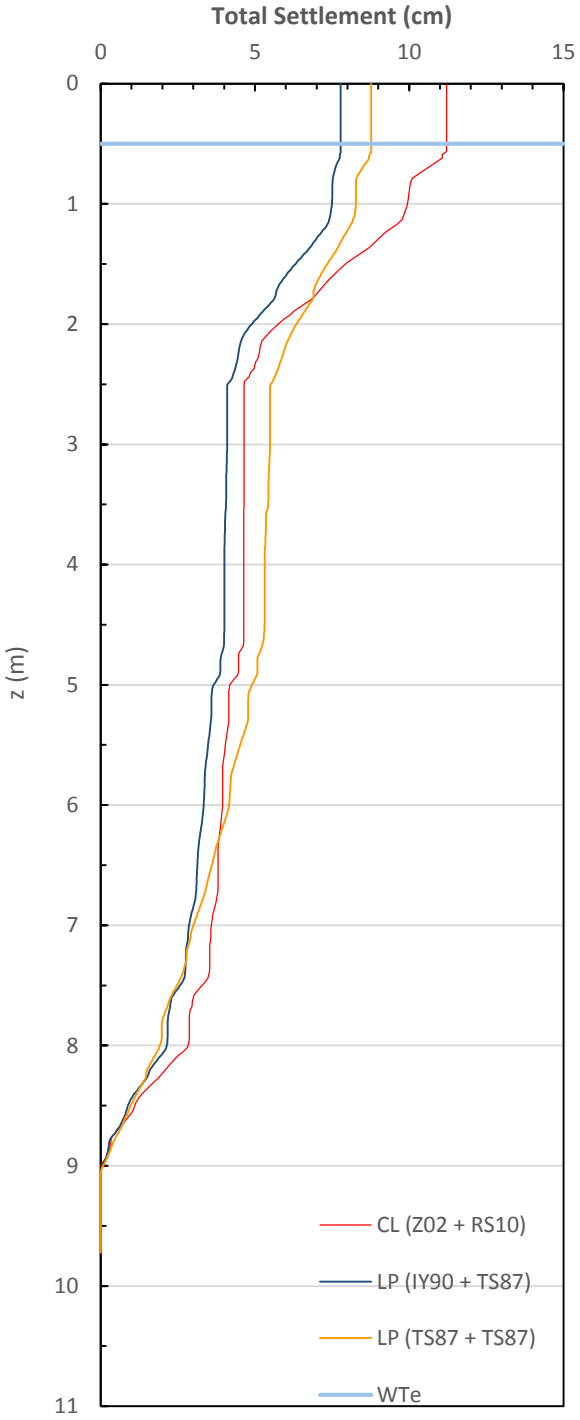

Figure 72- Total Settlement estimated by LiquefyPro and CLiq for CPT-KAN-26

5.5.3. CPT-KAS-19

In the database, the information for this location suggests that no liquefaction was observed, along with a settlement estimation from digital elevation models in the range of 0 to 10 cm. It is possible to observe

the stratification performed for the location of this CPT along with a plot of its data in section 4.3, Figure 56.

5.5.3.1. Liquefaction Evaluation

Figure 73 presents the I_C values estimated by LiquefyPro and CLiq and the resemblance between both estimations is not as clear as in the other two case studies previously assessed. The differences noticed at shallow depths are caused once again by the non-implementation of the limit value of 1.7 to C_Q, recommended in Youd et al. (2001). However, it is also observed some differences at higher depths (4.5 m and 6 m) that are not caused by this issue, once high C_Q values are only related with low overburden pressure at shallow depths. An analysis to the calculation report concludes that the differences appear at points in which the input sleeve friction was null. As the software products cannot handle null or negative values of this parameter, once that they will be introduced in logarithmical functions, they need to surpass this issue. The procedure adopted by CLiq was replacing null and negative sleeve friction values for 0.01 kPa and 0.01 MPa for the normalized tip resistance, what allows posterior calculations without modifying the accuracy of the results. LiquefyPro does not state what it is performing in order to outpace this issue, although a different approach in the overcoming of this problem may be the reason of the disagreement noticed.

This profile is composed essentially in its upper region by clay-like soils (silt), apart from a thin layer at the depth of 1.5 m and an even thinner at 5 m deep. Below 6.5 m the soil is mainly constituted by sand-like material. The analysis to the I_C plot is in agreement with the soil profile presented in Figure 56.

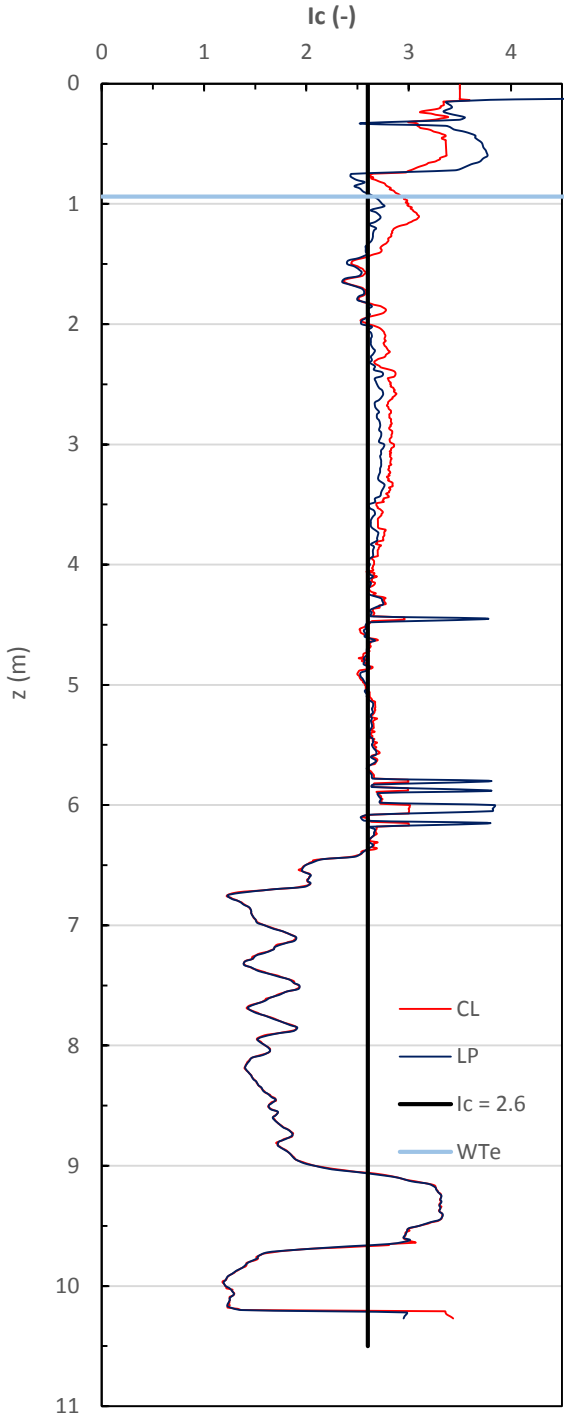

Figure 73- I_C estimated by LiquefyPro and CLiq for CPT-KAS-19

When assessing the comparison of the CRR estimated values in Figure 74a), it was noticed a huge discrepancy between the three software products, so it was decided to check in each software how were they estimating CRR. It was noticed in the tabular presentation of the calculation values of CLiq that it was not implementing correctly the expression for the relationship $q_{c1N,cs}$-$CRR_{7.5}$ ($Q_{tn,cs}$-$CRR_{7.5}$ if implemented Robertson 2009) proposed by Robertson and Wride (1998) in equation (12). The method

suggests a limit of $q_{c1N,cs}$ = 160 for this relationship, however it was noticed that CLiq extended it until $q_{c1N,cs}$ = 200, without any reference at it in its user's manual or in the report provided after each calculation. In order to understand the reason of this modification to the original method, the software developers were contacted, forwarding the problem to Professor Doctor Peter Robertson, one of the authors of the implemented method and developer of CLiq, that promptly replied saying that the relationship was extended to capture denser soils and larger earthquake loading. This modification is noticed in Figure 75, where it is presented CRR alongside $q_{c1N,cs}$ and I_C, in order to understand that in depths where the soil's I_C is lower than the threshold (I_C=2.6), the CRR calculation is performed until $q_{c1N,cs}$ = 200. For values above this limit the software assigns a value of CRR = 4.0 (this value was modified herein, in order to be in agreement with the limits imposed in LiquefyPro and Settle ^{3D})

A similar issue related with the relationship $q_{c1N,cs}$-$CRR_{7.5}$ was noticed in LiquefyPro, with this software not implementing the limit of $q_{c1N,cs}$ = 160 proposed by the method. However, it is not known what value was implemented as the new limit for the relationship, or even if there is a limit implemented. Figure 76 presents a comparison of the plots of I_C, $q_{c1N,cs}$ and CRR, in order to understand that the only threshold implemented in CRR calculation is an I_C value of 2.6.

In Figure 77 it is compared the plots of I_C, CRR and FS estimated by Settle^{3D}, as it was noticed an issue in the implementation of the threshold for I_C. In this case, unlike the other two case histories, it is noticed that the CRR estimated by Settle^{3D} is more conservative than the calculated by LiquefyPro and CLiq, once it was observed that it was defining more layers as liquefiable (Figure 74b)). Since the intermediate calculations cannot be extracted from Settle^{3D}, like I_C, it was implemented the I_C from CLiq in Figure 77a), once it was already used to obtain the FC values to input in Settle^{3D}. It is then possible to observe that this software is not implementing the threshold of 2.6 for I_C as the method suggests, once it is calculating CRR for soil with I_C greater than this value. In some cases this issue causes Settle^{3D} to define clay-like soils as liquefiable, as it can be seen in Figure 77c) at a depth around 4 m.

As this case history is not represented in the Green et al. (2014) case study, it is not possible to compare the obtained liquefiable layers with the defined as critical in this study, however, by comparing the evaluation of LiquefyPro and Settle^{3D} with the stratification performed on chapter 4 and presented in Figure 56, it is noticed that the liquefiable layers emerge in the Fine to Medium Sand strata, which is reasonable.

The observations based on aerial photographs in the database, classify this site as a location where no liquefaction was observed, whereas the evaluation performed predicts liquefaction in some layers with a medium thickness about 20 cm in depths around 4 m and 6.5 m. The lack of accuracy in the observations in the database, related with the quality and the light conditions of the photographs used may be the reason of this disagreement between them.

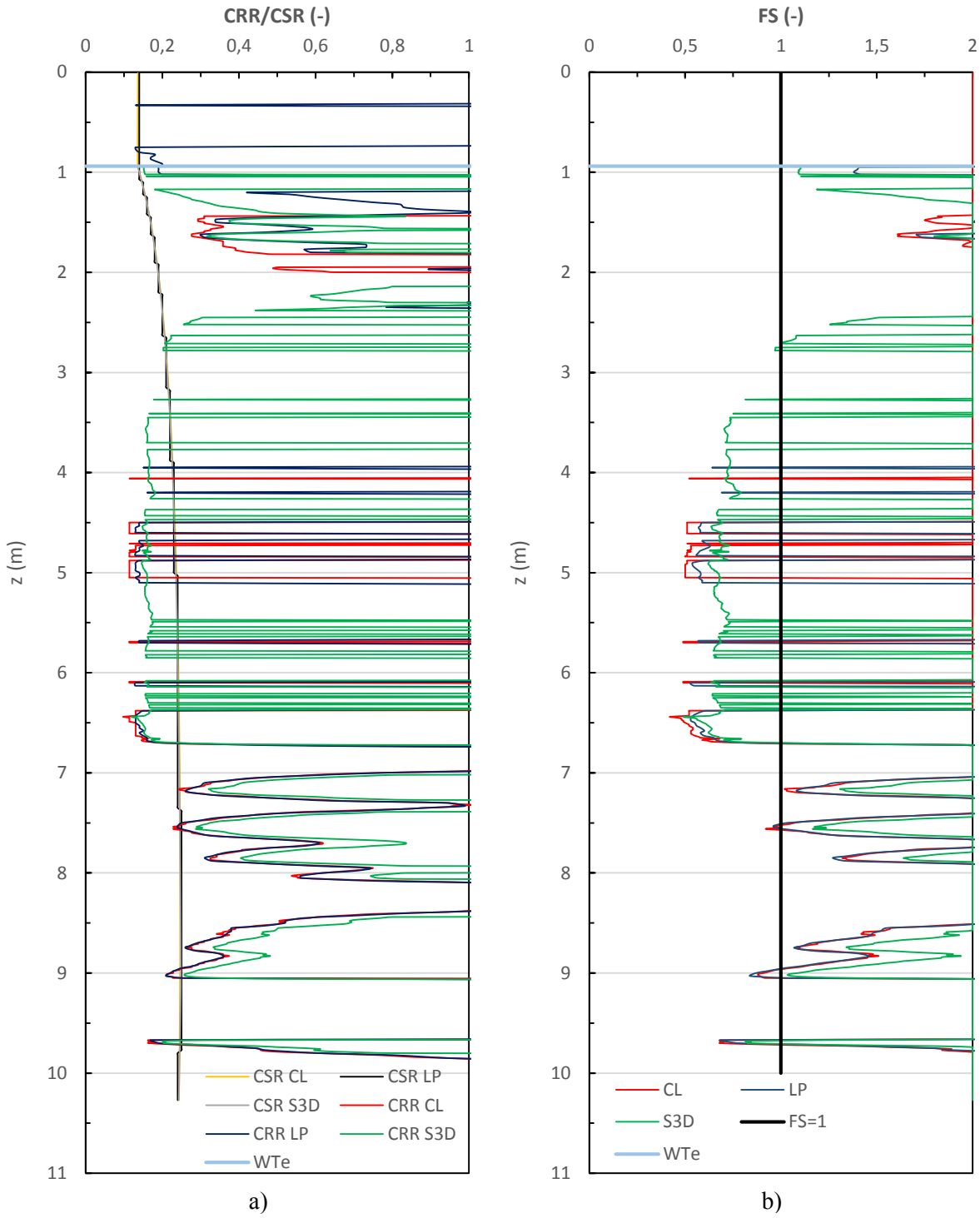

Figure 74- Comparison of parameters estimated by LiquefyPro, CLiq and Settle^{3D}: a) CRR and CSR; b) FS

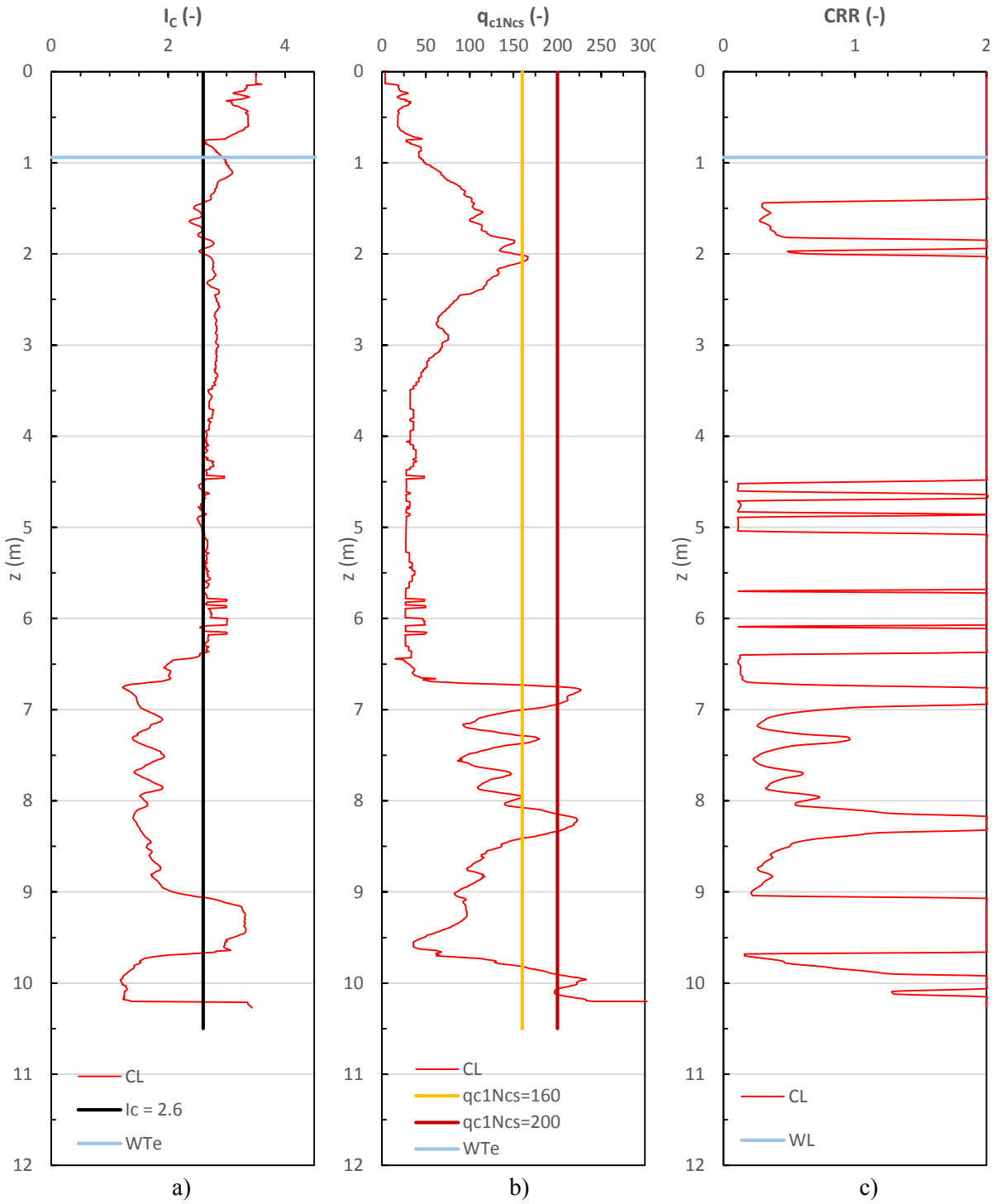

Figure 75- Comparison of parameters estimated by CLiq: a) I_C; b) q_{c1Ncs}; c) CRR

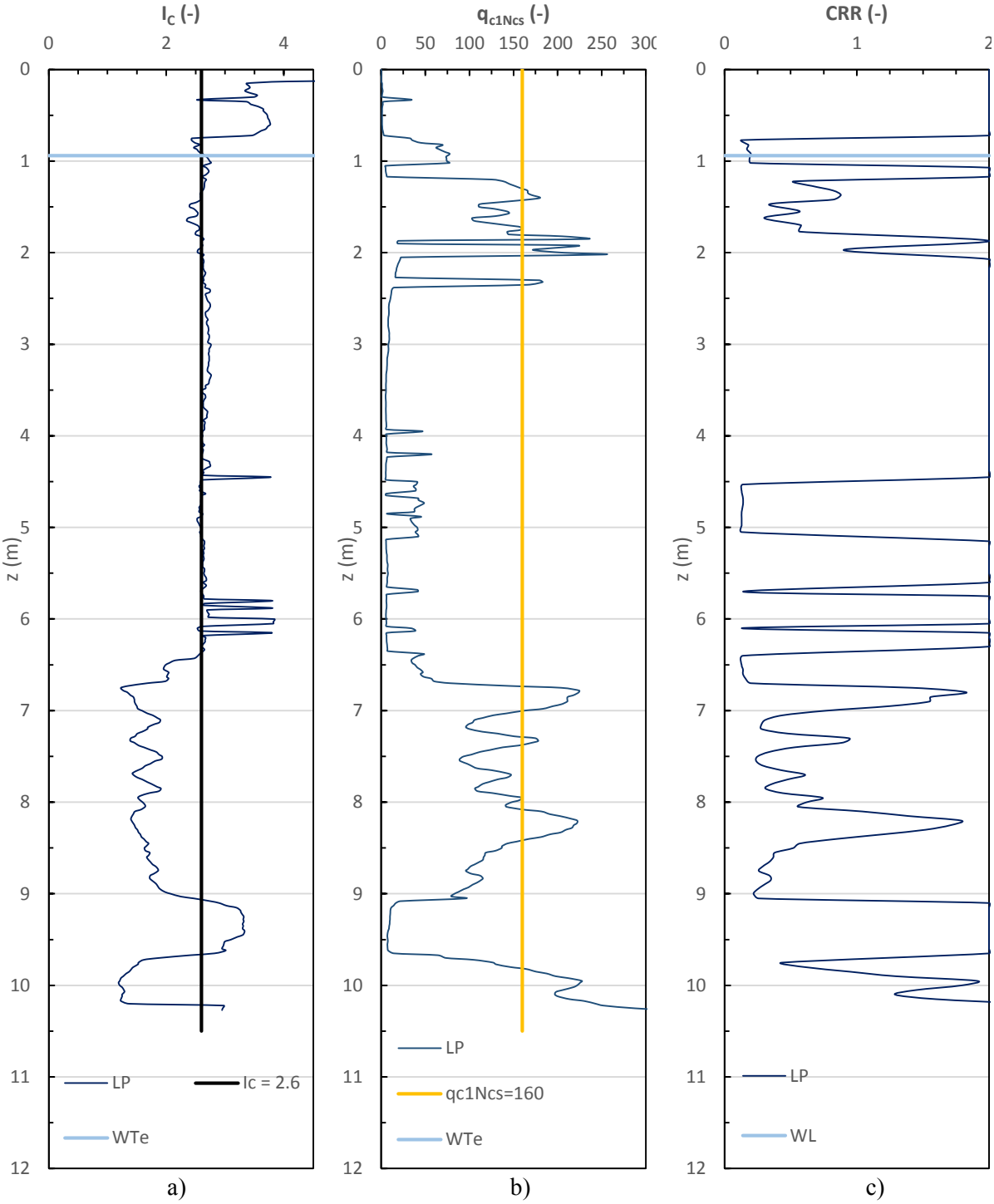

Figure 76- Comparison of parameters estimated by LiquefyPro: a) I_C; b) q_{c1Ncs}; c) CRR

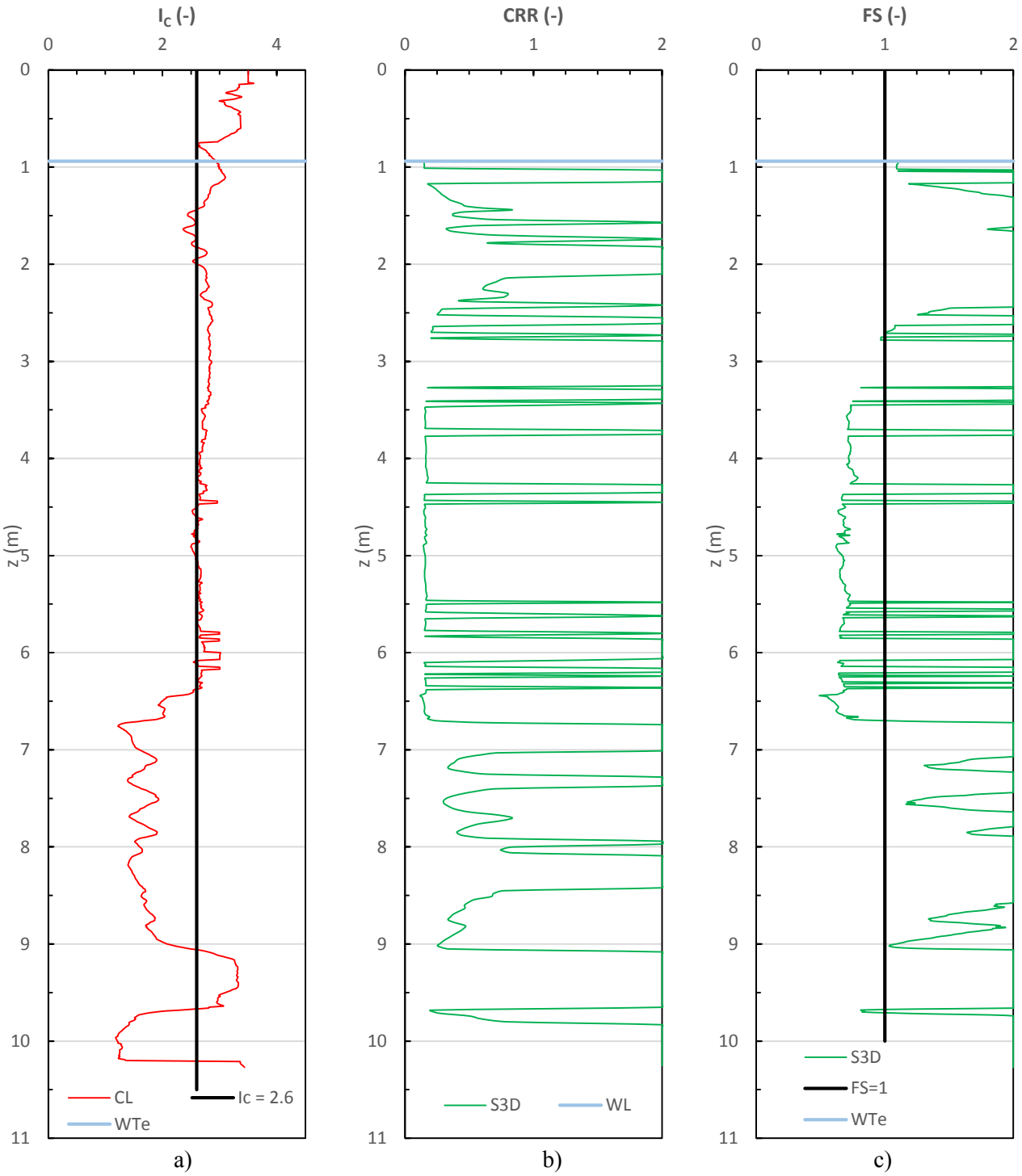

Figure 77- Comparison of parameters estimated by Settle 3D: a) I_C; b) CRR; c) FS.

5.5.3.2. Liquefaction-Induced Settlements

Figure 78 presents the estimation of settlements performed by CLiq and LiquefyPro, grounded in the same methods presented previously. For saturated soils, the method implemented by CLiq (Zhang et al.,

2002) provides once again the most conservative estimation, providing higher settlements in liquefiable layers than the methods implemented by LiquefyPro. Once more, Tokimatsu and Seed (1987) provide results more uniform along the soil column than Ishihara and Yoshimine (1992) and Zhang et al. (2002), whose results are more influenced by liquefiable layers. Regarding the computed ground settlements, Tokimatsu and Seed (1987) predicts a value around 4 cm, while Ishihara and Yoshimine (1992) estimation is between 4 and 4.5 cm. The method implemented in CLiq is more conservative, providing a ground settlement over 5 cm.

In Figure 78b) it is possible to observe the estimations for dry soils settlements performed by both LiquefyPro and CLiq. CLiq (Robertson and Shao, 2010) predicts the settlement of a single layer at a depth around 0.75 m, causing a ground settlement of 0.0007 cm, a negligible value. In LiquefyPro (Tokimatsu and Seed, 1987) is not capable of providing an estimation for this soils, what may be explained by the short precision noticed in the output of the results.

Figure 79 presents the total settlement predicted by both software products for the location of CPT-KAS-19. The estimation available in the database, provided by Digital Elevation Models, presents a settlement in the range of 0-10 cm, after the 2011 Christchurch event. All the values predicted by both LiquefyPro and CLiq are within this range, thus this products reply in a decent way the information in the database.

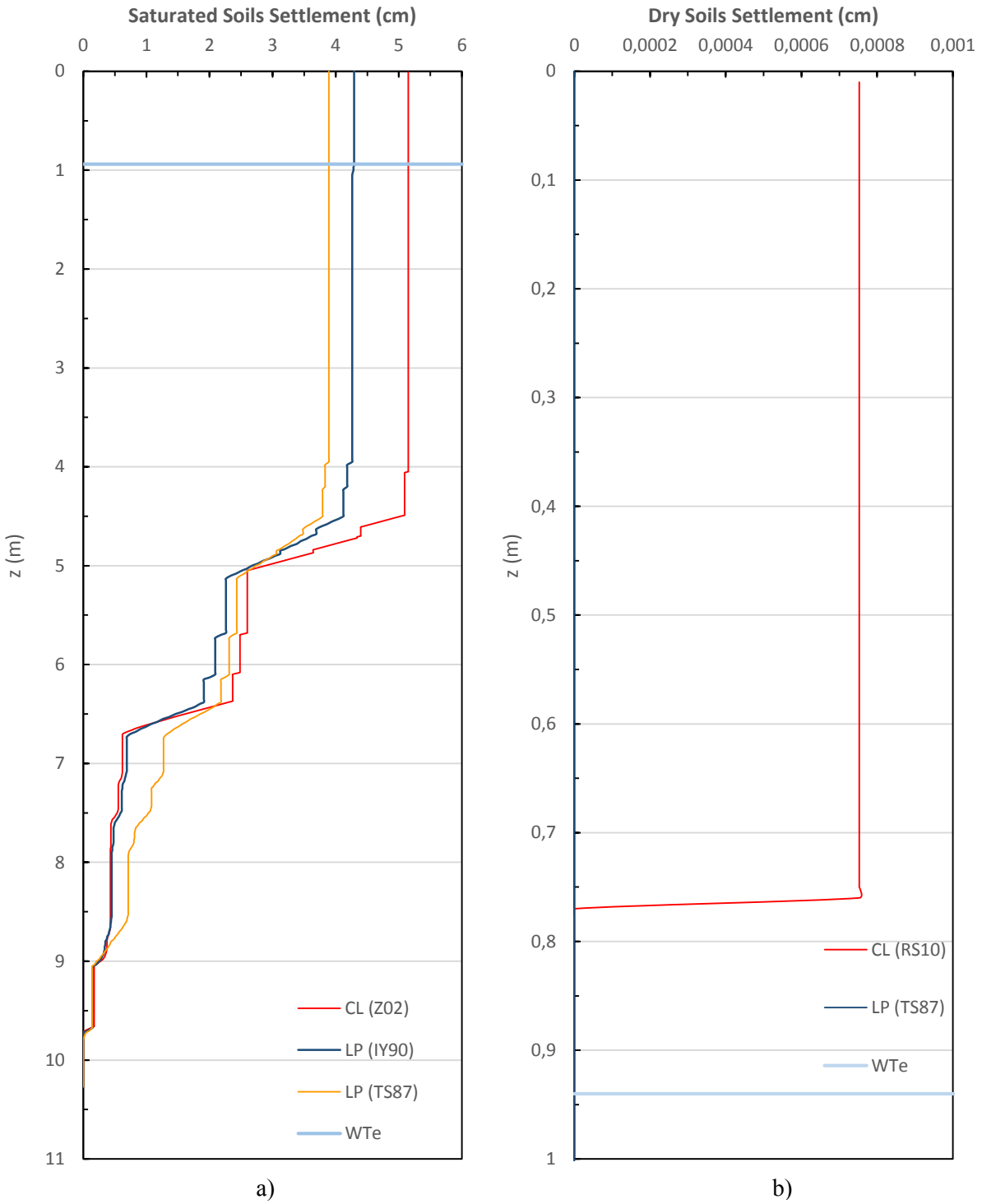

Figure 78- Estimation of settlements after LiquefyPro and CLiq for CPT-KAS-19: a) saturated soils; b) dry soils

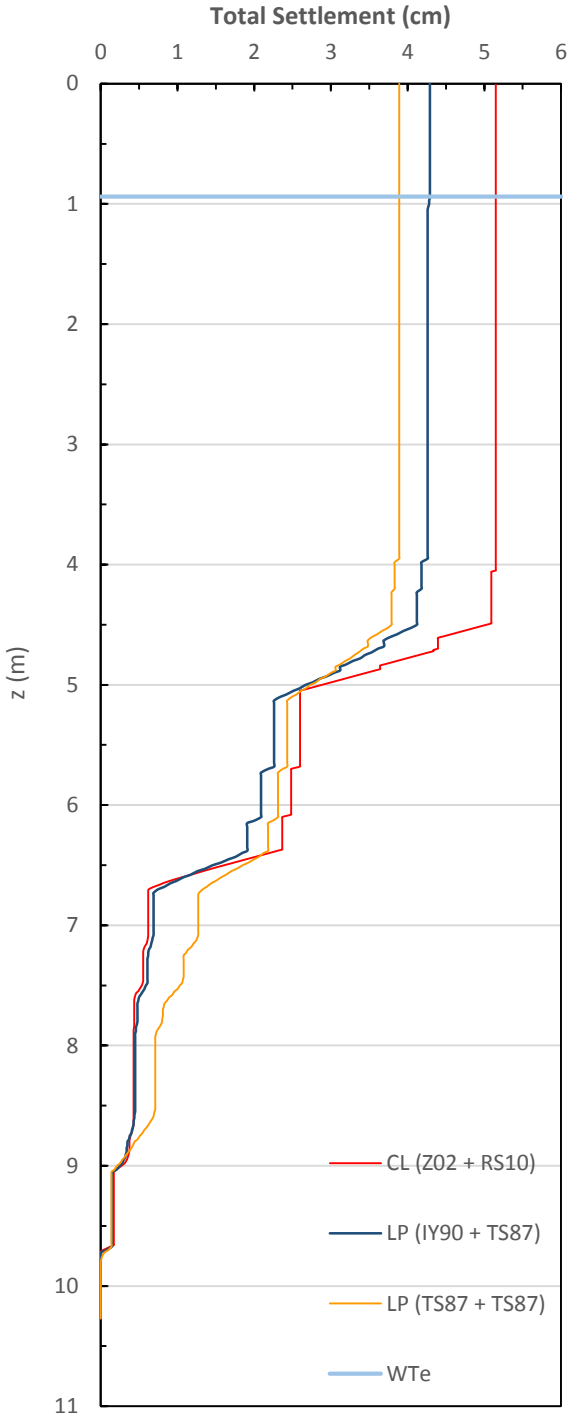

Figure 79- Total Settlement estimated by LiquefyPro and CLiq for CPT-KAS-19

5.6. DISCUSSION

In this part it is made a brief review of each software, presenting their limitations and errors in the implementation of Robertson and Wride (1998), noticed in the previous validation performed. A

summary of the aspects and capabilities of each software is given and a final comparison of the three software packages with the results obtained from the liquefaction assessments and the information available in NZGD is made. All these information are finnally summarised in tabular format.

5.6.1. LIQUEFYPRO

During the validation, in the assessment of this software it was noticed a limitation on the fines correction. The implemented Modified Robertson and Wride method (Robertson and Wride, 1998) performs a fines correction presented in chapter 2.2.1.1. in equations (20), (21) and (22). However, it was noticed that LiquefyPro was not implementing the suggestion of $K_C = 1.0$ for values of I_C between 1.64 and 2.36 and a normalized friction ratio, F, lower than 0.5% (equation (22)), proposed in order to consider the soils within this range as loose clean sands, instead of sands containing fines. This issue was noticed in the validation of CPT-KAN-26 and it is observed in Figure 69. It may produce considerable differences in the final results of the liquefaction evaluation, by defining layers as non-liquefiable that would be considered liquefiable if the method was followed, as noticed in Figure 70b).

It was also noticed that LiquefyPro does not apply on Robertson and Wride (1998) the threshold of 1.7 to the overburden stress correction factor proposed in Youd et al. (2001), what produces high unreasonable values of this parameter at shallow depths, due to low overburden pressure, which influences I_C values at shallow depths. It can be observed in Figure 64, Figure 68 and Figure 73.

The non-implementation of the limit value for $q_{c1N,cs}$ of 160, as suggested by the method, in the $q_{c1N,cs}$-$CRR_{7.5}$ relationship, can be observed in Figure 76. However, it was not possible to understand if any other limit is being implemented.

The procedure implemented by LiquefyPro in order to correct the negative values of the CPT log is not presented, however it does not have a considerable impact in the evaluation.

Comparing the results of the liquefaction evaluations and the settlements estimations performed in LiquefyPro for the three case histories, it can be concluded that its assessments predict in a reasonable manner what was registered after the 2011 Christchurch earthquake, except for the settlement in the location of CPT-NBT-03, where LiquefyPro predicted a higher value than the obtained in the database, and in CPT-KAS-19, where the liquefaction evaluation provided some liquefiable layers, in contrast with the observations that registered no liquefaction in the CPT location. However, this disagreement is partially due to the lack of accuracy when obtaining these parameters that are available in NZGD, therefore the analysis performed by the software cannot be classified as imprecise, based on only this. Also, from the methods available in this software to estimate liquefaction-induced settlements in saturated soils, when implementing Ishihara and Yoshimine (1992) it was noticed in the estimations for every case history a greater contribution for the ground settlement of layers defined as liquefiable, whereas Tokimatsu and Seed (1987) predicted a settlement almost uniform of the entire soil column. According to Juang et al. (2013), after Ueng et al. (2010), the settlement after earthquake is mainly caused by liquefied soil, whereas the settlement contributed by the soil layer that did not liquefy is very small, thus, Ishihara and Yoshimine (1992) provides a more accurate estimation than Tokimatsu and Seed (1987). It should also be noted that the fact that LiquefyPro has to convert CPT data into SPT in order to be possible to perform a settlement estimation, may produce some error in the final results.

Table 11 summarizes the characteristics of LiquefyPro and its limitations, noticed not only during the validation but also in the validation of the three case histories.

Table 11- Summary of LiquefyPro characteristics

	LiquefyPro
CRR	Seed and De Alba (1986); Suzuki et al. (1997); Robertson and Wride (1997); Modified Robertson and Wride.
MSF	NCEER.
Dry Soil Settlements	Tokimatsu and Seed (1971).
Saturated Soil Settlements	Tokimatsu and Seed (1971); Ishihara and Yoshimine (1992).
CSR / r_d	Seed and Idriss (1971) / Liao and Whitman (1986).
Output	I_C; CRR; CSR; FS; Dry Soil Settlements; Saturated Soil Settlements; Total Settlements
Limitations	CPT data input limited to 1200 rows; Does not state what procedure it implements in the correction of negative and null CPT data values; Little flexibility offered to the user in the calculation methodology; Implementation of the fines content correction different than the suggested by Robertson and Wride (1998); Does not implement the limit suggested by the method of 160 to the $q_{c1N,cs}$-$CRR_{7.5}$ relationship; Does not implement the limit of 1.7 to C_Q, as suggested in Youd et al. (2001).

5.6.2. SETTLE^{3D}

Of the three software products assessed, Settle^{3D} is definitely the one that provides less accurate estimations, being noticed several flaws in the implementation of the methods, associated to other limitations already discussed. The "opacity" in the presentation of the calculation results, makes difficult to know what are the modifications applied to the method and at which steps the software is implementing it differently. However, by comparing its results with the estimations of the other software products, it was noticed that the issues might be related with the fines content correction, where Settle^{3D} also presents some flaws in the input. The fact that this software is not implementing the I_C threshold of 2.6 (noticed in Figure 77), or it is estimating I_C different than the method (the values estimated by Settle^{3D} of this parameter are not provided) in Robertson and Wride (1998), can induce in error, once it predicts liquefaction in layers whose I_C is greater than 2.6. On the other hand, for I_C values below 2.6, this software is less conservative than the other two software products presented by overestimating the soil's resistance, what can be observed in Figure 65, Figure 70 and Figure 74.

Settle^{3D} does not allow to estimate liquefaction-induced settlements if the analysis is based on CPT data, so it is only possible to compare the results from the liquefaction evaluation with the scale of liquefaction observed in the database. The results provided by this software present disagreement with the observations of liquefaction based on aerial photographs, more specifically in CPT-KAS-19, where

Settle^{3D} predicts liquefaction of several layers, against the results of the other two software products and the post-earthquake observations available in NZGD.

Table 12- Summary of Settle3D characteristics

	Settle^{3D}
CRR	Robertson and Wride (1997); Modified Robertson and Wride (1998); Boulanger and Idriss (2004); Moss et al. (2006) – deterministic; Moss et al. (2006) – probabilistic.
MSF	Tokimatsu and Seed (1987); Idriss (1999); Andrus and Stokoe (1997); Idriss and Boulanger (2008); Youd and Noble (1997); Cetin et al. (2012).
Dry Soil Settlements	-
Saturated Soil Settlements	-
CSR / r_d	Seed and Idriss (1971) / Idriss (1999); Kayen (1992); Cetin et al. (2004); Liao and Whitman (1986a).
Output	CRR; r_d; CSR; FS; PL – if a probabilistic method is selected
Limitations	Implementation of a single water table in liquefaction evaluation; Little flexibility offered to the user in the calculation methodology; Fines Content needs to be defined by user, even that it implements methods that perform Fines correction based on CPT data; Does not implement the threshold of 2.6 for I_C; MSF expressions do not include NCEER recommendation; Estimation of settlements is not provided for CPT-based liquefaction assessments; Intermediate calculations are not presented.

5.6.3. CLIQ

It was noticed during $CRR_{7.5}$ calculation, a modification to Robertson and Wride (1998) method and its expressions for $q_{c1N,cs}$-$CRR_{7.5}$, more precisely in equation (12). CLiq extends the relationship to $q_{c1N,cs}$ values of 200, slightly beyond the original limit of 160. In order to understand the reason of this modification, the software developers were contacted and they forwarded the question to Professor Peter Robertson, who was very helpful and prompt in his reply, and justified the modification with the necessity to capture denser soils and larger earthquake loading.

The estimations provided by this software are generally in agreement with the post-earthquake information available in NZGD, apart from the predicted settlement for CPT-NBT-03 (Figure 67) and the occurrence of liquefaction for CPT-KAS-19, as discussed. However, the reason of this disagreement may be related with the lack of accuracy in the obtainment of the post-earthquake information in NZGD.

When comparing the results of the assessments made in CLiq with LiquefyPro it is noticed a great resemblance between both calculations, although the values estimated by this software are usually more conservative, especially regarding the settlements estimations, noticed in Figure 67, Figure 72 and Figure 79. Nevertheless, CLiq presented a proper implementation of the method with great accuracy, it allows more user control than LiquefyPro, presents all of the intermediate calculations in a friendly way and incorporates some of the more recent methods available in the literature, hence it was the software selected for validation of the developed Mathcad tool in the following chapter.

Table 13-Summary of CLiq characteristics

	CLiq
CRR	Robertson and Wride (1998); Robertson (2009); Moss et al. (2006); Idriss and Boulanger (2008); Boulanger and Idriss (2014).
MSF	NCEER (2001) – same as Youd et al. (2001); Moss et al. (2006); Idriss and Boulanger (2008).
Dry Soil Settlements	Robertson and Shao (2010).
Saturated Soil Settlements	Zhang et al. (2002); Idriss and Boulanger (2008).
CSR / r_d	Seed and Idriss (1971) / Blake (1996);
Output	$CRR_{7.5}$; MSF; r_d; CSR; FS; PL; LPI; Liquefaction Volumetric Strain; Saturated Soil Settlement; Dry Volumetric Strain; Dry Soil Settlement; Total Settlement; Probabilistic Settlement.
Limitations	Modification implemented on Robertson and Wride (1998), changing the limit of the $q_{c1N,cs}$-$CRR_{7.5}$ relationship from 160 (as the method suggests) to 200.

6

VALIDATION OF THE DEVELOPED TOOL

6.1. INTRODUCTION

After the assessment of the software packages, performed in chapter 5, it was concluded that CLiq presented better capabilities, by implementing in an accurate manner the latest methods available, providing information on the intermediate calculations in a clear way and allowing great user control over the input. Due to all this, it was the selected software to validate against the Mathcad developed tool, presented on chapter 3. In the development of this tool it was implemented some assumptions also made by CLiq, noticed while assessing it and that appear to be very reasonable (the influence of some modifications made to the methods will be assessed on a sensitivity analysis to the tool, presented hereafter).

6.2. CHARACTERISTICS OF THE VALIDATION

In order to perform an accurate comparison, it was implemented the same methodology on both CLiq and the Mathcad tool (with exception for r_d), presented in Table 14. Note that, although both are capable to estimate the probabilistic settlement, CLiq only presents this parameter's plot, not providing its values, thus this comparison will not be made.

Table 14- Methodology implemented on the tool validation

Parameters	Implemented Methods
CRR	Robertson (2009)
MSF	NCEER
CSR	Seed and Idriss (1971)
R_d	Liao and Whitman (1986) / Blake (1996)
Dry Soils Settlement	Robertson and Shao (2010)
Saturated Soils Settlement	Zhang et al. (2002)

The validation was grounded on the comparison of some parameters considered relevant, estimated from the calculation of both CLiq and the developed Mathcad tool. The selected parameters are:

- I_C;
- $Q_{tn,cs}$;
- $CRR_{7.5}$
- CSR;
- FS;
- P_L;
- LPI;
- Saturated Soils Volumetric Strain, ε_v;
- Saturated Soils Settlement, S_s;
- Dry Soils Volumetric Strain, ε_{vol};
- Dry Soils Settlement, S_d;
- Total Settlement, S_t.

For the validation of the developed tool it was only selected a case history, since it was considered unnecessary to check every single one, once that both products run on the same methods and assumptions. The case selected was CPT-NBT-03, in which location was observed moderate to severe liquefaction and a settlement in the range of 10 to 20 cm, according to the information in NZGD already presented herein.

6.3. COMPARISON OF THE PARAMETERS CALCULATED

The comparison of the selected parameters presented above was made by plotting the calculation results of both approaches.

In all of the presented parameters it is noticed a great resemblance between both estimations, in some plots the estimations are even identical. The parameters that present greater differences are $Q_{tn,cs}$, ε_{vol} and S_d and will be presented and discussed in this chapter. The soil profile for the case history implemented herein is presented in chapter 4 and Figure 52.

In the legend hereafter the developed Mathcad tool is referred to as MC.

6.3.1. LIQUEFACTION EVALUATION

By consulting Figure 80b) it is noticed some differences in the estimations of $Q_{tn,cs}$, only observed for depths in which I_C is greater than 2.7 (Figure 80a)), so by assessing the intermediate calculations of CLiq, it was noticed that in the calculation of K_C, CLiq implements equation (20) for I_C values greater than 2.7, whereas the Mathcad tool defines a value of 1.0 for soils in this range. However, by observing Figure 81 it can be concluded that this disagreement will not produce any error in the calculation of $CRR_{7.5}$, since CLiq implements correctly equation (26), based on Q_{tn}, in the calculation of this parameter for I_C values greater than 2.7.

The implementation of different r_d expressions produces a slight disagreement between CSR at higher depths (Figure 81b)) and consequently in FS (Figure 82a)), however this issue is of little significance, since it is only noticed at depths over 14 m and it does not produce differences in the layers defined as liquefiable in both software products.

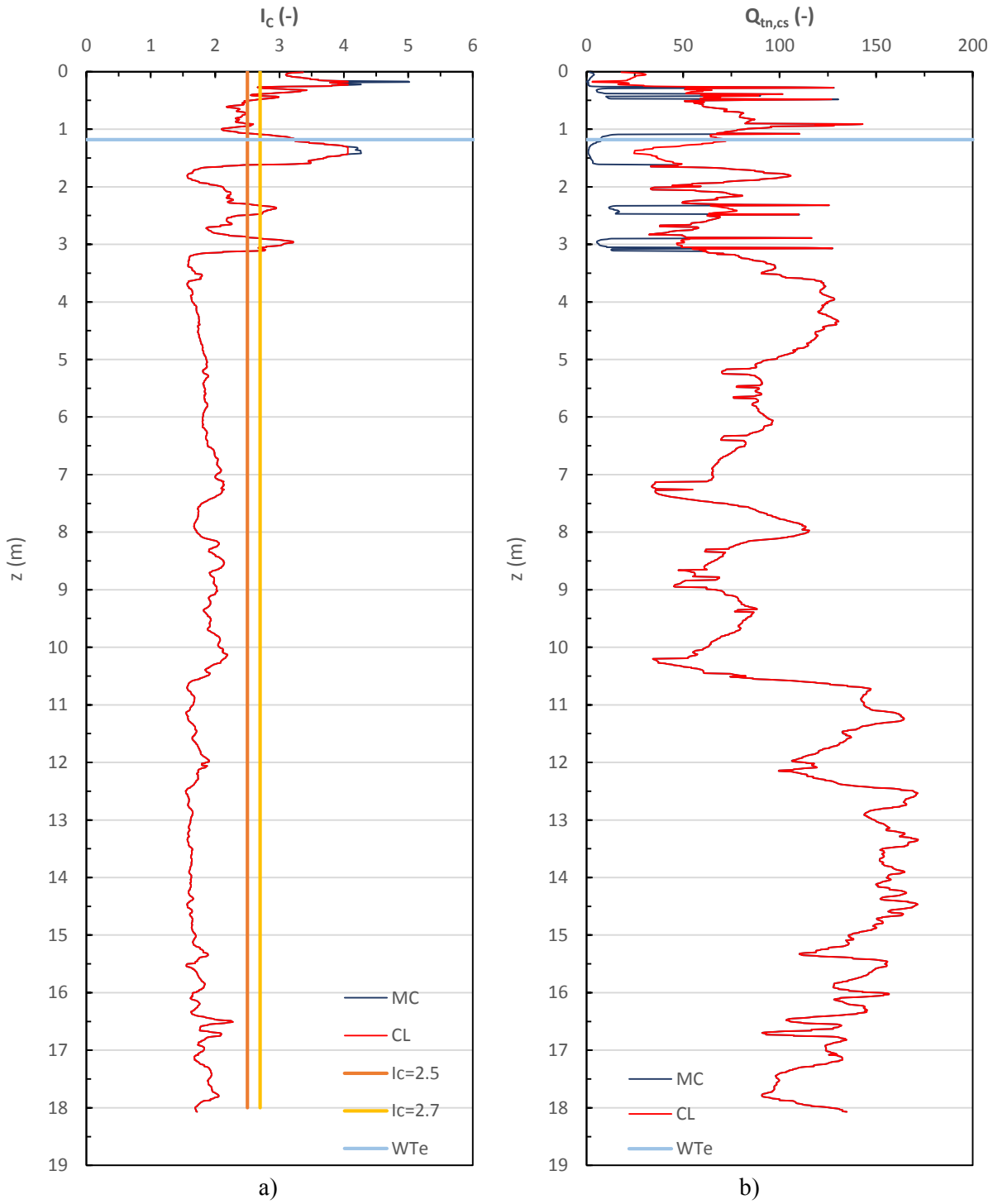

Figure 80- Comparison of parameters estimated from the developed tool and CLiq for CPT-NBT-03: a) I_C; b) $Q_{tn,cs}$.

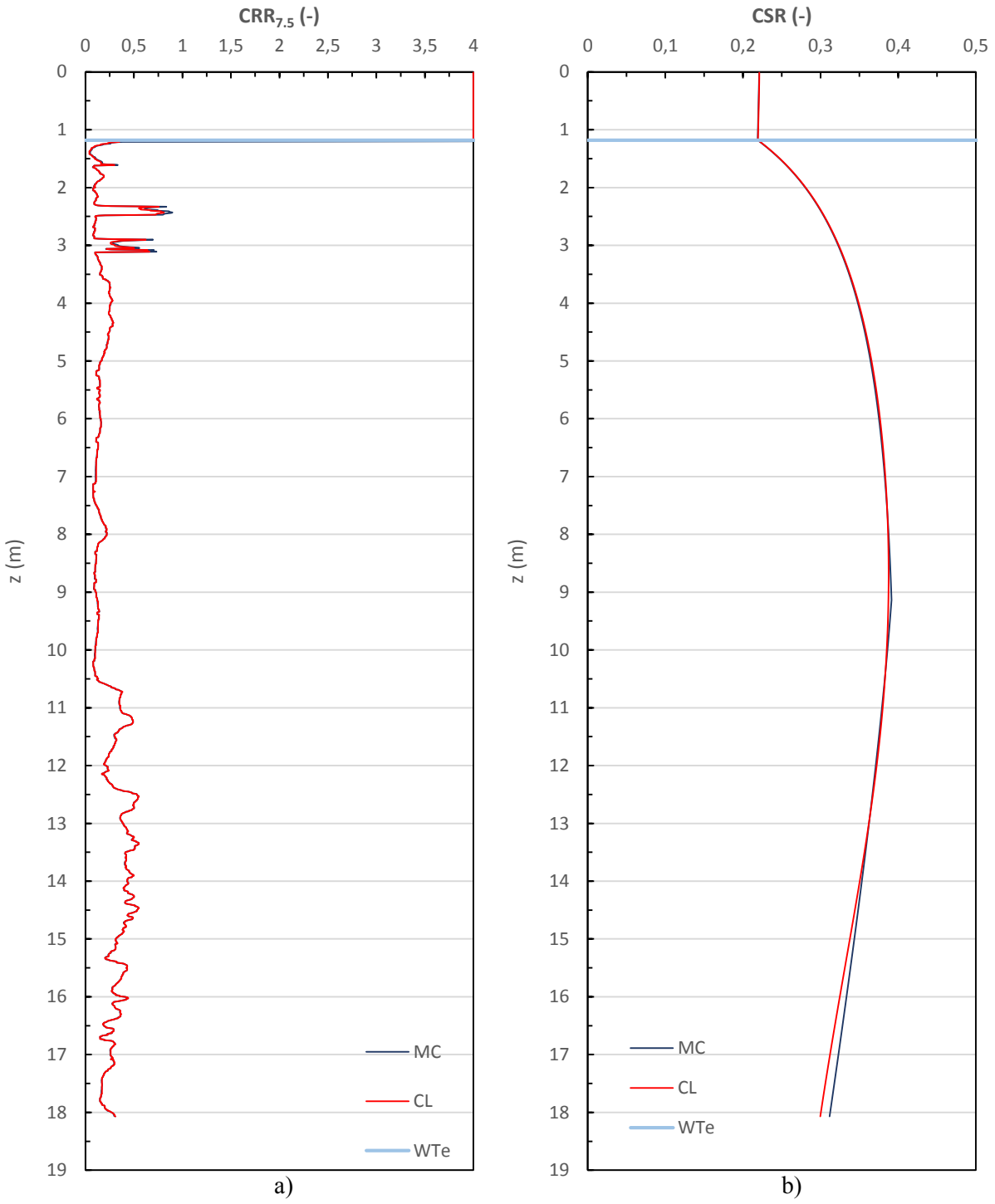

Figure 81- Comparison between parameters estimated from CLiq and the developed Mathcad tool for CPT-NBT-03: a) $CRR_{7.5}$; b) CSR

As mentioned previously, it is noticed in Figure 82a) a minor gap between both FS estimations at great depths due to the different r_d expressions implemented. As LPI and P_L are directly estimated from FS, this issue has an impact on their comparison plots in Figure 82b) and Figure 82c) respectively. However, it has little influence, causing no differences in the final evaluation of CLiq and the Mathcad tool.

Comparing the results of the liquefaction assessment performed with the information available in the database regarding the effects of the 2011 Christchurch earthquake event in the location of CPT-NBT-03, it is noticed an agreement with the moderate to severe liquefaction observed for this same site. Figure 82a) presents the factor of safety against liquefaction predicting a huge liquefiable layer of about 6 m thick, starting at the depth of 5 m, together with other 4 liquefiable layers between the water table and a depth of 4 m. The LPI value obtained of 22 (Figure 82b)) corresponds to a very high liquefaction severity, based on the Iwasaki et al. (1982) classification, and major liquefaction severity in the scale proposed by Luna and Frost (1998), both presented in section 2.3. Regarding PL in Figure 82c), about 5 layers with a considerable thickness are associated with a probability of liquefaction of 100%, while one third of soil column has more than 75% chance of liquefaction. Thus, combining FS, LPI and P_L estimated after a CPT-based liquefaction analysis using the Robertson (2009) and comparing them with the information recorded, it may be concluded that the assessment performed is reasonably consistent with the registered observations.

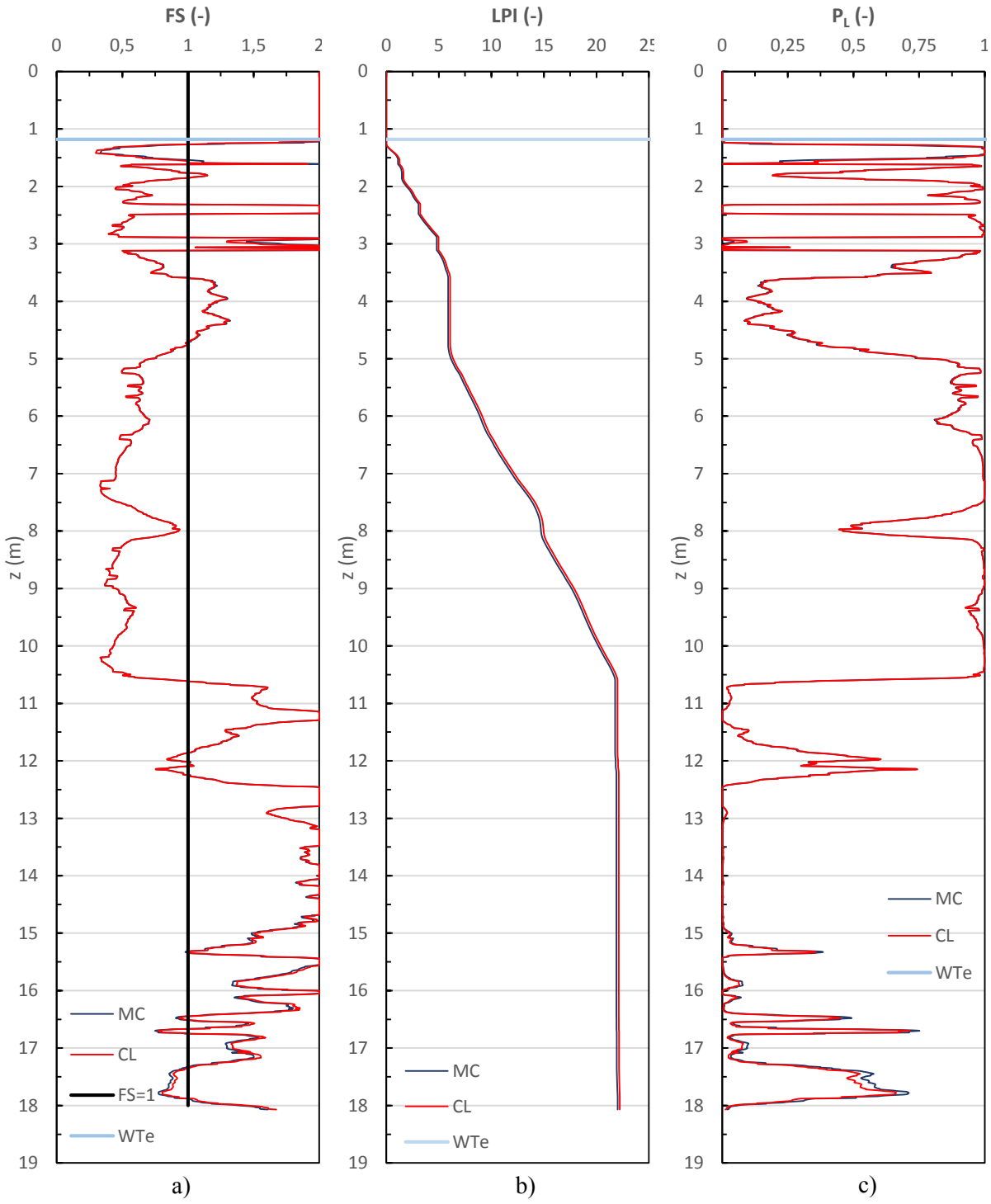

Figure 82- Comparison of parameters estimated by CLiq and Mathcad tool: a) FS; b) LPI; c) P_L

6.3.2. LIQUEFACTION-INDUCED SETTLEMENTS

It was also noticed some differences in the plot of the volumetric strain for saturated soils, ε_v, presented in Figure 83a), especially at greater depths. It was consulted the tabular information on CLiq, with the

intermediate parameters and it was noticed a different implementation of the expressions for ε_v proposed by Zhang et al. (2002). As it was mentioned in chapter 2 and later in chapter 3, these expressions are only available for specific values of FS, so in the tool it was decided to perform linear interpolation to obtain ε_v for FS values where the expressions of equation (57) are undefined, as suggested in the Technical Specification for Liquefaction Evaluation of CPT Investigations by the New Zealand Geotechnical Database. On the other hand, it was observed that CLiq was implementing a proximal interpolation instead. However, the fact that it is being implemented a different approach to deal with this issue, does not produce considerable differences in the results, as it can be noticed in Figure 83.

Other parameters that indicated less resemblance were the dry soils volumetric strain, ε_{vol}, and consequently the dry soils settlement, S_d, presented in Figure 84. The estimations for ε_{vol} were based in both cases on the method proposed by Robertson and Shao (2010) and presented in chapter 2.4.2. and both, CLiq and the MC tool, implemented a slight modification of the original method, by assuming K_0 = 1 in equation (67), for the whole profile. The calculation report, provided after each calculation performed in CLiq, presents a flowchart with the calculation sequence implemented in CLiq for the estimation of settlements in dry soils, and it matches with the procedure implemented in the tool, thus the reason of these slightly differences is unknown. However, the shape of the curve with the evolution of volumetric strains and settlement in depth is very similar between both CLiq and the tool, and the values predicted are extremely low, with a ground settlement of 0.006 cm in the more conservative prediction.

Regarding the ground settlement in Figure 85, it was noticed some differences between the assessment estimations and the vertical ground movements recorded in NZGD. Both CLiq and the Mathcad tool predict a settlement around 25 cm, while the database, based on Digital Elevation Models, recorded a settlement in the range of 10 to 20 cm in the same location. As mentioned previously, the settlement values in the database are not so accurate, due to the errors inherent in the mapping based on LiDAR, having an accuracy of ±15 cm, according to the Map Layer Description, available in the NZGD. Therefore, it can be concluded that the CPT-based liquefaction evaluation, using Robertson (2009) procedure, performed by the tool and CLiq, provide an accurate estimation.

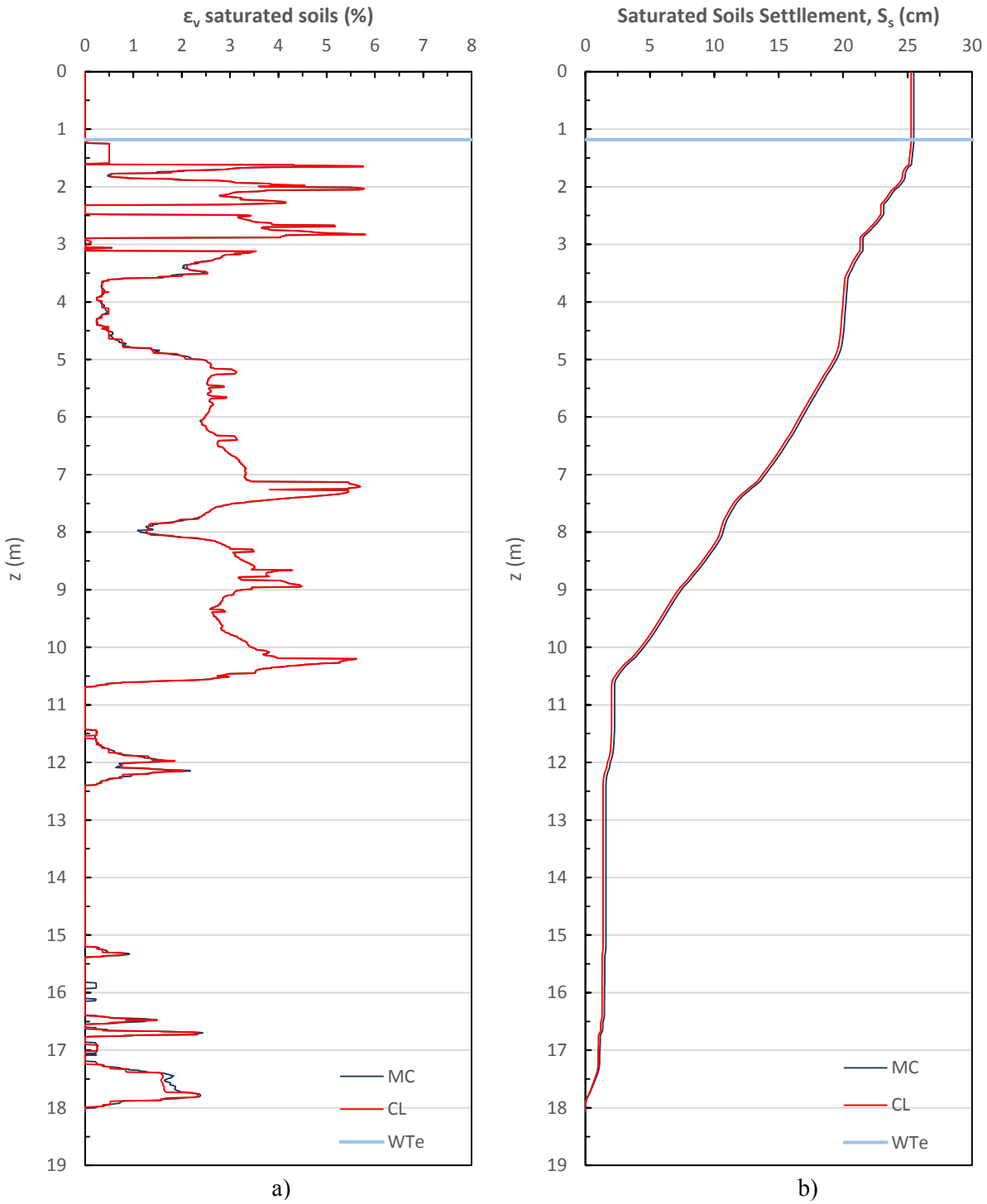

Figure 83- Comparison of saturated soils settlement related parameters estimated by CLiq and Mathcad tool for CPT-NBT-03: a) ε_v; b) S_s

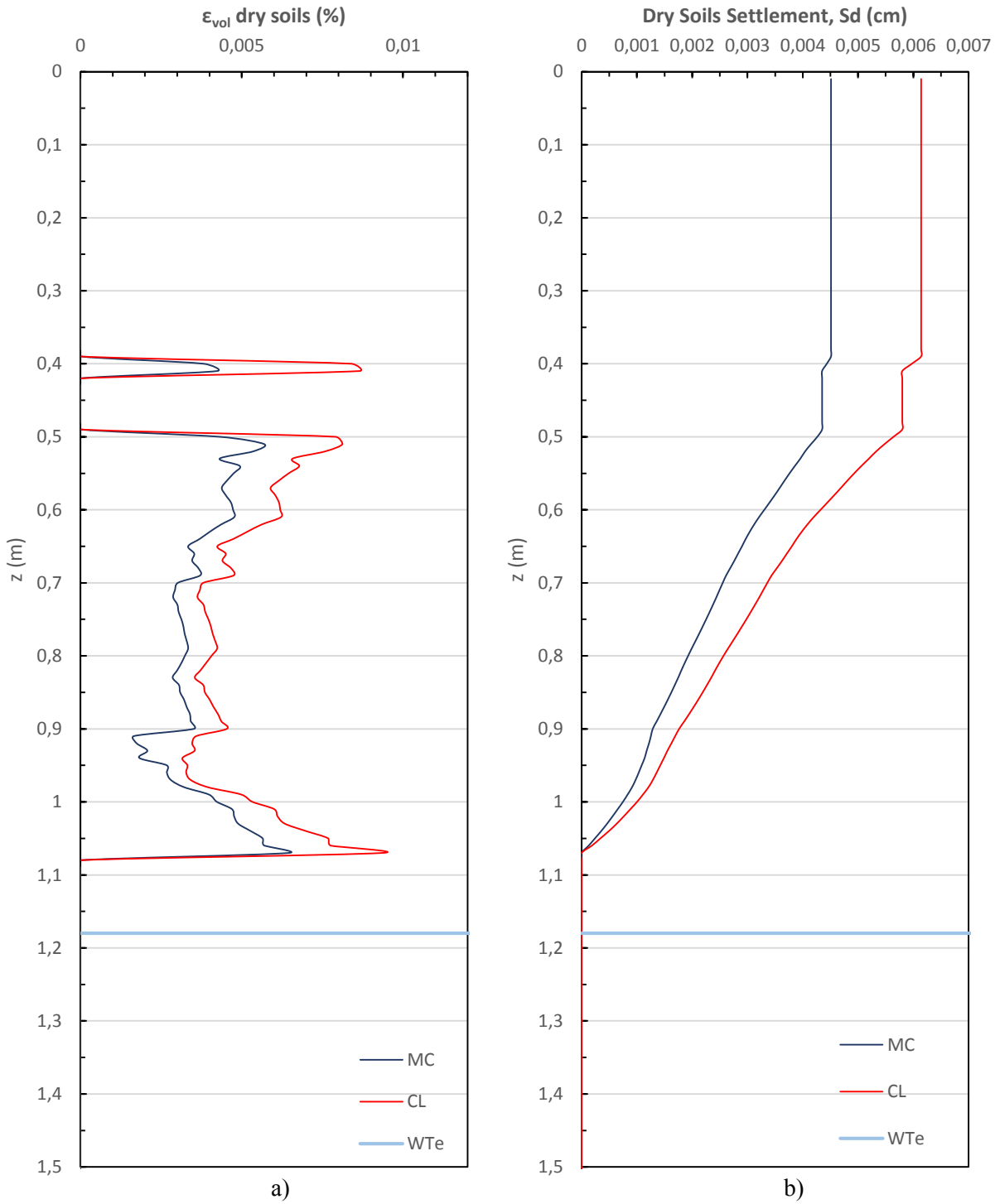

Figure 84- Comparison of dry soils settlement related parameters for CPT-NBT-03: a) $\varepsilon_{vol.}$; b) S_d.

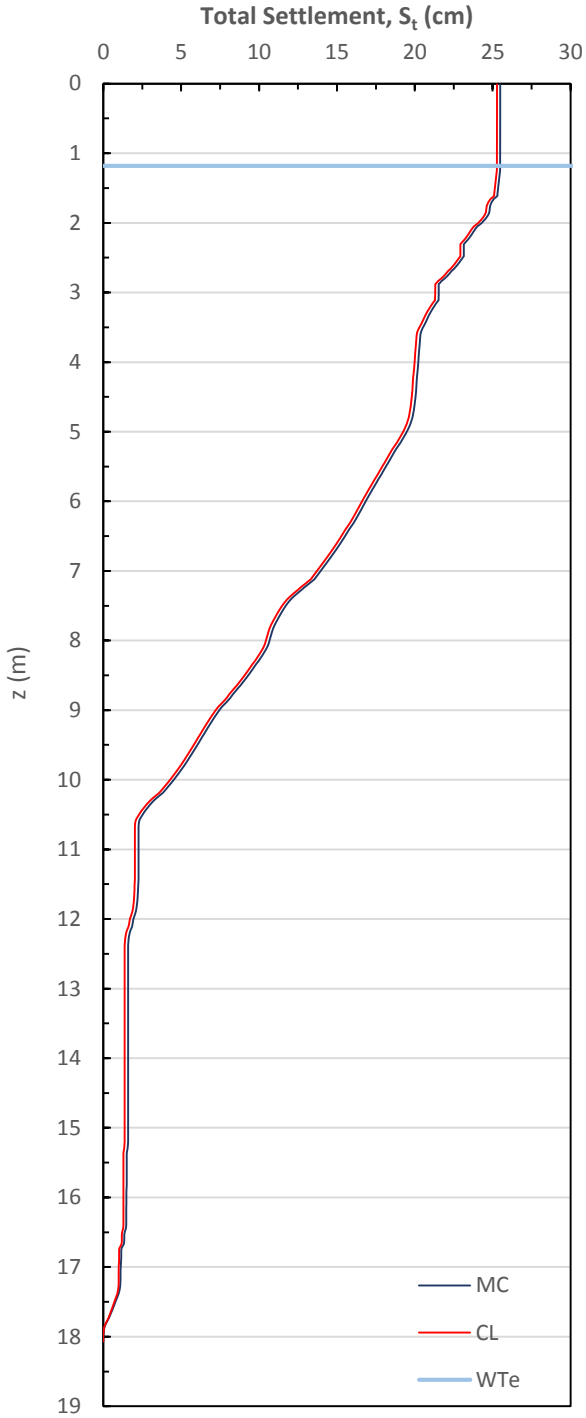

Figure 85- Comparison of the total settlement estimated by CLiq and the developed tool for CPT-NBT-03.

6.4. SENSITIVITY ANALYSIS

A sensitivity analysis was carried out in the tool to assess the influence in the results of the modifications made to the implemented methods.

As mentioned previously in section 3.2.1.5., it was implemented on the Mathcad tool a modification to the correlation $CRR_{7.5}$-$Q_{tn,cs}$ proposed in Robertson (2009), after Robertson and Wride (1998) and presented on equations (12) and (13). In this chapter, the influence of this modification is assessed by comparing the results of two liquefaction analysis performed, with and without the modification implemented. The analysis is only performed for one CPT profile of the three presented, selected by considering the number of points falling in the range between 160 (limit of the correlation proposed by the method) and 200 (limit implemented in the tool).

A quick analysis to the $Q_{tn,cs}$ values estimated for each CPT in the case histories concludes that CPT-NBT-03 has 113 points falling in the range of 160-200, while CPT-KAN-26 has 30 points and CPT-KAS-19 has 58. Thus, the case history selected is CPT-NBT-03, once it is the most affected by this modification. The influence in the results is assessed in Figure 86.

As it can be noticed in Figure 86, the extension of the $CRR_{7.5}$-$Q_{tn,cs}$ relationship to a $Q_{tn,cs}$ value of 200 only produces differences on the plot of $CRR_{7.5}$ (Figure 86a)). Once the affected values have a high resistance, the modification does not produce any changes in FS (Figure 86b)), thus it does not have any impact on the liquefaction evaluation. As the following steps of the assessment (LPI, P_L and estimation of settlements) are based on FS values, they do not suffer any alteration as well and for that reason they are not presented herein.

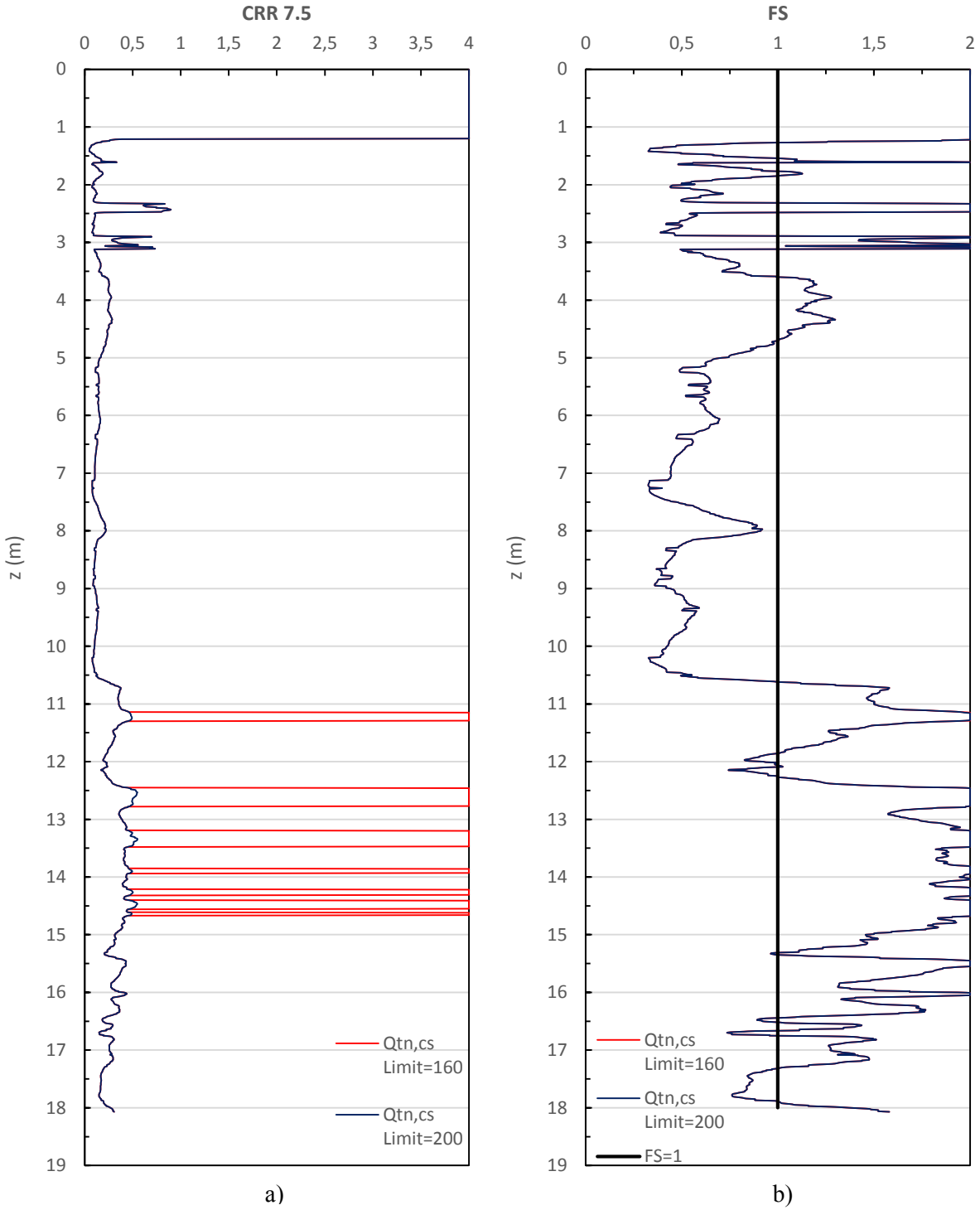

Figure 86- Results of sensitivity analysis performed to the Mathcad tool regarding the extension of the limit value for the $CRR_{7.5}$-$Q_{tn,cs}$ relationship : a) $Q_{tn,cs}$; b) FS

6.5. DISCUSSION

The comparison of the results estimated from the developed tool and CLiq presented a great agreement between both, although with some noticed differences but with no influence on the final results.

The only parameters whose values presented considerable differences between the two estimations are related with the settlement of dry soils, being observed a disagreement in the comparison of both calculations for ε_v and S_s (Figure 84). The reason behind this issue is not clear, since the tool followed the exact same method implemented in CLiq, with the same consideration for K_0. However, since the total ground settlement for dry soils in all the assessed cases contributes marginally to the total settlement (in this case it is less than 0.03% of the total settlement), it can be considered that this disagreement has no great influence on the results.

By assessing the implementation of Robertson (2009) method, it was noticed that CLiq performs some modifications to the original method presented herein that are not mentioned in its manual. According to the published method, the estimation of the fines correction factor, K_C, should not be performed for I_C values greater than 2.7, however CLiq does it, implementing equation (20) for I_C values within this range. The modification implemented to the method will affect $Q_{tn,cs}$ values, calculated based on K_C, but will not influence $CRR_{7.5}$ calculation, once the calculation of this parameter for I_C values greater than 2.7 is based on Q_{tn} values.

It was also noticed that different assumptions were made in the implementation of the Zhang et al. (2002) expressions in equation (57) for the calculation of ε_v. The Mathcad tool performs linear interpolation to extend these expressions to FS values where they are not defined, whereas CLiq performs proximal interpolation. The difference between both assumptions is merely mathematical, and the disagreement produced is very small, for this case history.

The developed tool strictly follows the methods implemented for liquefaction evaluation and settlement estimation apart from some minor modifications, as the extension of the relationship $Q_{tn,cs}$-$CRR_{7.5}$. However, as the sensitivity analysis performed in section 6.4. presents, this modification has no influence in the results. When compared the parameters obtained with the results from CLiq, it is noticed great agreement between both, with some minor differences in some cases but with little reflection on the final results. Considering all this and the fact that CLiq provides some of the latest methods available in the literature, offers the user a great control over some calculation parameters and has great transparency, providing in tabular and graphical form intermediate parameters and calculation results, it may be concluded that this software provides accurate results in liquefaction assessments and represents a useful tool to the engineering practice. However, the only method validated against the tool for liquefaction evaluation was the Robertson (2009) (Robertson and Wride (1998) was validated against two other commercial software products in chapter 5), thus to have a clearer image on this software, a validation should be performed for the other methods available in CLiq, like the probabilistic Boulanger and Idriss (2014). Within the aim of this thesis, the tool has been developed to implement the latest and widely used method for liquefaction assessment in engineering practice, i.e. the Robertson (2009) method, as was concluded through the literature review presented in chapter 2 and in accordance with recent project work within CH2M.

7
CONCLUSION

7.1. FINAL DISCUSSION

Within the context of the ongoing developments in the wider earthquake engineering community, this research project aims at creating an in-house soil liquefaction assessment tool based on a well-established empirical relationship using CPT measurements. The need for such a tool has been established following recent project experience in CH2M using commercial software, LiquefyPro, which operates essentially as a "black box code" using some techniques which are now superseded, and offering very little, if any, flexibility for adaptation or update as new techniques have become available.

The first important step in this work was to carry out a comprehensive literature review of methods for the assessment of soil liquefaction and estimation of associated settlements. This review, presented in Chapter 2, together with recent project experience within CH2M, enabled the identification of the Robertson and Wride (1998) method with the update by Robertson (2009), as the most widely used one. Regarding settlements, it was established that the method proposed by Zhang et al., 2002 was the most recent published one developed using CPT data.

A CPT-based in-house tool was developed using Mathcad, in order to implement in a transparent and user friendly way the Robertson (2009) method for liquefaction assessment and the Zhang et al. (2002) method for settlement estimation. The development of the tool is presented in chapter 3.

Within the aim of this thesis, three software packages used in engineering practice, namely CLiq, developed by Geologismiki with the collaboration of Professor Doctor Peter Robertson, LiquefyPro by CivilTech and Settle3D (liquefaction add-on) from Rocscience were assessed. The comparison of these three software products was carried out by implementing the Robertson and Wride (1998) method in each case, using CPT data from an extensive archive of case histories available in the New Zealand Geotechnical Database, created after the 2010-2011 Canterbury earthquake sequence. The seismic parameters were also taken from NZGD, obtained from the closest strong motion stations to the locations of the selected CPT profile, recording the 2011 Christchurch earthquake, the event that produced more liquefaction damage within the 2010-2011 Canterbury sequence. The existence of a database with a full set of high-quality data available was crucial for the development of this study, since it provided not only geotechnical and seismic data, but also post-earthquake information, relevant to compare with the liquefaction analysis results. The NZGD database is presented and the case histories selected for the comparison of the three software packages were discussed in chapter 4.

The comparison of the three software products consisted in comparing against each other the parameters estimated during the calculation by plotting them. This validation is discussed in further detail in chapter 5, where the main capabilities and limitations found for each software are presented and discussed.

During the assessment of LiquefyPro some limitations were found, mostly related with the implementation of the Robertson and Wride (1998) method, as the software is not following the proposed fines content correction and is not defining a limit for the $q_{c1N,cs}$-$CRR_{7.5}$ relationship. Another issue was found in the input, related with the limit imposed for the number of rows of CPT data, requiring the user to manipulate the data if it exceeds the limit, in order to perform the analysis. However, all of these noticed limitations did not produce a major error in the calculation results, since the comparison with the post-earthquake information in the database and another validated software presented some agreement in the values.

The assessment of the liquefaction add-on in Settle^{3D} did not have the same result, with several limitations noticed and a huge disagreement with the information in the database and the other two software packages assessed. Considering that this software does not provide any intermediate parameters apart from the normalized input data and the final results of the calculation, it is not possible to affirm with certainty which modifications were implemented in the method, and the reason of them. The comparison of the results obtained with Settle^{3D} did not match the other two software products. It is suspected that Settle^{3D} might wrongly implement the fines content correction. An issue was also noticed in the input, related with the definition of the fines content for the different soil layers. Although Robertson and Wride (1998) performs an estimation of the fines content based on the CPT data in order to implement the fines content correction, Settle^{3D} requires the user to input a fines content for the soil. The issues in this software are also extended to the definition of the threshold for I_C, since it was noticed that Settle^{3D} was not implementing any value for it, producing estimations of liquefiable layers and liquefaction evaluations different than the performed by the other two software products. In addition, this software does not allow to estimate liquefaction-induced settlements if the analyses are based on CPT data, which represents a major limitation since CPT is generally the preferred basis for liquefaction evaluation by the engineering community and an analysis of estimated settlements is essential for understanding the impact of occurrence of liquefaction at some specific location.

In the validation of CLiq it was only noticed one modification to Robertson and Wride (1998), also related with the limit for the $q_{c1N,cs}$-$CRR_{7.5}$ relationship, although in this case it is known the new limit implemented of 200. In an e-mail conversation with the developer of the method and collaborator in the development of this software, Professor Doctor Peter Robertson, it was clear that this modification was implemented in order to capture denser soils and larger earthquake loading. CLiq demonstrated great accuracy in its calculations, versatility achieved through user control over the parameters and transparency through clear presentation of the intermediate parameters. CLiq was therefore judged to be the most reliable and flexible commercial software tool for liquefaction assessment and was selected for validation against the developed in-house tool.

The validation of CLiq against the in-house tool is presented with further detail in chapter 6. It was based on one of the case histories selected from NZGD and it followed Robertson (2009), an update of the previous Robertson and Wride (1998) method. The tool strictly follows the method as published, and produces almost identical results as CLiq, apart from a disagreement in the values of $Q_{tn,cs}$, since it was noticed that CLiq was implementing differently the expression to obtain K_C for I_C values greater than 2.7. However, this difference does not affect in any way the final results of the analysis, since in the following steps of the calculation, $CRR_{7.5}$ is estimated based on Q_{tn} for I_C values in that range. The comparison of the settlement for dry soils showed a minor disagreement between CLiq and the in-house tool, although the reason behind it is not clear. Nevertheless, as this parameter has little influence on the total settlement, this difference does not produce a significant error.

The development of the in-house tool has provided a means for independent validation of commercial software. The use of Mathcad offers transparency and flexibility, essential to the understanding of the

operation implemented in CLiq or other similar products, which can otherwise seem like an analytical "black box". Having a means of independently checking calculations in a transparent way is particularly important in engineering practice and especially for projects in heavily regulated sectors such as nuclear or petrochemical. The in-house tool will therefore be very useful for increasing confidence in design calculations on future projects.

The in-house tool has also enabled the identification of the capabilities and limitations of available existing software products with respect to current liquefaction assessment methods. Owing to the flexibility of the Mathcad platform, the in-house tool will facilitate the introduction of new analysis methods as they become available.

7.2. RECOMMENDATIONS FOR FURTHER DEVELOPMENTS

The implemented tool follows the method for liquefaction assessment based on CPT data presented by Robertson (2009) as an update of the widely used procedure of Robertson and Wride (1998). A further development of this work could include the implementation of other liquefaction assessment procedures presented herein, for example the method of Boulanger and Idriss (2014), allowing the user to have control over the methodology used within the calculation.

In this work the developed tool has been validated against CLiq (by Geologismiki), identified as the most accurate, reliable and complete commercially available tool for the assessment of liquefaction based on CPT data following the Robertson and Wride (1998) procedure. As a potential further development, the tool could also be used to formally validate LiquefyPro, Settle^{3D} and any other software available in the market. Within the scope of the current project, it was not possible to fully understand the reasons behind some differences noticed between the estimations of some parameters using different software packages. This was especially the case for parameters estimated using Settle^{3D}. Further assessment of this software may therefore be beneficial.

The initial concept in the development of the tool was to implement various liquefaction assessment procedures presented herein, so the user would have control over the methodology used within the calculation and could adapt it to each specific project. However, in the scope of this thesis, it was only possible to adopt Robertson (2009). It would be valuable to add some other procedures, as the Robertson and Wride (1998) or the Boulanger and Idriss (2014), in order to allow a direct validation of the software packages that do not embody Robertson (2009) and to support a further validation of CLiq.

Another potential extension of the current tool would be to include SPT-based liquefaction assessment methods, to complement the CPT-based approach. This could have application to the assessment of sites for which CPT data is not available, which is sometimes the case for existing assets for which only historical ground investigation data are available.

The new tool could be used to explore further the sensitivity of outputs to input parameters which commercial software do not allow to adjust. Areas that could be explored are for example the effect on the liquefaction assessment of the selection of some parameters like K_0 or the choice of the magnitude scaling factor, MSF.

REFERENCES

Ambraseys, N.N. (1988). Engineering seismology: Part I. In *Earthquake Engineering and Structural Dynamics*, pp. 1-50, John Wiley and Sons, New Jersey.

Andrus, R., Stokoe, K.H. (1997). Liquefaction resistance based on shear wave velocity. In *Proceedings of NCEER Workshop on Evaluation of Liquefaction Resistance of Soils.*

Bal, A.A. (1996). *Valley fills and coastal cliffs buried beneath an alluvial plain evidence from variation of permeabilities in gravel aquifers, Canterbury Plains, New Zealand.* Journal of Hydrology (35):1-27.

Been, K. and Jeffries, M.G. (1985). *A State Parameter for Sands*. Geotechnique, 35(2): 99-112, Institute of Civil Engineers, London.

Blake, T.F. (1996). Personal Communication as cited in Youd et al. (2001).

Bishop, A.W. (1973). *The Stability of Tips and Spoil Heaps.* Quarterly Journal of Engineering Geology and Hydrogeology, 6(3-4): 335-376, The Geological Society, London.

Boulanger, R. W. (2003). *High Overburden Stress Effects in Liquefaction Analyses.* Journal of Geotechnical and Geoenvironmental Engineering, 129(12): 1071–1082, American Society of Civil Engineers, Reston.

Boulanger, R.W. and Idriss, I. M. (2004). *Evaluating the Potential for Liquefaction or Cyclic Failure of Silts and Clays.* Report no. UCD/CGM-04/01. Center for Geotechnical Modeling. University of California.

Boulanger, R.W. and Idriss, I. M. (2006). *Liquefaction Susceptibility Criteria for Silts and Clays.* Journal of Geotechnical and Geoenvironmental Engineering, 132(12): 1413–1426, American Society of Civil Engineers, Reston.

Boulanger, R.W. and Idriss, I. M. (2007). *Evaluation of Cyclic Softening in Silts and Clays.* Journal of Geotechnical and Geoenvironmental Engineering, 133(6): 641–652, American Society of Civil Engineers, Reston.

Boulanger, R.W. and Idriss, I.M. (2014). *CPT and SPT based Liquefaction Triggering Procedures Report No. UCD/CGM-14/01* Center for Geotechnical Modeling, pp134. Department of Civil and Environmental Engineering Report, University of California, Davis.

Brackley, H. L. (2012). Geological information relevant to the liquefaction hazard assessment and liquefaction susceptibility zoning. In *Review of Liquefaction Hazard Information in Eastern Canterbury, Including Christchurch City and Parts of Selwyn, Waimakariri and Hurunui Districts,* Environment Canterbury Regional Council, Christchurch.

Bray, J. D. and Sancio, R. B. (2006). *Assessment of Liquefaction Susceptibility of Fine Grained Soil.* Journal of Geotechnical and Geoenvironmental Engineering, 132(9): 1165 – 1177, American Society of Civil Engineers, Reston.

Brown, L.J., Weeber, J.H. (1992). *Geology of the Christchurch Urban Area. Scale 1:250000.* Institute of Geological and Nuclear Sciences Geological Map 1. Lower Hutt, Institute of Geological and Nuclear Sciences.

Brown, L.J., Wilson, D.D., Moar, N.T.,Mildenhall, D.C. (1988). *Stratigraphy of the Late Quaternary Deposits of the Northern Canterbury Plains, New Zealand.* New Zealand Journal of Geology and Geophysics, 31: 305-335, Royal Society of New Zealand, Oxford.

Browne, G.H., Naish, T.R. (2003). *Facies Development And Sequence Architecture Of A Late-Quaternary Fluvial-Marine Transition, Canterbury Plains And Shelf, New Zealand: Implications For Forced Regressive Deposits*. Sedimentary Geology, 158: 57-86, Elsevier.

Browne, G.H., Field, B.D., Barrell, D.J.A., Jongens, R., Bassett, K.N., Wood, R.A. (2012). *The Geological Setting of the Darfield and Christchurch Earthquakes.* New Zealand Journal of Geology and Geophysics, 55(3): 193-197, Royal Society of New Zealand, Oxford.

Castro, G. and Poulos, S.J. (1977). *Factors Affecting Liquefaction and Cyclic Mobility.* Journal of Geotechnical Engineering Division, 106(6): 501 – 506, American Society of Civil Engineers, Reston.

Cetin, K.O. (2000). *Reliability-Based Assessment of Seismic Soil Liquefaction Initiation Hazard.* Ph.D. dissertation, University of California.

Cetin, K.O. and Bilge, H.T. (2012). *Performance-Based Assessment of Magnitude (Duration) Scaling Factors.* Journal of Geotechnical Engineering Division, 138(3): 324 – 334, American Society of Civil Engineers, Reston.

Cetin, K.O., Seed, H. B., Der Kiureghian, A., Tokimatsu, K., Harder, L.F., Jr., Kayen, R. E., Moss, R. E. S. (2004). *Standard Penetration Test- Based Probabilistic and Deterministic Assessment of Seismic Soil Liquefaction Potential.* Journal of Geotechnical and Geoenvironmental Engineering, 130(12): 1314–1340, American Society of Civil Engineers, Reston.

CivilTech Software (2008). LiquefyPro: Liquefaction and Settlement Analysis Software Manual, Version 5, Palo Alto, California.

Dashti, S., Bray, J., Pestana, J., Riemer, M., Wilson, D. (2010). *Mechanisms of Seismically Induced Settlement of Buildings with Shallow Foundations on Liquefiable Soil.* Journal of Geotechnical and Geoenvironmental Engineering, 136(1): 151 – 164, American Society of Civil Engineers, Reston.

Eurocode 8: Design of Structures for Earthquake Resistance-Part 5: Foundations, Retaining Structures and Geotechnical Aspects. British Standard BS EN1998-5:2004.

Forsyth, P.J., Barrell, D.J.A., Jongens, R. (2008). *Geology of the Christchurch Area.* Institute of Geological and Nuclear Sciences 1:250000 geological map 16. Lower Hutt, New Zealand.

Golesorkhi, R. (1989). *Factors Influencing the Computational Determination of Earthquake-Induced Shear Stresses in Sandy Soils.* Ph.D. dissertation, University of California.

Guide Specifications for LRFD Seismic Bridge Design (2009). American Association of State Highway and Transportation Officials.

Green, R.A., Cubrinovski, M., Cox, B., Wood, C., Wotherspoon, L., Bradley, B., Maurer, B. (2014). *Select Liquefaction Case Histories from the 2010-2011 Canterbury Earthquake Sequence.* Earthquake Spectra, 30(1): 131-153, Earthquake Engineering Research Institute, Oakland.

Idriss, I.M. (1999). An update to the Seed-Idriss simplified procedure for evaluating liquefaction potential. In *Proceedings of TRB Workshop on New Approaches to Liquefaction.* Publication No. FHWA-RD-99-165. Federal Highway Administration, Washington.

Idriss, I.M. and Boulanger, R.W., (2008). *Soil Liquefaction During Earthquakes.* Earthquake Engineering Research Institute. MNO-12.

Ishihara, K. (1985). Stability of natural deposits during earthquakes. In *Proc., 11th Conf. on Soil Mechanics and Foundation Engineering Vol.1,* pp. 321-376, Balkema, Rotterdam.

Ishihara, K. and Yoshimine, M. (1992). *Evaluation of Settlements in Sand Deposits Following Liquefaction During Earthquakes.* Soils and Foundations, 32(1): 173-188. Japanese Geotechnical Society, Tokyo.

Iwasaki, T., Tatsuoka, F., Tokida, K.I., Yasuda, S. (1978). A practical method for assessing soil liquefaction potential based on case studies at various sites in Japan. In *Proceedings of the 2nd International Conference on Microzonation*, pp. 885-896, National Science Foundation, Washington D.C.

Iwasaki, T., Tokida, K., Tatsuoka, F., Watanabe, S., Yasuda, S., Sato, H. (1982). Microzonation for soil liquefaction potential using simplified methods. In *Proceedings of the 3rd International Conference on Microzonation*, pp. 1310-1330, Seattle.

Juang, C.H., Ching, J., Wang, L., Khoshnevisan, S., Ku, C.S., (2013). *Simplified procedure for estimation of liquefaction-induced settlement and site-specific probabilistic settlement exceedance curve using cone penetration test (CPT).* Canadian Geotechnical Journal, 50(10): 1055-1066, National Research Center, Ottawa.

Kayen, R.E., Mitchell, J.K, Seed, R.B., Lodge, A. Nishio, S., Coutinho, R. (1992). Evaluation of SPT, CPT and shear wave based methods for liquefaction potential assessment using Loma Prieta data. In *Proceedings of the 4th Japan-U.S. Workshop on Earthquake Resistant Design of Lifeline Facilities and Countermeasures for Soil Liquefaction*, Vol. 1, pp. 177-204.

Kim, D., Shin, Y., Siddiki, N. (2010). *Geotechnical Design Based on CPT and PMT*. Indiana Department of Transportation and Purdue University, Indiana.

Koppejan, A. W., van Wamelan, B. M., Weinberg, L. J. H. (1948). Coastal flow slides in the Dutch province of Zeeland. In *Proceedings of 2nd Conference in Soil Mechanics and Foundation Engineering*, pp. 89-96, Rotterdam.

Kramer, S. (1996). *Geotechnical Earthquake Engineering*. Prentrice Hall, New Jersey.

Ku, C.S., Juang, C.H., Chang, C.W., Ching, J. (2011). *Probabilistic Version of the Robertson and Wride Method for Liquefaction Evaluation: development and application.* Canadian Geotechnical Journal, 49(1): 27-44, National Research Centre, Ottawa.

Liao, S.S.C. and Whitman, R.V. (1986). *Overburden Correction Factors for SPT in Sand.* Journal of Geotechnical Engineering, 112(3): 373-377, American Society of Civil Engineers, Reston.

Luna, R. and Frost, J. D. (1998). *Spatial Liquefaction Analysis System.* Journal of Computing in Civil Engineering, 12(1): 48-56. American Society of Civil Engineers, Reston.

Lunne, T., Robertson, P.K., Powell, J.J.M. (1997). *Cone Penetration Testing in Geotechnical Practice.* Blackie Academic, pp 312, EF Spon/Routledge Publ., New York.

Matos Fernandes, M. (2006). *Mecânica dos Solos – Conceitos e Princípios Fundamentais.* FEUP Edições, Faculdade de Engenharia da Universidade do Porto.

Matos Fernandes, M. (2011). *Mecânica dos Solos - Introdução à Engenharia Geotécnica.* FEUP Edições, Faculdade de Engenharia da Universidade do Porto.

Mogami, T., and Kubo, K. (1953). The Behaviour of Soil During Vibration. *In Proceedings of the 3rd International Conference on Soil Mechanics and Foundation Engineering, Vol.1*, pp.152-153, ICOSOMEF, Zurich.

Moss, R.E.S., Seed, R.B., Kayen R.E., Stewart, J.P., Der Kiureghian, A., Cetin, K.O. (2006). *CPT-Based Probabilistic and Deterministic Assessment of In-Situ Seismic Soil Liquefaction Potential*. Journal of Geotechnical and Geoenvironmental Engineering, 132(8): 1032-105, American Society of Civil Engineers, Reston.

Moss, R.E.S., Kayen R.E., Tong, L.-Y., Liu, S.-Y., Cai, G.-J., Wu, J. (2009). Reinvestigating liquefaction and non-liquefaction case histories from the 1976 Tangshan earthquake. In *Pacific Earthquake Engineering Research Center Report 2009/2012.* Pacific Earthquake Engineering Center, Berkeley.

Moss, R.E.S., Kayen R.E., Tong, L.-Y., Liu, S.-Y., Cai, G.-J., Wu, J. (2011). *Retesting of Liquefaction and Non-Liquefaction Case Histories from the 1976 Tangshan Earthquake.* Journal of Geotechnical and Geoenvironmental Engineering, 137(4): 334–343, American Society of Civil Engineers, Reston.

Olsen, R. S. and Malone, P.G. (1988). Soil classification and site characterization using the cone penetrometer test. In *Penetration Testing 198*, pp. 887-893, De Ruiter Balkema, Rotterdam.

Olsen, R.S. and Mitchell, J.K. (1995). CPT stress normalization and prediction of soil classification. In *Proceedings of the International Symposium on Cone Penetration Testing, CPT 95,* pp. 257-262. Swedish Geotechnical Society, Linkoping.

Pradel, D. (1998). *Procedure to Evaluate Earthquake-Induced Settlements in Dry Sandy Soils.* Journal of Geotechnical and Geoenvironmental Engineering, 124(4): 364–368, American Society of Civil Engineers, Reston.

Pyke, R., Seed, H.B., Chan, C.K. (1975). *Settlement of Sands Under Multidirectional Shaking.* Journal of Geotechnical and Geoenvironmental Engineering, 101(4): 379–398, American Society of Civil Engineers, Reston.

Ramsey, N. (2010). *Some Issues Related to Applications of the CPT.* Paper presented at 2nd International Symposium on Cone Penetration Testing, CPT10, California.

Robertson, P.K. (1990). *Soil Classification Using the Cone Penetration Test.* Canadian Geotechnical Journal, 27(1): 151-158, National Research Center, Ottawa.

Robertson, P.K. (1994). Suggested terminology for liquefaction. In *Proceedings of the 47th Canadian Geotechnical Conference,* pp. 277-286, N.S. CGS., Halifax.

Robertson, P.K. (2004). *Evaluating Soil Liquefaction and Post-Earthquake Deformations using the CPT*. /Keynote Lecture. Geotechnical and Geophysical Site Characterization/. Ed. A. Viana da Fonseca and P.W. Mayne. Vol. 1, pp 233-249. Millpress, Rotterdam.

Robertson, P.K. (2008). *Interpretation of the CPT: a unified approach.* Manuscript submitted to the Canadian Geotechnical Journal.

Robertson, P.K. (2009). *Performance based earthquake design using the CPT.* Proc., IS Tokyo Conf. CRC Press/Balkema, Taylor and Francis Group, Tokyo.

Robertson, P.K. and Wride, C.E. (1997). Cyclic liquefaction and its evaluation based on SPT and CPT: Seismic Short Course on Evaluation and Mitigation of Earthquake Induced Liquefaction Hazards. In *Proceedings of the NCEER Workshop on Evaluation of Liquefaction Resistance of Soils,* San Francisco.

Robertson, P.K. and Wride, C.E. (1998). *Evaluating cyclic liquefaction potential using the cone penetration test*. Canadian Geotechnical Journal, 35(3): 442-459, National Research Center, Ottawa.

Robertson, P.K., and Cabal, K.L., (2010). Estimating soil unit weight from CPT. In *2nd International Symposium on Cone Penetrating Testing*, May 2010, Huttington Beach.

Robertson, P.K. and Shao, L. (2010). Estimation of seismic compression in dry soils using the CPT. *Fifth International Conference on Recent Advantages in Geotechnical Earthquake Engineering and Soil Dynamics.* San Diego, CA.

Robertson, P.K. and Cabal, K.L. (2015). *Guide to cone penetration testing 6th Edition.* Gregg Drilling & Testing, Inc. 6th Edition, Signal Hill, California.

Rocscience Inc. (2014). Settle3D Liquefaction Analysis Theory Manual, Version 3.0, Toronto.

Rodrigues, C., Amoroso, S., Viana da Fonseca, A., Cruz, N. (2014). *Estudo do risco de liquefação das areias de Aveiro a partir de ensaios SCPTU e SDMT.* Actas do 14º Congresso Nacional de Geotecnia. Cavaleiro, V. e Machado do Vale, J. (Eds.) UBI, Covilhã.

Scawthorn, C. (2006). A brief history of seismic risk assessment. In *Risk Assessment, modelling and decision support*, pp. 5-81, Springer Berlin Heidelberg, Heidelberg.

Seed, H.B. and Idriss, I. M. (1971). *Simplified Procedure for Evaluating Soil Liquefaction Potential.* Journal of the Soil Mechanics and Foundations Division, 107(9): 1249-1274, American Society of Civil Engineers, Reston.

Seed, H.B. and Silver, M.L. (1972). *Settlement of Dry Sands During Earthquakes.* Journal of Soil Mechanics and Foundations Division, 98(4): 381-397, American Society of Civil Engineers, Reston.

Seed, H.B. and De Alba, P. (1986). Use of SPT and CPT tests for evaluating the liquefaction resistance of sands. In *Proceedings of INSITU'86, ASCE Spec. Conference on Use of In Situ Testing in Geotechnical Engineering* , New York, American Society of Civil Engineers.

Seed, H. B., Idriss, I. M., Arango, I. (1983). *Evaluation of Liquefaction Potential Using Field Performance Data.* Journal of Geotechnical Engineering, 109(3): 458-482, American Society of Civil Engineers, Reston.

Seed, H. B., Idriss, I. M., Makdisi, F., Banerjee, N. (1975). *Representation of Irregular Stress Time Histories by Equivalent Uniform Stress Series in Liquefaction Analysis, Report No. EERC 75-29.* Earthquake Engineering Research Ctr., University of California.

Seed, H.B., Tokimatsu, K., Harder, L.F., Chung, R.M. (1985). *Influence of SPT Procedures in Soil Liquefaction Resistance Evaluations.* Journal of Geotechnical Engineering, 111(12): 1425-1445, American Society of Civil Engineers, Reston.

Silver, M. L. and Seed, H.B. (1971). *Volume Changes in Sands during Cyclic Loading.* Journal of Soil Mechanics and Foundations Division, 97(9): 1171-1182, American Society of Civil Engineers, Reston.

Suzuki, Y., Koyamada, K., Tokimatsu, K. (1997). Prediction of liquefaction resistance based on CPT tip resistance and sleeve friction. In *Proc. XIV Intl. Conf. on Soil Mechanics and Foundation Engineering*, pp. 603-606, Hamburg.

Taylor, M.L., Cubrinovski, M., Haycock, I. (2012). *Characterization of Ground Conditions in the Christchurch Central Business District.* Australian Geomechanics Journal, 47(4): 43-57, Australian Geomechanics Society, Stt. Ives.

Terzaghi, K., and Peck, R. B. (1967). *Soil Mechanics in Engineering Practice, Second Edition.* John Wiley and Sons, New York.

Tokimatsu, K. and Seed, H. B. (1987). *Evaluation of Settlements in Sands due to Earthquake Shaking*. Journal of Geotechnical Engineering, 113(8): 861-879, American Society of Civil Engineers, Reston.

Ueng, T.S., Wu, C.W., Cheng, H.W., Chen, C.H. (2010). *Settlements of saturated clean sand deposits in shaking table tests*. Soil Dynamics and Earthquake Engineering, 30(1-2): 50-60, Elsevier.

Youd, T.L. (1984). Recurrence of liquefaction at the same site. In *Proceedings of the 8th World Conference on Earthquake Engineering, Vol. 3,* pp. 231-238, Prentice-Hall, New Jersey.

Youd, T. L. (1993). *Liquefaction-Induced Lateral Spread Displacement (Report No. NCEL-TN-1862).* Naval Civil Engineering Laboratory, Port Hueneme, California.

Youd, T.L., and Idriss, I.M. (1997). *Proceedings of the NCEER Workshop on Evaluation of Liquefaction Resistance of Soils.* Technical report NCEER (Vol. 97). National Center for Earthquake Engineering Research (NCEER).

Youd, T.L. and Noble, S.K. (1997) Liquefaction criteria based on statistical and probabilistic analyses. In *Proceedings of the NCEER Workshop on Evaluation of Liquefaction Resistance of Soils*

Youd, T.L., Idriss, I.M, Andrus, R.D., Arango, I., Castro, G., Christian, J.T., Dobry, R., Finn, W.D.L., Harder, L.F., Hynes, M.E., Ishihara, K., Koester, J.P., Liao, S.S.C., Marcuson, W.F., Martin, G.R., Mitchell, J.K., Moriwaki, Y., Power, M.S., Robertson, P.K., Seed, R.B., Stokoe, K.H. (2001). *Liquefaction resistance of soils: summary report from the 1996 NCEER and 1998 NCEER/NSF Workshops on evaluation of liquefaction resistance of soils*. Journal of Geotechnical and Geoenvironmental Engineering, 127(4): 297 – 313, American Society of Civil Engineers, Reston.

Zhang, G., Robertson, P.K., Brachman, R.W.I. (2002) *Estimating liquefaction-induced ground settlements from CPT for level ground.* Canadian Geotechnical Journal, 39(5): 1168-1180, National Research Center, Ottawa.

CLiq User's Manual: (http://geologismiki.gr/Documents/CLiq/HTML/index.html) Access date: 21/03/2016

Learning from Building Failures: (https://buildingfailures.files.wordpress.com/2014/02/tiltedbuilding.jpg) Access date: 19/06/2016

National Centers for Environmental Information : (http://www.ngdc.noaa.gov/hazardimages/picture/show/1436) Access date: 19/06/2016

New Zealand Geotechnical Database: (https://www.nzgd.org.nz/) Access date: 20/04/2016

U.S.GeotechnicalSurvey:(http://geomaps.wr.usgs.gov/sfgeo/liquefaction/image_pages/boils_fissure22.html) Access date: 16/04/2016

APPENDIX

In this appendix is presented the worksheet implemented in the developed Mathcad tool.

CPT-Based Liquefaction Assessment

INPUT DATA

CPT Profile and Soil Parameters

Insert CPT file:

CPT :=
CPT_1324_AGS01.xls

$z_1 := CPT^{\langle 0 \rangle}$ $q_1 := CPT^{\langle 1 \rangle}$ $f_1 := CPT^{\langle 2 \rangle}$

Select Unit Weight estimation procedure:

Unit_Weight :=
Default Value
Estimate (Robertson and Cabal, 2010)

Insert default value for unit weight if selected: $\gamma_s := 18 \frac{kN}{m^3}$

Groundwater Depths

Water Unit Weight: $\gamma_w := 9.81 \frac{kN}{m^3}$

Water Table during earthquake: $WT_e := 1.10m$

Water Table during CPT test: $WT_i := 2m$

Seismic Parameters

Peak Ground Acceleration, PGA (g): $PGA := 0.17$

Earthquake Magnitude: $M := 6.20$

Choose between NCEER and Boulanger and Idriss aproaches for MSF:

MSF :=
NCEER (1997)
Idriss and Boulanger (2008)

LIQUEFACTION EVALUATION

$z := \text{for } j \in 1..\text{last}(z_1)$ $\quad a_{j-1} \leftarrow z_{1_j} \text{ if } z_{1_0} = 0$ $\quad a_{j-1} \leftarrow z_{1_{j-1}} \text{ if } z_{1_0} \neq 0$ $\quad a$

$q := \text{for } j \in 1..\text{last}(q_1)$ $\quad a_{j-1} \leftarrow q_{1_j} \text{ if } q_{1_0} = 0$ $\quad a_{j-1} \leftarrow q_{1_{j-1}} \text{ if } q_{1_0} \neq 0$ $\quad a$

$f := \text{for } j \in 1..\text{last}(f_1)$ $\quad a_{j-1} \leftarrow f_{1_j} \text{ if } f_{1_0} = 0$ $\quad a_{j-1} \leftarrow f_{1_{j-1}} \text{ if } f_{1_0} \neq 0$ $\quad a$

$z := z \cdot m$ $\qquad q := q \cdot MPa$ $\qquad f := f \cdot MPa$

CORRECTION OF NEGATIVE CPT VALUES

$j := 0..\text{last}(z)$

$q_{c_j} := \begin{cases} 0.01MPa & \text{if } q_j \le 0 \\ q_j & \text{otherwise} \end{cases}$ $\qquad f_{s_j} := \begin{cases} 0.01kPa & \text{if } f_j \le 0 \\ f_j & \text{otherwise} \end{cases}$

$\gamma_j := \begin{cases} \gamma_s & \text{if Unit\_Weight} = 1 \\ \left[0.27 \cdot \log\left[\frac{\left(f_{s_j} \cdot 100\right)}{q_{c_j}} \right] + 0.36 \cdot \log\left(\frac{q_{c_j}}{100kPa} \right) + 1.236 \right] \cdot \gamma_w & \text{if Unit\_Weight} = 2 \end{cases}$

CPT Data Plots:

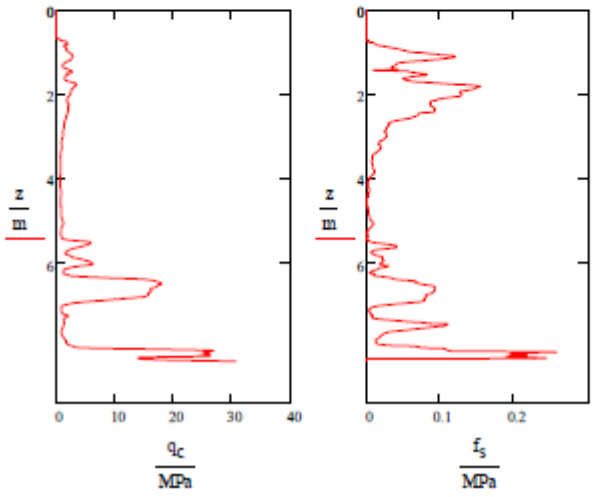

CRR CALCULATION *Robertson (2009)*

$\sigma_{v0} := \overrightarrow{(\gamma \cdot z)}$

$\sigma_{v0\_ef_j} := \begin{cases} \left[\sigma_{v0_j} - \gamma_w \left(z_j - WT_i \right) \right] & \text{if } z_j > WT_i \\ \sigma_{v0_j} & \text{otherwise} \end{cases}$

$$a := \text{for } j \in 0..\text{last}(z)$$

$$n_j \leftarrow 1$$

$$C_{N_j} \leftarrow \min\left[\left(\frac{100\text{kPa}}{\sigma_{v0\_ef_j}}\right)^{n_j}, 1.7\right]$$

$$F_{r_j} \leftarrow \left[f_{s_j}\cdot\frac{100}{\left(q_{c_j}-\sigma_{v0_j}\right)}\right]$$

$$Q_j \leftarrow \left[\left(q_{c_j}-\sigma_{v0_j}\right)\cdot\frac{C_{N_j}}{100\text{kPa}}\right]$$

$$I_{C_j} \leftarrow \left[\left(3.47-\log\left(Q_j\right)\right)^2+\left(1.22+\log\left(F_{r_j}\right)\right)^2\right]^{0.5}$$

$$n1_j \leftarrow \min\left[0.381\cdot I_{C_j}+\left[0.05\cdot\left(\frac{\sigma_{v0\_ef_j}}{100\text{kPa}}\right)\right]-0.15, 1\right]$$

while $\left|n1_j - n_j\right| > 0.01$

$$n_j \leftarrow n1_j$$

$$C_{N_j} \leftarrow \min\left[\left(\frac{100\text{kPa}}{\sigma_{v0\_ef_j}}\right)^{n_j}, 1.7\right]$$

$$F_{r_j} \leftarrow f_{s_j}\cdot\frac{100}{\left(q_{c_j}-\sigma_{v0_j}\right)}$$

$$Q_j \leftarrow \left(q_{c_j}-\sigma_{v0_j}\right)\cdot\frac{C_{N_j}}{100\text{kPa}}$$

$$I_{C_j} \leftarrow \left[\left(3.47-\log\left(Q_j\right)\right)^2+\left(1.22+\log\left(F_{r_j}\right)\right)^2\right]^{0.5}$$

$$n1_j \leftarrow \min\left[0.381\cdot I_{C_j}+\left[0.05\cdot\left(\frac{\sigma_{v0\_ef_j}}{100\text{kPa}}\right)\right]-0.15, 1\right]$$

$$\text{output} \leftarrow \text{augment}\left(n1, C_N, F_r, Q, I_C\right)$$

$$n := a^{\langle 0\rangle} \qquad C_N := a^{\langle 1\rangle} \qquad F_r := a^{\langle 2\rangle} \qquad Q := a^{\langle 3\rangle} \qquad I_C := a^{\langle 4\rangle}$$

$$I_{C\_2.6_j} := 2.6$$

Soil Parameters Plots:

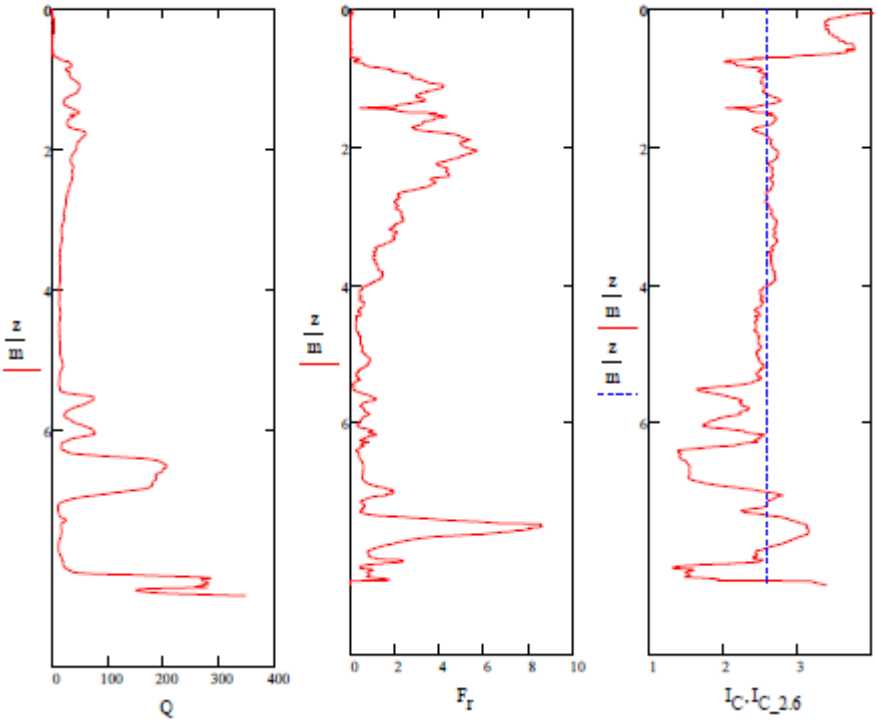

$$K_C := \text{for } j \in 0..\text{last}(z)$$
$$a_j \leftarrow 1 \text{ if } I_{C_j} \le 1.64 \vee I_{C_j} \ge 2.7$$
$$a_j \leftarrow 5.581 \cdot (I_{C_j})^3 - 0.403 \cdot (I_{C_j})^4 - 21.63 \cdot (I_{C_j})^2 + 33.75 \cdot I_{C_j} - 17.88 \text{ if } I_{C_j} > 1.64 \wedge I_{C_j} \le 2.6$$
$$a_j \leftarrow 1 \text{ if } I_{C_j} > 1.64 \wedge I_{C_j} < 2.36 \wedge F_{r_j} < 0.5$$
$$a_j \leftarrow 6 \cdot 10^{-7} \cdot (I_{C_j})^{16.76} \text{ if } I_{C_j} > 2.5 \wedge I_{C_j} < 2.7$$
$$a$$

$$Q_{m\_cs_j} := \begin{cases} K_{C_j} \cdot Q_j & \text{if } K_{C_j} \ne 0 \\ 0 & \text{otherwise} \end{cases}$$

Q_{tn_cs} Plot:

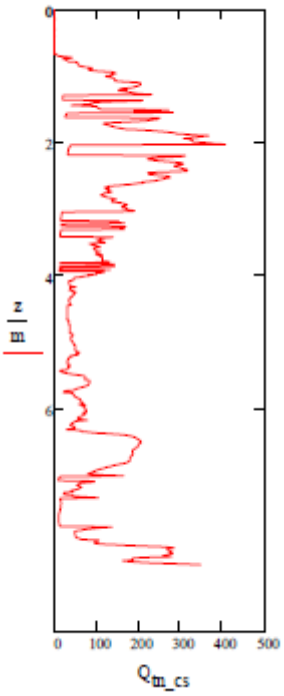

$$CRR_{7.5} := \left| \begin{array}{l} \text{for } j \in 1 + \frac{WT_e}{cm} \ldots \text{last}(z) \\ \quad \left| \begin{array}{l} a_j \leftarrow 93 \cdot \left(\frac{Q_{tn\_cs_j}}{1000} \right)^3 + 0.08 \text{ if } Q_{tn\_cs_j} \geq 50 \wedge Q_{tn\_cs_j} < 200 \\ a_j \leftarrow 0.833 \cdot \left(\frac{Q_{tn\_cs_j}}{1000} \right) + 0.05 \text{ if } Q_{tn\_cs_j} < 50 \\ a_j \leftarrow 0.053 \cdot Q_j \text{ if } I_{C_j} \geq 2.7 \\ a_j \leftarrow 4 \text{ otherwise} \end{array} \right. \\ \text{for } j \in 0 \ldots 1 + \frac{WT_e}{cm} \\ \quad a_j \leftarrow 4 \\ a \end{array} \right.$$

$CRR_{7.5}$ Plot:

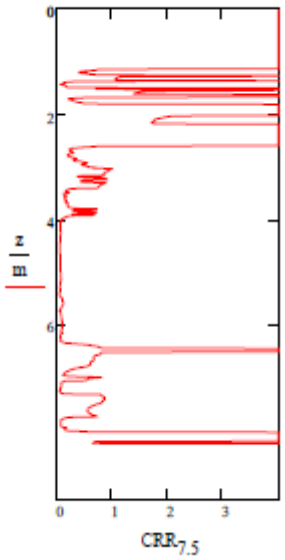

MSF CALCULATION *NCEER*

$$MSF_{max_j} := \min\left[1.09 + \left(\frac{Q_{m\_cs_j}}{180}\right)^3, 2.2\right]$$

$MSF_1 :=$ for $j \in 0..\text{last}(z)$

$a_j \leftarrow \frac{174}{M^{2.56}}$ if MSF = 1

$a_j \leftarrow 1 + \left(MSF_{max_j} - 1\right)\cdot\left(8.64\cdot e^{\frac{-M}{4}} - 1.325\right)$ if MSF = 2

a

$$CRR_j := CRR_{7.5_j}\cdot MSF_{1_j}$$

CSR CALCULATION *Seed and Idriss (1971)*

$$\sigma_{v0\_efl_j} := \begin{cases} \left[\sigma_{v0_j} - \gamma_w \cdot \left(z_j - WT_e\right)\right] & \text{if } z_j > WT_e \\ \sigma_{v0_j} & \text{otherwise} \end{cases}$$

STRESS REDUCTION FACTOR *Liao and Whitman (1986)*

$$r_d := \text{for } j \in 0..\text{last}(z)$$
$$a_j \leftarrow 1 - 0.00765 \cdot \frac{z_j}{m} \quad \text{if } z_j < 9.15m$$
$$a_j \leftarrow 1.174 - 0.0267 \cdot \frac{z_j}{m} \quad \text{if } z_j \geq 9.15m \wedge z_j < 23m$$
$$a$$

$$CSR_j := 0.65 \cdot PGA \cdot \left(\frac{\sigma_{v0_j}}{\sigma_{v0\_efl_j}}\right) \cdot r_{d_j}$$

CSR and CRR Plot:

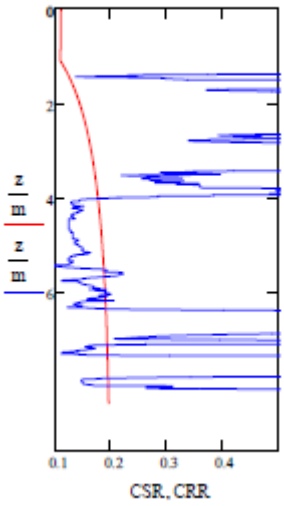

FACTOR OF SAFETY

$$FS := \text{for } j \in 1 + \frac{WT_e}{cm}..\text{last}(z) \qquad FS_{1_j} := 1$$
$$a_j \leftarrow \min\left(2, \frac{CRR_j}{CSR_j}\right)$$
$$\text{for } j \in 0..1 + \frac{WT_e}{cm}$$
$$a_j \leftarrow 2$$
$$a$$

Factor of Safety Plot:

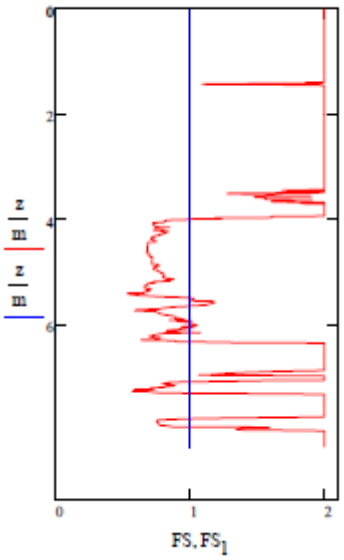

PROBABILITY OF LIQUEFACTION

Ku et al. (2011)

$$P_{L_j} := 1 - pnorm\left[\frac{\left(0.102 + \ln\left(FS_j\right)\right)}{0.276}, 0, 1\right]$$

Probability of Liquefaction Plot:

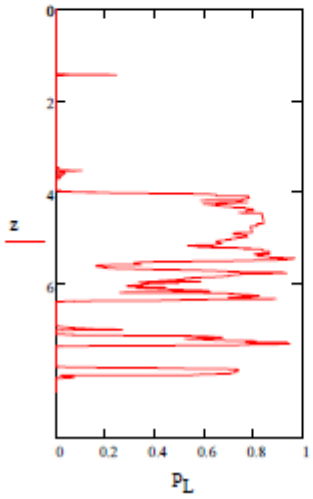

LIQUEFACTION POTENTIAL INDEX

Iwasaki et al. (1978)

$$w_j := 10 - 0.5 \cdot \frac{z_j}{m}$$

$$h := \left| \begin{array}{l} \text{for } j \in 1 .. \text{last}(z) \\ \quad a_j \leftarrow z_j - z_{j-1} \\ a \end{array} \right.$$

$$F1_j := \begin{cases} 1 - FS_j & \text{if } FS_j < 1 \\ 0 & \text{otherwise} \end{cases}$$

$$LPI := \left| \begin{array}{l} c_0 \leftarrow w_0 \cdot F1_0 \cdot \frac{h_0}{m} \\ \text{for } j \in 1 .. \text{last}(z) \\ \quad c_j \leftarrow w_j \cdot F1_j \cdot \frac{h_j}{m} + c_{j-1} \\ c \end{array} \right.$$

LPI Plot

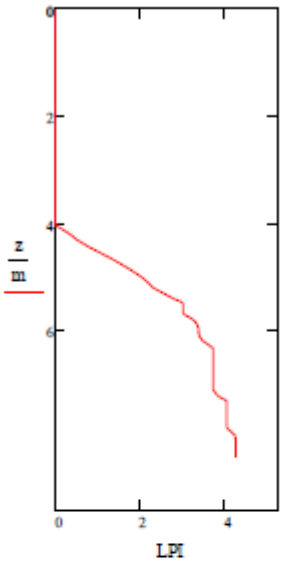

$$Liquefaction\_Severity := \left| \begin{array}{l} a \leftarrow \text{"Little to none"} \quad \text{if } LPI_{last(z)} = 0 \\ a \leftarrow \text{"Minor"} \quad \text{if } LPI_{last(z)} > 0 \wedge LPI_{last(z)} \leq 5 \\ a \leftarrow \text{"Moderate"} \quad \text{if } LPI_{last(z)} > 5 \wedge LPI_{last(z)} \leq 15 \\ a \leftarrow \text{"Major"} \quad \text{if } LPI_{last(z)} > 15 \\ a \end{array} \right.$$

LPI	Liquefaction Severity
LPI=0	Little to none
0<LPI<5	Minor
5<LPI<15	Moderate
15<LPI	Major

Liquefaction_Severity = "Minor"

SETTLEMENTS ESTIMATION

SATURATED SOIL *Zhang et al. (2002)*

$$q_{0_j} := Q_{tn\_cs_j}$$

$$\varepsilon_{v1} := \text{for } j \in \frac{WT_e}{cm} - 1 .. \text{last}(z)$$

$$a_j \leftarrow 102 \cdot \left(q_{0_j}\right)^{-0.82} \text{ if } FS_j \le 0.5 \wedge q_{0_j} \ge 33 \wedge q_{0_j} \le 200$$

$$a_j \leftarrow 102 \cdot (33)^{-0.82} \text{ if } FS_j \le 0.5 \wedge q_{0_j} < 33$$

$$a_j \leftarrow 102 \cdot \left(q_{0_j}\right)^{-0.82} \text{ if } FS_j > 0.5 \wedge FS_j \le 0.6 \wedge q_{0_j} \ge 33 \wedge q_{0_j} \le 147$$

$$a_j \leftarrow 102 \cdot (33)^{-0.82} \text{ if } FS_j > 0.5 \wedge FS_j \le 0.6 \wedge q_{0_j} < 33$$

$$a_j \leftarrow \frac{FS_j - 0.5}{0.1} \cdot \left[2411 \cdot \left(q_{0_j}\right)^{-1.45} - 102 \cdot \left(q_{0_j}\right)^{-0.82}\right] + 102 \cdot \left(q_{0_j}\right)^{-0.82} \text{ if } FS_j > 0.5 \wedge FS_j \le 0.6 \wedge q_{0_j} \ge 147 \wedge q_{0_j} \le 200$$

$$a_j \leftarrow 102 \cdot \left(q_{0_j}\right)^{-0.82} \text{ if } FS_j > 0.6 \wedge FS_j \le 0.7 \wedge q_{0_j} \ge 33 \wedge q_{0_j} \le 110$$

$$a_j \leftarrow 102 \cdot (33)^{-0.82} \text{ if } FS_j > 0.6 \wedge FS_j \le 0.7 \wedge q_{0_j} < 33$$

$$a_j \leftarrow \frac{FS_j - 0.6}{0.1} \cdot \left[1701 \cdot \left(q_{0_j}\right)^{-1.42} - 102 \cdot \left(q_{0_j}\right)^{-0.82}\right] + 102 \cdot \left(q_{0_j}\right)^{-0.82} \text{ if } FS_j > 0.6 \wedge FS_j \le 0.7 \wedge q_{0_j} \ge 110 \wedge q_{0_j} \le 147$$

$$a_j \leftarrow \frac{FS_j - 0.6}{0.1} \cdot \left[1701 \cdot \left(q_{0_j}\right)^{-1.42} - 2411 \cdot \left(q_{0_j}\right)^{-1.45}\right] + 2411 \cdot \left(q_{0_j}\right)^{-1.45} \text{ if } FS_j > 0.6 \wedge FS_j \le 0.7 \wedge q_{0_j} \ge 147 \wedge q_{0_j} \le 200$$

$$a_j \leftarrow 102 \cdot \left(q_{0_j}\right)^{-0.82} \text{ if } FS_j > 0.7 \wedge FS_j \le 0.8 \wedge q_{0_j} \ge 33 \wedge q_{0_j} \le 80$$

$$a_j \leftarrow 102 \cdot (33)^{-0.82} \text{ if } FS_j > 0.7 \wedge FS_j \le 0.8 \wedge q_{0_j} < 33$$

$$a_j \leftarrow \frac{FS_j - 0.7}{0.1} \cdot \left[1690 \cdot \left(q_{0_j}\right)^{-1.46} - 102 \cdot \left(q_{0_j}\right)^{-0.82}\right] + 102 \cdot \left(q_{0_j}\right)^{-0.82} \text{ if } FS_j > 0.7 \wedge FS_j \le 0.8 \wedge q_{0_j} \ge 80 \wedge q_{0_j} \le 110$$

$$a_j \leftarrow \frac{FS_j - 0.7}{0.1} \cdot \left[1690 \cdot \left(q_{0_j}\right)^{-1.46} - 1701 \cdot \left(q_{0_j}\right)^{-1.42}\right] + 1701 \cdot \left(q_{0_j}\right)^{-1.42} \text{ if } FS_j > 0.7 \wedge FS_j \le 0.8 \wedge q_{0_j} \ge 110 \wedge q_{0_j} \le 200$$

$$a_j \leftarrow 102 \cdot \left(q_{0_j}\right)^{-0.82} \text{ if } FS_j > 0.8 \wedge FS_j \le 0.9 \wedge q_{0_j} \ge 33 \wedge q_{0_j} \le 60$$

$$a_j \leftarrow 102 \cdot (33)^{-0.82} \text{ if } FS_j > 0.8 \wedge FS_j \le 0.9 \wedge q_{0_j} < 33$$

$$a_j \leftarrow \frac{FS_j - 0.8}{0.1} \cdot \left[1430 \cdot \left(q_{0_j}\right)^{-1.48} - 102 \cdot \left(q_{0_j}\right)^{-0.82}\right] + 102 \cdot \left(q_{0_j}\right)^{-0.82} \text{ if } FS_j > 0.8 \wedge FS_j \le 0.9 \wedge q_{0_j} \ge 60 \wedge q_{0_j} \le 80$$

$$a_j \leftarrow \frac{FS_j - 0.8}{0.1} \cdot \left[1430 \cdot \left(q_{0_j}\right)^{-1.48} - 1690 \cdot \left(q_{0_j}\right)^{-1.46}\right] + 1690 \cdot \left(q_{0_j}\right)^{-1.46} \text{ if } FS_j > 0.8 \wedge FS_j \le 0.9 \wedge q_{0_j} \ge 80 \wedge q_{0_j} \le 200$$

$$a_j \leftarrow \frac{FS_j - 0.9}{0.1} \cdot \left[64 \cdot \left(q_{0_j}\right)^{-0.93} - 102 \cdot \left(q_{0_j}\right)^{-0.82}\right] + 102 \cdot \left(q_{0_j}\right)^{-0.82} \text{ if } FS_j > 0.9 \wedge FS_j \le 1.0 \wedge q_{0_j} \ge 33 \wedge q_{0_j} \le 60$$

$$a_j \leftarrow \frac{FS_j - 0.9}{0.1} \cdot \left[64 \cdot (33)^{-0.93} - 102 \cdot (33)^{-0.82}\right] + 102 \cdot (33)^{-0.82} \text{ if } \left(FS_j > 0.9 \wedge FS_j \le 1.0 \wedge q_{0_j} < 33\right)$$

$$a_j \leftarrow \frac{FS_j - 0.9}{0.1} \cdot \left[64 \cdot \left(q_{0_j}\right)^{-0.93} - 1430 \cdot \left(q_{0_j}\right)^{-1.48}\right] + 1430 \cdot \left(q_{0_j}\right)^{-1.48} \text{ if } FS_j > 0.9 \wedge FS_j \le 1.0 \wedge q_{0_j} \ge 60 \wedge q_{0_j} \le 200$$

$$
\begin{aligned}
&a_j \leftarrow \frac{FS_j - 1.0}{0.1}\cdot\left[11\cdot\left(q0_j\right)^{-0.65} - 64\cdot\left(q0_j\right)^{-0.93}\right] + 64\cdot\left(q0_j\right)^{-0.93} \quad \text{if } FS_j > 1.0 \wedge FS_j \le 1.1 \wedge q0_j \ge 33 \wedge q0_j \le 200\\
&a_j \leftarrow \frac{FS_j - 1.0}{0.1}\cdot\left[11\cdot(33)^{-0.65} - 64\cdot(33)^{-0.93}\right] + 64\cdot(33)^{-0.93} \quad \text{if } FS_j > 1.0 \wedge FS_j \le 1.1 \wedge q0_j < 33\\
&a_j \leftarrow \frac{FS_j - 1.1}{0.1}\cdot\left[9.7\cdot\left(q0_j\right)^{-0.69} - 11\cdot\left(q0_j\right)^{-0.65}\right] + 11\cdot\left(q0_j\right)^{-0.65} \quad \text{if } FS_j > 1.1 \wedge FS_j \le 1.2 \wedge q0_j \ge 33 \wedge q0_j \le 200\\
&a_j \leftarrow \frac{FS_j - 1.1}{0.1}\cdot\left[9.7\cdot(33)^{-0.69} - 11\cdot(33)^{-0.65}\right] + 11\cdot(33)^{-0.65} \quad \text{if } FS_j > 1.1 \wedge FS_j \le 1.2 \wedge q0_j < 33\\
&a_j \leftarrow \frac{FS_j - 1.2}{0.1}\cdot\left[7.6\cdot\left(q0_j\right)^{-0.71} - 9.7\cdot\left(q0_j\right)^{-0.69}\right] + 9.7\cdot\left(q0_j\right)^{-0.69} \quad \text{if } FS_j > 1.2 \wedge FS_j \le 1.3 \wedge q0_j \ge 33 \wedge q0_j \le 200\\
&a_j \leftarrow \frac{FS_j - 1.2}{0.1}\cdot\left[7.6\cdot(33)^{-0.71} - 9.7\cdot(33)^{-0.69}\right] + 9.7\cdot(33)^{-0.69} \quad \text{if } FS_j > 1.2 \wedge FS_j \le 1.3 \wedge q0_j < 33\\
&a_j \leftarrow \frac{FS_j - 1.3}{2.0 - 1.3}\cdot\left[0 - 7.6\cdot\left(q0_j\right)^{-0.71}\right] + 7.6\cdot\left(q0_j\right)^{-0.71} \quad \text{if } FS_j > 1.3 \wedge FS_j \le 1.4 \wedge q0_j \ge 33 \wedge q0_j \le 200\\
&a_j \leftarrow \frac{FS_j - 1.3}{2.0 - 1.3}\cdot\left[0 - 7.6\cdot(33)^{-0.71}\right] + 7.6\cdot(33)^{-0.71} \quad \text{if } FS_j > 1.3 \wedge FS_j \le 1.4 \wedge q0_j < 33\\
&a_j \leftarrow 0 \quad \text{otherwise}\\
&\text{for } j \in 0..\frac{WT_e}{cm} - 1\\
&\quad 0\\
&a
\end{aligned}
$$

$$
\varepsilon_{V_j} := \begin{cases} \varepsilon_{vl_j} & \text{if } I_{C_j} \le 2.7 \\ \min\left(0.5, \varepsilon_{vl_j}\right) & \text{otherwise} \end{cases}
$$

Saturated Soils Strain Plot:

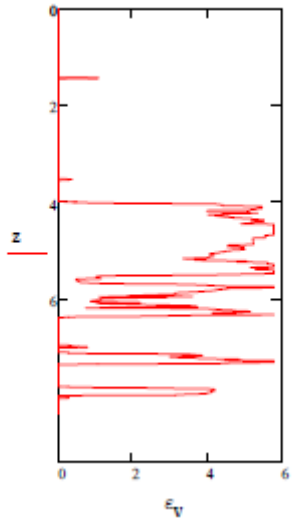

$$s_p := \left| \begin{array}{l} c_0 \leftarrow \varepsilon_{v_0} \cdot h_0 \cdot 0.01 \\ \text{for } j \in 1 .. \text{last}(z) \\ \quad c_j \leftarrow \varepsilon_{v_j} \cdot h_j \cdot 0.01 + c_{j-1} \\ c \end{array} \right.$$

$$s_{s_j} := s_{p_{\text{last}(z)}} - s_{p_j}$$

Saturated Soils Settlement Plot:

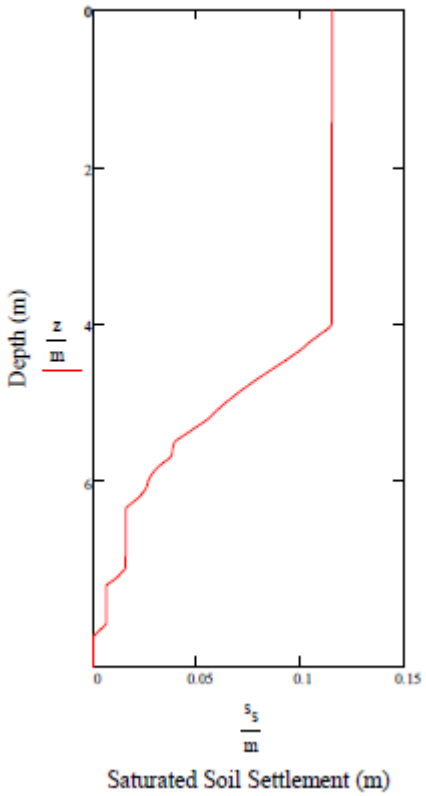

DRY SAND *Robertson and Shao (2010)*

$$N_{C_j} := (M - 4)^{2.17}$$

$$N_{1\_60c_j} := \begin{cases} \dfrac{Q_{m\_cs_j}}{8.5 \cdot \left(1 - \dfrac{I_{C_j}}{4.6}\right)} & \text{if } I_{C_j} < 2.6 \\ \dfrac{Q_j}{8.5 \cdot \left(1 - \dfrac{I_{C_j}}{4.6}\right)} & \text{if } I_{C_j} \geq 2.6 \end{cases}$$

$$N_{1\_60cs_j} := \begin{cases} 0.01 & \text{if } N_{1\_60c_j} = 0 \\ N_{1\_60c_j} & \text{otherwise} \end{cases}$$

$$G_{0_j} := 0.0188 \cdot \left(10^{0.55 \cdot I_{C_j} + 1.68}\right) \cdot \left(q_{c_j} - \sigma_{v0_j}\right)$$

$$\tau_{av_j} := 0.65 \cdot PGA \cdot \sigma_{v0_j} \cdot r_{d_j} \cdot \frac{1}{MSF_{1_j}}$$

$$R_{1_j} := \frac{\tau_{av_j}}{G_{0_j}}$$

$$a_{1_j} := 0.0389 \cdot \left(\frac{\sigma_{v0_j}}{100kPa}\right) + 0.124$$

$$b_{1_j} := 6400 \cdot \left(\frac{\sigma_{v0_j}}{100kPa}\right)$$

$$\varepsilon_{vol15_j} := \begin{cases} 0 & \text{if } I_{C_j} \geq 2.6 \\ \left[\gamma_{1_j} \cdot \left(\dfrac{N_{1\_60cs_j}}{20}\right)^{-1.20}\right] & \text{if } I_{C_j} < 2.6 \end{cases}$$

$$\varepsilon_{vol} := \left| \begin{array}{l} \text{for } j \in 0..\dfrac{WT_e}{cm} - 1 \\ \quad a_j \leftarrow \varepsilon_{vol15_j} \cdot \left(\dfrac{N_{C_j}}{15}\right)^{0.45} \\ \text{for } j \in \dfrac{WT_e}{cm} - 1 .. \text{last}(z) \\ \quad a_j \leftarrow 0 \\ a \end{array} \right.$$

$$s_{dl} := \left| \begin{array}{l} c_0 \leftarrow \varepsilon_{vol_0} \cdot h_0 \cdot \dfrac{1}{100} \\ \text{for } j \in 1 .. \text{last}(z) \\ \quad c_j \leftarrow \varepsilon_{vol_j} \cdot h_j \cdot \dfrac{1}{100} + c_{j-1} \\ c \end{array} \right.$$

$$s_{d_j} := s_{dl_{last(z)}} - s_{dl_j}$$

Dry Soils Settlement Plot:

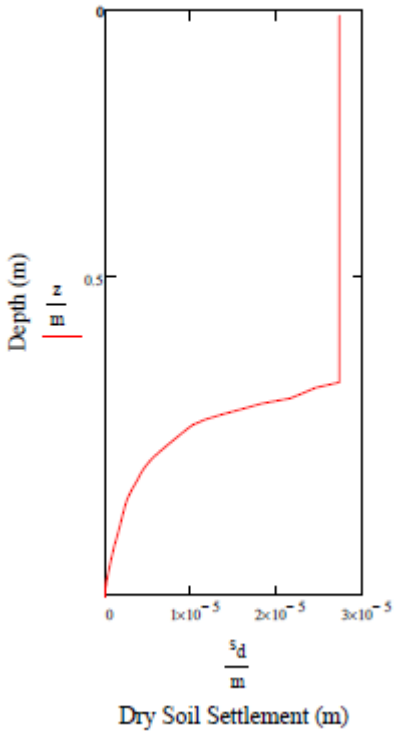

TOTAL SETTLEMENT

$s_{t_j} := s_{d_j} + s_{s_j}$

Total Settlement Plot:

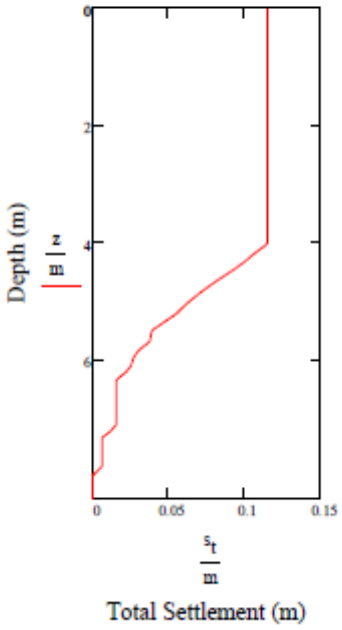

Probabilistic Settlement Juang et al. (2013)

$$\mu_p := \sum_j \left(\varepsilon_{v_j} \cdot h_j \cdot P_{L_j}\right)$$

$$\sigma_p := \sum_j \left[\left(\varepsilon_{v_j}\right)^2 \cdot \left(h_j\right)^2 \cdot P_{L_j} \cdot \left(1 - P_{L_j}\right)\right]$$

$$\mu_a := 1.2488 \cdot \mu_p$$

$$\sigma_a := 1.2488^2 \cdot \sigma_p + \mu_p^{\,2} \cdot (1.2488 - 0.5331)^2 + (1.2488 - 0.5331)^2 \cdot \sigma_p$$

$$\delta_a := \frac{(\sigma_a)^{0.5}}{\mu_a}$$

$x := 1 .. 60$

$$P_{S_x} := 1 - \text{pnorm}\left(\frac{\ln(x) - \ln\left(\frac{\mu_a}{m}\right)}{\sqrt{\ln\left(1 + \delta_a^{\,2}\right)}}, 0, 1\right)$$

Probabilistic Settlement Plot: